Structural and functional modifications of muscle proteins in response to glucosamine glycation

by

Yuliya Hrynets

A thesis submitted in partial fulfillment of the requirements for the degree of

Doctor of Philosophy

in

Food Science and Technology

Department of Agricultural, Food and Nutritional Science
University of Alberta

Abstract

High quality proteins can be isolated from meat processing by-products. The main quality attributes of these isolates are measured through their essential amino acid composition and functional properties, such as solubility, water holding and emulsification capacities, and gelation. The isoelectric solubilization and precipitation process (ISP) is a technology that can recover and valorize muscle proteins from these low value raw materials. This process involves acid and alkaline solubilization followed by precipitation of the proteins at their isoelectric point. Despite ISP provides a good protein recovery yield, solubility with this technique is a major problem due to partial denaturation as a consequence of the extreme acid/alkaline conditions applied. Protein-saccharide interactions through Maillard reaction (glycation) is a promising solution to solve this issue, since can produce novel glycoproteins with enhanced functionality (i.e. solubility). Hence, one of the main objectives of this thesis was to study the interaction between myofibrillar protein and reducing sugars using two different approaches: 1) a chemical glycation conducted at low temperatures (40°C) in a liquid environment and 2) an enzymatic glycosylation involving transglutaminase (TGase) as a catalyst conducted at 37°C. Glucosamine (GlcN), a popular amino sugar used to treat osteoarthritis, was chosen as a glycating agent due to its unique chemical characteristics. It is a fast glycating agent and could be used by TGase as an acyl acceptor to form an isopeptide bond between the glutamine in the myofibrillar protein and the free -NH_2 of a GlcN molecule. In the first part of the thesis, two studies were conducted. The first aimed to conjugate isolated actomyosin protein with glucosamine at 40°C in a liquid environment. Conjugation at 40°C for 8 h at a 1:3 protein:sugar ratio produced glycated myofibirillar proteins with enhanced solubility and emulsifying properties, particularly at the isoelectric point. In the second study, enzymatic glycosylation using TGase created a more stable

glycosylated myofibrillar protein at 25 and 37°C, possibly due to the formation of an isopeptide bond between glutamine and GlcN. It was possible to obtain stable glycoconjugates at these lower temperatures which also possessed increased solubility and emulsifying properties.

The 2nd part of the thesis was dedicated to understanding the unique chemistry of GlcN *in vitro* and how this would affect the structure of myoglobin, a major important globular protein found in muscle tissue. Two studies were conducted. The first focused to identify and quantify the main products of GlcN degradation at 37°C. GlcN produced a significant amount of α-dicarbonyl compounds (1000-6000 mg/kg of GlcN), particularly 3-deoxyglucosone and glucosone. GlcN cyclocondensation products, fructosazines and dihydrofructosazines, were also identified. The second study focused on the major structural changes of myoglobin in response to GlcN reactivity and degradation products. GlcN treatment may induce the production of fibrous aggregate in a relatively short time, while no such effect was observed for myoglobin glycated with glucose and acetyl-glucosamine. Overall, this thesis demonstrated that GlcN is a unique amino saccharide with the potential to be used in food applications (i.e. protein modification for improved solubility), and not only as a natural health product to treat osteoarthritis. However, further studies are necessary to evaluate the safety of GlcN as a food ingredient.

Preface

This thesis is an original work of Yuliya Hrynets. It is presented in manuscript format and consists of seven chapters.

The introduction (Chapter 1) defines the research problem, hypothesis and objectives of this work.

Chapter 2 is the literature review focuses on the Maillard reaction, its role in protein functionality modifications, and some aspects of glucosamine production and synthesis.

Chapters 3 to 6 constitute main body of the thesis.

Chapter 3 was published as Y. Hrynets, M. Ndagijimana, and M. Betti, "Non-enzymatic glycation of natural actomyosin (NAM) with glucosamine in a liquid system at moderate temperatures." *Food Chemistry*, vol. 139, issue 1-4, 1062-1072.

Chapter 4 was published as Y. Hrynets, M. Ndagijimana, and M. Betti, "Transglutaminase-catalyzed glycosylation of natural actomyosin (NAM) using glucosamine as amine donor" *Food Hydrocolloids*, vol. 36, 26-36.

Modified version of Chapter 5 was published as Y. Hrynets, M. Ndagijimana, and M. Betti, "Studies on the formation of Maillard and caramelization products from glucosamine incubated at 37˚C." *Journal of Agricultural and Food Chemistry,* vol. 63, issue 27, 6249-6261.

Chapter 6 was accepted for publication as Y. Hrynets, M. Ndagijimana, and M. Betti, "Rapid myoglobin aggregation through glucosamine-induced α-dicarbonyl formation". *PLosOne*.

The conclusion (Chapter 7) describes the outcomes of this research, with a brief discussion on the implications of possible glucosamine applications as a food ingredient and suggestions for future work.

I was responsible for the experimental design, data collection, analyses and manuscripts preparation in all the published and submitted manuscripts. Dr. M. Ndagijimana assisted with the technical part of experiment and the proof reading of manuscripts. Dr. M. Betti was the supervisory author and was directly involved in advisory input in the project's concept and work as it progressed, manuscript composition, editing and proof reading.

"…the Maillard reaction still holds many surprises, even after over one hundred years of research."

Hellwig and Henle, 2014

Dedication

To my parents, Viktor and Natalia Hrynets,
and in the memory of my beloved grandfather Ivan.

Acknowledgments

First and foremost I am very thankful to my principal supervisor Dr. Mirko Betti for his advice, problem guidance and inspiration offered throughout the course of this work. He was readily available to give constructive advice on issues all the time, after hours and on weekends to make me understand and do my work in the right way.

I wish to express my sincere gratitude and appreciation to my supervisory committee members Dr. Michael Gänzle and Dr. Jonathan Curtis for their valuable suggestions during meetings. Your challenges during the committee meetings made me to go from simple observation of the phenomenon to understanding the reason behind it. Thank you for always prompt replies and help whenever I needed.

Thank you to the external examiner Dr. Phillip Y. K. Choi who was willing to be my examiner during candidacy and final examinations bringing different perspective in a food science world.

Thank you to Dr. Thomas Henle who took time out is his schedule and agreed to be an external examiner.

I am very grateful to Dr. Maurice Ndagijimana for all his explanations, in particular chromatography techniques. Thank you for resolving all my technical and methodological questions with patience and skill.

Thank you Jack Moore from Institute of Biomolecular Design for helping me with mass spectrometry analyses.

Thank you Dr. Wayne Moffat for helping with circular dicroism spectropolarimetry analyses.

Appreciation also goes to Jody Forslund who kept on track with my PhD programm and was approachable for questions; and Holly Horvath who was very helpful, especially with my TA's responsibilities.

Many thanks are due to my closest friend Dr. Christine Liu for always being my very trustful "comrade".

Thank you Henan Wang for all years of sharing the same office and been together through all of the moments of graduate studies. I will have good memories of IFT conference in summer 2012.

I would like to thank to my family in Edmonton. My aunt Elena, cousin Pavel and his wife Maria. Thank you for forgiving me my "always busy" and "no time". I am very grateful for all the support you gave me throughout these years.

I thank all who in one way or another contributed to the completion of this research.

Table of Contents

Abstract ii

Preface iv

Dedication v

Acknowledgments vi

List of Figures xii

Abbreviations xv

CHAPTER 1. General Introduction 1

CHAPTER 2. Protein modifications by glycation (the Maillard reaction) or glycosylation (enzyme–aided) as approaches to improve functionality 6

2.1. Protein modification to increase functionality 6

2.2. Non-enzymatic glycosylation of protein: the technology 7

2.2.1. Maillard reaction and its pathways 7

2.2.2. Dry vs wet protein modification 11

2.2.3. Novel discoveries about the Mallard reaction and its potential application for protein modification 13

2.3. An example of protein which require modification: Muscle protein isolate 14

2.4. Protein glycosylation by enzymatic approach 21

2.5. Aminosugars as glycating agents 24

2.5.1. Glucosamine production 24

2.5.2. GlcN application: supplements against arthritis 25

2.5.3. Hexosamine biosynthesis pathway (HBP) 26

2.5.4. Glucosamine stability: autocondensation products 29

2.5.5. GlcN as a potential food ingredient 30

2.5.6. Glycation as a promising tool for protein functionality improvement 32

CHAPTER 3. Non-enzymatic glycosylation of natural actomyosin (NAM) with glucosamine in a liquid system at moderate temperatures. 33

3.1. Introduction 33

3.2. Material and Methods 35

3.2.1. Materials 35

3.2.2. Extraction of Natural Actomyosin (NAM) 36

3.2.3. Glycation of Natural Actomyosin (NAM) 36

3.2.4. Assessment of the Maillard reaction evolution by UV-Vis spectroscopy 37
3.2.5. Protein oxidation measurement 37
3.2.6. Evaluation of protein solubility 38
3.2.7. Study in a model lysine-glucosamine system 39
3.2.8. Sample pre-treatment and digestion prior to matrix-assisted laser desorption/ionization time-of-flight mass spectrometry (MALDI-TOF/TOF-MS) analyses 40
3.2.9. Evaluation of glycoconjugation by MALDI-TOF/TOF-MS 41
3.2.10. Emulsifying activity index (EAI) and emulsion stability index (ESI) 41
3.2.11. Data analyses 42
3.3. Results and discussion 43
3.3.1. UV-Vis absorbance spectrum 43
3.3.2. Effect of frozen storage on glycation parameters 48
3.3.3. Protein oxidation during frozen storage 50
3.3.4. Protein solubility profiles as a function of pH 51
3.3.5. Model study in lysine-glucosamine system 53
3.3.6. Protein glycation by MALDI-TOF/TOF-MS 56
3.3.7. Emulsifying properties 59
3.4. Conclusions 61
CHAPTER 4. Transglutaminase-catalyzed glycosylation of natural actomyosin (NAM) using glucosamine as amine donor: functionality and gel microstructure 63
4.1. Introduction 63
4.2. Material and Methods 65
4.2.1. Materials 65
4.2.2. Methods 65
4.3. Results and Discussion 71
4.3.1. Evaluation of protein glycosylation by MALDI-TOF/TOF-MS 71
4.3.2. Confirmation of enzymatic glycosylation by Orbitrap-LC-MS 74
4.3.3. Effect of glycosylation on solubility 75
4.3.4. Emulsifying properties 77
4.3.5. Dynamic rheological behaviour 81
4.3.6. Impact of glycosylation on NAM gels microstructure 84

4.4. Conclusions 87
CHAPTER 5. Studies on the formation of Maillard and caramelization products from glucosamine incubated at 37˚C. 88
5.1. Introduciton 88
5.2. Materials and Methods 91
5.2.1. Chemicals 91
5.2.2. Experimental design 91
5.2.3. Incubation of GlcNAc, Glc-NH_3 and GlcN aliquots 92
5.2.4. Preparation of α-dicarbonyls and glucosamine reaction mixtures 92
5.2.5. Spectrophotometric measurements 93
5.2.5. Free α-dicarbonyl compounds: extraction, identification and quantitation 93
5.2.6. Statistical analysis 96
5.3. Results and Discussion 97
5.3.1. UV-Vis and fluorescence profiles of non-enzymatic modification of GlcNAc, Glc-NH_3 and GlcN over time 97
5.3.2. Identification and quantitation of the major α-dicarbonyls produced from GlcN degradation by UHPLC and mass spectrometry analyses 100
5.3.3. Condensation products from non-enzymatic modification of GlcN 106
5.4. Conclusions 111
CHAPTER 6. Rapid myoglobin aggregation through glucosamine-induced α-dicarbonyl formation 112
6.1. Introduction 112
6.2. Materials and Methods 114
6.2.1. Materials 114
6.2.2. Experimental design 115
6.2.3. Preparation of glycoforms of myoglobin 115
6.2.4. Matrix asisted laser desorption/ionisation time-of-flight mass spectrometry (MALDI-TOF-MS) 116
6.2.5. Liquid chromatography–electrospray ionization mass spectrometry (LC-ESI-MS) 116
6.2.6. Assay of carbonyl formation 117
6.2.7. Extraction of α-dicarbonyl compounds 117

6.2.8. Separation of the quinoxalines derivatives of α-dicarbonyl compounds by UHPLC-UV 118
6.2.9. Identification and quantitation of quinoxaline derivatives 118
6.2.10. Direct infusion orbitrap mass spectrometry analyses (DIMS) 119
6.2.11. Determination of myoglobin forms 119
6.2.12. Soret absorbance spectroscopy 119
6.2.13. Circular dichroism (CD) spectra acquisition and analyses 119
6.2.14. Intrinsic fluorescence measurements 120
6.2.15. Thioflavin T (ThT) fluorescence spectroscopy 120
6.2.16. Transmission electron microscopy (TEM) 121
6.2.17. Statistical analyses 121
6.3. Results 121
6.3.1. Mass spectrometric glycoform profiling of myoglobin 121
6.3.2. Glycation induces myoglobin oxidative modifications through carbonyl formation 128
6.3.3. Identification and quantitation of the major α-dicarbonyl compounds in Mb-GlcN 130
6.3.4. Mb-Fe^{3+}-reducing activity of GlcN 135
6.3.5. Conformational changes of myoglobin during glycation in the presence of glucosamine 137
6.4. Conclusions 143
CHAPTER 7. Conclusions, implications and future research 144
Bibliography 148
Appendix A. 169
Appendix B. 170
Appendix C. 171
Appendix D 172
Appendix E 173
Appendix F 174
Appendix G. 175
Appendix H. 176
Appendix I. 177
Appendix J 178

List of Tables

Table 2.1. Summary of the major studies on the effect of glycation through the Maillard reaction on muscle protein functionality……18

Table 3.1. Emulsion activity index (EAI) and emulsion stability index (ESI) of native and glycated NAM……..……60

Table 5.1. Retention times and precursor ions of the peaks reported in Figure 5.2…….…....101

Table 5.2. Concentrations of five different α-dicarbonyl compounds found in GlcN incubated over time……105

Table 6.1. Retention time, structure, MS and MS/MS data of the α-dicarbonyl compounds detected Mb-GlcN conjugates……132

List of Figures

Figure 2.1. Amadori and Heyns rearrangements leading to the Amadori (A) and Heyns (B) compounds……..……..9

Figure 2.2. Structures of the main myofibrillar proteins……..15

Figure 2.3. Schematic representation of the conjugation mode of polysaccharide with protein through the Maillard reaction……..……..20

Figure 2.4. A simplified schematic representation of hexosamine biosynthesis pathway (HBP)……..……..28

Figure 2.5. Formation of dihydroxyfructosazine, fructosazine and deoxyfructosazine from D-glucosamine…….……30

Figure 3.1. Experimental variables for actomyosin conjugation with different sugars via the Maillard reaction in a liquid system…….37

Figure 3.2. UV-Vis absorbance spectra of NAM-GlcN (A) and NAM-Glc (B) conjugates over time..……44

Figure 3.3. Difference in the molecular structure between glucosamine and glucose……45

Figure 3.4. Hierarchal clustering of protein-sugar UV-Vis absorbance data for actomyosin extracted from fresh chicken *Pectoralis major*……..…….47

Figure 3.5. Hierarchal clustering of protein-sugar UV-Vis absorbance data for actomyosin extracted from frozen chicken *Pectoralis major*…….49

Figure 3.6. Solubility of actomyosin as dependent on pH, type of sugar and protein to sugar ratio……..52

Figure 3.7. Orbitrap LC-MS spectrum of Lys-GlcN conjugates at 0 (A), 2 (B) and 8 (C) hours of incubation and proposed Schiff base structures (inset 1)…….……..54

Figure 3.8. MALDI-TOF/TOF mass spectra of non-treated actomyosin (A), and actomyosin conjugated with glucosamine (B) or glucose (C) at 40˚C for 8 hours at 1:3 protein to sugar ratio……..58

Figure 3.9. MALDI-TOF/TOF mass spectra of non-treated actomyosin (A), and actomyosin conjugated with glucosamine (B) or glucose (C) at 40˚C for 12 hours at 1:6 protein to sugar ratio……..……59

Figure 4.1. MALDI-TOF/TOF mass spectra of non-treated actomyosin (A), and actomyosin conjugated with glucosamine at 1:1 (B) or 1:3 (C) protein to sugar ratio via enzymatic reaction of TGase at 25˚C for 6 hours.……....72

Figure 4.2. Relative percentages of glycation and glycosylation endowed to protein during the conjugation reaction at different reaction conditions.…….....……..73

Figure 4.3. pH-dependent solubility profiles of controls and enzymatically glycosylated actomyosin at different conditions.……...…...……..76

Figure 4.4. Mean values and standard deviations of the mean droplet size ($d_{4,3}$) at 0 and 3 days of storage ($\Delta\ d_{4,3}$) for non-treated and glycosylated NAM at pH 5.0 (A) and 7.5 (B)….……...78

Figure 4.5. Particle size distribution profiles of control and glycosylated NAM at pH 5.0 (A) and 7.5 (B) determined initially and after 3 days of storage……..……..80

Figure 4.6. Changes in dynamic viscoelastic behaviour (DVB) of proteins glycosylated with GlcN by the mean of TGase at different conditions. ……81

Figure 4.7. Cryo-scanning electron microscopy images of the gels produced from non-treated and glycosylated actomyosin after slush of the sample with liquid nitrogen at the atmospheric pressure……..….85

Figure 5.1. Derivatization reaction of α-dicarbonyl compounds with *o*-phenylenediamine (OPD) to give their corresponding quinoxalines……..94

Figure 5.2. UV-Vis absorbance (A) and fluorescence spectra (B) profiles of GlcNAc (1A, 1B), Glc-NH_3 (2A, 2B) and GlcN (3A, 3B) as a function of heating time from 0 to 12 days.……..98

Figure 5.3. UHPLC analyses of quinoxaline derivatives of α-dicarbonyl compounds produced from GlcN incubation over time……..……...101

Figure 5.4. MS/MS spectra and structures of quinoxaline α-dicarbonyl compounds produced during GlcN degradation…….103

Figure 5.5. Mass spectrum of GlcN incubated at 0.5 (A) and 3 (B) days and directly infused into the LTQ Orbitrap – MS instrument.……107

Figure 5.6. Proposed structures and theoretical monoisotopic molecular weights (M_w) of cyclocondensation products of GlcN only or GlcN and α-dicarbonyl compounds……...109

Figure 5.7. Absorbance (A) and fluorescence emission (B) spectra of incubated equimolar mixtures of GlcN and α-dicarbonyl compounds……..……..110

Figure 6.1. MALDI-TOF/TOF mass spectra of Mb incubated at 37ºC for various times in the presence of GlcNAc, Glc and GlcN……..123

Figure 6.2. A deconvoluted ESI-MS spectra of Mb incubated at 37ºC for various times in the presence of GlcNAc, Glc and GlcN.……..……..…126

Figure 6.3. Protein oxidation (carbonyl content) in Mb and Mb conjugated with GlcNAc, Glc and GlcN from 0 to 12 days...……..129

Figure 6.4. UHPLC analyses of quinoxaline derivatives of α-dicarbonyl compounds produced from Mb-GlcN conjugates over time.……..……131

Figure 6.5. Concentration of the major α-dicarbonyl compound produced during incubation of Mb in the presence of GlcN from 0 to 12 days.……..…….133

Figure 6.6. (A) Decrease in Soret band absorbance; (B) images and the percentages of metmyoglobin (MetMb), deoxymyoglobin (DeoMb) and oxymyoglobin (OxyMb) in native Mb and Mb-GlcN conjugates over glycation period from 0.5 to 12 days…….……136

Figure 6.7. (A) Fluorescence emission spectra (B) far-UV spectra analyses; (C) secondary structure composition; (D) maximum fluorescence intensity of Thioflavin T (λ=482 nm)…….....…139

Abbreviations

AGEs - advanced glycation end-products
ANOVA - analysis of variance.
AO – alginate oligosaccharide
CD – circular dichroism
COS - chitosan oligosaccharide
DA - diacetyl
3,4-DGE-3,4-dideoxyglucoson-3-ene
3-D - 3-deoxyglucosone
DTPA - diethylene triamine pentaacetic acid
ESI- electrospray ionization
FDA - Food and Drug Administration
G - glucosone
GAGs – glycosaminoglycans
GFAT - glutamine:fructose-6-phosphate-aminotransferase
Glc -glucose
GlcN- glucosamine
GlcN-6-P - glucosamine-6-phosphate
GlcNAc- *N*-acetyl-glucosamine
GO - glyoxal
GRAS - generally regarded as safe
HA- hyaluronic acid
HBP - hexosamine biosynthesis pathway
HPA - hydroxypyruvaldehyde
LOD - limit of detection
LOQ - limit of quantification
MALDI-TOF - matrix assisted laser desorption/ionization-time of flight
MGO - methylglyoxal
MR – Maillard reaction
MS - mass spectrometry
MS/MS - tandem mass spectrometry
NAM – natural actomyosin
nd - not detectable
NHP -natural health product
OPD - *o*-phenylenediamine
PDA - photo diode array detector
SPE- solid phase extraction
TEM - transmission electron microscopy
TFA - trifluoroacetic acid
TGase – transglutaminase
ThT – thioflavin T
UHPLC - ultrahigh performance liquid chromatography
USDA - United States Department of Agriculture
α-DC - alpha-dicarbonyl compound

CHAPTER 1. General Introduction

During my previous studies at the M.Sc. level, I was involved in a research to recover functional myosin and actin muscle proteins from meat and fish processing by-products (Hrynets et al. 2010, 2011 a,b). The technology studied and optimized was based on the concept of "pH-shifting". This technique can efficiently and sustainably solubilize and recover muscle protein for the preparation of processed meat products or other food applications like, for instance, protein films (Betti and Xu, 2010) and coatings. The technology is now known as the isoelectric solubilization/precipitation process, and has been widely applied to isolate proteins from underutilized fish and poultry species and meat processing by-products. The research on this was important because it linked the laboratory work to the pilot plant development where the technology was later scaled-up (Khiari et al. 2014). A scheme of the extraction is reported in Appendix A. A slurry of mechanically separated meat in water (1:5, w/w) is adjusted to pH 2.5 to solubilize proteins, which then is precipitated at pH 5.2, centrifuged and recovered to create an isolate with around 15% protein and 1% fat on a wet-basis. The wet protein isolate is spray- or freeze-dried in order to create a shelf-stable protein powder with protein content around 90%. Structural modifications, functionality (solubility, emulsification capacity and stability, foaming and gelation) and sensorial characteristics of protein isolates in several products have been studied (Omana et al. 2012 a,b; Khiari et al. 2013, 2014). One of the issues observed was the reduced solubility, likely due to protein denaturation occurring during solubilization of the slurry at pH 2.5 and during the freeze-drying process (Yongsawatdigul and Park, 2004; Kristinsson and Hultin, 2004; Khiari et al., 2013). Thus, it is important to find solutions to this issue in order to increase the application of muscle protein isolates in the food industry. For instance, Proliver, a Belgian based protein manufacturer, produces innovative protein powders extracted from

chicken or turkey meat parts. These powders are then used for meat, soup and savoury, and sport and health nutrition applications (Proliver, 2015). Prospector, a US Company, also produces chicken protein isolates, which they propose to use in protein shakes, drinks and other health and sports foods (Prospector, 2015). International Dehydrated Foods, Inc. also manufactures beef and turkey meat powders which could be employed for making snacks, bars, breads, powder shake mixes and ready-made meals (IDF, 2015).

At the end of my M.Sc. studies, a PhD focusing on improving the functionality of the isolated muscle proteins, particularly solubility and gelation, was undertaken. In this regard, two major technologies were emphasized in literature: enzymatic hydrolysis with commercial proteases or protein-saccharide interaction through the Maillard reaction. The enzymatic hydrolysis of food proteins to increase solubility was a field highly investigated already, and this technique likely result in lack of gelation properties due to protein fragmentation and possibly bitter-testing peptides (Visessanguan and An 2000; Saha and Hayashi, 2001). So attention was paid to the less well known protein-saccharide interaction instead. Several studies were conducted to enhance the functionality of myofibrillar proteins through saccharide interactions, and were particularly focused on fish proteins. At the same time, only one study was conducted on poultry protein. Furthermore, the main technology used for developing neoglycoproteins through protein-saccharide interaction was based on the Maillard reaction (glycation) conducted in dry conditions between proteins and reducing mono-, di- and polysaccharides.

Even though the studies on protein glycation by the Maillard reaction showed positive outcomes, the industrial application of dry glycation to proteins has not been scaled up and commercialized. The reasons for this were attributed to difficulties in controlling the extent of glycation, uneven distribution of reactants (Kato, 2002), long reaction time (Zhu et al. 2008), possible protein

denaturation (French et al. 2012), undesirable colour changes (Tanaka et al. 1999) and formation of anti-nutritional compounds (Brands, 2000).

In an attempt to combine the production of novel glycoproteins with enhanced functionality such as solubility, and possibly bioactivity, the development of conjugates between muscle proteins and glucosamine in a liquid state via the Maillard reaction at the early stage was hypothesized. Glucosamine (GlcN; 2-amino-2-deoxy-glucose) is an aminosugar widely used through the world as a dietary supplement to treat osteoarthritis, and is prescribed as a drug in the European Union. It is produced from the by-products of the marine industry through hydrolysis of chitin polysaccharide.

During preliminary studies on a model system composed of bovine serum albumin and GlcN in both water and phosphate buffer, it was observed that GlcN was a good glycating agent at ambient and moderate temperatures (25-50˚C) as judged from the rapid colour development visible to the naked eye. This was also confirmed by some available literature reporting a higher reactivity of GlcN as compared to fructose, galactose, glucose or xylose when reacting with cysteine at 125˚C for 25 min (Kraehenbuehl, 2008).

Furthermore, based on the previous experience on the use of transglutaminase (TGase) to cross-link muscle protein isolates (Hrynets et al. 2011c) it was hypothesized that this enzyme could be used to create novel bioconjugates between muscle protein and GlcN. TGase catalyzes the acyl-transfer reactions between a γ-carboxyamine group of a peptide- or protein-bound glutamyl residue and a primary amino group of various substrates. The hypothesis was based on the concept that GlcN could act as an amine donor (or acyl acceptor) and thus could be incorporated to the glutamine residues of muscle proteins via the TGase-catalyzed reaction. This approach was previously demonstrated, where 6-aminohexyl-1-thio-β-D-galactopyranoside, a synthetized

aminosaccharide, was introduced into vegetable proteins, like β-gliadins or legumin (Colas et al. 1993).

Hence, the objective of this thesis was to design a novel glycoprotein between muscle protein and glucosamine using chemical and enzymatic approaches. To meet these objectives four experiments were conducted and divided into two main parts.

The first part (the studies described in Chapters 3 and 4) was devoted in proving the feasibility of producing functional glycoconjugates in the liquid state at moderate temperature based on the higher reactivity of GlcN and on the catalyzing effect of TGase.

Specific objectives were:

1. To prove the glycation and glycosylation feasibility at the laboratory level.
2. To optimize the conditions to achieve maximum GlcN conjugation.
3. To test the functionality of the glycoconjugates obtained.

The second part of this thesis (described in Chapters 5 and 6) was devoted to understanding the reasons behind the higher reactivity of GlcN towards protein. No clear explanation on this phenomenon has been provided previously. For instance, the positive outcomes of the first part of the experiment were obtained without a complete understanding of the reactions system. Hence the specific objectives of the second part of this thesis were:

1. To study the main degradation products of GlcN *in vitro* model system.
2. To investigate the effect of GlcN degradation products on structural modifications of myoglobin.

Two main experiments were conducted in this regard. The first was focused on understanding the chemistry of degradation of GlcN *in vitro* at 37˚C. It was hypothesized that GlcN, being a

Heyns compound (an unstable intermediate from the Maillard reaction between fructose and NH_3), can produce reactive intermediates, i.e. α-dicarbonyls. Next, an *in vitro* study was conducted to specifically study the structural modification of myoglobin, another relevant protein found in muscle tissue, in the presence of GlcN. Myoglobin is widely used for model studies due to its availability and well-known structure.

CHAPTER 2. Protein modifications by glycation (the Maillard reaction) or glycosylation (enzyme–aided) as approaches to improve functionality

2.1. Protein modification to increase functionality

Protein is an essential component of the diet needed for human survival. Apart from the nutritional value, protein provides unique functional properties in foods affecting their behaviour during preparation, processing and storage. They also significantly contribute to the sensorial and quality attributes of the food system (Wrolstad, 2005). Nutritional quality, availability of source, and cost are all important factors for protein applications in food, however a key component is a satisfactory functional property profile. The functional role of protein is mainly ascribed as solubility, the abilities to form emulsions, foams, gels, and the ability to retain fat or water (Liu et al. 2012). Consequently these functional properties influence the selection of the processing methods and final qualitative characteristics of the product. Numerous studies have been performed to expand commercial use for a variety of protein types in various food applications. Strategic and selective structural modifications often alter protein functionalities to make them better food ingredients (Hamada et al. 2004). Protein modifications are well-studied and show possible approaches for modifying physico-chemical and functional properties. These modifications include chemical and enzymatic hydrolysis, protein deamidation, succinylation, acetylation, and phosphorylation. Among different types of modifications developed in research laboratories, not all can be used in food applications due to potential health hazards, since non-food ingredient are sometimes required in some of these methods. Also, methodological issues or simply the inability to scale the process up or transfer it from laboratory to industrial plant, make the system unfeasible.

The Maillard reaction (MR) has been proposed as a relatively simple and safe strategy to improve protein functionalities, since it occurs naturally and there is no need for additional non-

food grade chemicals. Under controlled conditions of time, pH and moisture, heat-induced MR is a promising approach for the modification of food protein functionality (Gerrard, 2002). The MR introduces covalent bonds between proteins and carbohydrates, both of which are food components. MR synthetic glycoprotein was proposed to be called neoglycoprotein (Saeki, 1997). Owing to the positive aspects of the MR it remains one of the most complicated, interesting, and productive reactions in food science; research continues to harness it to produce food ingredients with improved properties (Joubran, 2013). Due to the importance and popularity of MR in food protein modification, many research papers and several reviews have been written on the subject recently (Liu et al. 2012; Oliveira et al. 2014; Song and Zhao, 2013). For this reason, this chapter can bring forward the main subjects that are currently being discussed. In relation to this thesis, this review emphasizes the production of novel glycoprotein, its functionality in a model system, and the chemistry of the sugar used in the reaction.

2.2. Non-enzymatic glycosylation of protein: the technology

2.2.1. Maillard reaction and its pathways

The MR has been detected in heated, dried or stored foods and naturally in the mammalian organism. For food scientists MR is unquestionably important as being responsible for changes in colour, flavour, texture and nutritive value in a variety of processed foods. Whereas in medicine, *in vivo* ageing and complications of diabetes are ascribed to undesirable protein glycation due to excess of sugar reaction with proteins and impairing their functionalities.

The MR is of great importance in food manufacturing, and it is used almost everywhere from the baking industry to our day to day life to make food more flavourful. Along with MR, this reaction is so-called glycation, non-enzymatic glycosylation or simply “browning”. Since 1993 the terms became more distinguishable, where glycation (or non-enzymatic glycosylation) is a result of a sugar molecule, fructose or glucose, bonding to a protein or lipid without the

controlling action of an enzyme. This is differentiated from enzyme-catalyzed glycosylation, where sugars are attached to asparagine or serine side chains through glycosidic linkages to form glycoproteins *in vivo*. Glycation is a relatively haphazard process that impairs the functioning of biomolecules, whereas glycosylation occurs at defined sites on the target molecules with specific biological functions (Lis and Sharon, 1993). The reaction was named after its discoverer French biochemist Louis Camille Maillard, who was the first to report that aqueous solutions consisting of amino acids and reducing sugars turning progressively brown during heating (Maillard, 1912). Since 1940's the chemistry of the MR has been extensively investigated, particularly, in relation to the formation of flavour and color compounds in food and model systems, using variety of proteins, amino acids and reducing sugars. The importance of MR in food science and nutrition is undisputed, at the same time the research is growing beyond these fields, including medicine and pharmaceutical worlds.

MR is a sequence of reactions, beginning with the covalent bond between the amine groups and carbonyl compounds. As proposed by Hodge (1953) the reaction is divided into "early", "advanced" and "final" stages, which are highly dependent on the reaction conditions and distinguished by the characteristic reaction product (Silván et al. 2011; Hellwig and Henle, 2014). The main participants of the MR are biomolecules with free amine groups like proteins, nucleotides and some phospholipids. Amines have several properties that are responsible for their extensive reactivity. Paramount is their ability to act as nucleophiles by possessing a lone pair of electrons on the nitrogen atom. The properties of the carbonyl group are primarily those of the carbon-oxygen double bond, which is both strong and reactive. The early stages of the Maillard reaction are depicted in Figure 2.1.

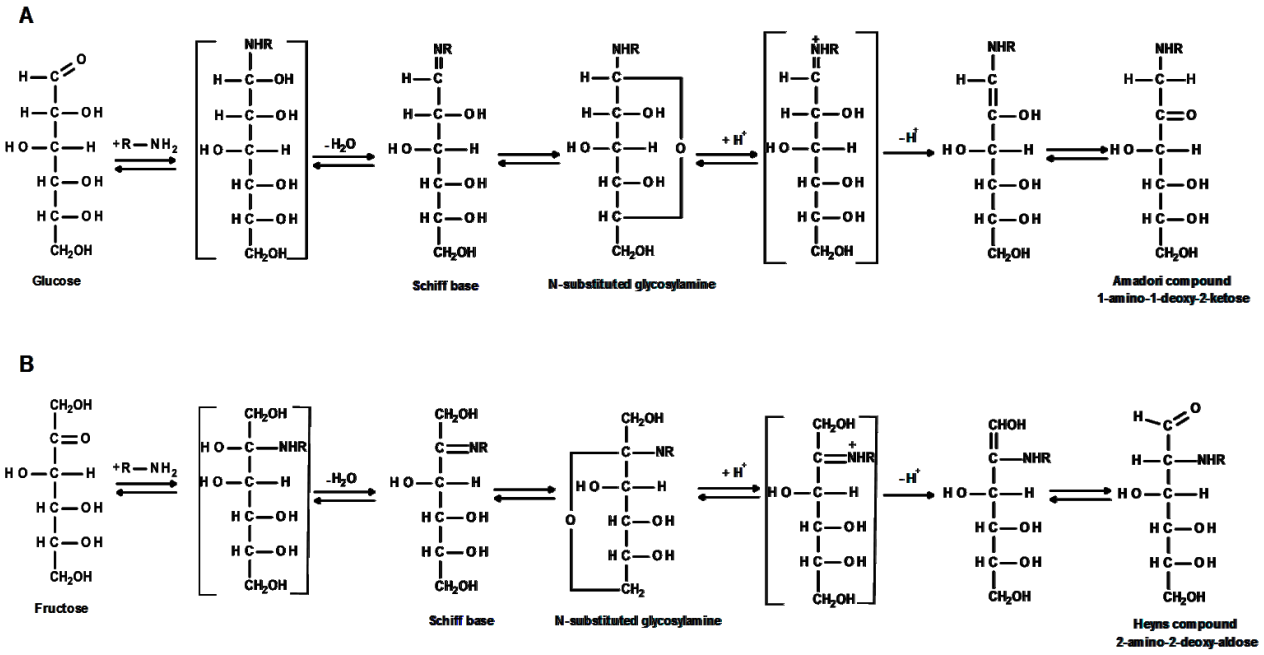

Figure 2.1. Amadori and Heyns rearrangements leading to the Amadori (A) and Heyns (B) compounds. The structures are reproduced from Nursten (2005).

The initial step of MR involves the reaction between a reducing sugar and an amino acid to form an addition product. The addition product dehydrates to form the corresponding imine referred to as Schiff base, which cyclized to form the N-glycosylamine. From the perspective of nutritive value, the glycosylamines are hydrolyzable and the free amino acid and sugar are usually re-generated and therefore nutritionally available (Dills, 1993). N-glycosylamine from aldose sugars undergoes the Amadori rearrangement and is converted to a 1-amino-1-deoxy-2-ketose (in the case of glucose, to 1-amino-1-deoxy-2-fructose, Figure 2.1 A). Derivatives from amino acids and ketoses (ketosylamines), in an analogous way to the Amadori rearrangement, undergo what is known as the Heyns rearrangement (Figure 2.1 B) (Davidek and Davidek, 2003). This arrangement was called after Kurt Heyns, a chemist at the Chemical Institute of the University of Hamburg (Hellwig and Henle, 2014), who observed the formation of D-glucosamine in the reaction of fructose with ammonia (Heyns and Koch, 1952). No color changes are usually observed at this stage of reaction (Damodaran, 2008), however the nutritional value can be

reduced due to irreversible modification of lysine residues, along with other proteinogenic amino acids such as arginine, tryptophan, and isoleucine (Dworschak, 1980). Depending on pH, temperature and time, Amadori products are degraded via several pathways during the advanced stages of the MR to deoxyosone intermediates, which are highly reactive α-dicarbonyl compounds (Henle et al. 1996), including 3-deoxyglucosone, (3-DG), 1-deoxyglucosone (1-DG), methylglyoxal (MGO), glyoxal (GO) and butanedione (Popova et al. 2010). These further react with the N-termini of lysine or arginine side chains of proteins leading to the formation of an advanced glycation end-products (AGEs). For instance, pyrraline is the result of reaction between lysine residue with 3-DG; MGO reacts with lysine residues to form N^{ε}-(carboxyethyl)lysine (CEL) or methylglyoxal-lysine dimer (MOLD) whereas N^{ε}-(carboxymethyl)lysine (CML) and glyoxal-lysine dimer (GOLD) are formed on reaction of GO with lysine (Friedman, 1996). Further rearrangements occur later in the advanced stage, including cyclisation, dehydration, retroaldolization, rearrangements and condensation. In the final stages of the MR melanoidins defined as polymeric high molecular weight, brown-coloured end-products containing nitrogen are formed (Henle et al. 1996; Bekedam et al. 2006). Though, the definite structure of variety of melanoidins unidentified, several mechanisms of their formation were proposed, including 1) cross-linking of low-molecular weight coloured substances to free amino groups of lysine or arginine of protein (Hofmann et al. 1998); 2) furan or pyrrole unit which upon polycondensation form repeating units of melanoidins (Heyns and Hauber,1970; Tressl et al. 1998); 3) a skeleton made up from proteins cross-linked by MR reaction products (i.e. melanoproteins) (Hofmann, 1999). In general it is well recognised that the advanced stages of the MR are much more complex in comparison to earlier stages. In this

regard, a substantial amount of studies were conducted to comprehend variety of MR-derived products.

2.2.2. Dry vs wet protein modification

Several factors, including temperature, time, pH, water activity, intrinsic properties of reactants, and the protein:sugar ratio all influence the yields and types of Maillard reaction products (MRPs). MRPs can determine structure, physico-chemical characteristics and functional properties of modified food proteins (Oliver et al. 2006). To introduce glycosyl units into food protein by MR, both solution (wet MR) and dry conditions can be used. However, the most studied and popular method to synthesize glycoconjugate is by dry-heating - so called solid-state heating. It involves the mixing of proteins and sugars, lyophilisation and heating under controlled temperature and humidity. The reaction is generally performed at 40-60˚C and 40-70% relative humidity (Saeki, 1997). Due to several reasons dry-heating method is not feasible for industrial scale production (Zhu et al. 2010). For instance, the application of freeze-drying is still a costly method for food industry. Equilibration to the desired water activity and control of relative humidity are the other factors limiting industrial scaling up (Oliver et al. 2006). In the case of muscle protein, freezing followed by drying can lead to denaturation and/or aggregation, which consequently causes problems with functionality (Leblanc and Leblanc, 1992; Gatlin et al. 2008). Thus, it is a regular practice to use cryprotective substances, sorbitol and sucrose, when freezing muscle protein. The reaction time required for globular proteins to be glycated may take over 2-3 weeks (Zhu et al. 2008), which is also not industrially practical. Here it is not easy to control the extent of the reaction, and the products are usually a mixture of intermediate and/or advanced MR products that have a light yellow or brown color (Akhtar and Dickinson, 2003; Zhu et al. 2008). In addition, after the reaction, the powders should be dissolved and the

conjugates purified by some technique. Presumably, during the storage of the powders, the reaction still may progress to advanced MR stages, where the conjugates possess reduced functionalities compared to early stage conjugates (Corzo-Martínez et al. 2011). Considering these factors, dry-heating is costly for industrial point of view and prevent the marketing of conjugates as food ingredients (Zhu et al. 2010).

Zhu et al. (2008, 2010) was the first to attempt to create protein−polysaccharide conjugates in aqueous solutions and to limit the MR to the very initial stage (Schiff base) to obtain a white color product. These authors showed that conjugates obtained from mixing 10% whey protein isolates (WPI)−30% dextran, incubated at 60°C for 24 h, were composed mainly of Schiff base. As the MR between proteins and polysaccharides in aqueous solution proceeds more slowly compared to dry-heating (Morgan et al. 1998), it was feasible to terminate the MR at the initial stage. However, a strong aroma was noted and a yellow color appeared with prolonged incubation time (>24 h). In terms of functionality, WPI-dextran conjugates (Zhu et al. 2010) has significantly improved heat stability when subjected to 80˚C for 30 min, remaining soluble at pH 3.2-7.5 in contrast to native WPI. The emulsifying ability and stability of WPI-dextran emulsions were greatly improved compared with the native WPI or natural commercial glycoprotein emulsifier, such as gum arabic.

In the study from Qi et al. (2009) functional soybean acid-precipitated protein (SAPP)-dextran conjugates were produced in an 80% ethanol-reacting system at 50˚C for 6 h, along with a 95% ethanol-reacting system at 60˚C for 24 h. Compared to the classical dry-heating, the reaction time of in both ethanol systems was largely shortened. Emulsifying activity and heat stability of SAPP-dextran conjugates were improved significantly compared to SAPP alone. Niu et al. (2011) also employed MR under wet conditions with xylose, glucose, lactose, dextran and

maltodextrin to improve the functionalities of wheat germ protein (WGP). The conjugates were produced at pH 11 at 90˚C for 20 min. The authors reported that conjugation resulted in improved both emulsion properties and solubility at the range from pH 5.0 to 10.0. For instance the solubility at the isoelectric point (pI) of modified WGP was three times higher as compared to native protein. While the MR in aqueous conditions is much less studied than for dry-conditions, these represented the first studies to demonstrate its potential application for food protein modification.

2.2.3. Novel discoveries about the Mallard reaction and its potential application for protein modification

Protein aggregation in food has been studied previously in relation to product structure and texture, with controlled aggregation being an essential part of many food processing techniques (Totosaus et al. 2002). In the last decade protein aggregation is becoming an increasingly important topic in the areas of biochemistry and biomedicine. There is a growing implication of the amyloid fibril, a particular form of aggregated protein, and its precursors, in the pathology of an increasing number of human neurodegenerative diseases (Dobson et al. 2001). In general, amyloids are a class of insoluble proteinaceous substances formed from misfolded proteins (Iannuzzi et al. 2013). When amyloid fibrils are analyzed with transmission electron microscopy (Sunde and Blake, 1997), they are visualized as long unbranched fibrils, and have the ability to bind to specific dyes (Krebs et al. 2005). They also show a typical cross-β pattern when analyzed by X-ray diffraction (Sunde and Blake, 1997).

In recent food science literature, amyloid fibrils have been proposed as new functional macromolecules in proteinaceous foods. Fibrillization of whey protein isolate greatly improves its foaming properties (Oboroceanu et al. 2014), where amyloid-like fibrils from β-Lactoglobulin (β-Lg) have potential as efficient thickening and gelling agents in food (Loveday et al. 2014).

These modifications from globular monomers to fibrils were achieved by heating protein dispersions above their denaturation temperatures (~80˚C) at a low pH for 15 to 20 h. Other food proteins under the same conditions, including kidney bean phaseolin, soy and hen lysozyme, were also shown to form amyloidal nanofibrils (Liu and Zhong, 2013). A new evolution of the technique was proposed by Liu and Zhong (2013), who produced nanofibrils from WPI after dry-state incubation with lactose. These authors showed that an arrangement of the lactose on nanofibril surface provided steric hindrance and enabled dispersibility and thermal stability in a variety of pH and ionic conditions, in contrast to the poor dispersibility and heat instability of WPI nanofibrils.

In another study from Dave et al. (2014), freeze-dried powder mixtures of β-Lg-lactose were incubated for 3 d, while β-Lg-glucose incubated for 8 h at 40˚C. The glycoconjugates were further heated at 80˚C at pH 2.0 for 2-24 h to promote self-assembly of nanofibrils. This study showed that steric constraints introduced by sugar residues substantially inhibited the self-assembly of glycated β-Lg fragments into fibrils, with the effect being greater for the larger lactose moiety, where even the extent of lactosylation was less than glycosylation.

2.3. An example of protein which require modification: Muscle protein isolate

A variety of protein isolates are produced from low valued products of cheese and casein manufacturing (i.e. whey protein isolate), soy (i.e. soy protein isolate), fish (i.e. fish protein isolate) or meat (i.e. poultry protein isolate) industries. One of the methods to recover the protein for food purposes having a GRAS (Generally Regarded as Safe) status in the United States (FDA, 2004) is the isoelectric solubilization/precipitation method (also called pH-shifting). Due to its good potential to be transferred from laboratory to industrial scale production, it has been subjected to numerous studies, particularly in recovery of myofibrillar and sarcoplasmic protein

from fish (Kim et al. 2003) and beef (DeWitt et al. 2002). Later, the process was also applied and optimized in increasing the value of poultry processing by-products (Hrynets et al. 2010, 2011 a, b). It involves solubilising muscle proteins by subjecting finely homogenised fish/meat mince to either low pH (~2.5-3.0) or high pH (~10.0-12.0) at low temperatures. Solids such as bones, neutral fat and disrupted cellular lipid membranes are then removed by centrifugation. The soluble protein is then precipitated by adjusting the pH to the pI of the myofibrillar proteins to give a protein isolate (Hrynets et al. 2010). Myosin, in *pre-rigor* muscle, and actomyosin, in *post-rigor* muscle, are myofibrillar proteins which contribute to the functionality of processed meat products (Smith, 2001). The structures of myosin and actin are depicted in Figure 2.2. Myosin is a multidomain protein with two large heavy chains and four light chains arranged into an asymmetrical molecule with two globular heads attached to a long rod-like tail (Visessanguan and An, 2000). Actin is a globular protein that polymerizes to form long filaments (F-actin).

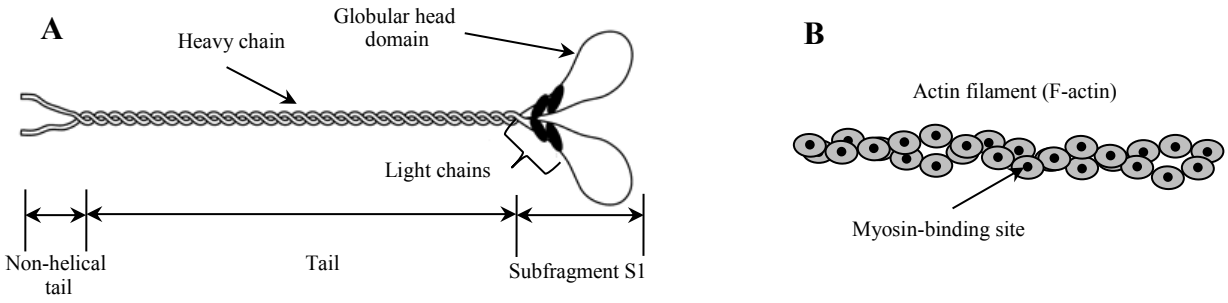

Figure 2.2. Structures of the main myofibrillar proteins: (A) myosin molecule showing the globular head region, light chains, the α-helical tail, short non-helical tail and subfragment S-1; (B) actin filament showing myosin-binding site. Myosin structure is reproduced with modifications from Conti and Adelstein (2008).

Protein isolate can be frozen like surimi (concentrated fish myofibrillar protein) or dried for further utilization. Several studies showed that recovered proteins recently have a potential to be used as an ingredient in food products due to their low price and high nutritive value (Geirsdottir,

2005; Shaviklo et al. 2010a; Khiari et al. 2013, 2014). Functional properties and stability of protein play important roles in food formulations and have a critical impact on the general sensory acceptance of formulated products (Damodaran, 2008). Even though studies reported positive outcome when protein was used as a part of marinating or injection brine formulation, there is still a need to improve their functional properties to maximize their utilization (Khiari et al. 2014). As proteins undergo partial denaturation during pH-shifting, final isolates shows lack in solubility (Yongsawatdigul and Park 2004). In addition, the drying process to produce a powder also reduces functionality (Shaviklo, 2010b, Khiari et al. 2013). Solubility is one of the most important protein functionality, since it further influences emulsifying, gel-forming abilities and water holding capacity. To address these shortcomings and maximize the functional usability of protein, extensive research continues with the objective to create commercially successful methods for protein modifications. The majority research related to improving the solubility of these recovered proteins has focused on enzymatic hydrolysis with a variety of commercially available proteases. However, the most serious problem in the practical use of the hydrolysates is the residual bitter taste caused by the release of peptides containing hydrophobic amino acids (Saha and Hayashi, 2001). A decrease in molecular weight could also lead to the partial loss of the gelling ability (Visessanguan and An, 2000). Among a number of treatments that focus on the modification of several molecular properties of proteins, the MR could be one of the most promising methods used to improve protein functionality, since it does not require the addition of objectionable chemical reagents, and thus additional cost. Several excellent general reviews concerning protein modification by the MR have been written (Oliver et al. 2006; Sanmartin et al. 2009; Oliveira, 2014), therefore the focus of this section is dedicated to muscle protein modification as pertinent to this thesis. Originally, glycation of myofibrillar proteins has been

studied (Brown et al. 1990; Syrovy and Hodny, 1992), with the purpose to investigate metabolic changes with aging and diabetes.

The first attempt to glycate carp (*Cyprinus carpio*) myofibrillar proteins for improving its functionality as a food material was performed by Saeki et al. (1997), who upon glycation of fish myofibrillar proteins with glucose (1:9, w/w ratio) in a dry-state, found an increase in solubility and emulsifying properties of neoglycoprotein at a high ionic strength. Table 2.1 summarises the major studies conducted to enhance the functionalities of muscle proteins. Saeki and Inoue (1997) also used 9-fold the amount of glucose over protein weight to make the myofibrillar protein of carp soluble in a low ionic strength (0.1 M NaCl) medium. The same effect was shown by Saeki and Tanabe (1999) in protein-glucose/ribose conjugates. An increase in solubility at low ionic strength (0.1 M NaCl) was suggested to be due to solubilization of myosin and the dissociation of myosin filaments in myofibrils (Tanabe and Saeki, 2001). To further explore this theory, Katayama et al. (2004) separately glycated two myosin subfragments referring to the globular head portion (subfragment-1 (S-1) and the long coil helical tail (rod). They reported that inhibition of myosin molecule self-assembly occurred as a result of the increase in negative charge repulsion among myosin molecules, also and due to the introduction of the glycosyl units onto the surface of the rod region of myosin. Katayama and Saeki (2007) supported these results and showed that myosin rods from carp and scallop (*Pecten yesoensis*) became soluble in 0.1 M NaCl (pH 7.5), where their filament-forming ability was weakened with the progress of glycation with glucose.

Table 2.1. Summary of the major studies on the effect of glycation through the Maillard reaction on muscle protein functionality.

Study	Protein	Carbohydrate	Reaction conditions			Findings
			Water activity	Temperature (˚C)	Duration	
Saeki (1997)	Carp myofibrillar proteins	Glucose	0.65	40, 50, 60	3-24 h	Neoglycoproteins showed higher solubility in 0.5 M NaCl, and its emulsifying properties were superior to unglycated protein.
Saeki and Inoue (1997)			0.4-0.65	40	0-48h	Myosin and actin became solubilized in low ionic strength (0.01-0.16 M NaCl) solution upon glycation at 1:9 protein:sugar ratio (w/w)
Saeki and Tanabe (1999)	Carp myofibrillar proteins	Glucose Ribose	0.65	60	0-8 h	Increased solubility of glycated protein in low ionic strength media. Glycation with ribose was more rapid at lower temperature.
Nakamura et al. (2005)	Scallop tropomyosin	Glucose, ribose, maltose, maltotriose	0.35	60	0-15 days	Enhanced allergenicity at the early stage of the Maillard reaction by glycation will all tested sugars, except maltotriose
Katayama and Saeki (2004)	Shellfish muscle proteins	Glucose	0.5-0.95	50	0-30 h	Marked increase in solubility upon conjugation at 1:18 protein to glucose ratio (w/w).
Yanagimoto et al. (1992)	Salmine (protamine)	Xylose	Aqueous solution	100	0-60 h	The antibacterial activity of glycated salmine against *Bacillus subtilis* increased at the beginning of the Maillard reaction. Gram-negative bacteria were not sensitive to glycated protein.
Nishimura et al. (2011)	Chicken myofibrillar proteins	Glucose, maltose	0.35	60	6 h	Improved solubility at low ionic strength medium (0.1 M), improved thermal stability at 1:6 protein:sugar ratio (w/w). Antioxidative function.
Wahyuni et al. (1998, 1999)	Fish sarcomplasmic proteins	Glucose, glucose-6-phosphate	0.65	60	0 to 12 h	Improved thermal stability and emulsifying properties upon glycation.
Sato et al. (2000, 2003,2005)	Fish myofibrillar proteins	Alginate oligosaccharide	0.35-0.65	40	0-120 h	Significant improvement in protein solubility in a low ionic strength medium (0.16 M).
Maitena et al. (2004)	Carp myosin	Alginate oligosacchride	0.35-0.4	40	0-48 h	Improved solubility at low ionic strength, at pI in particular. Improved thermal stability.
Takeda et al. (2007)	Salmon myofibrillar proteins	Alginate oligosacchride	0.05-0.95	60	0-3 h	Improved solubility by up to 40%. Maintained solubility after storage at -25 for 60-90 d. Suppressed protein denaturation during storage.
Fujiwara et al. (1998)	Carp myofibrillar proteins	Dextran	0.65	20-60	0-72 h	Improved thermal stability and emulsifying properties of glycated protein.
Tanaka et al. (1999)	Salmine (protamine)	Dextran	0.65	160-200	0-2 h	Increase in solubility during early stages of the Maillard reaction, while decrease in solubility during the advanced reaction stages. Improved antibacterial activity against Gram-negative bacteria (*Pseudomonas fluorescens* and *P.aeruginosa*).
Matsudomi et al. (1994)	Salmine (protamine)	Galactomannan	0.79	60	0 to 12 h	The emulsifying activity was six times and the emulsion stability of the conjugate more than 10 times higher than those of protamine. Slight decrease in bactericidal activity by conjugation.

The majority of the studies to produce neoglycoproteins from muscle were focused on improving the functionality of fish muscle protein, and less attention was devoted to muscle proteins from other sources. For instance, one study reported from Nishimura et al. (2011) incubated myofibrillar protein extracted from chicken muscle with glucose or maltose for 6 h at 60˚C in a dry-state. When the ratio of the weights of the protein and glucose or maltose had respectively reached 1:6 or 1:3-5, the solubility of each type of glycated protein in a 0.1 M NaCl was significantly improved. When the myofibril and maltose reaction was extended to 36 h, the glycated protein did not undergo denaturation when held at 50˚C for 2 h.

The combination of sarcoplasmic proteins extracted from blue marlin (*Makaira mazara)* and glucose-6-phosphate with suitable conjugation conditions can improve protein solubility. This is shown to be due to hydrophilicity of the covalently attached phosphate groups during the early stages of the MR (Wahyuni et al. 1998). At the same time glycation with glucose had less pronounced improvement in protein functionalities. A number of studies aiming to produce neoglycoconjugates from muscle proteins were performed in the presence of small molecular weight monosaccharides, which is possibly due to the fact that monosaccharides usually react faster than di-, oligo- or polysaccharides (Saeki, 2012). At the same time glycation with polysaccharides has also been explored; in particular, the effect of oligo- and polysaccharides attachment was shown to greatly improve emulsifying properties and protein stability against thermal denaturation. The schematic representation of a conjugation reaction and the formation of protein-galactomannan conjugates proposed by Kato (2002) is shown in Figure 2.3.

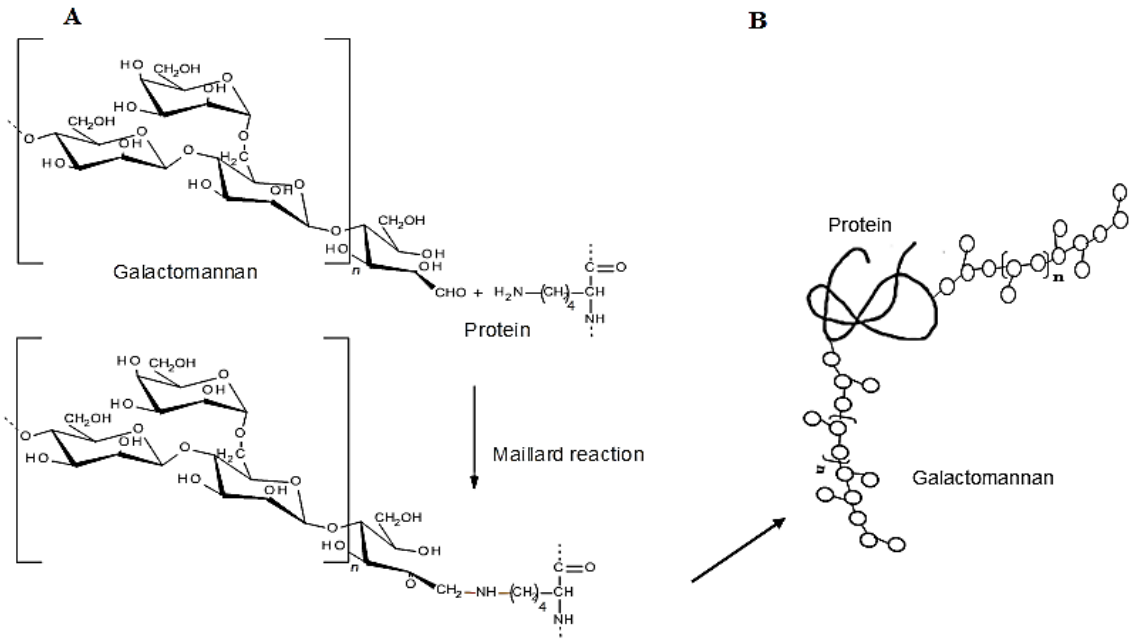

Figure 2.3. Schematic representation of the conjugation mode of polysaccharide with protein through the Maillard reaction (A) and the resulting protein-polysaccharide conjugate (B). The figure is reproduced from Kato (2002).

The protective effect exerted by polysaccharides is an important area of investigation, because myofibrillar proteins are susceptible to thermal denaturation or denaturation by freeze-drying (Saeki, 2012). Various kinds of protein have been shown to be stabilized by conjugation with dextran, chitosan, galactomannan and alginate oligosaccharide. Protein stabilization is likely due to the suppression of protein-protein aggregation by the glycosyl units, where an increase in the length of the attached glycosyl results in a higher thermal stability (Kato, 2002). Sato et al. (2000) prepared neoglycoprotein by conjugating alginate oligosaccharide (AO) with carp myofibrillar protein at 1:9 protein:oligosaccharide ratio (w/w) and reported a 20% increase in solubility at pH 7.5 within 4 h of glycation. In the study from the same research group (Sato et al. 2003), not only solubility, but also emulsifying properties and thermal stability of carp myofibrillar proteins were increased when conjugated with AO. When the total available lysine loss reached 17% (after 3 h) or 46% (after 48 h), both an increased solubility and acidic shift in

pI of protein were reported. Similar results on improved protein functionalities, solubility and thermal stability in particular, were later reported in carp myosin-AO (Maitena et al. 2004, Sato et al. 2005), salmon-AO (Takeda et al. 2007) and carp myofibrillar protein-dextran conjugates (Fujiwara et al. 1998). Matsudomi et al. (1994) reported that by conjugating a major protein of salmon and herring (salmine) with galactomannan, excellent emulsifying properties were attained. Similar results have been achieved by others, where emulsifying capabilities of salmine-dextran conjugates became 4 to 5 times greater than untreated protein during the early stage of the MR at 180 to 190˚C, yet were significantly decreased at the advanced MR stages (Tanaka et al. 1999). The mechanism proposed for the improvement of protein emulsifying properties by sugar conjugation, in particular with polysaccharides, is possibly due to the partial protein unfolding leading to the slight exposure of hydrophobic areas (Kato, 2002), which then can be adsorbed onto the surface of the oil droplets. At the same time, the hydrophilic sugar portion attracts water molecules leading to the establishment of highly solvated layers near the interface. This increases the repulsive forces between neighbouring oil droplets, and prevents coalescence (Evans, 2013).

2.4. Protein glycosylation by enzymatic approach

An alternative approach to modify the functionalities of proteins could be by using the catalytic power of enzymes. For instance, enzyme-mediated conjugation (glycosylation) may be useful for site-specific conjugation due to its strict substrate specificity and amenability to mild reaction conditions. Three types of enzymes could be considered to catalyze the glycosylation reaction: glycosyltransferases, glycosidases and transglutaminases (Colas et al. 1993). Glycosyltransferases (EC 2.4) are responsible for *in vivo* glycosylation reactions, but their utilization for *in vitro* applications is limited by the lack of commercially available enzymes

capable of direct catalytic reaction for the attachment of glycosyl residues to amino acid side chains. Strict specificity towards glycosyl donor and acceptor restricts their exploitation as a general method for modifying food proteins. Glucosidases (EC 3.2) use readily available donor substrates and have less specificity for acceptors. However, the use of glycosidases in synthesis is a process with two major limitations: the low transglycosylation yield and the product hydrolysis (Milosavic 2012). Transglutaminases, however, do not present those drawbacks. Transglutaminase (TGase; EC 2.3.1.13, protein-glutamine γ-glutaminyl-transferase) catalyzes the acyl-transfer reactions between a γ-carboxyamine group of a peptide- or proteins-bound glutamyl residue and a primary amino group of various substrates. TGase exhibits a higher specificity towards glutamine residues as the acyl donor and lower specificity towards the acyl acceptor, thus the ε-amino group of lysine as well as many primary amines and ammonia can act as substrates (Folk, 1969). In the absence of amine substrates, TGase catalyzes the hydrolysis of the γ-carboxyamide group of the glutaminyl residue, resulting in deamidation. When the ε-amino group of a peptide-bound lysyl residue is the substrate, peptide chains are covalently connected through ε-(γ-glutamyl)-lysine isopeptide bond (Kieliszek and Misiewicz, 2014). During each reaction one molecule of ammonia is generated. The first TGase, cytoplasmic TGase2, was identified in guinea pig liver almost 50 years ago (Sarkar et al. 1957), and since then TGases have been identified in different vertebrate and invertebrate animals (Noguchi et al. 2001), plants (Del Duca et al. 2000) and microorganisms (Ando et al. 1989). Industrial applications of animal TGases have been investigated (Traoré and Meunier, 1991; Oh et al., 1993), however not applied industrially. TGase separation and purification from animal sources is difficult, and make them costly and scarcely available and impractical at larger scale. In early 1980 a Ca^{2+}-independent TGase was obtained from the microorganism *Streptoverticillium mobaraense,* and since 2002

this source of TGase has a GRAS status (FDA 2002). Due to the possibility to achieve mass production of mTGAse by microbial fermentation at a low cost for industry, a large number of studies were designed on improvement of protein functionality, texture in particular (Kobayashi et al. 1998). In this regard majority of studies focused on the use of TGase for protein cross-linking, including actomyosin of turkey, beef and tilapia (Akamittath and Ball, 1992; Kim et al. 1993; Worratao et al. 2003), dairy (Jaros et al. 2006), egg yolk and white (Sakamoto et al. 1994, Lim et al. 1998), fish (Joseph et al. 1994) and wheat flour dough (Basman et al. 2002) and soy (Babiker, 2000) proteins. mTGase is also used to produce protein or composite edible films (Porta et al. 2011). The latest review on applications of TGase in food industry is from Kieliszek and Misiewicz (2014), and confirms a great interest and potential of this enzyme in successful food protein modifications. Less attention however has been paid to exploring TGase as a glycosylation agent. For instance, Colas et al. (1993) used TGase to covalently attach 6-aminohexyl-1-thio-β-D-galactopyranoside to glutamine residues performing the reaction at 37˚C. After full or partial blocking of lysines with toxic sodium cyanoborohydrate, 18 and 57 glycosyl units per mole of β-gliadins or legumin were incorporated. These corresponded to a degree of glycosylation of 15.7% for gliadins and 25.7 % for legumin. Glycosylaiton of both proteins resulted in increased solubility at their pI by up to 30%. The solubility of gliadin in the acidic pH range increased by 15-20% as compared to the non-treated protein. Fan et al. (2014) reported that mTGase effectively catalyzed the incorporation of collagen chains onto the chitosan backbone within 1 h at 37˚C. The introduction of collagen to chitosan increased the hydrophilicity of chitosan, enabling the production of a collagen-chitosan water-soluble derivative. Same authors have reported synthesized collagen-chitosan exhibits significant antioxidant activity cell viability, and have proposed it could be used for skin reparative and

pharmaceutical fields (Fan et al. 2014). When considering versatility, speed and efficiency of this enzymatic process, protein-protein and protein-sugar coupling could provide a promising technology for the new applications.

2.5. Aminosugars as glycating agents

In the previous section it was described that efficiency and outcomes of glycation dependent on the type of the saccharide used. There are several aminosugars, including 2-amino-2-deoxy-D-mannose, 2-amino-2-deoxy-D-galactose and 2-amino-2-deoxy-D-glucose that could have a potential to be incorporated into the protein. Since, GlcN is the most available amino sugar which also reported to have a nutraceutical application it was chosen in this study as a glycating agent.

2.5.1. Glucosamine production

Glucosamine (chitosamine) is an aminosaccharide that occurs in acetylated and polymerized forms of chitin, a poly-beta-1,4-*N*-acetylglucosamine (GlcNAc). Chitin occurs in a wide variety of species, from invertebrates to fungi and microorganisms. Arthropod shells (exoskeletons) are the most easily accessible sources and contain 20-50% chitin on a dry weight basis. From a practical viewpoint, shells of crustaceans, such as crabs and shrimps, are conveniently available as wastes from seafood processing industries, and are used for the commercial production of chitin (Kurita, 2001). Other potential sources for chitin production include krill, insects, clams, oysters, fungi and some microorganisms (i.e. *Aspergillus niger*). Antarctic krill (*Euphausia superba*) is likely to be the most promising source in the future; the potential annual catch of this crustacean is as high as 100 mt, which can yield about 2.0 mt of chitin (Venugopal, 2011).

Chitin is water insoluble due to its intermolecular hydrogen bonds (Pillai et al. 2009). Chitosan, chitin-derivative soluble in aqueous dilute acids can be obtained by deacetylation using 40-50%

aqueous alkali at 100-160˚C for a few hours. Depending on the reaction conditions, the degree of deacetylation usually varies from 70 to 95% (Hussain et al., 2013).

GlcN is obtained from chitin by a hydrolysis where crude chitin is deacetylated and depolymerized to GlcN hydrochloride in the presence of hydrochloric acid solution. The hydrolysis procedure varies slightly, but in general is performed with concentrated HCl at 90-100˚C for 1 to 2 h (Sibi et al. 2013). D-glucosamine hydrochloride has a faintly sweet, slightly astringent taste. When used in beverages, for instance, a minimal effect on taste was reported (Kralovec and Barrow, 2008).

2.5.2. GlcN application: supplements against arthritis

D-Glucosamine is the biochemical precursor of most nitrogen-containing sugars in humans and is found naturally in the form of glucosamine-6-phosphate (Roseman, 2001). One hypothesis is that nutritional supplementation with GlcN would provide the symptomatic relief for osteoarthritis was developed more than 30 years ago by D`Ambrosio et al. (1981). Now, GlcN preparations are a popular non-vitamin, non-mineral dietary supplement commonly used to prevent and treat joint pain and osteoarthritis in humans (Weimer et al. 2014), and are taken at a suggested dose of 1.5 g daily (Navarro et al. 2015). Commercially available products in the GlcN market include GlcN·HCl, GlcN·SO_4, *N*-acetyl-GlcN and GlcN-chondroitin sulfate formulation. GlcN·SO_4 products have generally been more popular in Europe, whereas GlcN·HCl products have dominated North America. When these preparations enter the stomach, an acidic environment representing normally pH 2.5, both salts dissociate completely and the aminosugar component is identical (Block et al. 2010). The popularity of the sulphate formulation was originally due to claims that the sulfate anion can stimulate synthesis of the chondroitin sulphate (van der Kraan et al. 1988, Cordoba and Nimni, 2003). This assumption was later found to have

conflicting results (Qu et al. 2007; Block et al. 2010). Regardless, due to inconclusive randomized control trials its effectiveness on joint pain and function is highly debated (Jordan et al. 2003; Zhang et al. 2008). Despite this, it is still among the most commonly used supplement by older adults in both the US and Europe (Griffith et al. 2012). The growing geriatric population is expected to continue boosting global sales of glucosamine supplements. Global sales of GlcN supplements reached almost $2 billion in 2008, which represents an increase of about 60% compared with 2003, with anticipated growth through 2013 reaching $2.3 billion (Heller, 2009). Global GlcN demand was 23,208.0 metric tons in 2013 and is expected to reach 57.868.8 metric tons by 2020 (US Market research report, 2014). In terms of regulations, Health Canada defines GlcN formulations as dietary supplements, known also natural health product (NHP). In the United States, GlcN formulations are not approved by the Food and Drug Administration (FDA) for medical use in humans and are classified as a dietary supplement (Hubbard, 2012). In Australia, GlcN are registered as dietary supplements rather than prescription medications, as in the European Union (Burdett and McNeil, 2012).

2.5.3. Hexosamine biosynthesis pathway (HBP)

Physiologically amino sugars are synthesized through the metabolic pathway called the hexosamine biosynthesis pathway (HBP), consuming 2-5% of glucose (Figure 2.4). Upon entering the cell through the action of glucose transporters (GLUT) (Vigetti et al. 2014) glucose is converted to glucose-6-phosphate (G-6-P), which is then transformed to fructose-6-phosphate by the enzyme glucose-6-phosphate isomerase (F-6-P). F-6-P is further converted to glucosamine-6-phosphate (GlcN-6-P) by the rate-limiting enzyme glutamine:fructose-6-phospahte aminotransferase (GFAT), which uses glutamine as an amino donor. Besides this endogenous production, GlcN provided exogenously can be actively transported from the

extracellular tissue into the cells by glucose transporters; insulin facilitates this GlcN transport into cells (Heart et al. 2000). In the cell, GlcN is directly phosphorylated by hexokinase (HK) yielding GlcN-6-P, thus by-passing the rate limiting aforementioned pathway. In the next steps, GlcN-6-P is acetylated to N-acetylglucosamine-6-P (GlcNAc-6-P) from acetyl-CoA catalyzed by GlcN-P-N-acetyltransferase. At this point, exogenous GlcNAc, which comes into the cell through bulk endocytosis and is phosphorylated by the salvage pathway enzyme *N*-acetylglucosamine kinase (NAGK), can also enter the hexosamine pathway (Wellen et al. 2010). GlcNAc-6-P is further converted to GlcNAc-1-P by phosphoacetylglucosamine mutase. GlcNAc-1-P is then transformed into uridine diphosphate-*N*-GlcNAc (UDP-GlcNAc) by the action of UDP-*N*-GlcNAc pyrophosphorylase. UDP-GlcNAc is the precursor for all other amino sugars that are necessary for the biosynthesis of glycoproteins, glycolipids, and proteoglycans (Schleicher and Weigert, 2000; Salazar et al. 2014).

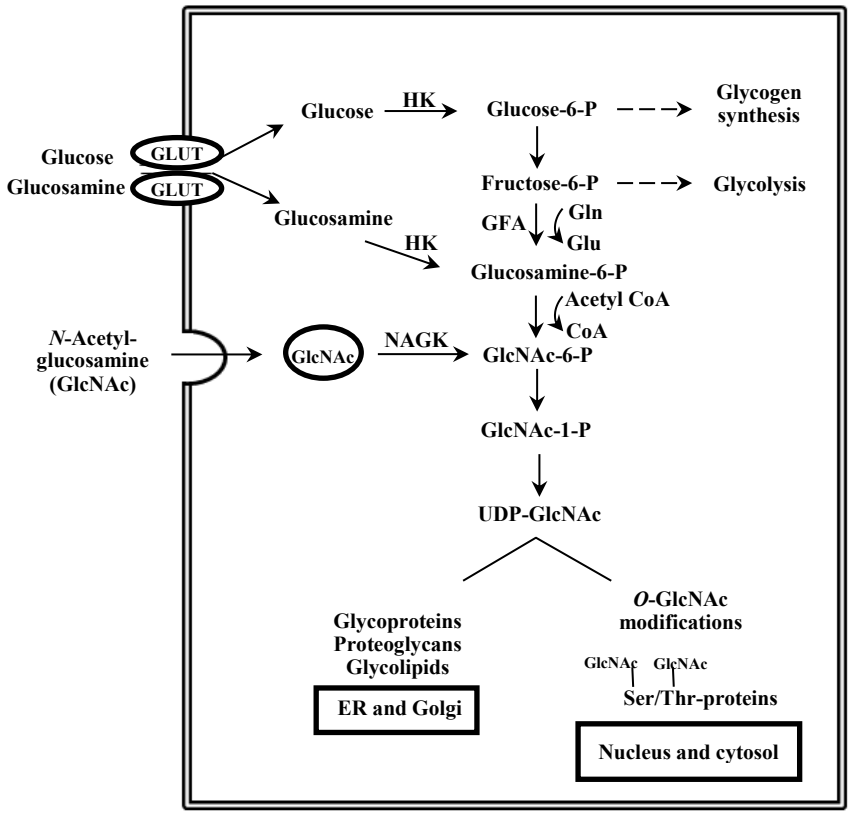

Figure 2.4. A simplified schematic representation of hexosamine biosynthesis pathway (HBP). Glucosamine and N-acetyl-glucosamine are endogenously synthesized from glucose via HBP or may be obtained exogenously from supplements. HK: hexokinase; GlcNAc: N-acetyl-glucosamine; NAGK: N-acetylglucosamine kinase; GFAT: glucosamine fructose-6-phosphate aminotransferase; GlcNAc-6-P: N-acetyl-glucosamine-6-phosphate; GlcNAc-1-P: N-acetyl-glucosamine-1-phosphate; UDP-GlcNAc: uridine diphosphate (UDP)-N-acetyl-glucosamine.

In the early work of Kohn et al. (1961) the metabolism of GlcN, GlcNAc and Glc was studied in normal rats that were deprived of food. The purpose was to understand their comparative rates of oxidation, conversion to liver glycogen, incorporation GlcN into macromolecular liver components, and excretion in the urine. This study reported that GlcN was not extensively oxidized to CO_2 or converted to liver glycogen and a considerable amount was excreted in the urine. The remaining portion of GlcN was suggested to be incorporated into glycoproteins or mucopolysaccharides (GAGs). Glc was demonstrated to serve as a poor precursor of protein-bound GlcN, but was readily converted to liver glycogen and oxidized to CO_2. GlcNAc

metabolism was intermediate between Glc and GlcN in oxidation, incorporation into macromolecules and excretion.

In humans the endogenous production of GlcN is in the range of 4-20 g/day or 12 g/day (Vosseler et al. 2002; Wells et al. 2003), and the amount of GlcN found in a healthy human serum is around 0.04 mmol/L. GlcN supplements are usually taken orally and in humans are 90% is absorbed. Humans with daily GlcN intake of 23.1 mg/kg of body weight achieve GlcN serum level of around 0.06 mmol/L (Anderson et al. 2005).

2.5.4. Glucosamine stability: autocondensation products

Numerous studies have investigated the effectiveness of oral doses of GlcN alone or in combination with chondroitin in treating osteoarthritis. However, none of these studies have considered whether it is the GlcN itself and/or one or more of its autocondensation products which exerts this effect. Previous studies (Candiano et al. 1988, Zhang et al. 2004) showed that GlcN can not only glycate protein, but also undergo autocondensation under simulated physiological conditions (37°C, pH 7.4) *in vitro*. A major product of GlcN autocondensation was 2,5-bis(tetrahydroxybutyl)pyrazine (dihydroxyfrtuctosazine) (Figure 2.5). Kashige et al. (1995) described that dehydrochlorinated product of GlcN showed greater DNA breaking activity than the original GlcN·HCl, mainly attributed to the dihydroxyfructsazine generated by the condensation of two GlcN molecules. In connection to this, the diverse reaction with GlcN during *in vitro* incubation and thus its instability, indicate a need for further understanding of GlcN rearrangement products. This is especially true when higher reaction temperatures may be involved.

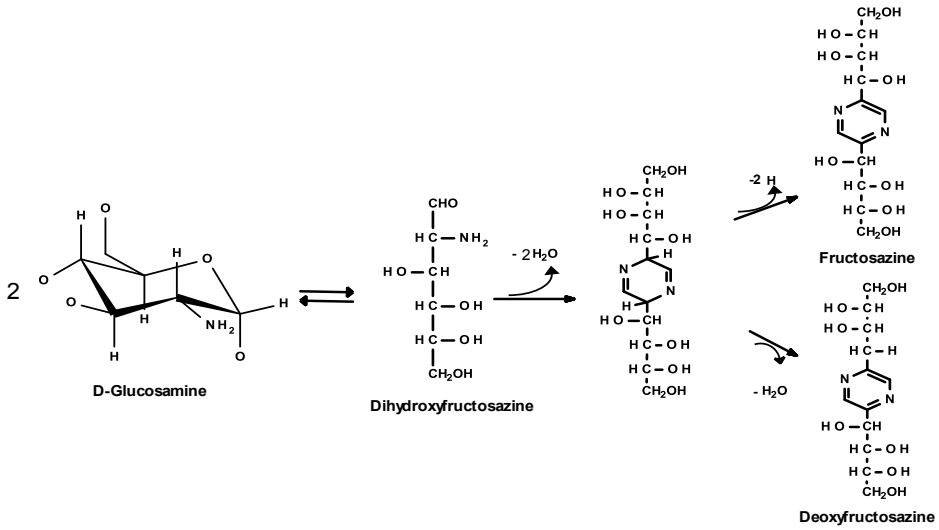

Figure 2.5. Formation of dihydroxyfructosazine, fructosazine and deoxyfructosazine from D-glucosamine. The structures are reproduced from Kashige et al. (1995).

2.5.5. GlcN as a potential food ingredient

As mentioned before for North America and US, GlcN is regulated as a dietary supplement. Nevertheless, in the past several companies have attempted to use GlcN as a food ingredient. For instance, SoBeSport System line from Pepsi is a GlcN-containing drink. Coca-Cola and Procter@Gamble also produced a GlcN-containing drink called "Elations". Other GlcN-containing drinks are available, including Super Glucosamine and Glucosamine Drink Mix from Action-Labs, Logic Juice4Joints from the Health Company in United Kingdom, and Joint Juice in US. GlcN extracted from *Aspergillus niger* (Regenasure brand) from Cargill Inc. was approved to market as a novel ingredient in fruit juices and "smoothies", soft drinks, fermented milk-based products, dried beverage mixtures and sports drinks at 750 mg/per daily serving (EFSA, 2009). However, in the US, GlcN does not have a GRAS status and thus cannot be used in foods and beverages. Though GlcN-containing beverages are sold as supplements the FDA has become concerning about defining these drinks as supplements and has been targeting these products. The main reason why GlcN is not GRAS approved is there have been no clinical

studies proving GlcN consumption is safe in young children, pregnant woman and diabetics (Kralovec and Barrow, 2008).

In addition, the Federal Institute for Risk Assessment in Germany showed that food supplements containing GlcN pose a health risk for patients taking anticoagulants, since GlcN can amplify the anti-blood clotting effects of drugs and lead to haemorrhages (BfR, 2012). According to the same authorities, diabetics and/or individuals with impaired glucose tolerance may have a health risks associated with GlcN supplements (BfR, 2012).

Regardless, due to the consistent increasing popularity of GlcN supplements, the food industry is trying to produce novel GlcN-enriched foods. Uzzan et al. (2007) prepared milk based dietary supplements by enriching fat-free milk with 6.25 mg/mL GlcN hydrochloride (equivalent to 750 mg/serving). Preliminary trials with GlcN revealed that heating at 100˚C or higher caused destabilization of the milk proteins, expressed by aggregation and precipitation of milk proteins in the heat exchanger. Yet, heating at 80˚C or lower did not destabilize proteins when held for 2 min. When processed in milk beverage at a pH of around 6.5, GlcN was found to be very labile. The nutraceutical manufacturer suggests that the pH should be lowered to approximately 4.5.

In addition, GlcN and its derivatives, deoxyfructosazines (DF), were also found in tobacco and anticipated to be precursors of toxicants in smoke and at the same time influencing sensory properties of the cigarettes. For instance, after analyses of different tobacco types Moldoveanu et al. (2011) found between 0 to 608 mg/kg and 26 to 1886 mg/kg of 2,5-DF and GlcN, respectively. The source of GlcN and 2,5-DF was due to presence of fructose and ammonia which reacted to form GlcN, which further condensed to produce fructosazines.

2.5.6. Glycation as a promising tool for protein functionality improvement

Positive results described in this literature review may infer that glycation with the aid of the MR could be a promising technique to increase the value of muscle protein isolates. Along with natural occurrence without need to add toxic compounds, glycation improves functional properties of protein. At the same time, more studies are needed to be conducted to assess the industrial scale-up opportunities for proteins glycated via the MR. If production of neoglycoproteins via the MR proved industrially feasible this new product could be considered as a "novel food". Indeed, this should be subjected to further testing to ensure safety for human consumption (Sanmartin et al. 2009). In consideration of the disputable issues of beneficial and unfavourable effects of the MR, AGEs in particular, more studies are needed to investigate the physiological fate of such modified food proteins. The details regarding proteolysis during digestion and the absorption of modified amino acid derivatives (Henle et al. 1996) are among a few questions to be studied.

CHAPTER 3. Non-enzymatic glycosylation of natural actomyosin (NAM) with glucosamine in a liquid system at moderate temperatures.

3.1. Introduction

The functional behaviour of proteins is one of the most important aspects which determines their technological usability, described in terms of solubility, emulsification others. As this functionality is vital in food processing, many efforts have been made to develop new food ingredients with improved properties. Among the number of studies on functionality improvement, non-enzymatic glycation, so-called Maillard reaction, has received much attention as a natural way to produce glycoconjugates with upgraded functional properties. The Maillard reaction is initiated by the interaction between the free amino groups in protein and carbonyl groups of a reducing sugar to produce an imine (Schiff base) (Dutta et al. 2006). This adduct further rearranges into the Amadori product which, upon dehydration and rearrangements, forms highly reactive deoxyosones - potent precursors of protein cross-links (Elgawish et al. 1996). Advanced glycation end products (AGEs), generated at the late stages of the Maillard reaction, are affiliated with diabetic complications and other diseases (Hsu and Zimmer, 2010).

The Maillard reaction, as a tool for glycation, was reported to be superior to other systems, since no objectionable chemical reagents are required for the reaction to proceed (Saeki, 2012). For instance, the solubility of scallop (Katayama et al. 2002) and chicken myofibrillar proteins (Nishimura et al. 2011) were highly improved with the progress of the Maillard reaction. In addition, emulsifying properties (Shu et al. 1998) and thermal stability (Fujiwara et al. 1998) of different proteins have also been upgraded via glycation.

The usual preparation of protein-carbohydrate complexes by Maillard reaction involves dry heating and storage of the lyophilized mixtures from 1 to 3 weeks (Zhu et al. 2008). Despite substantial evidence of functionality improvement by glycation in a dry conditions, its

application in food technology is limited. The limitations are attributed to difficulties in controlling the extent of glycation, uneven distribution of reactants (Kato, 2002), long reaction time (Zhu et al. 2008), possible protein denaturation (French et al. 2002), undesirable color changes (Tanaka et al.1999) and formation of antinutritional compounds (Brands et al. 2000). In view of the drawbacks of current glycation techniques, no feasible industrial scale up method is available, thus no commercially produced conjugate ingredients have been obtained (Zhuo et al. 2013).

Water activity (a_w) of the reaction mixture plays an important role in the rate of numerous Maillard reaction pathways, as it is responsible for molecular mobility, protein conformation, surface area and accessibility of reactive amino groups in protein (Oliver, 2011). In a recent study (Qi et al. 2010) attempting to overcome drawbacks of glycation in dry conditions, acid precipitated soya protein-dextran conjugates were prepared in a 80% or 95% ethanol-reacting system at 50˚C for 6 h or 60˚C for 24 h, respectively. Zhu et al. (2008) also reported formation of whey protein-dextran complexes in a liquid medium at 60˚C for 24 h.

The main myofibrillar proteins, myosin and actin are the most important muscle proteins for technological purposes. Actomyosin, the main state of actin and myosin in *post-mortem* muscle, is accepted to be an unstable heat sensitive molecule (Jacobson and Henderson, 1973). Correspondingly, moderate temperature of reaction is an essential factor for actomyosin glycation. According to previous reports, if elevated temperatures and advance stages of reaction are used during protein glycation in solution, protein denaturation and polymerisation are likely to occur (Igaki et al. 1990). Therefore, there is a strong need to establish a method suitable for glycation of muscle proteins in wet conditions. Concurrently with water activity, the nature of reducing sugars considerably influences the reaction rate and consequently protein functionality

(Oliver, 2011). The reactivity of reducing sugars in the Maillard reaction has been reported to increase with decreasing molecular weight (Jouppila, 2006).

Glucosamine (GlcN) is an amino sugar that is important for the biosynthesis of glycated proteins and lipids. It is a major constituent of glycosaminoglycans and glycolipids, important for the structure and function of cartilage in the joints of human body (Henrotin et al. 2012). Thus, it is widely applied as a dietary supplement for osteoarthritis treatment. Glucosamine is mainly obtained by acid hydrolysis of chitin, the second most abundant polymer in nature and a major component of insect exoskeletons, crustacean shells and fungal cell walls (Jalal et al. 2012). Kraehenbuehl et al. (2008) reported higher reactivity of GlcN as compared to fructose, galactose, glucose or xylose when reacting with cysteine at 125˚C for 25 min. If such a fast reactivity occurs during glycation it would be expected to increase the rate of the reaction and avoid usage of elevated reaction temperatures. Taking into account that GlcN possesses amino and hydrophilic hydroxyl groups (Chung et al. 2006), its incorporation into actomyosin could be a practical strategy to improve muscle protein functionality. Therefore, the aim of this study is to demonstrate the possibility of actomyosin glycation with GlcN by Maillard reaction in a liquid medium at moderate temperatures, with faster reaction rates, and to investigate its contribution to functionality mediated by glycoproteins.

3.2. Material and Methods

3.2.1. Materials

Fresh chicken breast was obtained from the local store. Analytical grade D-(+)-Glucosamine hydrochloride, D-(+)-Glucose (Glc), L-Lysine, potassium phosphate monobasic and dibasic were purchased from Sigma-Aldrich (St. Louis, MO, USA). Other chemicals and reagents used were

of analytical grade. All buffers were prepared with Milli-Q purified distilled water (Millipore, Bedford, MA, USA).

3.2.2. Extraction of Natural Actomyosin (NAM)

Actomyosin from chicken *Pectoralis major* was extracted according to the method described by Benjakul, Visessanguan, Ishizaki and Tanaka (2001) with slight modifications. Briefly, chicken breast muscle (fresh or frozen) was homogenised in chilled 0.6 M KCl at 1:10 (w/v) for 2 min in a homogeniser (Fisher Scientific, Power Gen 1000 S1, Schwerte, Germany). Homogenate was centrifuged at 5000*g* for 40 min at 4˚C using Avanti® J-E refrigerated centrifuge (Beckman Coulter Inc., Palo Alto, CA, USA). Three volumes of chilled deionized water were added to precipitate NAM. After centrifugation at 5000*g* for 30 min at 4˚C the pellet was re-suspended in chilled 50 mM potassium phosphate buffer solution (PBS) (pH 7.5) containing 0.5 M KCl. The precipitate was collected by centrifugation at 5000*g* for 10 min at 4˚C. The pellet from the final centrifugation step is hereafter called "natural actomyosin" or NAM.

3.2.3. Glycation of Natural Actomyosin (NAM)

Experimental design for NAM glycation is presented in Figure 3.1. As follows, mixtures of NAM and sugars (Glc or GlcN) in ratios of 1:1, 1:3 and 1:6 (w/w) were dissolved in 50 mM PBS (pH 7.5) in the presence of 0.5 M KCl. The pH values of the solutions were adjusted by careful addition of 0.1 M HCl or 0.1 M KOH. The aliquots of the solutions were incubated in an Innova 44 (New Brunswick Scientific, USA) shaker under constant agitation. After incubation unreacted carbohydrate moieties were removed by ultrafiltration employing Amicon Ultra 3K membrane (molecular weight cut-off of 3.000 NMWL; Millipore Corporation, Bedford, MA, USA). To study the effect of different reaction temperatures, NAM-Glc and NAM-GlcN solutions at different ratios were heated at 25, 37 and 40˚C from 0 to 12 h. To elucidate the effect of different

protein to sugar ratios NAM-Glc and NAM-GlcN solutions were incubated at different temperatures with samples withdrawn every 2 hours of reaction. At least three individual reaction conditions were performed.

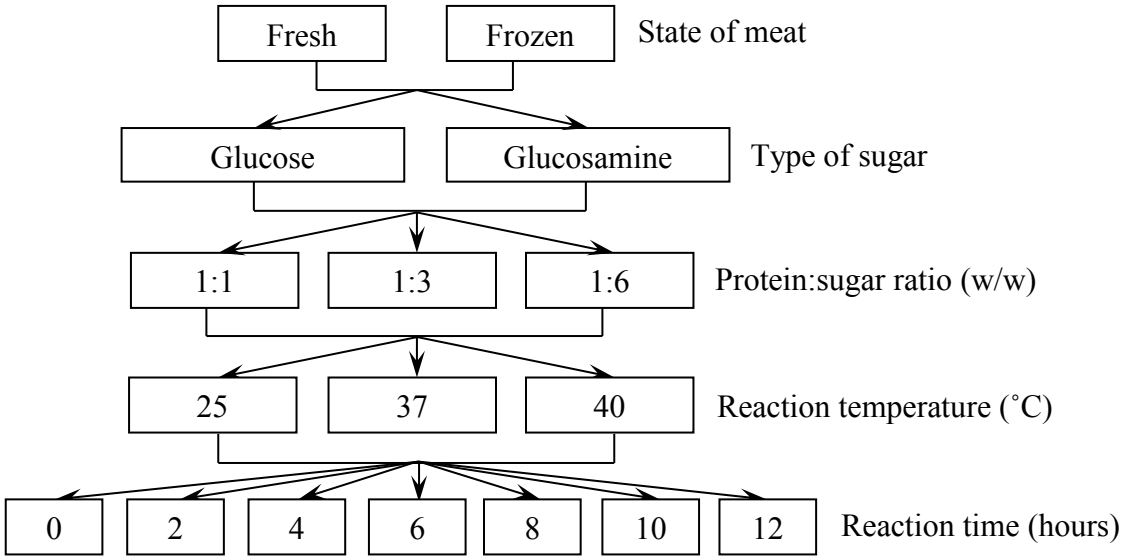

Figure 3.1. Experimental variables for actomyosin conjugation with different sugars via the Maillard reaction in a liquid system.

3.2.4. Assessment of the Maillard reaction evolution by UV-Vis spectroscopy

To confirm glycation occurrence and assess the extent of the Maillard reaction, UV-Vis spectroscopy analyses were performed. Glycated proteins in 50 mM PBS (pH 7.5) in presence of 0.5 M KCl were analyzed using a spectrophotometer (Beckman Instruments, Fullerton, CA, USA). The samples were diluted 11 times, loaded into 96-well microplate (200 μL) and scanned from 280 to 500 nm. Glc or GlcN solutions were analyzed under the same conditions.

3.2.5. Protein oxidation measurement

Determination of carbonyl level in proteins is used as an index of the extent of protein oxidative damage. Content of carbonyl groups in NAM extracted from fresh or frozen chicken breast were detected by reactivity with 2,4-dinitrophenylhydrazine (DNPH) to form protein hydrazones

according to Chan et al. (2011). NAM solutions were diluted to a protein concentration ranging from 0.7 to 1.0 mg/mL and precipitated with 10% TCA (w/v). After centrifugation (2000*g*, 10 min, 4˚C) the blank was treated with 4 mL of 2 M HCl and the test samples (pellet) with 4 mL of 0.2% DNPH (w/v) in 2 M HCl. The tubes were incubated for one hour at 25˚C in the dark with agitation every 10 min. After precipitation with 10% TCA, the solutions were further centrifuged to collect the protein precipitates. Next, the pellet was washed 2 times with 1 mL of ethanol-ethyl acetate (1:1, v/v), precipitated with 10% TCA and centrifuged. The final precipitate was dissolved in 2 mL 6 M guanidine hydrochloride in 20 mM potassium PBS (pH 6.5). Carbonyl group content was determined spectrophotometrically (V-530, Jasco Corporation, Tokyo, Japan) at a wavelength of 365 nm for the DNPH-treated samples against an HCl control. Protein concentration was calculated from the absorbance at 280 nm in the HCl control using a standard bovine serum albumin (BSA) in guanidine. The carbonylation level was calculated using absorption coefficient of 22,000 $M^{-1}cm^{-1}$ for protein hydrazones and expressed as nmol of DNPH fixed/mg of protein.

3.2.6. Evaluation of protein solubility

The solubility of glycated and control samples was determined according to the method of Montero et al. (2008). One mL of each sample or control solution was added to glass test tubes and the pH was adjusted to end points ranging from 2.0 to 12.0. The final volume was then attuned to 2 mL with distilled water having the same pH as the sample solution. After centrifugation (9000*g* for 15 min at 4°C) protein content of the clear supernatant and original suspension was determined according to the Biuret assay (Gornall et al. 1949) using BSA as a reference protein. The solubility of glycated and control NAM was expressed as the percent of the protein in the supernatant to that of the protein solution before centrifugation. The ionic

strength post-ultrafiltration was calculated for glycated samples using a conductivity meter (Oakton Acorn CON 6, Vernon Hills, IL, USA) calibrated prior to the measurements. Thereafter, the ionic strength of the samples set was adjusted to 0.5 M KCl.

3.2.7. Study in a model lysine-glucosamine system

For the purpose of the study in the model system, mixture of GlcN and Lysine (Lys) at 1:3 (w/w) ratio in a 50 mM PBS was incubated at 40˚C under constant agitation. After predetermined heating time (0, 2 and 8 hours) obtained samples were immersed in ice for rapid cooling. Aliquots were further analysed by Orbitrap-LC-MS. Solutions of GlcN separately were prepared, incubated and analysed at the same conditions as described above.

3.2.7.1. LC-MS analyses

Mixture of Lys-GlcN obtained from different incubation times were dissolved in aqueous 25% (v/v) acetonitrile and 0.2% (v/v) formic acid. Nanoflow HPLC (Easy-nLC II, Thermo Scientific) coupled to the LTQ XL-Orbitrap hybrid mass spectrometer (Thermo Scientific, Bremen, Germany) was used to resolve and analyse the samples. Nanoflow chromatography and electrospray ionization were accomplished by using a PicoFrit fused silica capillary column (ProteoPepII, C18) with 100µm inner diameter (300Å, 5µm, New Objective). Samples solutions were injected onto the column at a flow rate of 3000 nL/min and resolved at 500 nL/min using 30 min linear ACN gradients from 5 to 50% v/v aqueous ACN in 0.2% v/v formic acid. The mass spectrometer was operated in data-dependent acquisition mode, recording high-accuracy and high-resolution survey Orbitrap spectra using external mass calibration, with a resolution of 60000 and m/z range of 100-2000. Ten most intense multiply charged ions were sequentially fragmented by using collision induced dissociation, and spectra of their fragments were recorded

in the linear ion trap; after two fragmentations all precursors selected for dissociation were dynamically excluded for 60 s.

3.2.7.2. Detection of ammonia (NH_3)

To verify the release of NH_3 in the course of Lys glycation with GlcN, the mixture of GlcN and Lys at 1:3 (w/w) ratio in a 50 mM PBS was incubated at 40˚C for 0, 2 and 8 hours under constant agitation. The NH_3 concentration of the produced conjugates was measured immediately with the commercial ammonia quantitative determination kit (Sigma, St. Louis, MO, USA), according to the manufacturer's instructions. The assay is based on the following reaction: NH_3 reacts with α-ketoglutaric acid (KGA) and reduced nicotinamide adenine dinucleotide phosphate (NADPH) in the presence of the L-glutamate dehydrogenase (GDH) to form L-glutamate and oxidized nicotinamide adenine dinucleotide phosphate ($NADP^+$).

$$KGA + NH_4^+ + NADPH \xrightarrow{GDH} L\text{-}Glutamate + NADP^+ + H_2O$$

The oxidation of NADPH to $NADP^+$ results in a decrease in the absorbance at 340 nm that is proportional to the concentration of NH_3.

3.2.8. Sample pre-treatment and digestion prior to matrix-assisted laser desorption/ionization time-of-flight mass spectrometry (MALDI-TOF/TOF-MS) analyses

Control and glycated samples were diluted in a ratio of 1:1 with sample buffer containing 5% β-mercaptoethanol. After heating for 5 min (Thermomixer R, Eppendorf North America, Westbury, NY), 20 µL of the sample was loaded on 4-20% Mini-PROTEAN TGX precast gel (Bio-Rad Laboratories, Inc., Hercules, CA). After running in a Mini-PROTEAN tetra cell attached to a PowerPac Basic electrophoresis apparatus (Bio-Rad Laboratories Inc., 1000 Alfred Nobel Drive, Hercules, CA, USA) samples were stained with Coomassie Brilliant Blue. Afterward, excised gels were reduced with 10 mM β-mercaptoethanol, alkylated with 50 mM

iodoacetamide, washed with 100 mM ammonium bicarbonate/acetonitrile (1:1, v/v) solution and dried in a SpeedVac (AES 2000, Savant Instruments Inc., Farmingdale, NY, USA). Dried gel bands were subjected to overnight proteolytic digestion at 37˚C with 0.2 μg of trypsin. After incubation, peptides were extracted with 30 μL of 100 mM ammonium bicarbonate followed by extraction with 30 μL solution containing 5% formic acid and 50% acetonitrile in water twice and dried to ~15 μL in a SpeedVac.

3.2.9. Evaluation of glycoconjugation by MALDI-TOF/TOF-MS

With the aim of knowing the relative amount of carbohydrates linked covalently to NAM, MALDI-TOF/TOF-MS analyses were carried out. For this purpose, the samples (obtained as described in the section above) were diluted tenfold in 50% acetonitrile/water + 0.1% trifluoroacetic acid. One μL of each sample was mixed with one μL of α-cyano-4-hydroxycinnamic acid (4-HCCA, 10 mg/mL in 50% acetonitrile/water + 0.1% trifluoroacetic acid). One μL of the sample/matrix solution was then spotted onto a stainless steel target plate and allowed to air dry. All mass spectra were obtained using a Bruker Ultraflex MALDI-TOF/TOF-MS (Bruker Daltonic GmbH, Bremen, Germany). Ions were analyzed in positive mode after acceleration from the ion source by 25 kV. External calibration was performed by use of a standard peptide mixture.

3.2.10. Emulsifying activity index (EAI) and emulsion stability index (ESI)

The measurements of emulsifying activity and stability indexes were conducted according to the method described by Moure et al. (2002) with slight modifications. 3 mL of protein solution (2 mg/mL in 50 mM PBS (pH 7.5), containing 0.5 M KCl) was added to 1.0 mL of corn oil. The mixture was homogenised by using Power Gen 1000 S1 homogeniser (Fisher Scientific, Schwerte, Germany) operated for 1 min at setting 3. Immediately after homogenization, 0.05 mL

of emulsion was diluted to 5 mL with 0.1% sodium dodecyl sulphate (SDS) solution and the absorbance of the sample was measured at 500 nm against 0.1% (w/w) SDS solution blank using a spectrophotometer (V-530, Jasco Corporation, Tokyo, Japan). The effect of pH on EAI was determined by careful pH adjustment to 3.0 or 10.0 with a set of KOH and HCl of different concentrations.

The EAI was calculated from the following equation:

$EAI = 2.33 \times A_0$

where A_0 is the absorbance estimated just after emulsion preparation. The emulsion stability index was determined by measuring the absorbance of these emulsions after 10 min of standing. The ESI was calculated as follows:

$ESI = 10 \times [A_0/(A_0 - A_{10})]$,

where A_{10} is the absorbance determined after 10 min.

3.2.11. Data analyses

The experiment was replicated at least three times. All the data were expressed as means ± standard deviation. Significance of difference was determined by analysis of variance (ANOVA) using statistical analysis system computer software (SAS, Version 9.0, NC, USA). Means were compared using Tukey's adjustment at the 95% confidence interval.

The results from UV-Vis spectra were analyzed by using bidimensional hierarchical clustering analyses (heat map) performed within the programming and visualisation environment R version 2.10.1. (Ihaka and Gentleman, 1996). The heat map was developed based on 126 samples (average from 3 repetitions) × 40 wavelength values for fresh and frozen NAM separately. In the graph each column represented a wavelength, each row represented a different glycation treatment and the color of each square corresponded to the magnitude of absorbance values, with

green representing higher values and red representing lower values. The raw data underwent a Z-score transformation with the cells colored accordingly:

$$Z = \frac{\text{Observed value - Average}}{\text{Standard deviation}}$$

3.3. Results and discussion

3.3.1. UV-Vis absorbance spectrum

In the current study Maillard-type carbohydrate-protein conjugates were produced by the reaction between free amino groups of NAM and carbonyl groups of Glc or GlcN. The extent of protein glycation is an important factor in the beneficial and detrimental effects on protein functionality (Oliver et al. 2006). Hence, this study focused on determining the best conditions to achieve high yields of conjugation, along with avoiding protein polymerization and minimizing the formation of undesirable reaction side products. To achieve this objective the study was designed as depicted in Figure 3.1. Buffered solutions of NAM/Glc or NAM/GlcN at different protein to sugar ratios (1:1; 1:3 or 1:6) were incubated at 25, 37 or 40˚C with aliquots collected at different time intervals. The progress of reaction over time was monitored with UV-Vis spectroscopy. Typical spectra obtained for NAM-GlcN and NAM-Glc conjugates are shown in Figure 3.2 A and B, respectively. Due the large number of variables not all spectra are presented, however the results from all spectra are summarised in a heat map (described in the following part of this chapter).

UV-Vis absorption spectra profiles demonstrated that the rate of Maillard reaction products formation was dependent on the type of sugar, its concentration, reaction time and temperature. The absorbance values at 280-320 nm (Zhu et al. 2008) obtained from NAM-GlcN conjugates were higher as compared to those of NAM-Glc. Increase in the amount of sugar in the reaction

mixture also resulted in increases of the absorbance values at 280-320 nm. Continuous rise of absorbance values was observed as heating time increased.

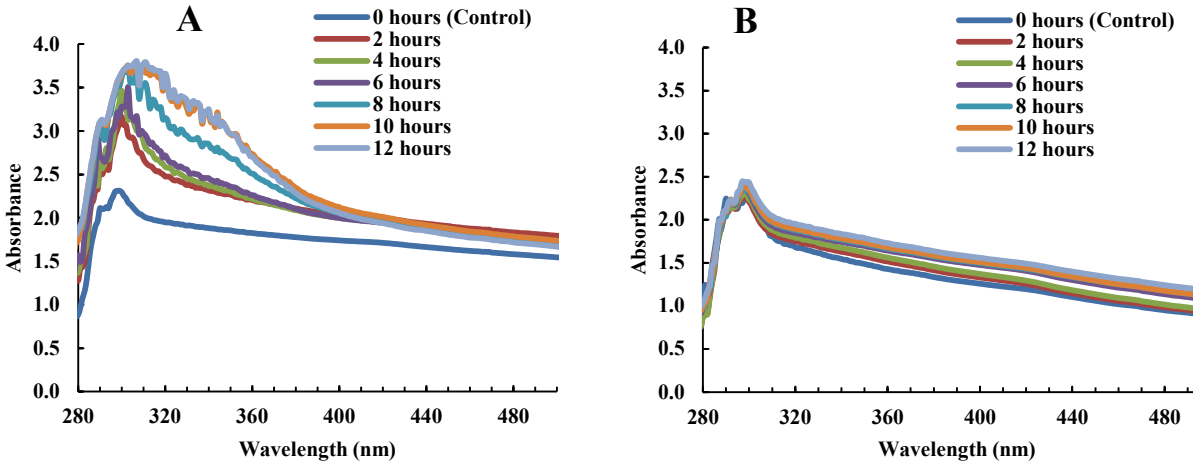

Figure 3.2. UV-Vis absorbance spectra of NAM-GlcN (A) and NAM-Glc (B) conjugates over time. The reaction was performed at 40˚C at 1:3 protein-carbohydrate ratio from 0 (control) to 12 hours.

The highest absorbance readings were obtained when a 1:6 protein to carbohydrate ratio was used and increased mainly after 6 hours of incubation. The rate of product formation was faster when GlcN was used as compared to Glc. NAM-Glc or NAM-GlcN mixture at the beginning of reaction corresponded to the absorbance maximum in the range from 287 to 290 nm, which might be dominated by contributions from the Tyr, Phe and Trp side-chains (Jamin and Lacapere, 2007). Upon glycation the bathochromic shift was observed in the region of 305-307 nm depending on the reaction variables. This shift was achieved faster and was more evident for the samples glycated with GlcN as compared to Glc. Previously, Zhu et al. (2008) reported that conjugation between whey protein and dextran resulted in the peak shift from 304 nm to 307 or 310 nm after 48 or 72 h of reaction. The authors assigned λ_{max} of 304 to the Schiff base formation, while 307-310 nm were attributed to the formation of Amadori compounds or intermediate stages of the glycation reaction. In the model reaction of 2,4-

dihydroxybenzaldehyde (DNBA-P) with aminocaproic acid, Schiff base formation was observed at λ_{max} of 296 nm (Blonski et al. 2007). Although, the reaction between DHBA-P with lysine residues of aldolase resulted in Schiff base formation at 311 nm. Zhu et al. (2008) proposed that the different values for shift λ_{max} reported in previous studies were related to the different environments of the Schiff bases. As presented in Figure 3.2 A and B, besides the absorption at the corresponding λ_{max} there was a tailing absorption which extended to the visible wavelength region. This may indicate the formation of some chromophores, acquired from the rearrangement products of the Maillard reaction (Zhu et al. 2008).

Higher reactivity of GlcN compared to other sugars (i.e. fructose, galactose, glucose, etc.) when reacted with cysteine at a 4:1 molar ratio was observed by Kraehenbuehl et al. (2008). Greater acceleration in glycation rate by GlcN might be related to the difference in the molecular structure as compared to Glc (Figure 3.3).

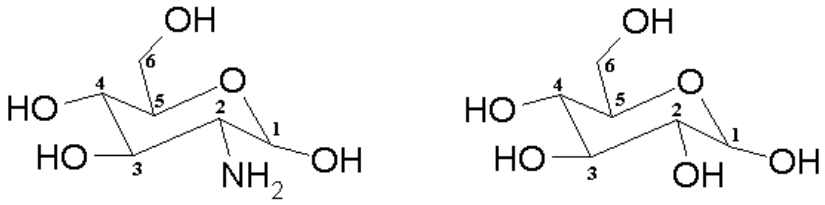

Figure 3.3. Difference in the molecular structure between glucosamine and glucose.

It is speculated here that GlcN might convey higher catalytic activity for non-enzymatic browning by a specific mechanism related to the presence of a primary amine at the C-2 position in the pyranose ring. The close proximity of this amino group to the reactive anomeric center apparently might be responsible for GlcN higher reactivity.

Because of GlcN amino group, the condensation between GlcN molecules or GlcN molecules with their products in solution may occur (Zhang et al. 2004). GlcN has been reported to undergo spontaneous dimerisation and rearrangement, forming deoxyfructosazine and 2,5-bis-

(tetrahydroxybutyl)pyrazine and other products (Jun et al. 2003). In view of this, it is expected that the reaction mixture contained not only glycoconjugates and unreacted protein/sugar, but also the products derived from GlcN autocondensation and/or rearrangement. In the current study GlcN solutions were also separately incubated as a carbohydrate control (data not shown). The increase in absorbance values over time was observed at 1:6 protein to sugar ratios using 40˚C for incubation. The results from all UV-Vis spectra for NAM extracted from fresh meat are summarised in a heat map (Figure 3.4).

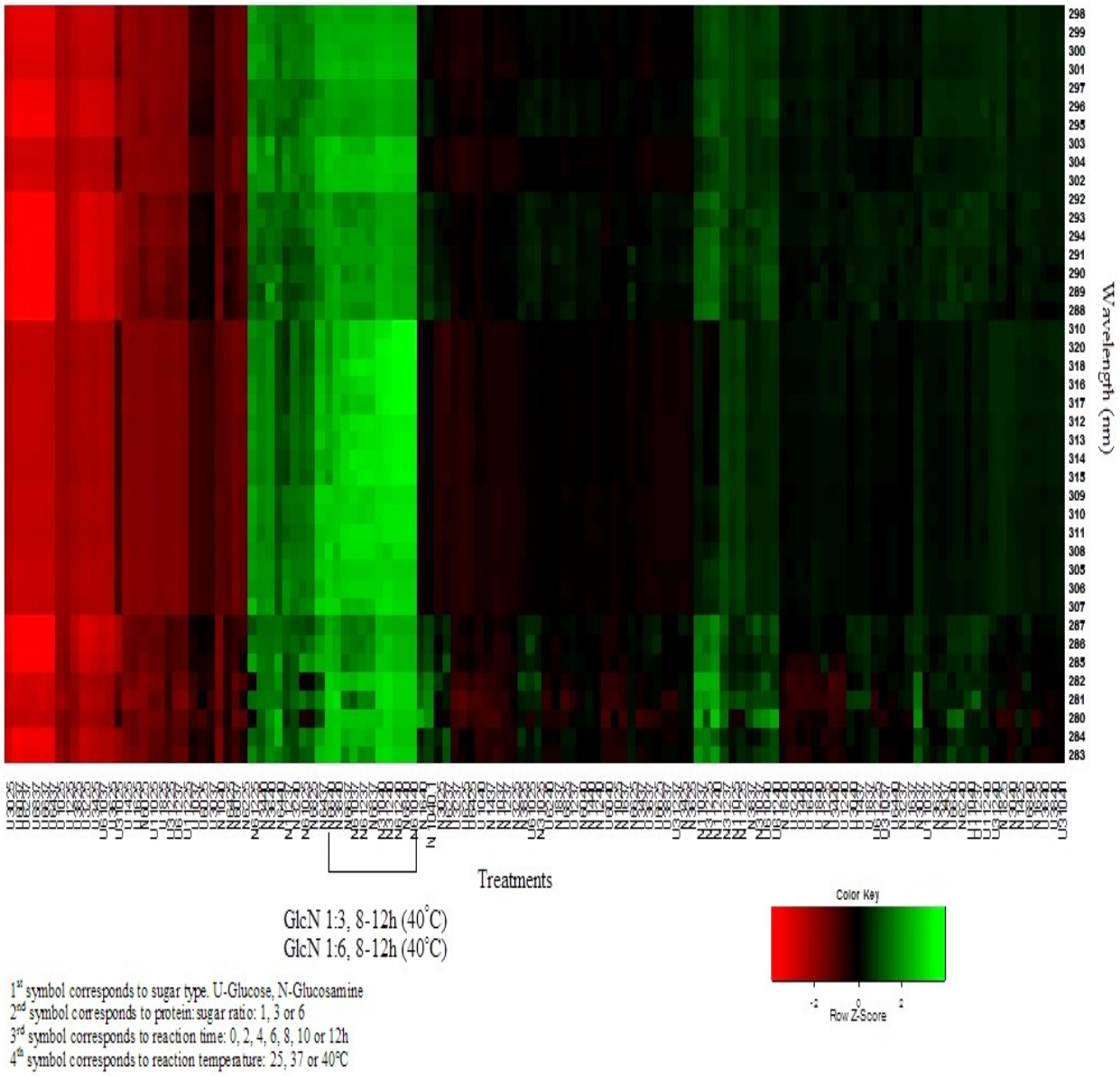

Figure 3.4. Hierarchal clustering of protein-sugar UV-Vis absorbance data for actomyosin extracted from fresh chicken *Pectoralis major*. The vertical axis represent individual wavelength (280-320 nm). The horizontal axis represents individual glycation treatments. The colors in each cell indicate the absorbance of a particular sample relative to the mean level from all samples for the specific wavelength. The color scale extends from bright green (maximum absorbance) to bright red (minimum absorbance). The heat map was developed based on 126 samples (average from 3 repetitions) × 40 wavelength values.

Described here for the first time for glycation analyses, this method allows for visualization of large-scale experimental data in a single graph, helping to explore and interpret results more efficiently. From the heat map it is evident that samples glycated with Glc formed clusters tightly together, colored in bright red on the left side of the heat map. The central part of the heat map consisted of clusters with treatments displaying the highest absorbance, which corresponded to GlcN glycated samples (bright green). Accordingly, the following treatments were selected as optimal for glycation reactions: 1:3 NAM-GlcN incubated from 8 to 12 hours and 1:6 NAM-GlcN from 6 to 10 hours of reaction at 40˚C.

3.3.2. Effect of frozen storage on glycation parameters

Frozen storage is an important practise used for preservation of muscle-based food. Allowing for longer storage time and better production control, it is also necessary for the purpose of transportation and export. Even though frozen storage is applied to slow down undesirable biochemical reactions in meat, cell disruption due to formation of ice crystals might have negative effects on meat physicochemical properties and subsequently its functionality (Soyer et al. 2010). Due to the changes during frozen storage, conditions for glycation for this type of meat might significantly differ from those which are optimal for fresh meat.

In this respect, determination of the optimal conditions to produce NAM glycoconjugates from frozen material was included into the experimental design (Figure 3.1). NAM was extracted from frozen (3 weeks; -20˚C) chicken breast, glycated and analyzed by UV-Vis spectroscopy in the same way as described above for fresh NAM. Collected UV-Vis spectra were organised into the heat map (Figure 3.5).

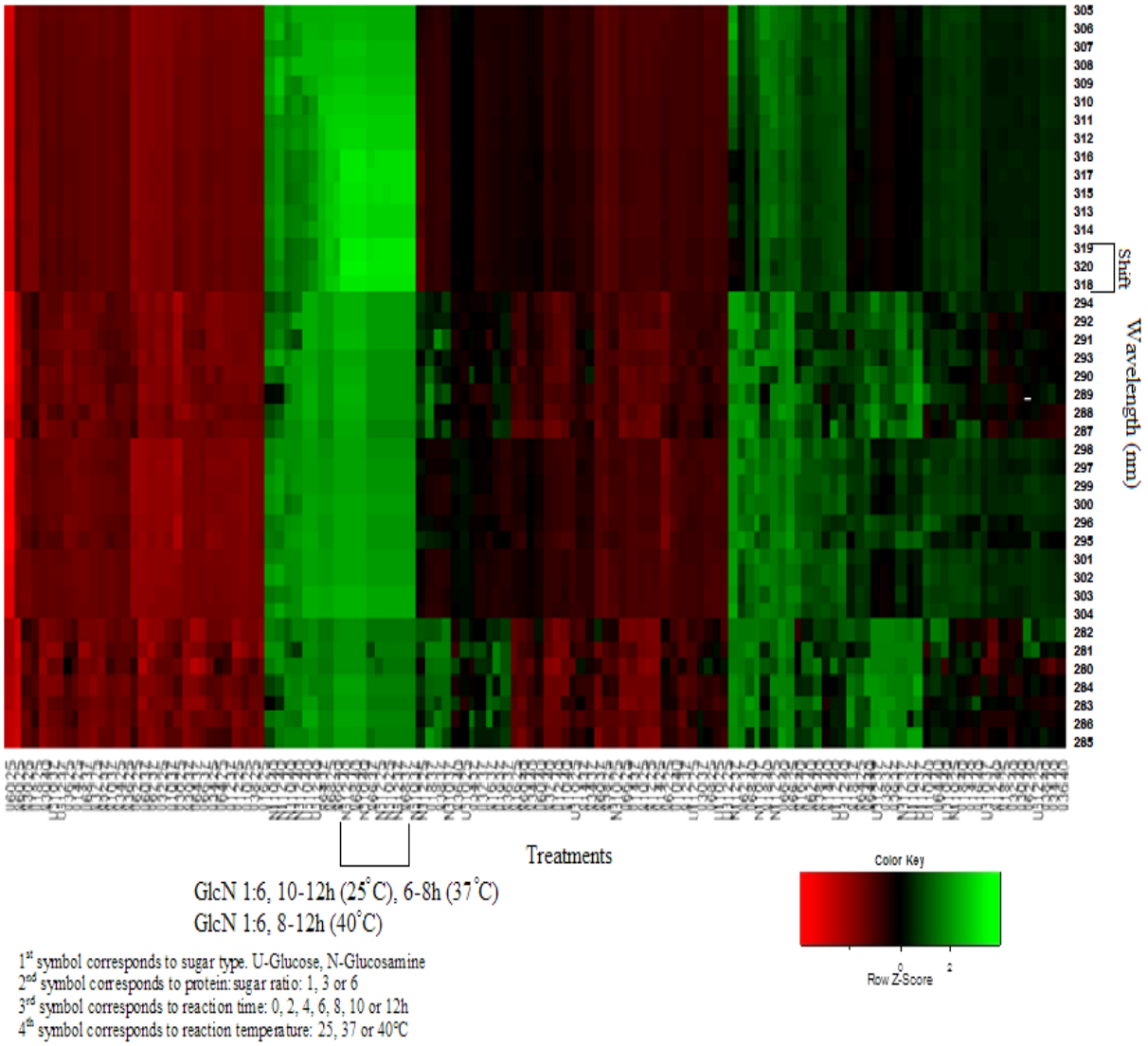

Figure 3.5. Hierarchal clustering of protein-sugar UV-Vis absorbance data for actomyosin extracted from frozen chicken *Pectoralis major*. The vertical axis represent individual wavelength (280-320 nm). The horizontal axis represents individual glycation treatments. The colors in each cell indicate the absorbance of a particular sample relative to the mean level from all samples for the specific wavelength. The color scale extends from bright green (maximum absorbance) to bright red (minimum absorbance). The heat map was developed based on 126 samples (average from 3 repetitions) × 40 wavelength values.

For the UV-Vis absorbance there was an evident shift to the longer wavelength (318-320 nm) as compared to the fresh, where clustering was observed at broader range of wavelength. This shift corresponded to the samples incubated at 25, 37 and 40˚C at different NAM/GlcN ratios. Moreover, the glycation proceeded slightly faster even at lower temperatures, as compared to the fresh meat system. This suggests that freezing of NAM prior to glycation might be responsible for the acceleration of the reaction rate. It was also observed that after 8 hours of incubation, frozen NAM-GlcN sample solutions developed a slightly yellow color. Even though a faster time of glycation seems to be a positive aspect here, there is a chance that glycation may not to be limited to the initial stages of the Maillard reaction, proceeding further to Amadori or the AGEs. This might negatively impact protein functionality by causing higher occurrence of protein cross-linking and faster accumulation of unwanted reaction products. At the same time, considering the complexity of the Maillard reaction, it would be beneficial to gain further insight into the parameters allowing for better control of the reaction at these particular conditions.

3.3.3. Protein oxidation during frozen storage

There are reports in the literature indicating that frozen storage promotes oxidative deterioration of proteins, causing production of carbonyl compounds. For example, Soyer et al. (2010) found that freezing of chicken leg meat over 3 months at -7˚C led to significant increases in carbonyl content. To further elucidate the effect of frozen storage, the amount of carbonyl groups in fresh and frozen NAM was measured. The amount of carbonyls significantly increased (p = 0.0059) from 2.14 to 2.92 nmoles carbonyls/mg protein. This result was in agreement with the report of Chan et al. (2011) who found that the amount of carbonyls significantly increased from 1.72 to 2.0 nmol carbonyls/mg protein during frozen storage of turkey breast meat. It has been reported that oxidation subjects proteins to unfolding, enhancing the exposure of certain protein segments

and reactive amino acid residues (Li et al. 2012). In this case, higher availability of Lys exposed for reaction with Glc or GlcN might be the reason for the faster reaction rate in frozen NAM systems. However, the increase in absorbance values at earlier incubation times and shifts in wavelength were predominant for GlcN glycoconjugates, as compared to Glc. This suggests that carbonyls produced by NAM oxidation can be attacked by nucleophiles, such as -NH_2 of GlcN. Thus, one possible explanation for the glycation rate differences between fresh and frozen NAM with GlcN, is the simultaneous involvement of two functional groups from sugar molecules (aldehyde and primary amine) and protein (protein-bound -NH_2 and carbonyl groups).

3.3.4. Protein solubility profiles as a function of pH

On the basis of the optimum reaction variables selected from the heat map for fresh NAM, the following reaction conditions were designed: 40˚C, 1:3 and 1:6 protein to carbohydrate ratio during 4, 8 and 12 hours of incubation. In order to determine the optimum time of incubation and conclude the best protein to carbohydrate ratio, protein solubility was tested at pH values of 3, 5, 7, 8 and 10 (preliminary test; data not shown). It was found that at a 1:3 protein to carbohydrate ratio, higher solubility was obtained for the samples incubated for 8 hours as compared to those incubated at 4 and 12 hours. Whereas NAM incubated at 1:6 protein to carbohydrate ratio was more soluble after 12 hours of incubation. Even though the optimum incubation time was found to be the same for Glc and GlcN, solubility of NAM treated with Glc was significantly lower ($p < 0.05$). Based on this, the complete solubility profile of the Glc/GlcN glycated NAM was built as a function of pH for samples treated for 8 hours with 1:3 NAM-Glc/GlcN ratio and 1:6 protein:sugar ratio for 12 hours (Figure 3.6). The solubility of native NAM gradually decreased from pH 3 to 5, where it became the least soluble, corresponding to its pI. In contrast, the solubility of NAM glycated either with Glc or GlcN was improved, increasing from 6.6% to 28%

on average for glycoconjugates. The solubility of NAM glycated with GlcN was higher than those glycated with Glc, particularly in the pH range from 8 to 12. Chung et al. (2006) also reported that solubility of chitosan-glucosamine was higher as compared to chitosan-glucose, reaching the highest values after 3 days of incubation at 70˚C. Moreover, the same authors reported the formation of precipitates during dialysis for Glc glycated chitosan.

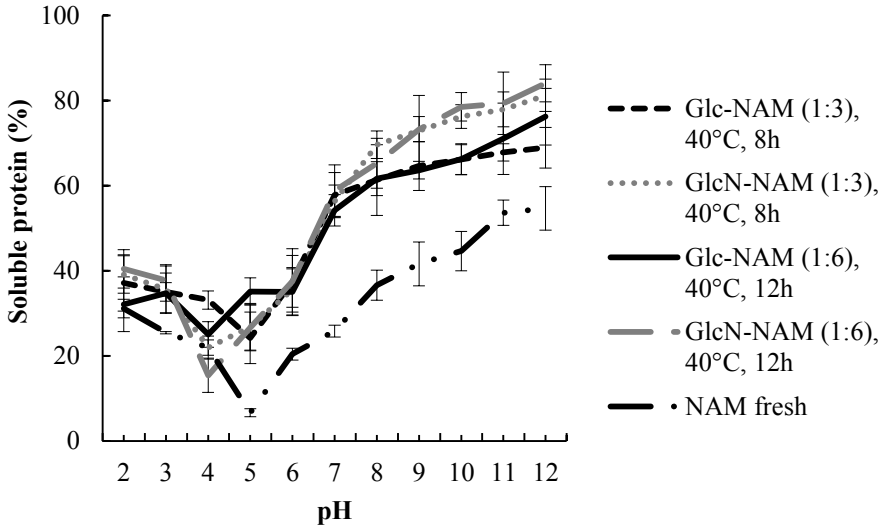

Figure 3.6. Solubility of actomyosin as dependent on pH, type of sugar and protein to sugar ratio. NAM-Glc/GlcN mixtures in weight ratios of 1:3 and 1:6 were incubated at 40˚C for 8 or 12 hours. Results are means of three independent experiments ± standard deviations.

There was only a slight difference in solubility between samples treated at 1:3 and 1:6 protein to sugar ratio for both Glc and GlcN. This possibly indicates that all available -NH_2 groups in protein reacted when 3-fold parts of sugar were in excess over protein. A further increase in the amount of sugar in the reaction mixture did not influence the solubility significantly. To render carp myofibrillar proteins soluble in low ionic strength media, Saeki (1997) used a 9-fold weight of glucose over protein. In comparison, Jimenez-Castano et al. (2005) found that conjugate formed at a 2:1 weight ratio of dextran to β-Lg exhibited higher solubility in the pH range from 3 to 9 as compared to native protein. Such a difference in the amount of sugar required for

successive grafting might be dictated by the size and reactivity of the reactants, as well as amphipathicity and molecular flexibility of protein (Jung et al. 2006).

The average increase in solubility at pH 7-12 as a result of glycation with GlcN was 23% as compared to native protein. In addition, the shift in isoelectric point to acidic values was observed for the samples glycated with Glc at 1:6 protein to sugar ratio and for GlcN at 1:3 and 1:6 ratios. This shift was expected, as protein becomes more acidic upon glycation since sugar attachment leads to the neutralisation of positive charges on protein (Luthra and Balasubramanian, 1993). However, this explanation mainly applies to Glc. GlcN, which carries its own $-NH_2$ group, was not expected to induce the pI shift. Judging from the difference in molecular structure between Glc and GlcN (Figure 3.3), the explanation of pI shift may possibly involve the $-NH_2$ group of GlcN in the progress of glycation.

3.3.5. Model study in lysine-glucosamine system

A plausible reason for the isoelectric point shift to more acidic values for GlcN glycoconjugates might be the liberation of ammonia from NAM-GlcN conjugate during reaction. To clarify this, the model study in amino acid-sugar system was designed. Lysine is a very reactive amino acid towards glycation. Histidine, tryptophan, and arginine residues also react but to a lesser extent (Ames, 1992). The mass spectra for the study in the model system are presented in Figure 3.7.

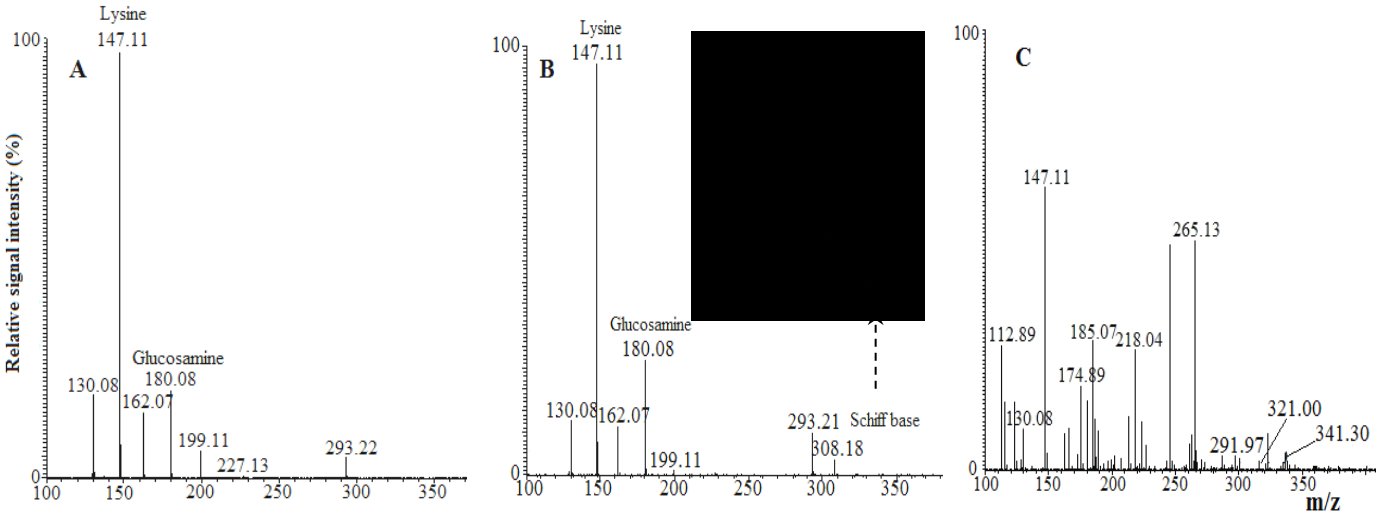

Figure 3.7. Orbitrap LC-MS spectrum of Lys-GlcN conjugates at 0 (A), 2 (B) and 8 (C) hours of incubation and proposed Schiff base structures (inset 1).

At time 0 (control, Figure 3.7 A), two prominent peaks with m/z 147.11 and 180.08 Da corresponding to protonated molecular ions $[M+H]^+$ of Lys and GlcN, respectively, were observed. After two hours of incubation (Figure 3.7 B) the early glycation product (Schiff base) formation was detected, corresponding to the protonated ion with molecular weight of 308.18 Da, calculated based on the mass shift of + 161 Da. This mass shift was calculated based on water release upon GlcN to protein (Lys) attachment. In the samples that had been heated for 8 hours (Figure 3.7 C), a decrease in peak intensity was found for Lys and GlcN. Ions with m/z of 308.18 were not detected after 8 hours of glycation, but a new ion with m/z 291.97 was formed possibly due to ammonia liberation [(Lysine+GlcN)-(H_2O+NH_3)]. Due to the presence of the -NH_2 group on GlcN it may undergo variable reactions, including autocondensation and rearrangements. The products of this reaction were not found at 0 and 2 hours of glycation, but were identified after 8 hours. For instance, an ion with m/z 321.00 indicated the presence of GlcN autocondensation product with further rearrangement to give 2,5-

bis(tetrahydroxybutyl)pyrazine (Candiano et al. 1988). The same authors also reported a peak at m/z 185.07. However the structure of the product associated with that molecular mass was not indicated. Further evidence of GlcN autocondensation adducts is a peak of m/z 341.30, which derives from GlcN dimerisation (Kerwin et al. 1999). Ion peaks of m/z 321.00 and 185.07 with higher intensities were also identified in the sample, where GlcN was incubated without Lys (data not shown). This further confirms the assignments of those peaks to GlcN rearrangement products.

Therefore, the proposed pathway of ammonia release during Lys glycation with GlcN appears to be possible and the obtained results could be extended to the NAM-GlcN system. This model gives a preliminary indication of the involvement of ammonia release during GlcN-Lys conjugation and its influence on protein isoelectric point. It is also possible that the pI shift is induced by blocking the $-NH_2$ group of covalently attached GlcN by other free GlcN molecules or compounds deriving from rearrangements products of GlcN alone or NAM-GlcN conjugates. Therefore, more detailed investigation is necessary to figure out the mechanism and kinetics behind the course of glycation with GlcN.

3.3.5.1. Verification of ammonia (NH_3) release in the model system

To further confirm the results obtained from mass spectrometry about ammonia release in the model study, the enzymatic assay kit was used. It was revealed that 3.3% of NH_3 was released after 8 hours of glycation, validating the information attained from the mass spectrometry analyses. This finding also clarifies the mechanism of the higher reactivity of GlcN compared to Glc; the presence of $-NH_2$ group adjacent to the reactive aldehyde group, accelerates the release of NH_3 during initial phase of glycation. In comparison, the acetylated form of GlcN (*N*-acetyl-glucosamine) normally found in the connective tissue of human body has lower reactivity due to

the presence of an amide bond (Greene and Wuts, 1999). It appears that in biological system acetylation of amino sugars is a strategy to control their reactivity.

The proposed mechanism also suggests that aldehyde group of GlcN is an acceptor of nucleophilic -NH_2 groups from amino acids. Notwithstanding, when proteins are oxidized with formation of carbonyls (i.e. freezing) glucosamine can also act as a nucleophile donor through -NH_2 group. Moreover, this result also demonstrate that shift in pI of NAM might be caused by NH_3 liberation in the progress of glycation with glucosamine.

3.3.6. Protein glycation by MALDI-TOF/TOF-MS

To determine the relative levels of the glycated proteins MALDI-TOF/TOF-MS analyses were performed. Previous reports indicated the usefulness of this approach to study the glycation in vivo and in vitro, since the number of Glc molecules that condense onto the protein can be evaluated by the mass increase (Lapolla et al. 2000). This task is also simplified since the majority of ionized peptides from MALDI are singly charged, thus observed mass/charge (m/z) ratios of peaks denote the mass of the peptide. In this study, solutions of NAM, separately or glycated with Glc or GlcN were incubated at 40˚C for 8 or 12 h, at different protein to sugar ratios. Thereafter, native and glycated NAM was digested with endoprotease trypsin to produce a set of peptides, which were further analyzed by MALDI-TOF/TOF-MS. The difference of +162 Da between control (peptides from non-treated NAM) and glycated peptides was attributed to attachment of Glc residue within particular treatment and loss of water molecule (Meltretter and Pischetsrieder, 2008). As this study is the first focusing on MALDI-TOF/TOF-MS analyses of muscle protein glycation with GlcN, no information is available on the possible mechanism of this reaction and thus identification of GlcN-protein glycation products. In addition, as shown in the model Lysine-GlcN study possible ammonia liberation during NAM reaction with GlcN

might have an impact on the calculation of molecular weight of the resulting glycation product. In this respect, calculation of glycation for GlcN-NAM conjugates was performed in two ways. First, each detected mass shift of +161 Da represented the successive increase of one GlcN residue as a result of Schiff base formation at the initial stages of Maillard reaction and further dehydration. Second, a + 144 Da shift in molecular mass indicated a single glycation due to the loss of both water and ammonia. It is worth mentioning that the mass shift (Δm = 161 Da) was confirmed by the model study (Lysine-GlcN) as being suitable for subsequent calculation of Shiff base formation between NAM and GlcN.

The profiles from various treatments (Figures 3.8 and 3.9) showed that the relative number of the glycated peptides varied among treatments. The highest percentage of glycated peptides was found for NAM-GlcN (1:3) conjugates, reaching 32% of the total peptides. In contrast, 14% of glycopeptides were produced by conjugation with Glc. Only a slight increase (on average about 1%) in glycation level was observed with an increase in the sugar amount to 6-fold over protein and prolonged reaction time (12 hours) for both Glc and GlcN. These results are supported by the findings of the protein solubility study, where the highest values were obtained for samples glycated with GlcN, as compared to those with Glc. It is also in agreement with observations that increase in the amount of sugar does not considerably influence the level of glycation, as well as protein solubility.

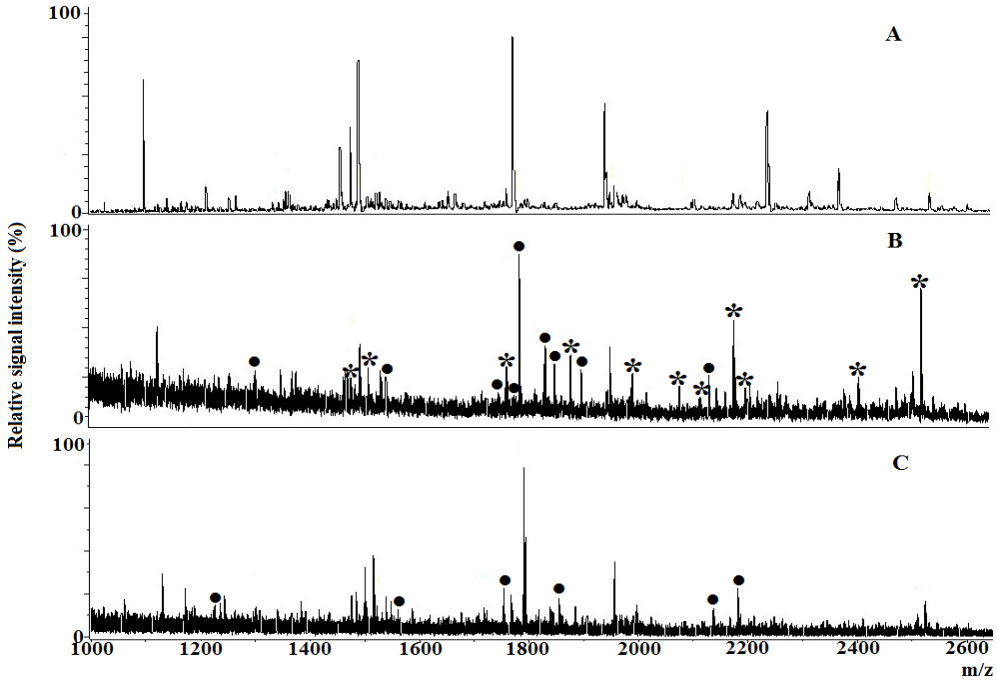

Figure 3.8. MALDI-TOF/TOF mass spectra of non-treated actomyosin (A), and actomyosin conjugated with glucosamine (B) or glucose (C) at 40˚C for 8 hours at 1:3 protein to sugar ratio. The data were obtained after total digestion with trypsin. The filled circle refers to Mw obtained from a mass shift of 161 (GlcN-H_2O) or 162 (Glc-H_2O). The stars indicated Mw obtained from a mass shift of 144 (GlcN-H_2O-NH_3).

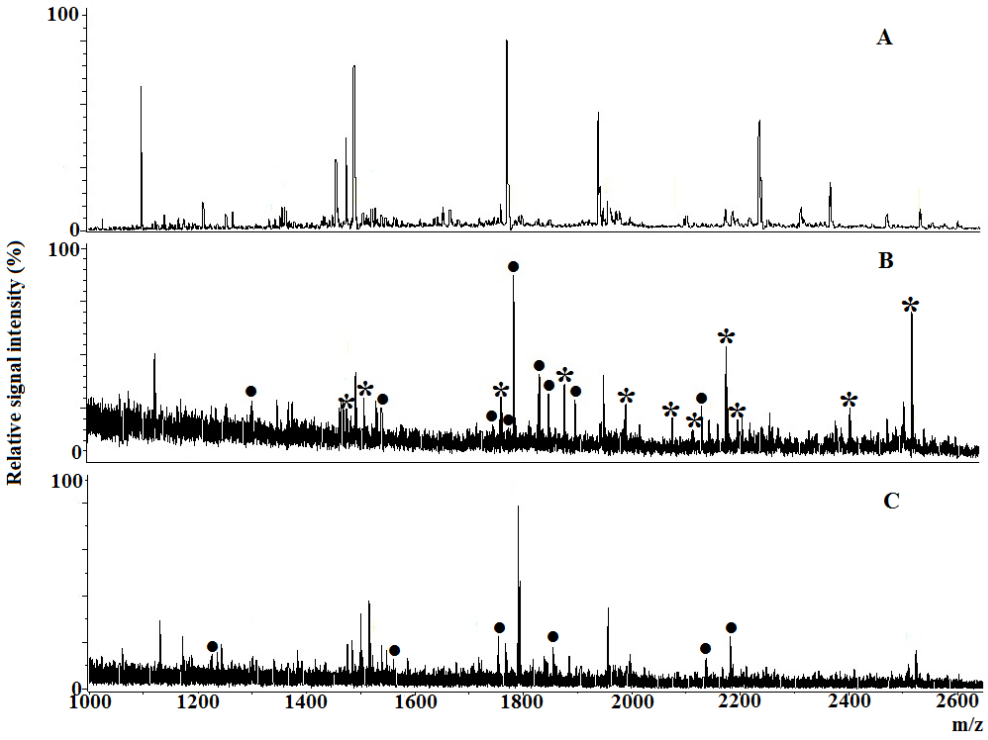

Figure 3.9. MALDI-TOF/TOF mass spectra of non-treated actomyosin (A), and actomyosin conjugated with glucosamine (B) or glucose (C) at 40˚C for 12 hours at 1:6 protein to sugar ratio. The data were obtained after total digestion with trypsin. The filled circle refers to Mw obtained from a mass shift of 161 (GlcN-H_2O) or 162 (Glc-H_2O). The stars indicated Mw obtained from a mass shift of 144 (GlcN-H_2O-NH_3).

With the increase in incubation time up to 12 hours (Figure 3.9), the number of peptides calculated by the second method (considering ammonia release) doubled, supporting the proposed explanation of ammonia liberation as a reason for a shift in isoelectric point for NAM-GlcN conjugates.

3.3.7. Emulsifying properties

Among the dominant properties for protein's favourable industrial application is the ability to emulsify fat and form a stable emulsion. Emulsifying properties of non-treated NAM and NAM glycated with Glc or GlcN at different pH values were determined and the results are presented in Table 3.1.

Table 3.1. Emulsion activity index (EAI) and emulsion stability index (ESI) of native and glycated NAM[1]

[1]Results are presented as mean (n=3) ± standard deviation. Dissimilar alphabetical letters within a column represent significant ($p < 0.05$) difference between mean.

Treatments	Emulsion activity index (EAI)			Emulsion stability index (ESI)		
	pH 3.0	pH 7.5	pH 10.0	pH 3.0	pH 7.5	pH 10.0
NAM non-incubated	2.6 ± 0.1^{c}	4.3 ± 0.7^{b}	6.0 ± 0.3^{b}	16.4 ± 3.6^{b}	19.7 ± 2.6^{bc}	38.6 ± 5.8^{bc}
NAM incubated (40˚C, 8h)	2.1 ± 0.2^{c}	4.0 ± 0.6^{b}	5.8 ± 0.6^{b}	15.2 ± 1.8^{b}	27.3 ± 2.7^{b}	27.7 ± 5.0^{c}
NAM-Glc (1:3, 40˚C, 8h)	3.9 ± 0.5^{b}	5.2 ± 0.7^{ab}	7.6 ± 0.9^{ab}	20.4 ± 2.9^{ab}	35.4 ± 3.6^{ab}	46.1 ± 2.7^{ab}
NAM-GlcN (1:3, 40˚C, 8h)	5.5 ± 1.3^{a}	6.5 ± 1.3^{a}	8.3 ± 1.1^{a}	26.2 ± 4.0^{a}	40.6 ± 6.1^{a}	55.6 ± 4.8^{a}
Level of significance	0.0012	0.0225	0.0152	0.0113	0.0339	0.0005

Emulsion activity index at all pH values was significantly higher for NAM-GlcN conjugates as compared to non-heated and incubated NAM. In contrast, the EAI of NAM-Glc conjugates was significantly higher from control NAM only at strongly acidic pH. At pH 3 significantly higher EAI was found for GlcN conjugates in comparison to those of Glc. Such a strong difference, particularly at this pH, was probably caused by the pI shift into acidic values for GlcN glycoconjugates, providing higher solubility and thus higher ability to emulsify fat particles. The results from ESI had the same trend as EAI, with significant improvement of emulsion stability for GlcN conjugates compared to that of control NAM. Although incorporation of Glc into NAM enhanced EAI, no significant improvement was brought to emulsion stability. Improvement in emulsifying properties of glycoconjugates, in particular NAM-GlcN, was possibly caused by changes in the amphiphilic properties of protein. It seems reasonable to propose that if proteins absorb at the oil-water interface and forming viscoelastic layer, while hydrophilic sugar residues orient towards water, prevention of oil droplets from coalescence occurred (Fujiwara et al. 1998). Moreover, as solubility is a determining factor in a protein's ability to form an emulsion its

improvement (Figure 3.6) upon glycation provides beneficial effects on emulsifying properties. Morgan et al. (1999) showed that lactosylation of β-Lg in dry conditions (50˚C, 48 hours) did not significantly modify the native protein structure, while the treatment in solution (60˚C, 130 hours) resulted in important structural changes. Thus, it is speculated here that protein structural modifications induced by glycation in liquid conditions might have a strong influence on its emulsifying activity and stability. This is especially related to NAM-GlcN conjugates, since a shift in protein pI confirms a higher degree of modification and hence changes in three-dimensional protein structure.

In previous studies by Fujiwara et al. (1998) it was found that myofibrillar proteins from carp developed excellent emulsifying properties during glycation with dextran. Saeki (1997) who incorporated Glc into carp myofibrillar protein also found that emulsifying properties of glycoconjugates were superior to that of unglycated protein.

3.4. Conclusions

This study offers important information about the glycation of muscle protein in a liquid environment achieved at moderate temperature and faster reaction rate. It also gives an insight into glycation by using protein, which undergoes oxidative changes as a result of frozen storage. The optimised method for muscle protein glycation proposed here leads to significant improvement in protein solubility, which is of primary importance in muscle food processing. The present work showed that use of GlcN for non-enzymatic glycation accelerates the speed of reaction, which allows in shorter time and lower temperatures sugar incorporation into protein, avoiding its heat denaturation. Further research is required to determine the mechanism of glycation with GlcN related to kinetics of the reaction. In addition, as GlcN is known to have

medical effects on joint health, it would be beneficial to evaluate the biological activity of those proteins to which GlcN was covalently attached.

CHAPTER 4. Transglutaminase-catalyzed glycosylation of natural actomyosin (NAM) using glucosamine as amine donor: functionality and gel microstructure

4.1. Introduction

The recovery of proteins from poultry and fish by-products for their utilization as food ingredients is of increasing interest in the food industry. One of the methods for protein extraction is using a pH-shifting process, based on acid/alkaline solubilization followed by precipitation at the pI (Hrynets et al. 2010). Even though the method results in the production of high-protein ingredients, partial denaturation during the extraction process affects its functionality, solubility in particular. As a result, the functional properties of these isolated proteins have to be further improved. For this purpose, a wide spectrum of modifications, such as deamidation, succinylation, acetylation, and others could be used (Saberi et al. 2008). However, not all of the currently existing methods have been extensively used or explored at industrial-scale processing. Recent, significant attention has been given to protein modification by covalent attachment of carbohydrates during the Maillard reaction (glycation), usually performed in dry-state conditions (Zhu et al. 2008). Despite substantial functional improvement using this dry-state process, its application in food technology is limited due to the difficulty of controlling the reaction, long reaction time, and formation of mutagenic compounds, such as advanced glycation end products (AGEs) (Brands et al. 2000; Zhu et al. 2008). Conducting the reaction in a liquid state would be preferable to overcome these limitations and make it viable for industrial scale up. For instance, the Maillard reaction may be limited to its very initial stage of Schiff base formation, obtaining a light colored product (Zhu et al. 2008). In this regard, in Chapter 3 a new method taking advantage of the higher reactivity of the amino sugar glucosamine as compared to glucose was proposed. A fast glycation rate at a moderate temperature in a liquid aqueous environment was demonstrated possible, with subsequent positive effects on protein

functionality. However, in order to further increase glycoconjugation efficiency at lower temperatures, a further reduction of browning, and the minimization of AGEs formation, glycosylation methods involving enzymes are proposed as a promising alternative.

Enzyme-mediated conjugation (glycosylation) may be very useful for site-specific conjugation due to its strict substrate specificity and amenability to mild reaction conditions. In this respect, glycosyltransferases and glycosidases might be considered as glycosylation catalysts (Colas et al. 1993). A glycosyltransferase (EC 2.4) catalyzed reaction uses a complex sugar nucleotide as the donor and has a very stringent substrate specificity (Ban et al. 2012). In comparison, glucosidase (EC 3.2) uses readily available donor substrates and has less specificity for acceptors. However, the low yield of transglycosylation is a major limiting factor to its usage in glycosynthesis (Milosavic, 2012). Transglutaminases (TGase; EC 2.3) belong to the group of acyltransferases, which are widely distributed in animal tissues, plants, and microorganisms. They are capable of catalysing acyl-transfer reactions between the γ-carboxyamide of protein/peptide glutaminyl residues (acyl donors) and various primary amines (acyl acceptors). When the ε-amino group of lysine residues act as acyl acceptors, ε-(γ-glutamyl)-lysine isopeptide bond is formed. In the absence of primary amines in the reaction system, water acts as acyl acceptor resulting in the deamidation of the glutaminyl residue (Hu et al. 2011). Since the enzyme recognizes a wide variety of primary amines (Folk, 1983), a variety of conjugates can be produced using TGase-mediated acyl-transfer reactions.

Glucosamine (GlcN) is a naturally occurring amino sugar that is a building block of glycosaminoglycans found in cartilage (Black et al. 2009). It is produced commercially by the hydrolysis of crustacean shells and exoskeletons, a by-product of the marine food production (Arbia et al. 2013). As an important constituent of joints, it is also known as a nutraceutical

proposed to reduce the incidence of osteoarthritis. Taking into consideration that GlcN possesses amino and hydrophilic hydroxyl groups (Chung et al. 2006), its incorporation into actomyosin via TGase would be useful for improvement of muscle protein functionality. Therefore, this study aimed: (1) to develop an enzymatic process for actomyosin glycosylation using TGase at two protein to glucosamine ratios (1:1 and 1:3) and two reaction temperatures (25 and 37˚C) and (2) to investigate its contribution on functionality. Actomyosin complex extracted from *Pectoralis major* of broiler chickens was used as a model protein. Sugar moieties covalently bound to actomyosin were evaluated using mass spectrometry techniques, while subsequent effects on functionality were evaluated by determining protein solubility, emulsifying properties, gelation behaviour and gel microstructure.

4.2. Material and Methods

4.2.1. Materials

Fresh chicken breast was obtained from a local store. D-(+)-Glucosamine hydrochloride, potassium phosphate monobasic and dibasic, sodium azide, guinea pig liver transglutaminase (EC 2.3.2.13), proteomics grade trypsin and ProteoMass peptides MALDI-MS calibration kit were purchased from Sigma-Aldrich (St. Louis, MO, USA). All the reagents and chemicals used in the study were of analytical grade.

4.2.2. Methods

4.2.2.1. Experimental design

Broiler chicken breasts were kept at 4˚C before treatments. Natural actomyosin (NAM) was extracted according to the procedure indicated in Section 4.2.2.2. Then buffered solutions of NAM:GlcN at 1:1 or 1:3 protein to sugar ratios were incubated at 25 and 37˚C for 6 hours with (+) or without (-) TGase (glycosylation and glycation, respectively). This duration was chosen to minimize the extent of glycation (Chapter 3) while providing enough time for glycosylation to

occur. Non-treated and incubated NAM at 25 and 37˚C without GlcN and TGase were also included as controls to ensure that changes in protein functionality are due from sugar incorporation. The entire experiment from NAM extraction through final glycosylated/glycated products was replicated 3 times. Functionality measurements (solubility, emulsion properties, gels microstructure, rheological behaviour) were also conducted in triplicate.

4.2.2.2 Extraction of natural actomyosin (NAM)

Actomyosin from chicken *Pectoralis major* was extracted following the method described in Chapter 3 (section 3.2.2.).

4.2.2.3. Enzymatic glycosylation of natural actomyosin (NAM)

Glycosylation was conducted based on the optimization study of Chapter 3. Mixtures of NAM and GlcN in ratios of 1:1 and 1:3 (w/w) were dissolved in 50 mM PBS (pH 7.5) in the presence of 0.55 M KCl. The pH of the solutions was adjusted to 7.5, when needed. The reaction was initiated by addition of 10 U of TGase/g of protein and 5 mM of $CaCl_2$. One enzymatic unit is defined as the amount needed to catalyse the formation of 1.0 μmol of hydroxamate per min from Z-Gln-Gly and hydroxylamine at pH 6.0 at 37˚C. Obtained aliquots were incubated in an Innova 44 (New Brunswick Scientific, Edison, NJ, USA) shaker under constant agitation for 6 h at 25 or 37˚C. To remove the enzyme and unreacted sugar, collected aliquots were subjected to an ultrafiltration membrane system with molecular weight cut-offs of 100 and 3 kDa (Amicon Ultra, Millipore Corporation, Bedford, MA, USA), respectively. The post-ultrafiltration ionic strength was measured for glycosylated samples using a conductivity meter (Oakton Acorn CON 6, Vernon Hills, IL, USA) calibrated prior to the measurements. Thereafter, the ionic strength of the sample set was adjusted to 0.55 M KCl.

4.2.2.4. Evaluation of protein solubility

The solubility of glycosylated and control samples was determined as described in Chapter 3 (section 3.2.6.).

4.2.2.5. Samples pre-treatment and digestion prior to matrix-assisted laser desorption/ionization time-of-flight mass spectrometry (MALDI-TOF/TOF-MS)

Control and glycosylated samples were diluted in a ratio of 1:1 with Laemmli sample buffer containing 5% β-mercaptoethanol and loaded (20 µl) onto a 4-20% Mini-PROTEAN TGX precast gel (Bio-Rad Laboratories, Inc., Hercules, CA, USA). SDS-PAGE was performed (Laemmli, 1970) in a Mini-PROTEAN tetra cell attached to a PowerPac Basic electrophoresis apparatus (Bio-Rad Laboratories, Inc.) at constant voltage of 200 V. After staining with Coomassie Brilliant Blue the excised gel pieces containing glycoprotein were reduced with 10 mM β-mercaptoethanol, alkylated with 50 mM iodoacetamide, washed with 100 mM ammonium bicarbonate/acetonitrile (ACN) (1:1, v/v) solution and dried in a Speed Vac (AES 2000, Savant Instruments Inc., Farmingdale, NY, USA). Dried gel bands were subjected to overnight proteolytic digestion at 37˚C with 0.2 µg of trypsin. Then, peptides were extracted with 30 µl of 10 mM ammonium bicarbonate, followed by extraction with 30 µl solution containing 5% formic acid and 50 % ACN in water twice and dried to ~15 µl in a Speed Vac.

4.2.2.6. Evaluation of glycoconjugation by MALDI-TOF/TOF mass spectrometry analyses

The samples obtained as described in section 2.2.5 were diluted 10-fold in 50% ACN/water + 0.1% trifluoroacetic acid. One µl of each sample was mixed with 1 µl of α-Cyano-4-hydroxycinnamic acid (4-HCCA, 10 mg/mL in 50% ACN/water + 0.1% trifluoroacetic acid). One µL of the sample/matrix solution was then spotted onto a stainless steel target plate and allowed to air dry. All mass spectra were obtained using a Bruker Ultraflex MALDI-TOF/TOF-

MS (Bruker Daltonic GmbH, Bremen, Germany). Ions were analyzed in positive mode after acceleration from the ion source by 25 kV. External calibration was performed by use of a standard peptide mixture (Mw = 700 to 3500 Da).

4.2.2.7. Orbitrap-LC-MS

Fractions containing tryptic peptides dissolved in aqueous 25% v/v ACN and 0.2% v/v formic acid were resolved and ionized by using nanoflow HPLC (Easy-nLC II, Thermo Scientific, West Palm Beach, FL, USA) coupled to the LTQ XL-Orbitrap hybrid mass spectrometer (Thermo Scientific). Nanoflow chromatography and electrospray ionization were accomplished by using a PicoFrit fused silica capillary column (ProteoPepII, C18) with 100 μm inner diameter (300 Å, 5 μm, New Objective, Inc., Woburn, MA, USA). Peptide mixtures were injected into the column at a flow rate of 3000 nl/min and resolved at 500 nl/min using 30 min linear ACN gradients from 5 to 50% v/v aqueous ACN in 0.2% v/v formic acid. The mass spectrometer was operated in data-dependent acquisition mode, recording high-accuracy and high-resolution survey Orbitrap spectra using external mass calibration, with a resolution of 60.000 and m/z range of 400-3000. The ten most intense multiply charged ions were sequentially fragmented by using collision induced dissociation and spectra of their fragments were recorded in the linear ion trap; after two fragmentations all precursors selected for dissociation were dynamically excluded for 60 s. The amino acid sequences of the resulting peptide fragments were obtained using Proteome Discoverer 1.3 (Thermo Scientific) and the Uniprot protein database (SEQUEST, Thermo Scientific). Search parameters included a precursor mass tolerance of 10 ppm and a fragment mass tolerance of 0.8 Da and peptides were searched with carbamidomethyl cysteine as a static modification and oxidized methionine as a dynamic modification.

4.2.2.8. Emulsion characterization

To prepare emulsions, 1 mL of corn oil and 3 mL of protein solution (2 mg/ml in 50 mM PBS containing 0.55 M KCl), were homogenised in Power Gen 1000 S1 (Fisher Scientific, Schwerte, Germany) for 1 min at setting 3. Sodium azide (0.01%) was added as an antimicrobial agent. Immediately after homogenization the emulsion was diluted 100-fold with 0.1% (w/v) sodium dodecyl sulphate (SDS) solution. The droplet size distribution of the emulsions was measured using laser light scattering analyzer Malvern Mastersizer 2000S (Malvern Instruments, Worcestershire, UK), performed at room temperature. The relative refractive index (*N*), i.e., the ratio of the refractive index of the emulsion droplets (1.47) to that of the dispersion medium (1.33), was 1.11. The emulsifying ability was assessed by checking the shape of the distributions and the value of the average droplet size ($d_{4,3}$), calculated as follows: $d_{4,3} = \sum n_i d_i^4 / \sum n_i d_i^3$, where n_i is the number of droplets with diameter d_i. The evolution of droplet size with time is the main parameter used to determine the emulsion stability due to instability phenomena that are affected by the droplet size. For this purpose, the changes in average droplet size ($\Delta\ d_{4,3}$) and size distributions after 3 days of storage at 4°C were evaluated.

4.2.2.9. Dynamic viscoelastic behaviour (DVB)

Dynamic rheological properties of NAM:GlcN conjugates and control samples (2 mg/mL protein in 50 mM PBS (pH 7.5) in the presence of 0.55 M KCl) were measured by oscillation tests. DVB upon thermal gelation was monitored on a controlled Physica MCR Rheometer (Anton Paar GmbH, Ashland, VA, USA) equipped with 25 mm parallel-plate geometry. The upper plate was lowered until the thickness of sample was adjusted to 1 mm and the excess was removed. Following this, the hood was lowered to prevent sample evaporation. The samples were heated from 10 to 80˚C at a rate of 2˚C min^{-1}. Preliminary amplitude sweeps over the range of γ = 0.1-

10% were used to determine the linear viscoelastic region (LVR). On the basis of this data, measurements were conducted by applying a controlled strain (0.5%) with a constant frequency set at 1 Hz. The storage modulus (G') and loss modulus (G'') were determined simultaneously throughout the heating.

4.2.2.10. Microscopy

Morphology of the internal structure of non-treated and glycosylated actomyosin was determined using a cryo-scanning electron microscopy (Cryo-SEM). In order to acquire better shape of the gel, the control and glycosylated samples (in 50 mM PBS, containing 0.55 M KCl) were concentrated to 8 mg/mL protein by dehydration in an Eppendorf Vacufuge concentrator (Brinkman Instruments, Westbury, NY, USA) for 6 h. The concentrated samples were then heated at 75 ˚C for 30 min (Cao et al. 2012). For the cryo-SEM, the gel samples were cut in small sizes with thicknesses of around 3 mm^3 and placed on the copper sample-holders. The copper holders were immersed in liquid nitrogen slush (-207˚C), then transferred into a cryo-preparation unit. The specimens were fractured with a blade in the preparation chamber and further warmed at -40˚C, 10^{-5} Torr vacuum for 30 min to sublime the water. Finally the fractured specimens were sputtered with gold coating (20 nm) and subjected to SEM (JEOL JSM-6301, JEOL Ltd., Tokyo, Japan). The samples were viewed under an accelerating voltage of 5 kV. Several digital images were collected at different magnifications.

4.2.2.11. Statistical analyses

Data were subjected to the Analysis of Variance (ANOVA) using the Statistical Analyses Software (SAS, Version 9.1, Cary, NC, USA). Comparison among means was evaluated by performing the studentized range test (Tukey's honestly significant difference test) at the 5% significance level.

4.3. Results and Discussion

4.3.1. Evaluation of protein glycosylation by MALDI-TOF/TOF-MS

The previous study (Chapter 3) revealed that the Maillard reaction between NAM and GlcN can occur at 25, 37 and 40˚C in relatively short time (8 h) and in a liquid environment. However, the extent of glycation was higher at 40˚C compared to 25 and 37˚C. Therefore, in order to minimize the impact of glycation and promote glycosylation the reactions should be conducted at the lower temperatures possible. For this reason 25 and 37˚C were chosen in this study.

The relative number of GlcN residues linked covalently to NAM was determined by MALDI-TOF/TOF-MS analyses. A mass increase of 162 Da between control (non-treated NAM) and glycosylated protein, accompanied by a loss of ammonia was attributed to GlcN attachment via TGase. A mass shift of + 161 Da indicated condensation between NAM and GlcN, and thus permitted the calculation of the amount of sugar attached as a result of non-enzymatic glycation (i.e. the Maillard reaction). Moreover, as shown in Chapter 3 possible liberation of ammonia during the reaction of NAM with GlcN may impact the molecular weight calculation for the resulting glycation product. Consequently, the calculation of adducts derived from the glycation reaction was performed in two ways: + 161 Da [(Peptide+GlcN)-H_2O] and + 144 Da [(Peptide+GlcN)-(H_2O+NH_3)].

Figure 4.1 represents an example of MALDI spectra obtained from NAM glycosylated with GlcN at 25 ˚C. The results from mass spectrometry, including controls (in the absence of enzyme), are summarised in Figure 4.2. The highest percentage of glycosylated peptides was found for NAM:GlcN (1:1) conjugates produced during the reaction at 37˚C, reaching 15% of the total peptides. No differences in percentages of glycosylated peptides derived from the

TGase-initiated reaction were observed among the other treatments, which on average corresponded to 10 % of the total peptides.

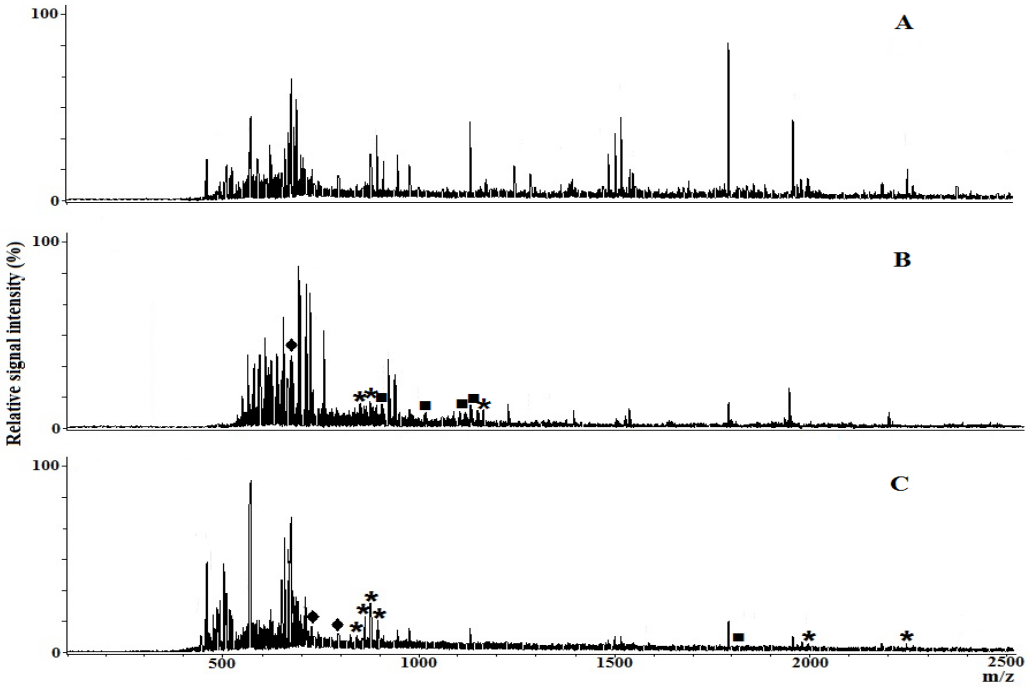

Figure 4.1. MALDI-TOF/TOF mass spectra of non-treated actomyosin (A), and actomyosin conjugated with glucosamine at 1:1 (B) or 1:3 (C) protein to sugar ratio via enzymatic reaction of TGase at 25˚C for 6 hours. The stars and filled squares refer to glycosylated or glycated peptides, respectively. Filled rhombuses indicated glycated peptides considering a release of 1 mol of H_2O and 1 mol of NH_3 during glycation with GlcN.

Mass spectrometry results showed that protein glycosylation can be achieved via an enzymatic reaction using TGase. This is the first study to demonstrate muscle protein glycosylation as a result of exploitating TGase. Jiang and Zhao (2010) reported GlcN incorporation into soybean protein isolates by the means of TGase; however the authors did not provide direct evidence that the glycoconjugates functionality improved due to the enzymatic reaction, rather than the Maillard one.

With respect to the Maillard reaction occurring concurrently with enzymatic glycosylation, higher relative percentages of glycated peptides were found when the reaction progressed at

37˚C as compared to those treatments performed at 25˚C (Figure 4.2). For instance, on average 5% of NAM peptides were glycated at 25˚C (average from both protein:sugar ratios) with a 4-fold percentage increase when 37˚C was used for glycosylation. It was found that at a 1:1 NAM:GlcN ratio and at 37˚C, the highest numbers of glycated peptides were produced from the Maillard reaction, reaching 23% of the total peptides.

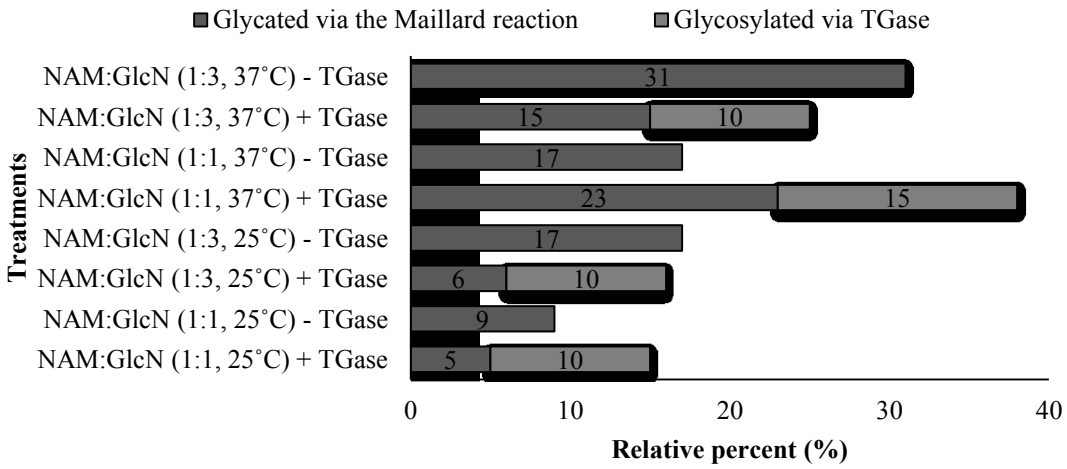

Figure 4.2. Relative percentages of glycation and glycosylation endowed to protein during the conjugation reaction at different reaction conditions. The percentages were calculated based on the data obtained from MALDI-TOF/TOF-MS analyses.

Figure 4.2 also provides deeper insight into the formation of glycoconjugation, showing not only the level of conjugation, but also how glycosylation and glycation compete during the conditions studied. In general, when conjugation is promoted by the addition of TGase, a reduction in glycation is observed. Specifically, at 25˚C, glycation was reduced by enzymatic glycosylation at both sugar concentrations. In contrast, at 37˚C (1:1, NAM:GlcN), the treatment with TGase resulted in an increased level of glycation. The reason for this specific observation is not immediately clear and deserves further investigation.

Even though AGEs were not determined, the moderate temperatures chosen in this study would be expected to reduce the formation of these products. For instance, in one study, Nε-

(Carboxymethyl) lysine (CML), one of the most abundant AGEs, was shown to increase significantly from 1.56 mmol/mol lysine at 35˚C to 11.09 mmol/mol lysine at 95˚C, with a sharp increase at 75˚C during 20 min heating in a glucose-lysine wet system (Fu et al. 2012). In the study conducted by Mottram et al. (2002), the temperature dependence of acrylamide, another Maillard reaction product, indicated its formation above 100˚C for 20 min. As mentioned previously, the competitiveness between enzymatic and non-enzymatic reaction also plays a role in AGEs formation. When TGase was included into the reaction mixture the amount of peptides derived from the Maillard reaction decreased in most of the treatments (except for 1:1 NAM:GlcN ratio at 37˚C).

Another advantage of using TGase-mediated glycosylation is the formation of a stable isopeptide bond between glucosamine and actomyosin (Greenberg et al. 1991) which would increase the stability of the glyconjugates during storage. The formation of glycoconjugates through Schiff base and Amadori rearrangement as a consequence of the Maillard reaction is not stable, and so would continue forming AGEs during storage (Tauer et al. 2004).

4.3.2. Confirmation of enzymatic glycosylation by Orbitrap-LC-MS

Since glycosylation by TGase is site-specific, an analytical technique that allows for confirmation of the occurrence of glycosylation as a result of the enzyme induced acyl-transfer reaction was required. Accurate mass capabilities and amino acid sequence information elucidated by Orbitrap-LC-MS allowed for assigning glycosylated sequences unambiguously by i) presence of glutamine (Q) in the NAM sequence and ii) comparison between non-treated and glycosylated peptide masses. The sequence information was subsequently used to verify that the glycosylated peptides were obtained specifically from the TGase-mediated reaction. The peptide sequence DSYVGDEA**Q**SK was identified in two treatments (1:1 NAM:GlcN ratio, 37˚C and

1:3 NAM:GlcN ratio, 25˚C) while the sequence I**Q**LVEEELDR was common to the treatments 1:1 NAM:GlcN ratio, 25˚C and 1:3 NAM:GlcN ratio, 25˚C. Peptides with the following sequences were identified in the treatment 1:3 NAM:GlcN ratio, 37˚C: IVESM**Q**STLDAEIR, VAE**Q**ELLDATER and DT**Q**IHLDDALR; none of them was similar to those identified in other treatments. Even though the primary sequence of protein is the same for all of the treatments, the secondary and tertiary structures, and thus the exposure of available glycosylation sites (Q) may be dependent upon protein conformation. The latter is linked to firstly reaction temperature and secondly to the sugar concentration (Rondeau et al. 2007). The incubation of NAM in presence of the higher amount of GlcN at 37˚C may have caused a different protein unfolding pattern and consequently a different exposure of glutamine residues. Moreover, recognizing that some of the sites may be glycated by the Maillard reaction (Figure 4.2), steric hindrance could partially block access to the nearby glutamine residues (Zheng et al. 2007), making it less accessible for TGase.

4.3.3. Effect of glycosylation on solubility

The solubility profiles derived from control and conjugated NAM are represented in Figure 4.3 A, B, C and D. In general, for control NAM the solubility at alkaline pHs was higher than at acidic pH likely due to the predominance of -COOH ionisable groups over -NH_2; as a matter of fact, it is known that the acidic amino acids glutamic and aspartic are higher compared to the basic ones in the myosin molecule (Pearson and Young, 1989). Therefore, additional effects on solubility due to glycosylation were expected to be more pronounced at alkaline pH values, rather than at acidic. However, a remarkable result was obtained in the treatment using a 1:1 NAM:GlcN ratio conjugated at 37˚C (Figure 4.3 C). For this treatment the solubility at pI increased from 8.7 to 34% as compared to non-treated NAM. Since the net charge of a protein at pI is zero, it is proposed that the solubility increase was primarily due to an increased

hydrophilicity conferred to the protein by GlcN attachment. The carbohydrate moiety of a glycosylated amino acid may have imposed a steric hindrance (Kihlberg and Elofsson, 1997), giving rise to protein solubility by preventing protein aggregation (Liu and Zhong, 2012).

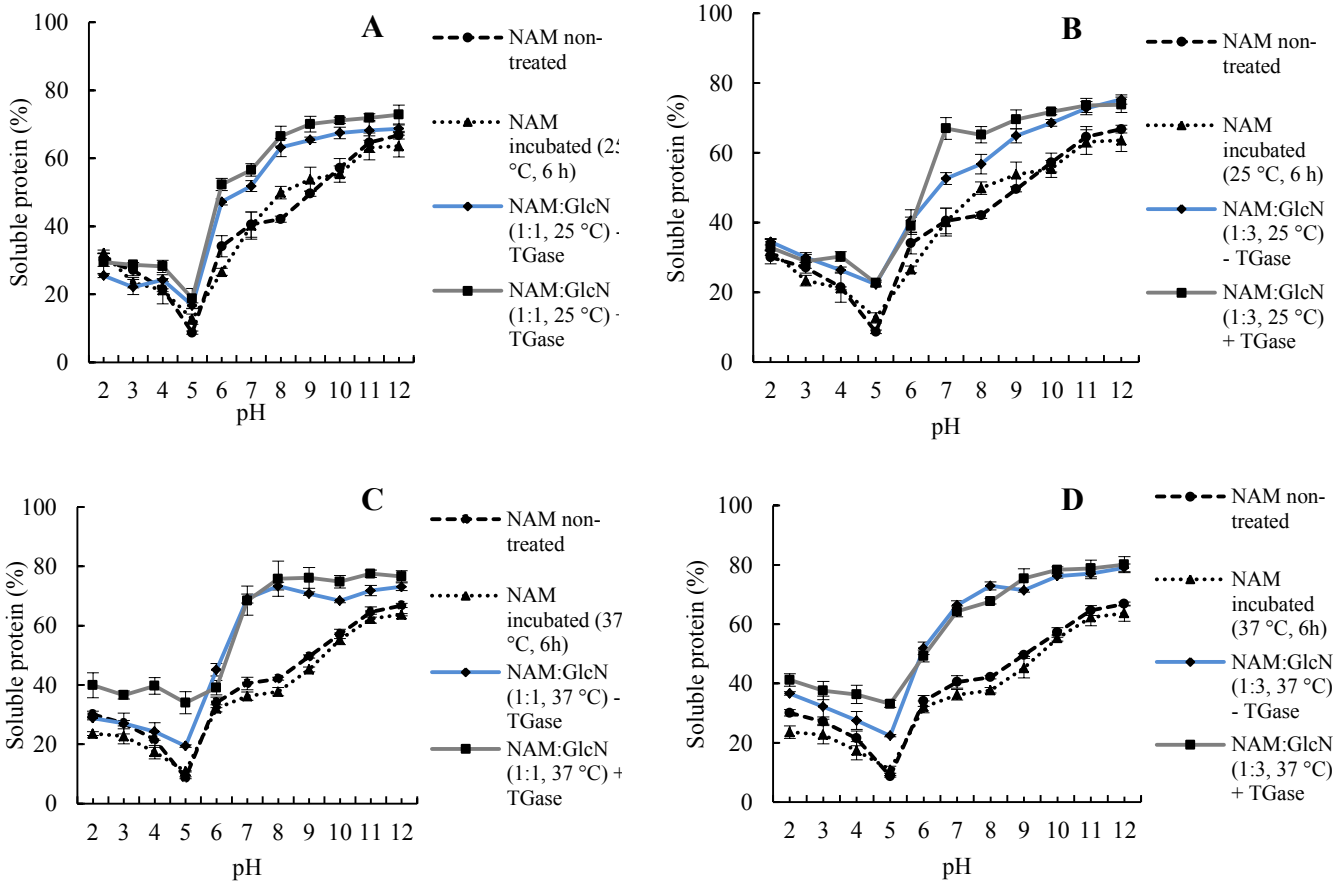

Figure 4.3. pH-dependent solubility profiles of controls and enzymatically glycosylated actomyosin at different conditions. Protein:sugar mixtures (1:1 or 1:3 ratio) were incubated at 25˚C (A, B) or 37˚C (C, D) for 6 h in the presence of TGase. Results are means of 3 independent experiments ± standard deviations.

Although a significant increase in solubility was found at pHs ranging from 7 to 10, this treatment also led to a substantial solubility increase at extreme acidic pHs. Based on the results from mass spectrometry, the highest level of glycoconjugation was also observed for this sample, accounting for 38%. Even though the extent of glycosylation was lower as compared to

glycation, the percentage of glycosylated peptides was the highest as compared to the other treatments (Figure 4.2). Therefore, the higher extent of glycoconjugation coupled with the highest level of enzymatic glycosylation made NAM more soluble at extreme acidic pHs. A possible explanation for this phenomenon could be an increased dissociation of the myosin chains as a consequence of the electrostatic repulsion from positively charged amino acids, which would be further increased by the additional effect of the hydrophilic GlcN moieties bound to NAM. In summary, in order to see a pronounced effect on the solubility of NAM under acidic conditions, which is desirable for food applications, higher levels of glycoconjugation need to be achieved.

When the sugar amount was increased to 3-fold over protein at the same reaction temperature (37˚C) (Figure 4.3 D), the large solubility improvement of TGase glycosylated NAM at extreme acidic and pI region was also obtained; however, there was a more pronounced influence from non-enzymatic conjugation (the Maillard reaction). This corresponds to results from mass spectrometry, where an increase in GlcN from 1 to 3 parts over NAM resulted in an increase in the amount of glycated peptides from 17 to 31%, respectively (Figure 4.2).

The same observation of the strong interference of the Maillard reaction on solubility was noticed when the reaction was conducted at 25˚C for both sugar ratios. There was no major difference in solubility between untreated and control-incubated NAM during the reactions at 25 and 37˚C. Also no large effect of protein to sugar ratio on solubility was found between non-treated and control-incubated NAM.

4.3.4. Emulsifying properties

As concluded from mass spectrometry and solubility analyses, enzymatic glycosylation was most effective at a 1:1 NAM:GlcN ratio. Even though higher number of glycoconjugates was found

for the reaction conducted at 37˚C, the reaction at 25˚C was also successful for glycoconjugation. For this reason, the emulsifying properties were evaluated for samples glycosylated at this specific ratio at both 25 and 37˚C reaction temperatures. Figure 4.4 illustrates the effect of glycosylation on the emulsion average particle size at different pHs (5.0 and 7.5) and times (0 and 3 d).

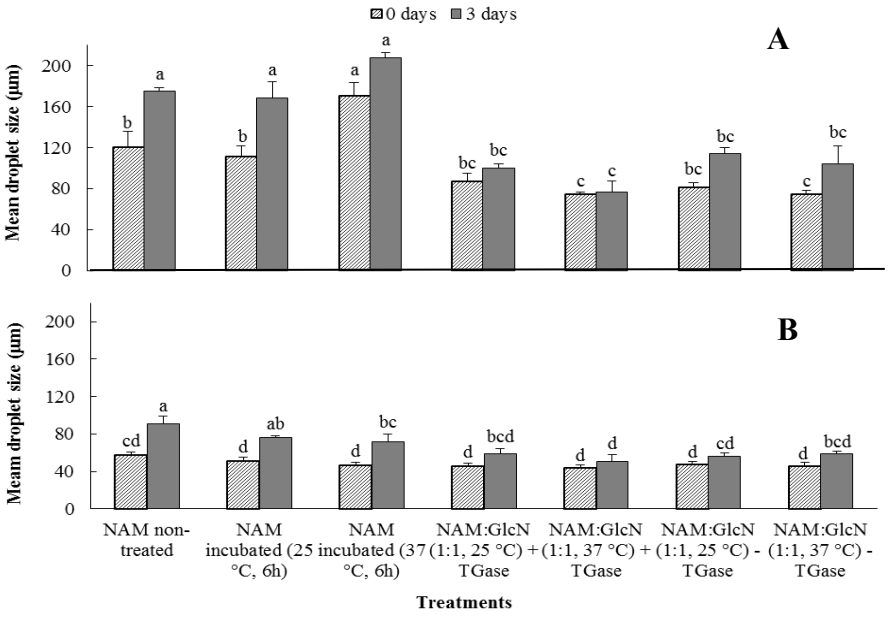

Figure 4.4. Mean values and standard deviations of the mean droplet size ($d_{4,3}$) at 0 and 3 days of storage ($\Delta\ d_{4,3}$) for non-treated and glycosylated NAM at pH 5.0 (A) and 7.5 (B). Means followed by the same letter do not differ each other ($p < 0.05$). Results are means of 3 independent experiments ± standard deviations.

The initial (0 d) average droplet size of non-treated and incubated NAM at pH 5.0 (Figure 4.4 A) was significantly higher ($p < 0.05$) as compared to those glycated and glycosylated NAM at 37˚C, indicating higher emulsifying ability of glycoconjugates (Nakamura et al. 2004). Even though no significant difference between glycated and glycosylated treatments was found, the glycoconjugates produced at 37°C showed the lowest average particle size. Three days of storage

caused a significant ($p < 0.05$) increase in particle size of non-treated NAM, suggesting its lower emulsion stability. In contrast, no significant changes ($p > 0.05$) occurred in the average particle size of glycated and glycosylated NAM at both temperatures. Moreover, the more stable emulsion ($\Delta\ d_{4,3}$ = 1.95 μm) was obtained for NAM enzymatically conjugated with GlcN at 37˚C, corresponding to the treatment where the highest amount of TGase-mediated glycosylation was found (Figure 4.2). The ability of glycoconjugates to form emulsions with higher stability could be attributed to improvement in protein solubility (Figure 4.3) and the formation of a sugar steric layer at the interface that provides stabilization against coalescence (Wong et al. 2011). An improvement in emulsifying properties at the pI appears especially promising for glycoprotein applications as potential emulsifiers.

Particle sizes of emulsions produced at pH 7.5 (Figure 4.4 B) were smaller than the particles prepared at pH 5.0 (Figure 4.4 A). This was expected as at pH 5.0 (the pI of NAM), since particles tend to flocculate due to a lack of electrostatic repulsion and particle dispersions are less stable. At 0 d, there was no significant difference among non-treated and NAM:GlcN conjugates. However, after 3 d of storage the particle size of non-treated NAM significantly ($p < 0.05$) increased, while glycoconjugates at both temperatures remained not statistically different from 0 d.

In order to gain more insight into the emulsion properties upon NAM glycosylation, particle size distribution was also compared among the treatments, where the most prominent impact on average particle size was found. In this respect, Figure 4.5 represents the particle size distribution (PSD) for NAM incubated (control) and glycosylated at 37°C at 0 and 3 d of storage at pH 5.0 (Figure 4.5 A) and 7.5 (Figure 4.5 B). PSD of control NAM at pH 5.0 was bimodal with peaks centered from 10 to 300 μm and 750 to 2200 μm. On the other hand, TGase-mediated

glycoconjugate particles presented unimodal distribution with sizes from 8 to 100 μm. These observations clearly correspond with the results presented in Figure 4.4 A, where significantly higher $d_{4,3}$ values were obtained for control-incubated NAM as compared to NAM glycosylated at 37°C. After storage, higher numbers of particles sized from 750-2200 μm appeared for control-incubated NAM, while very minor size increases in the region from 200 to 450 μm was observed for glycosylated NAM.

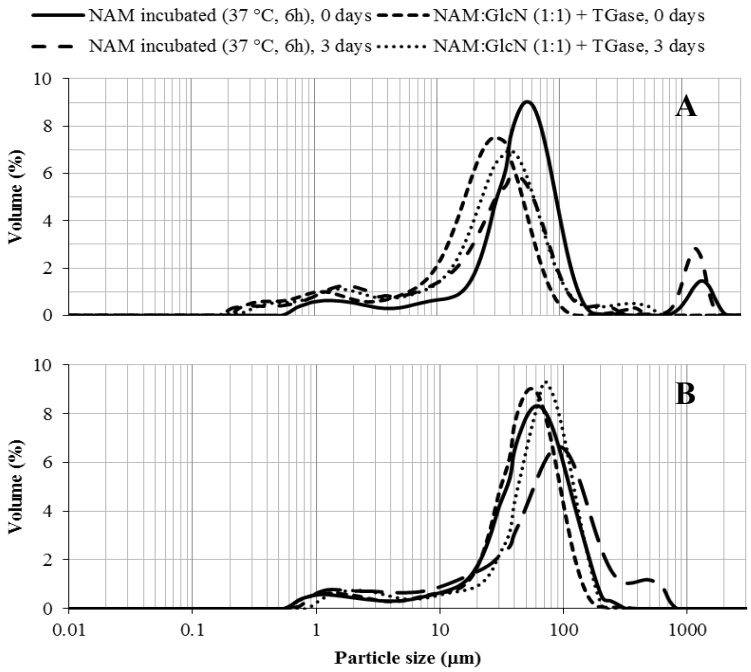

Figure 4.5. Particle size distribution profiles of control and glycosylated NAM at pH 5.0 (A) and 7.5 (B) determined initially and after 3 days of storage.

These results further confirm that glycosylation provides a stabilizing effect on the NAM emulsion against coalescence. As can be seen at pH 7.5 (Figure 4.5 B), the PSD of the emulsion prepared from control-incubated and glycosylated NAM were both monodispersed with an average size around 90 μm, probably due to the electrostatic force induced by protein charges at this pH. After storage, a new peak with particle sizes from around 360 to 630 μm appeared in

control-incubated NAM, while no peak was observed for glycosylated NAM, confirming the inferior stability of non-glycosylated proteins (Jourdain et al. 2008).

4.3.5. Dynamic rheological behaviour

Thermal gelation properties of NAM before and after conjugation with GlcN are shown in Figure 4.6 A and B.

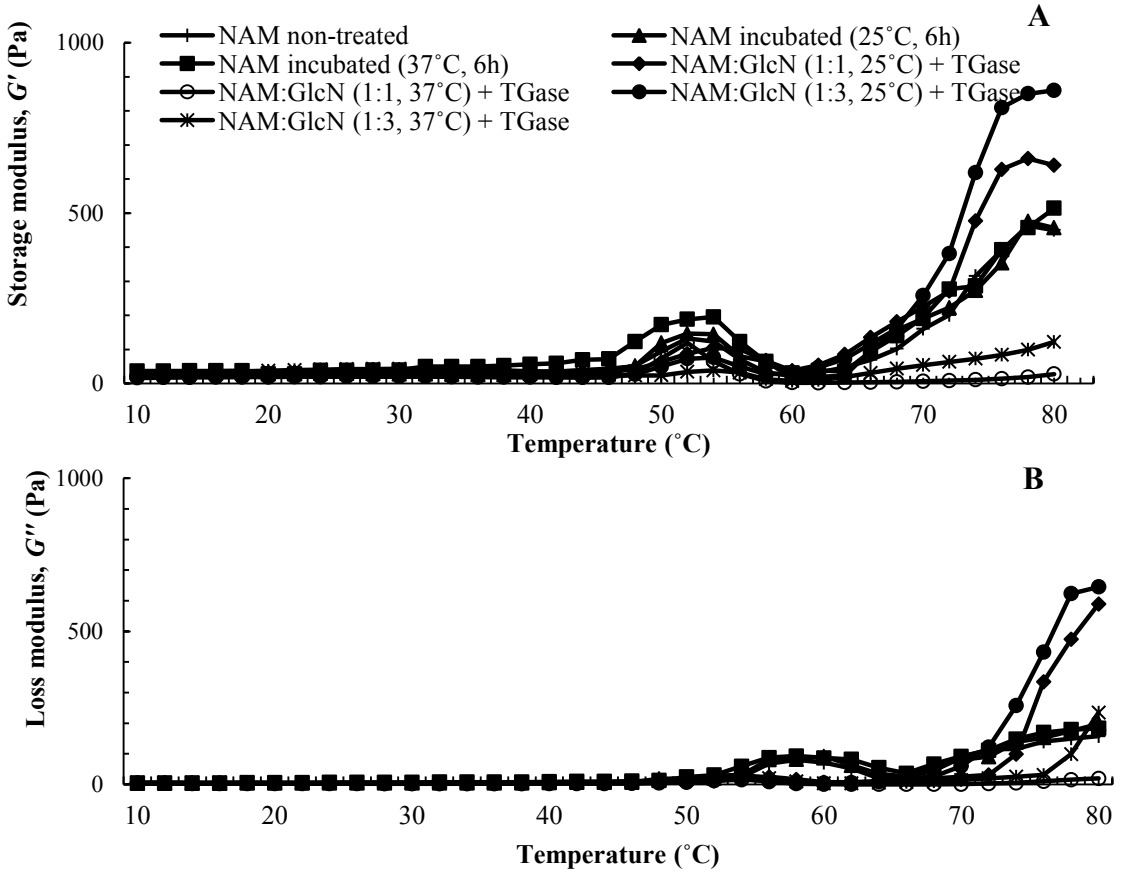

Figure 4.6. Changes in dynamic viscoelastic behaviour (DVB) of proteins glycosylated with GlcN by the mean of TGase at different conditions. The rheograms show storage modulus, *G′* (A) and loss modulus, *G″* (B) development during heating from 10 to 80˚C at 2˚C min^{-1}.

The development of storage moduli (*G′*) during heat-induced gelation of non-treated and control-incubated NAM could be virtually divided into three steps. *G′* of non-treated and control-incubated NAM started to rise with temperature increase, reaching a peak at 52-54˚C, associated with onset of gelation. The initial increase in *G′* of the control-incubated NAM (37˚C) was

observed at lower temperatures as compared to non-treated and NAM incubated at 25˚C. Incubation at higher temperatures (6 h, 37˚C) likely caused partial protein unfolding. An initial increase of G' indicated the first step of gelation, that could correspond to the protein unfolding and association of myosin filaments via hydrophobic interactions and disulfide linkages, resulting in the transformation from a viscous sol to an elastic network (Egelansdal et al. 1986). Upon further heating G' gradually decreased, reaching a minimum at 60˚C, indicating the second step of gelation. Similar behaviour was observed in chicken breast myosin (Xiong, 1997) and was postulated to be due to helix-to-coil transformation of myosin leading to a large increase in filamental fluidity. Markedly, descending of G' accompanied with an increase in G'' (liquid-like behaviour) (Figure 4.6 B), confirmed the onset of protein denaturation (unfolding) which enhanced the viscous component of non-treated and incubated NAM (Tahergorabi and Jaczynski, 2012). In addition, G'' for NAM incubated at 37˚C was higher in comparison to other controls, confirming higher protein unfolding at lower temperatures. Strasburg et al. (2008) also reported that at 50-60˚C conformational changes in light meromyosin (LMM) lead to formation of an open structure exposing hydrophobic regions and specific side chain groups, and leading to a decrease in G'. In addition, the drop in G' at these intermediate temperatures may be also related to dissociation of the actomyosin complex. The decline of G' after reaching the first peak has also been reported in fish myosin (Yongsawatdigul and Park, 1999) and chicken myofibrillar proteins (Xiong and Blanchard, 1994). Upon a further rise in temperature, the G' increased until 80˚C (3rd gelation step), indicating a structure build-up attributed to the formation of a permanent and irreversible protein network structure, initiated by the association of LMM via tail-to-tail interactions by the application of thermal energy. At 80˚C the magnitude of G' was considerably higher than that of the peak at 52˚C, suggesting higher elastic properties at the end of heat-

induced gelation. The G' pattern for NAM shown in this figure is very similar to the result of fish actomyosin (Benjakul et al. 2001).

Glycoconjugation strongly impacted the three different phases of thermal gelation. At the beginning of gelation the magnitude of G' (Figure 4.6 A) development for glycosylated samples was lower as compared to non-glycosylated NAM. For instance, at 52˚C the maximum G' value for non-treated NAM was reaching 133 Pa as compared to 78 Pa on average for glycoconjugates. Moreover, non-treated NAM reached the peak at a lower temperature than glycosylated, except for the reaction with 1:1 NAM:GlcN, at 37˚C. This implies that protein glycosylation increases thermodynamic stability by preventing unfolding of myosin globular heads and their further association. This consequently delays protein denaturation, impacting the progress of gelation. Joao et al. (1992) related the increased thermostability of glycosylated RNase to a decrease in structural mobility, rendering the protein more resistant to aggregation. Notably, the local effect from glycosylation could be transferred throughout the whole protein structure. Gervais et al. (1997) came to the same conclusion while studying the structural dynamics of glycosylated recombinant human granulocyte-colony-stimulating factor by using NMR spectroscopy. Among glycosylated samples the lowest G' was found for the samples treated at 37˚C at 1:3 NAM:GlcN ratio. In addition, the shift in maximum G' temperature was also found for this sample. This suggests that high amounts of carbohydrate moieties attached by glycation/glycosylation have a strong influence on gelation patterns, by protecting NAM from unfolding at lower temperatures. For instance, Sola et al. (1997) reported that increases in the degree of glycosylation shifted the maximum gelation temperatures to higher values. Protein aggregation at these temperatures was possibly prevented by stronger steric repulsions between NAM molecules due to the presence of higher amounts of GlcN on its surface, acting as molecular spacers (Baudys et al. 1995; Sola et

al., 1997). As heating proceeded to the final temperatures, NAM conjugated with GlcN at 25˚C exhibited higher G' (760 Pa on average for both sugar ratios) as compared to that of non-glycosylated protein (436 Pa). In contrast, the glycoconjugates produced at 37˚C may require higher temperatures in order to start the formation of the gel.

Only a slight increase in G'' (Figure 4.6 B) was observed for glycosylated NAM until the temperature reached ~70˚C, where G'' increased rapidly. This is in agreement with G', where less protein unfolding below 70˚C, lead to low viscosity of glycoconjugates. An additional temperature increase to 80˚C revealed that G'' was the highest for NAM conjugated with GlcN via TGase at 25˚C.

4.3.6. Impact of glycosylation on NAM gels microstructure

Even though rheological analysis is an important analytical technique for understanding gelling properties of glycosylated NAM it is also important to elucidate the relationship between rheological properties and gel structure, as well as visualising changes in the gel microstructure upon glycosylation. Gels are a challenge to prepare for electron microscopy by conventional methods due to their high water content. In contrast, cryo-SEM has been shown to preserve the fine microstructure of the samples since water within the sample is rapidly (~10 ms) frozen with liquid N_2, limiting ice-crystal formation (Dykstra, 1992). Partial water removal by controlled sublimation can significantly reduce sample distortion due to the dehydration process (Echlin, 1992). The microstructures of non-treated and glycosylated NAM at different reaction conditions are presented in Figure 4.7. In all the micrographs, the dark grey portions are protein strands and the black (empty) areas would be mainly occupied by water. Honeycomb structures appeared in non-treated samples and the samples enzymatically glycosylated at 25˚C at both GlcN ratios.

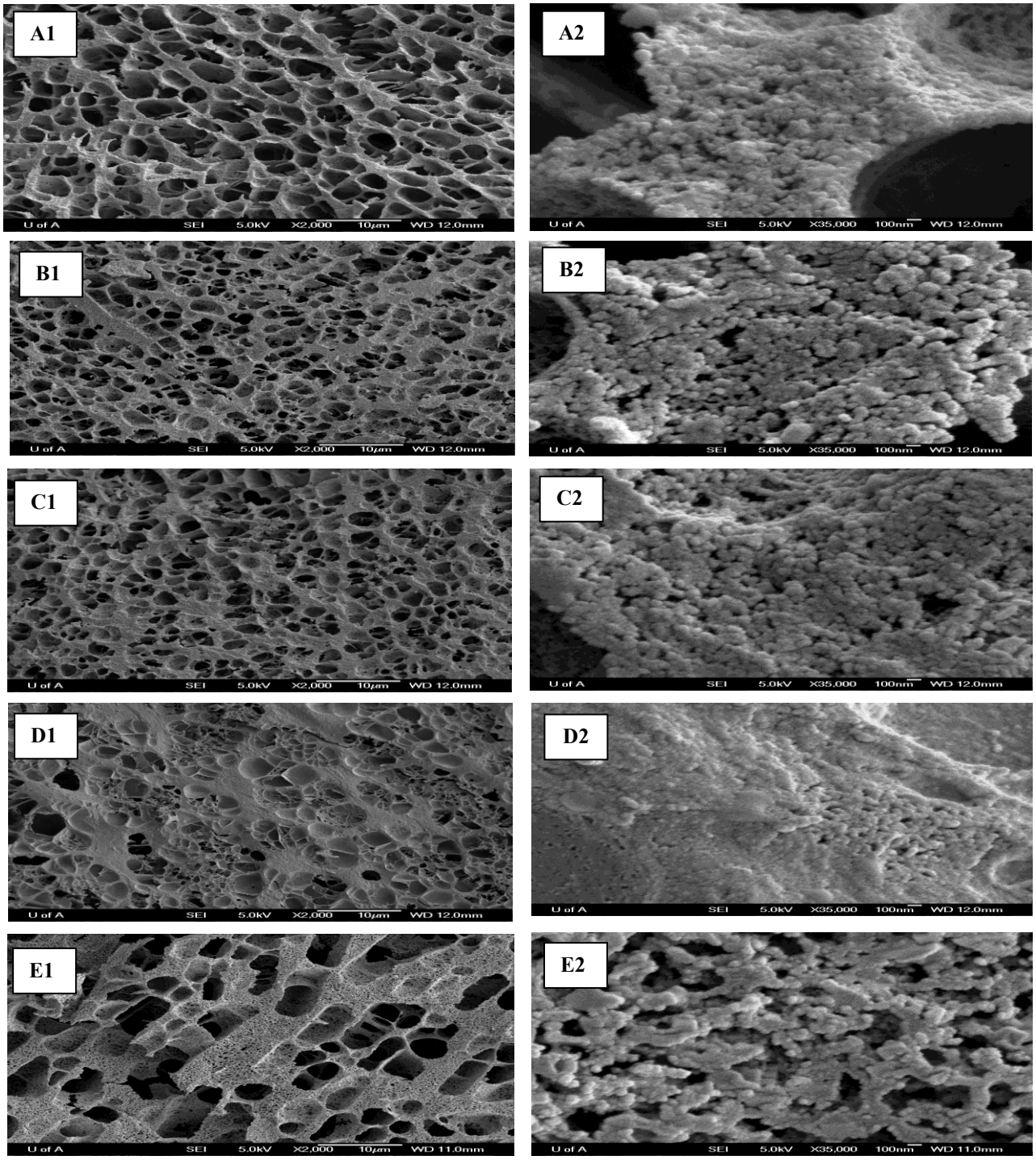

Figure 4.7. Cryo-scanning electron microscopy images of the gels produced from non-treated and glycosylated actomyosin after slush of the sample with liquid nitrogen at the atmospheric pressure. The scale bars are 10 μm (A1, B1, C1, D1, E1) and 100 nm (A2, B2, C2, D2, E2) in length. Non-treated actomyosin (A) and NAM:GlcN conjugates (1:1 or 1:3 ratio) were incubated at 25˚C (B, C) or 37˚C (D, E) for 6 h in the presence of TGase.

However, the structural units of the honeycomb network of non-treated samples were larger and characterized by higher elongation. The larger pore size and higher uniformity of non-treated NAM is particularly evident at high magnification of × 35.000 (Figure 4.7 A1). This may imply that non-treated NAM was able to form a fine protein network, which was capable of high water entrapment. These results were consistent with the rheological data (Figure 4.6 A), where the highest G' was observed for this sample at the temperature range from around 45 to 55˚C. No major difference was noticeable between samples produced at 25˚C with different NAM:GlcN ratios (Figure 4.7 C1 and D1). Only high magnification at × 35.000 (Figure 4.7 C2 and D2) could detect less dense and thinner-stranded structure of glycoconjugates at a 1:1 NAM:GlcN ratio as compared to those at a 1:3 NAM:GlcN ratio. Moreover, at a 1:3 NAM:GlcN ratio the proportion of pores with small size shifted to a population with extra small pores in comparison to glycoconjugates produced at a 1:1 NAM:GlcN ratio. This suggests that higher amounts of attached GlcN moieties result in gels with higher rigidity.

Enormous differences were observed in the microstructure of gels from the glycoconjugates produced during the reaction at 37˚C with a 1:1 NAM:GlcN ratio. The formation of a highly dense network with a more closed nature and a significant decrease in porosity was observed for this treatment. This is in accordance with the results of the dynamic viscoelastic behaviour, where the lowest gel elasticity at the end of the thermal gelation was observed (Figure 4.6 A). This suggests that high amounts of sugar residues grafted to protein by the TGase reaction, as confirmed by mass spectrometry analyses (Figure 4.2), prevents the latter from unfolding, the primary step responsible for gel matrix formation. This consequently interrupts the gelation process overall (Figure 4.6 A) and possibly describes different dynamics of unfolding and/or aggregation as compared to non-treated NAM. Increasing the sugar amount to 3 parts over

protein at the same reaction temperature resulted in a gel network characterized by wall-like structures among the strands and high internal integrity. The presence of minor pockets may be indicative of GlcN content in the sample network, minimizing protein-protein interactions (Lillard et al. 2009). These results coincided with the lowest *G′* at the temperature range from 45 to 55˚C and the second lowest at the end of the gelling. All this suggests that structural modification induced by GlcN attachment strongly determined the microstructure and consequently the rheological behaviour of the gel.

4.4. Conclusions

This study successfully demonstrated enzymatic muscle protein glycosylation using TGase. The optimized method results in an increase in protein solubility, a key functional attribute for industrial applications. Significant improvement in emulsifying properties of actomyosin glycoconjugates has strong potential for use as food emulsifiers. Current work showed that sugar attachment using TGase as catalysts can be achieved at lower temperatures and faster times as compared to those used for glycation. These in consequence lead to less protein denaturation. Glycosylation impacted rheological properties of actomyosin by delaying thermal aggregation. Cryo-SEM of glycosylated NAM gels elucidated differences in gel structure upon glycosylation at different conditions, confirming that higher levels of glycosylation result in weaker gel structures as determined by rheological analysis.

CHAPTER 5. Studies on the formation of Maillard and caramelization products from glucosamine incubated at 37˚C.

5.1. Introduciton

N-acetyl-glucosamine (GlcNAc, 2-acetamido-2-deoxy-D-glucose) is an essential component of mucopolysaccharides and chitin. Glycosaminoglycans (GAGs; mucopolysaccharides) are large complexes of negatively charged carbohydrate chains that are incorporated into mucous secretions, connective tissue, skin, tendons, ligaments and cartilage (Anderson et al. 2005). Deacetylation of GlcNAc leads to the formation of glucosamine, (GlcN, 2-amino-2-deoxy-D-glucose), an amino monosaccharide used by North American consumers as a dietary supplement to both reduce osteoarthritis pain and improve joint function (Block et al. 2010). It is believed that GlcN supplementation may stimulate synovial production of hyaluronic acid (HA) (Uitterlinden et al. 2008), a type of GAG responsible for the lubricating and shock-absorbing properties of synovial fluid in cartilage (Qu et al. 2006). For the industrial production of GlcN, chitin (Einbu and Varum, 2008) or chitosan, by-products of the shellfish processing industry, can be used as a starting material (Sibi et al. 2013). Different products are available on the market; the most common are GlcN sulfate ($GlcN{\cdot}SO_4$), GlcN-hydrochloride ($GlcN{\cdot}HCl$) and *N*-acetyl-glucosamine. In nature, amino monosaccharides biosynthesis is controlled by the hexosamine biosynthesis pathway (HBP), where GlcNAc is produced and used in several metabolic processes such as post-translational modification of proteins and GAGs synthesis (Schleicher et al. 2000). In mammalian species, for instance, glucosamine-6-phosphate (GlcN-6-P) is produced from the reaction between fructose-6-phosphate, obtained through glycolysis, and a glutamine residue due to the action of glutamine:fructose-6-phosphate-amidotransferase (GFAT). With exogenous GlcN, it is rapidly phosphorylated by hexokinase yielding GlcN-6-P. Following phosphorylation, GlcN-6-P is then *N*-acetylated to *N*-acetyl-GlcN-6-P via acetyl-CoA-mediated

reaction and consequently converted to UDP-GlcNAc, a precursor in synthesis of GAGs, proteoglycans and glycoproteins (i.e. *O*- and *N*-linked glycosylation) (Salazar et al. 2014). On the other hand, commercial production of chitosan oligosaccharide (COS) and GlcN are normally obtained by the deacetylation and hydrolysis of chitin, where the natural amide form is converted into an amino saccharides where the $–NH_2$ is free. Hence, chemically deacetylated GlcN is an equivalent aldosamine to the one firstly obtained by the German chemists Heyns and Koch in the early 1950's from the reaction of D-fructose with ammonia (Heyns and Koch, 1952). The Maillard reaction produces Amadori and Heyns rearrangements forming fructosamine (1-amino-1-deoxy-ketose) or glucosamine (2-amino-2-deoxy-aldose), depending if the initial sugar is an aldose (i.e. glucose) or a ketose (i.e. fructose), respectively. It is known that Amadori and Heyns compounds are unstable products undergoing enolization or oxidation reactions (Mottram and Elmore, 2010). On the contrary, GlcNAc, the amide derivative of GlcN, is a less reactive molecule due to the stabilizing effect of the acetylation on the free amino group.

Due to the popularity of GlcN to treat osteoarthritis, research on this compound has dramatically increased to demonstrate other activities. For instance, in addition to its chondro-protective action, several studies have reported an inhibitory effect of GlcN on different types of tumors in both humans and animals (Song et al. 2014; Chesnokov et al. 2014). The anti-tumor activity is postulated to be a selective effect on nucleic acid synthesis *in vivo*, since RNA and DNA synthesis in treated tumors were significantly inhibited, or alternatively, due to the alteration of glycosylation on the surface of target proteins (Kantor et al. 2013).

In food applications GlcN has been used to generate antimicrobial, antioxidant (Wu et al. 2014) and taste-enhancing compounds (Katsumata et al. 2008); to enrich beverages (Kralovec and Barrow, 2008) or milk (Uzzan et al. 207) and to modify proteins to enhance their functionality in

food systems. For instance, as per results described in Chapter 3 advantage of GlcN higher reactivity was taken to create novel glycoproteins at moderate temperatures resulting in an enhanced solubility and emulsification capacity.

At the same time, studies have reported a link between GlcN supplementation and diabetes complications (Nakamura et al. 2001; Hawkins et al. 1996) presumably due to GlcN-induced beta cell apoptosis and dysfunction (Zhang et al. 2010). Furthermore, Candiano et al. (1988) indicated that GlcN possesses reactivity at physiological temperatures producing fluorescent pyrazines compounds derived from the cyclocondensation between two GlcN molecules, which were later reported to cause DNA strand breakage (Kashige et al. 1995).

Some of the GlcN`s effects, for instance taste-enhancing and antimicrobial properties as well as protein modifications, are likely related to its high reactivity; however, to date no plausible explanations for this phenomenon have been provided. It is also surprising that only a few studies have focused on GlcN degradation at moderate temperatures (i.e. 37ºC) (Zhang et al. 2003; Horowitz, 1991) and, to best of our knowledge, no research has evaluated the formation of α-dicarbonyls (α-DCs) from this popular dietary supplement. It was expected that GlcN, a Heyns/Amadori-like compound, would rapidly form reactive intermediates like α-DCs and several advanced and stable condensation products as compared to GlcNAc. Hence, the main objective of this study was to investigate the chemistry of GlcN degradation *in vitro* (non-enzymatic degradation) and to compare it to GlcNAc and a reaction mixture containing Glc+NH_3 (Glc-NH_3). To meet this objective GlcNAc, Glc-NH_3 and GlcN were incubated at 37°C and α-DC were analyzed over time using liquid chromatography and Orbitrap mass spectrometry. Condensation products were also evaluated over time using both spectroscopic and mass spectrometric techniques.

5.2. Materials and Methods

5.2.1. Chemicals

N-acetyl-D-glucosamine (≥99% purity), D-glucose (≥99.5% purity), D-glucosamine hydrochloride (≥99% purity), potassium phosphate monobasic and dibasic, sodium azide, HPLC-grade solvents (acetonitrile, methanol, formic acid), glucosone (2-keto-D-glucose; ≥98.0% purity; M_W 178.14 Da), glyoxal (ethanedial; 40% in H_2O; M_W 58.04 Da), methylglyoxal (2-oxopropanal; 40% in H_2O; M_W 72.06 Da), diacetyl (butane-2,3-dione; ≥95.0% purity; M_W 86.09 Da) and 1,2-diaminobenzene were purchased from Sigma-Aldrich (St. Louis, MO). 3-deoxyglucosone (3-Deoxy-D-erythro-hexosulose; ≥95% purity; M_W 162.14 Da) was obtained from Cayman Chemical (Ann Arbor, MI). Ammonium hydroxide was purchased from Fisher Scientific. SPE tC-18 Sep-Pak Vac 6 cc columns were obtained from Waters (Milford, MA). Filtration membranes (0.22 μm) were from Millipore (Billerica, MA). Standard ion calibration solution (Pierce LTQ) for electrospray ionization in positive mode was purchased from Thermo Scientific (Rockford, IL, USA). All buffers and reaction mixtures were prepared with Milli-Q purified distilled water (Millipore, Bedford, MA, USA).

5.2.2. Experimental design

In this study the non-enzymatic degradation of GlcN, GlcNAc and Glc-NH_3 was evaluated over time at 0, 0.5, 1, 2, 3, 6 and 12 d in phosphate buffer at 37°C using UV/Vis and fluorescence spectroscopic analyses as well as mass spectrometric techniques. In the first part of the study, UV/Vis and fluorescence profiles were assessed over time to understand the major changes occurring during the degradation reaction of the monosaccharides. In this regard, a total of 42 tubes (2 tubes × monosaccharide × incubation time) were randomly placed within the incubator and the reaction was monitored over time. Three independent trials were conducted resulting in 6 replicates per treatment.

Since this exploratory test showed minimal changes in spectroscopic analyses in GlcNAc and Glc-NH_3 treatments, a dedicated study on α-DCs identification and production in GlcN samples was conducted using the same design as reported before. Liquid chromatographic separations and mass spectrometry techniques were used to identify and quantify the major degradation products. Finally, the last part of this study focused on the production of fluorescent and stable condensation products obtained by the reaction between the main α-DCs produced during GlcN degradation and GlcN. In this regard, selected α-DCs (glucosone (G), 3-deoxyglucosone (3-DG), glyoxal (GO) and methylglyoxal (MGO) were incubated with GlcN at equimolar concentrations for 0, 4, 8, 12, 24 and 48 h at 37°C, and their UV/Vis and fluorescence profiles recorded. Three tubes per selected α-DCs were incubated over time resulting in 6 replicates.

5.2.3. Incubation of GlcNAc, Glc-NH_3 and GlcN aliquots

15 mg/mL solutions of GlcNAc, Glc-NH_3 (equimolar mixture) and GlcN were prepared in 50 mM phosphate buffer. The pH of the final solutions, 7.4, was adjusted (Denver Instrument UltraBasic pH Meter) if necessary. NaN_3 was added to a final concentration of 0.02% to prevent microbial growth. The reaction mixtures were transferred into plastic screw-cap tubes, randomly arranged within an incubator (New Brunswick Scientific, Edison, NJ) and incubated at 37˚C. Samples aliquots were collected at 0.5, 1, 2, 3, 6 and 12 days. The controls were reaction solutions at zero hours. The pH value of the solution over time was monitored, but not adjusted during the reaction to enable a natural time course generation of reaction's reactive intermediates. Decrease in pH within 0.3-0.45/0.5 units was found for GlcN (6-12 reaction days, respectively) and 0.1 unit Glc-NH_3 solutions (12 reaction days).

5.2.4. Preparation of α-dicarbonyls and glucosamine reaction mixtures

Equimolar (2.5 mM) concentrations of GlcN and commercially available standards of G, 3-DG, GO and MGO were solubilized in 50 mM phosphate buffer (pH 7.4), containing 0.02% NaN_3. Controls included fresh and incubated solutions of GlcN and each α-DCs separately. All reaction mixtures were incubated at 37°C for 4, 8, 12, 24 and 48 h.

5.2.5. Spectrophotometric measurements

UV-Vis absorbance and fluorescence spectra of 15 mg/mL solutions of GlcNAc, Glc-NH_3 and GlcN were recorded using the Spectramax M5 multi-mode microplate reader (Molecular Devices, Sunnyvale, CA). For both analyses readings were taken with 1-cm quartz cuvettes and samples diluted (1:20, v/v) with 50 mM phosphate buffer (pH 7.4). The absorbance was recorded in the range of 200 to 500 nm. For fluorescence, the excitation wavelength was set at 347 and an emission was recorded from 364 to 600 nm. A blank (buffer) was subtracted from all spectra automatically. Absorbance (200-600 nm) and fluorescence (λ_{exc} = 347, λ_{em} = 364-600) of α-DCs standards separately or in the mixture with GlcN were measured in the same way at the concentration of 2.5 mM. For all GlcN-α-DCs mixtures, controls of incubated GlcN and respective incubated α-DCs for each time periods were subtracted.

5.2.5. Free α-dicarbonyl compounds: extraction, identification and quantitation

5.2.5.1. Solid-phase extraction (SPE) and derivatization procedure

The extraction procedure was based on a method reported by Papetti et al. (2014) with slight modification. Briefly, collected over time aliquots of GlcNAc, Glc-NH_3 and GlcN were spiked with 0.006 g of 1,2-diaminobenzene (*o*-phenylenediamine (OPD)), leading to the formation of the quinoxaline derivatives (Figure 5.1). pH was adjusted to 3.00 ± 0.02 with 4 M HCl and derivatized at 37°C for 1 h.

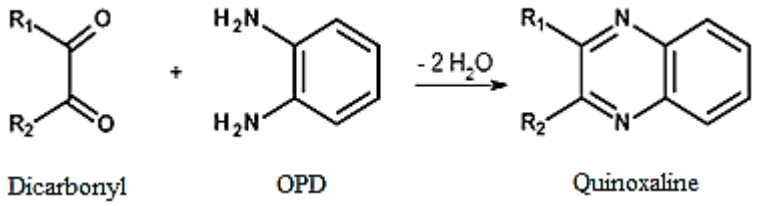

Figure 5.1. Derivatization reaction of α-dicarbonyl compounds with *o*-phenylenediamine (OPD) to give their corresponding quinoxalines.

The derivatized solution was passed through a preconditioned SPE cartridge (tC-18 Sep-Pak, Waters, Milford, MA, USA). The cartridge was washed with 2 mL of water, and quinoxalines were eluted with 4 mL of a MeOH/H_2O mixture (90/10, v/v) at a flow rate close to 2 mL/min. The first 1 mL was discarded, whereas the next 2 mL were used for analysis. The controls were treated exactly as collected sugar aliquots except no derivatizing agent was added. To ensure complete derivatization, a preliminary test was performed, where derivatization times of 0.5, 1, 2, 4 and 8 h were tested. The maximum peak area was reached after a derivatization for 1 h without further increase during the following longer derivatization time.

5.2.5.2. UHPLC–UV analysis of quinoxalines derivatives formed from α-dicarbonyl compounds and o-phenylenediamine

α-DCs analysis was conducted using an Ultrahigh Performance Liquid Chromatography apparatus (Shimadzu, Columbia, MD) consisting of two pumps LC-30AD, an SPD-M20A photo diode array detector (PDA), DGU–20A5 degasser, SIL–30AC autosampler (operated at 4°C) and CTO-20 AC column oven. The UHPLC system was controlled by a personal computer equipped with LabSolutions software operating in a Windows XP. The separation was achieved following the method described by Papetti et al. (2014) using Ascentis Express ES-C18 column (150 × 4.6 mm, 2.7 µm particles; Sigma-Aldrich, St. Louis, MO) with a UHPLC pre-column filter (UltraShield Analytical Scientific Instruments, Richmond, CA) operating at 25.0 ± 0.5°C and a flow rate of 0.3 mL/min. The binary mobile phase consisted of (A) 0.1% formic acid in water

and (B) methanol. The 120 min gradient is described as follows: 0–5 min (90–85% A), 5–13 min (85–80% A), 13–40 min (80% A), 40–65 min (80–70% A), 65–90 min (70–50% A), 90–100 min (50–0% A), 100–105 min (0% A), and 105–110 min (0–90% A); the column was then re-equilibrated with the initial mobile phase for 10 min. The injection volume was 5 μL. The PDA detector was set at 314 and 335 nm to record the peaks, and UV spectra recorded from 215 to 420 nm. Before injection sample solutions were filtered with PVDF syringe filter (13 mm, 0.22 μm; Millipore Millex, Billerica, MA, USA).

5.2.5.3. Identification and quantitation of quinoxaline derivatives

The identification of major α-DCs was based on comparison of their retention times of the reference compounds (quinoxalines derivatives of G, 3-DG, GO, MGO and DA) and spectral characteristics. For unequivocal identification of the major α-DCs, ten UHPLC peaks were manually collected and subjected to mass spectrometry analyses. The accurate mass and MS^n fragmentation patterns were compared to authentic standards and to the reference data. Mass spectrometry analyses were performed in duplicates.

For quantitation external calibration was used. Each quinoxaline derivative was diluted to the final concentrations ranging from 60 - 2000 (G), 30 - 2000 (3-DG), 4.5 - 50 (GO), 1.0 - 10 (MGO), and 1.25 - 7.5 μM for DA. Calibration curves were prepared for each trial and each concentration was analyzed in triplicate. The peak area was plotted against concentration and the regression equations were calculated. The correlation coefficients for all calibration curves were $R^2 \geq 0.999$. The average (from three trials) limit of detection (LOD) was calculated as 2.15 ± 0.07 (G), 0.27 ± 0.00 (3-DG), 0.13 ± 0.00 (GO), 0.09 ± 0.00 (MGO) and 0.18 ± 0.00 μM (DA). The average limit of quantification (LOQ) was determined as 6.52 ± 0.21 (G), 0.81 ± 0.01 (3-DG), 0.39 ± 0.01 (GO), 0.27 ± 0.01 (MGO), and 0.55 ± 0.02 μM (DA) by assuming a signal-to-noise

ratio (S/N) 3:1 for LOD and S/N 10:1 for LOQ. The following ranges of sample concentrations (in μM) were extrapolated from the calibration curves: 179 - 667 (G), 76 - 1290 (3-DG), 8.7 - 27 (GO), 2.8 - 6.5 (MGO) and 1.9 - 3.5 (DA). These values were then expressed as mg/kg GlcN.

5.2.5.4. Direct infusion orbitrap mass spectrometry analyses (DIMS)

Collected α-DCs fractions from UHPLC and GlcN aliquots (diluted in 50:50 (methanol:water, v/v)) were subjected to DIMS. All Orbitrap measurements were carried out by using the Ion Max electron spray ionization (ESI) source (Thermo Fisher Scientific) mounted on a LTQ Orbitrap XL (Thermo Scientific, San Jose, CA, USA). The Orbitrap mass analyzer was calibrated with standard ion calibration solutions (Pierce LTQ, Thermo Scientific). Following parameters were applied: sheath gas flow 15 arbitrary units, auxiliary gas flow 5 arbitrary units, and capillary temperature of 275°C. Samples (3 μl) were injected manually performing direct infusion using 100 μl syringe (Hamilton, Reno, NV, USA) and the on board syringe pump. DIMS analyses were performed at a mass resolution of 60.000 at m/z 400 and spectra were acquired over the range of m/z 50 - 2000. The automatic gain control (AGC) target was set to 1e6 and the maximum injection time to 250 ms. For MS/MS experiments, ions of interest were isolated with an isolation width of 1-2 Da and collision induced dissociation was conducted at varying voltages which were optimized for each sample. An activation time of 30 ms was used with a tube lens voltage of 110 V and a capillary temperature of 275°C. Data acquisition and processing were performed using Xcalibur software (Thermo Scientific).

5.2.6. Statistical analysis

Spectroscopic profiles obtained from UV/Vis and fluorescence analyses from the three different independent trials were averaged and reported as graphs. α-DCs production over time was subjected to the analysis of variance (ANOVA) using the PROC MIXED procedure of SAS (v.

9.3, SAS Institute Inc., Cary, NC). The model tested incubation time as a fixed variable and used the trial replication as a random variable. Tukey's honest significant difference ($p < 0.05$) multiple range test was conducted to determine differences between means.

5.3. Results and Discussion

5.3.1. UV-Vis and fluorescence profiles of non-enzymatic modification of GlcNAc, Glc-NH_3 and GlcN over time

UV-Vis and fluorescent profiles can be a useful and simple tool to understand the major changes occurring during a reaction. Solutions of GlcNAc, Glc-NH_3 and GlcN were incubated at 37°C in phosphate buffer from 0 to 12 days and their UV-Vis absorbance and fluorescence profiles (Figure 5.2 A and B) were recorded to monitor their stability over time.

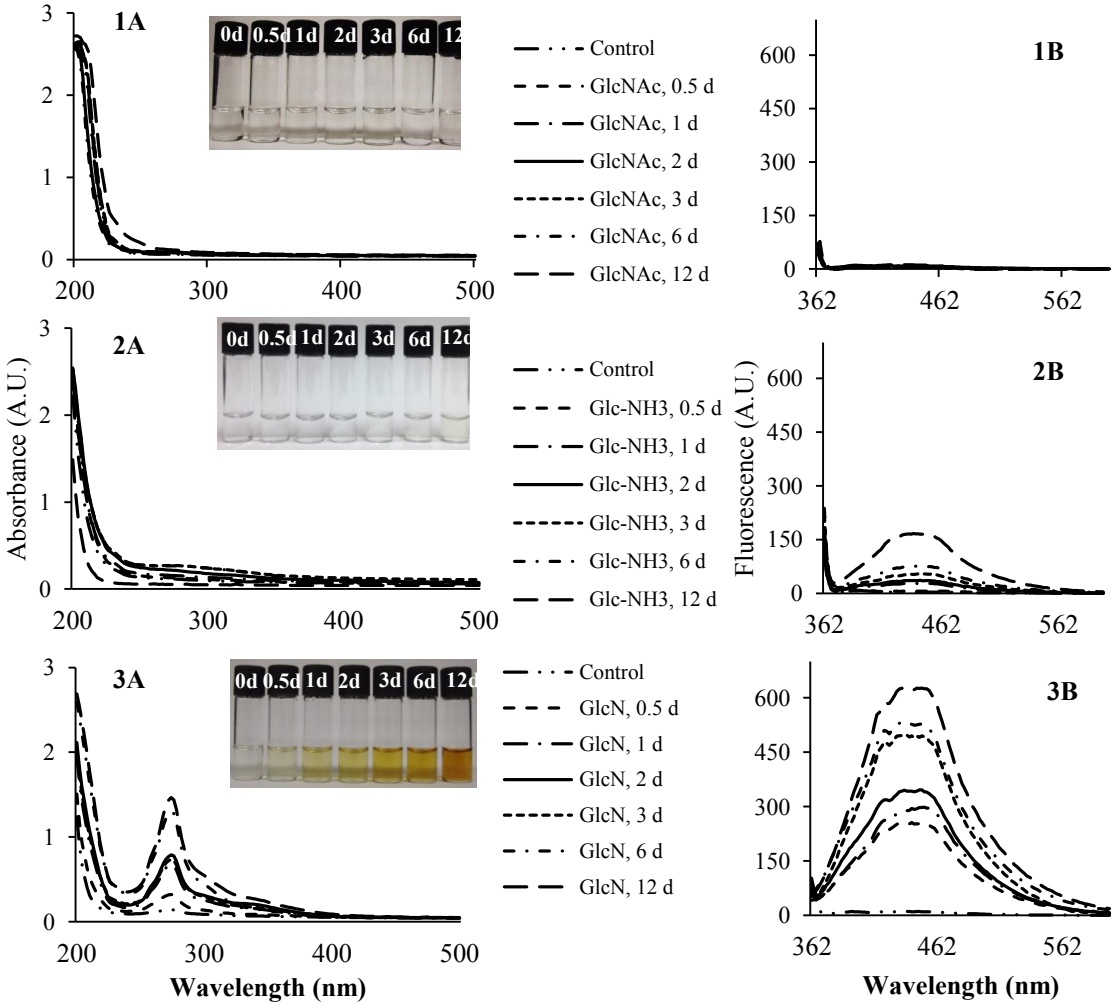

Figure 5.2. UV-Vis absorbance (A) and fluorescence spectra (B) profiles of GlcNAc (1A, 1B), Glc-NH_3 (2A, 2B) and GlcN (3A, 3B) as a function of heating time from 0 to 12 days. The values are expressed in arbitrary units (A.U.). Inset images (left) show photographs of the corresponding incubated reaction solutions. The images were taken for non-diluted experimental solution incubated at 15 mg/mL.

No major changes in the absorbance over time were obtained for GlcNAc, except a slight increase at λ = 220-235 at 12 days. Minor absorbance increase was observed in Glc-NH_3 mixtures. On the contrary, a steady increase of maxima of 274 and 320-360 were obtained for GlcN, suggesting a formation of products which absorb in the UV region. The increase in absorbance at 320 nm was lower than at 274 nm, however the formation of a light yellow color was apparent after 0.5 day incubation. The increase in UV absorbance at 274 and 320 nm was also reported by Zhang et al. (2004) who incubated 0.02 M GlcN at 37°C for 50 h in phosphate

buffer (pH 7.4). Increase in absorbance at 275 nm to was ascribed due to GlcN autocondensation and Maillard reaction products generation in the mixture of GlcN and fibrinogen/human serum albumin (Zhang et al. 2004). Candiano et al. (1988) and Horowitz (1991) indicated that the increase in UV absorption at around 274 nm is due to the formation of pyrazine compounds, which derive from the cyclocondensation between GlcN molecules; which have been confirmed by MS analysis (see the section about condensation products). At the same time increase at 320 nm was attributed to the formation of soluble pre-melanoidins (Fogliano et al. 1999), which was also confirmed by the production of light yellow-brown color over incubation time (Figure 5.1 3A, inset). In addition, this hyperchromicity at 320-340 nm was apparent at longer incubation times. No color production was observed for GlcNAc (Figure 5.2 1A inset); Glc-NH_3 mixture changes from slightly yellow to yellow over 6 to 12 days (Figure 5.2 2A inset), whereas the time course of color development by GlcN was changed from yellowish to brown. The fluorescence profile showed a progressive increase in the emission ($\lambda_{exc.}$ 347/$\lambda_{em.}$ 364-600 nm) intensity over time for GlcN. A broad peak was observed with a maximum intensity ranging from 420 to 450 nm. Glc-NH_3 also showed an increased fluorescence, however with significantly lower intensity and reaction velocity; at 12 days fluorescence emission was around three times lower as compared to GlcN. On the other hand, GlcNAs fluorescence profile did not change significantly over time. The wavelengths observed were typically used to assess the progress of the Maillard reaction, and more specifically, the development of advanced glycation products (AGEs) (Ferrer et al. 2005; Munanairi et al. 2007). Zhang et al. (2003) reported the increase in fluorescence intensity ($\lambda_{exc.}$ 340/$\lambda_{em.}$ 420 nm) during GlcN incubation at 37°C, and suggested an increase due to GlcN cyclocondensation and rearrangements. Candiano et al. (1988) came to the same conclusion and further proved that the increase in fluorescence emission at 430 nm (λ_{exc} = 362

nm) in lysine-GlcN reaction mixture was due to GlcN cyclocondensation. The same authors indicated that GlcN cyclocondensation products possessed optical and fluorescent properties of browning compounds, which in turn could explain an increase in color intensity over time (Figure 5.2 3A inset). These preliminary results suggest that with prolonged heating time GlcN cyclocondensation and a variety of rearrangements occur, thus the formation of higher molecular weight colored compounds.

5.3.2. Identification and quantitation of the major α-dicarbonyls produced from GlcN degradation by UHPLC and mass spectrometry analyses

In the previous section, UV and fluorescence analyses were discussed to evaluate the formation of the final stable products of GlcN degradation (i.e. GlcN-GlcN autocondensation products). However, GlcN, being a Heyns-like compound, it was expected the production of α-DCs, which in turn have the potential to generate a variety of condensation products. α-DC are highly reactive compounds, thus they were derivatized (condensation with OPD) to form stable quinoxalines, followed by UHPLC and MS analyses. Separation of quinoxalines achieved with chromatography (Papetti et al. 2014) allowed for identification of analytes. Figure 5.2 illustrates the representative UHPLC chromatogram of standard α-DCs compounds and α-DCs produced from GlcN incubated for 1 day.

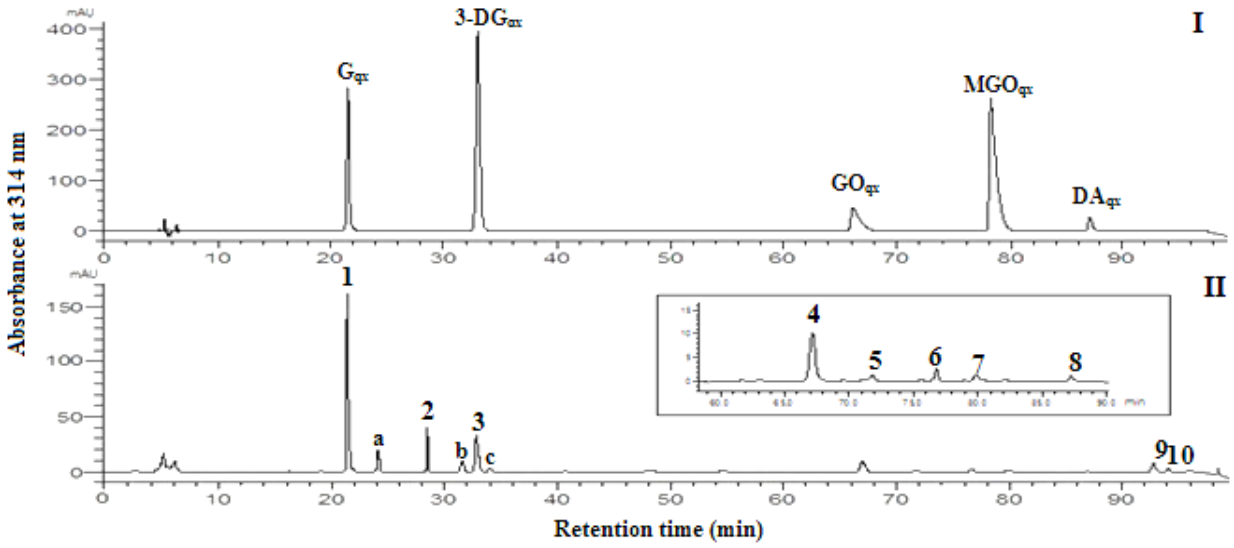

Figure 5.3. UHPLC analyses of quinoxaline derivatives of α-dicarbonyl compounds produced from GlcN incubation over time. (I) Chromatograms of a reference quinoxaline mixture of glucosone (G), 3-deoxyglucosone (3-DG), glyoxal (GO), methylglyoxal (MGO) and diacetyl (DA). (II) Representative chromatogram of GlcN incubated for 1 day, derivatized with OPD and acquired by UHPLC with UV detection at 314 nm. Numbers indicate the peaks of the quinoxalines of (1) G, (2) unidentified α-DC, (3) 3-DG, (4) GO, (5) HPA, (6) 3,4 - DGE, (7) MGO, (8) DA, (9) 4-GlcN-3-DG, (10) 4-G-3-DG and a, b, c peaks corresponding to non-OPD derived GlcN condensation products. Inset shows a zoomed-in view of the peaks eluted at 60-90 min.

Table 5.1. Retention times and precursor ions of the peaks reported in Figure 5.3.

Peak	Retention time (min)	Precursor ion $(M+H)^+$
1	21.5	251.1032
2	28.5	235.0973
3	33.2	235.1081
4	67.1	131.0611
5	71.8	161.0720
6	76.9	217.1707
7	79.9	145.0767
8	87.4	159.0925
9	93.0	396.3326
10	94.2	397.1812

For confirmation of the peaks for which commercial standards were available and the identification of unknowns, the major peaks were collected and further subjected to MS analyses. Eight peaks in the UV chromatograms (Figure 5.3 II) were identified by their pseudomolecular peaks ($[M + H]^+$, as detected by MS analyses (Table 5.1). Individual peaks 1-8 were identified as

being (1) glucosone, m/z = 251.1032; (2) unidentified α-dicarbonyl, m/z = 235.0973; (3) 3-deoxyglucosone, m/z = 235.1081; (4) glyoxal, m/z = 131.0611; (5) 3-hydroxy-2-oxo-propanal (hydroxypyruvaldehyde, HPA); m/z = 161.0720; (6) 3,4-dideoxyglucosone-3-ene, m/z = 217.1707; (7) methylglyoxal, m/z = 145.0767 and (8) diacetyl, m/z = 159.0925. Based on molecular weight and the reference data (Papetti et al. 2014) the peaks (9) and (10) were tentatively assigned to the quinoxaline derivatives of 2-amino-2-deoxy-4-glycosyl-5,6-dihydroxy-2-oxohexanal (4-GlcN-3-DG) and 4-glycosyl-5,6-dihydroxy-2-oxohexanal (4-Glc-3-DG), respectively (MS/MS fragmentation spectra are reported in Appendix B). The peaks denoted as (a), (b) and (c) showed the m/z in the range of 317 to 355 (refer to the MS spectra in Appendix C). The nature of these peaks is not clear, however it is suspected that they derived from a variety of condensation products of GlcN itself or GlcN with α-DCs (i.e. fructosazines). Hence, they are likely non-OPD condensed products, which are highly hydrophilic fructosazines missing the benzene portion of OPD, and despite their high molecular weight elute at early retention times in the hydrophilic part of the gradient. The product ions and structures of quinoxaline derivatives of the seven identified peaks are shown in Figure 5.4. For G_{qx} the molecular ion and subsequent losses of three water molecules were observed. Mittelmaier et al. (2011) found very similar fragmentation pattern with the loss of three water molecules, except the fragment ion at m/z 173.0 was dominant. Products ion spectra of 3-DG_{qx} and its dehydration product, 3,4-DGE_{qx} showed similar fragment ions, apart from the latter missing fragments at m/z 235.1081 and 171.0918.

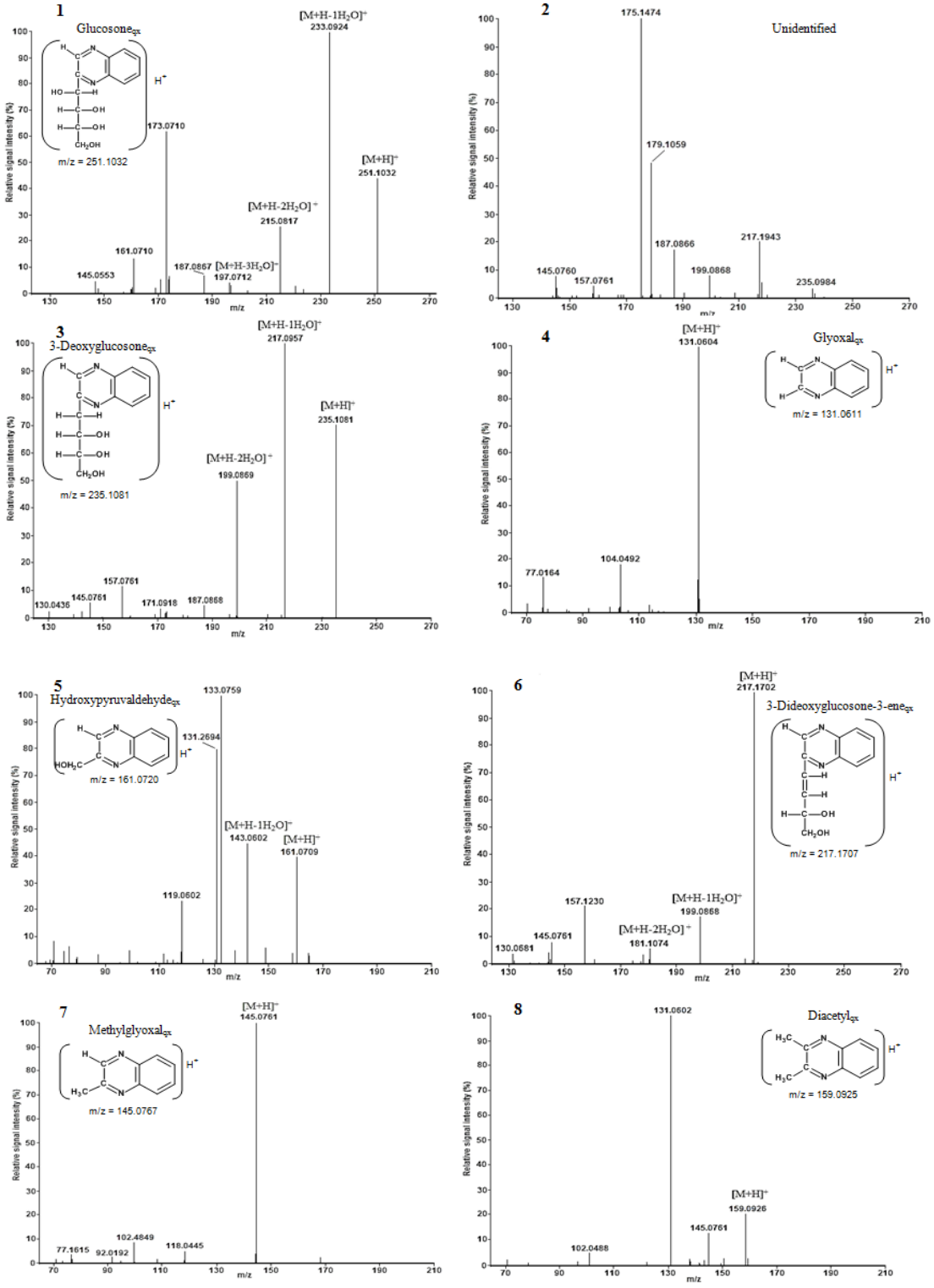

Figure 5.4. MS/MS spectra and structures of quinoxaline α-dicarbonyl compounds produced during GlcN degradation: (1) glucosone$_{qx}$, (2) unidentified α-DC$_{qx}$, (3) 3-deoxyglucosone$_{qx}$, (4) glyoxal$_{qx}$, (5) hydroxypyruvaldehyde$_{qx}$, (6) 3,4-dideoxyglucosone-3-ene$_{qx}$, (7) methylglyoxal$_{qx}$ and (8) diacetyl$_{qx}$. The respective quinoxaline precursor ions are shown in the Table 5.1.

The MS/MS of the unidentified α-dicarbonyl (peak 2) showed two similar fragment ions (m/z 145.0760/1 and 157.0761) with 3-DG_{qx}, and could be an indication of the presence of 1-deoxyglucosone (1-DG), 3-deoxygalactosone or 4-deoxyglucosone. However, the presence of DA supports the presence of 1-DG, being a precursor of DA (Shibamoto, 2014). There was a minimal tendency of fragmentation for GO_{qx} and MGO_{qx}, with three and five fragments, respectively, along with the highest intensity for precursor ions and fragment at m/z 77.0164 (77.1615 in MGO) typical for quinoxaline skeleton fragmentation (Pfeifer and Kron, 2010). As well as for DAqx four major MS/MS fragment ions were found. Under the described MS/MS conditions m/z 161.0709, 143.0602, 133.0759, 131.2694 and 119.0602 were identified as the main fragments of the parent molecule ion (m/z 161.0720) of HPA_{qx}. The fragments ions from eight identified α-DCs were in accordance with previously reported quinoxalines in various foods, such as high-fructose corn syrup (Gensberg et al. 2012), coffee, barley and soy sauce (Papetti et al. 2014) and honey (Mavric et al. 2008). The MS/MS fragmentation and proposed structures of 4-GlcN-3-DG and 4-G-3-DG are reported in the Appendix B. After identifying the α-DC presence, five of them were quantified and the concentrations expressed in mg/kg of GlcN are given in Table 5.1. It was found that G, 3-DG and GO were present in control samples, suggesting the partial degradation of GlcN while stored in powder. Even though a freshly ordered GlcN was used in the analyses, rapid development of α-DCs could be a possible explanation for their presence in the non-heated sample. The elevated temperatures (90°C for hydrolysis, 45°C for evaporation, etc.) used during GlcN's extraction could induce its degradation and thus dicarbonyl compounds development.

Table 5.2. Concentrations of five different α-dicarbonyl compounds found in GlcN incubated over time. All values are expressed as mg of α-dicarbonyl compound per kg of GlcN. The mean ± standard deviation of three independent experiments (n = 6) is shown.

α-DC	Free α-dicarbonyl compounds (mg/kg of GlcN)							
	0 d	0.5 d	1 d	2 d	3 d	6 d	12 d	*p*-value
G	709 ± 68^{e}	2634 ± 87^{b}	3245 ± 90^{a}	2710 ± 134^{b}	2443 ± 85^{bc}	2132 ± 89^{c}	1131 ± 68^{d}	**
3-DG	272 ± 19^{f}	451 ± 32^{e}	571 ± 27^{de}	583 ± 33^{cd}	707 ± 63^{c}	1905 ± 42^{b}	4535 ± 82^{a}	**
GO	11.2 ± 1.2^{e}	26.6 ± 2.1^{bc}	34.9 ± 3.4^{a}	28.4 ± 2.1^{b}	24.9 ± 1.6^{c}	17.7 ± 0.9^{d}	12.6 ± 1.1^{e}	**
MGO	nd	4.5 ± 1.3^{e}	5.5 ± 1.1^{de}	6.4 ± 1.0^{cd}	7.3 ± 0.8^{c}	8.7 ± 0.9^{b}	10.4 ± 2.3^{a}	**
DA	nd	2.1 ± 0.8^{d}	6.1 ± 1.1^{b}	6.9 ± 0.9^{a}	3.7 ± 1.0^{c}	nd	nd	**

G-glucosone; 3-DG–3-deoxyglucosone; GO-glyoxal; MGO-methylglyoxal; DA-diacetyl.

The values on the same line with different uppercase superscript letters differ significantly ($p < 0.05$).

nd - not detectable.

** Indicates $p < 0.0001$.

At the beginning of the incubation G was the most abundant α-DC compound followed by 3-DG. However, after 1 day incubation the concentration of G decreased significantly ($p < 0.05$) from 3245 to 1131 mg/kg GlcN, along with a significant increase in the amount 3-DG. At 0.5 and 1 day of incubation G concentration was around six times higher than 3-DG. After heating for 12 days concentration of 3-DG was four times higher than G. G is a product of oxidative degradation of Heyns compound, while 3-DG is formed non-oxidatively through enolization pathway (Kerler et al. 2010). These results suggest the prevalence of an oxidative pathway during the first days of incubation, whereas over time the enolization process dominates. The concentrations of the other α-DCs: GO, MGO and DA were significantly lower in comparison to G, 3-DG. Opposite relationship was observed between GO and MGO formation over time. While the concentration of GO significantly ($p < 0.05$) decreased from 34.9 mg/kg at 1 day to 12.6

mg/kg GlcN after 12 days, the amount of MGO significantly ($p < 0.05$) increased from 4.5 to 10.4 mg/kg GlcN. Several studies (Weenen, 1998; Yaylayan et al. 2000) suggested 3-DG as the precursor for MGO formation, which is based on the non-oxidative fragmentation of the retroaldolization pathway. Increase in 3-DG was accompanied with increasing concentrations of MGO over time (Table 5.2). In the model experiment of Thornalley et al. (1999) 0.09 μM MGO was formed from 50 μM 3-DG, which accounts for 0.18%. In the current study, at 0.5 d, MGO accounted for 1% of 3-DG, whereas with incubation up to 12 days the percentage decreased to 0.23. On the other hand, Hoffman et al. (1999) proposed GO production from G. DA reached the highest concentration at 2 days of incubation (6.9 mg/kg GlcN), dropped almost twice by 3 days and was not detected with prolonged incubation. Obtained results confirm our hypothesis that GlcN is an unstable amino sugar that degrades faster in phosphate buffer at 37°C, while GlcNAc is stable in the condition used in this study.

5.3.3. Condensation products from non-enzymatic modification of GlcN

As presented in Figure 5.2, incubation of GlcN results in an increased absorbance and fluorescence, suggesting products are generated over time. To further investigate, aliquots of GlcN incubated for half (Figure 5.5 A) and three days (Figure 5.5 B) were directly injected into a MS to obtain a compound profile. As shown in Figure 5.5 A and B, several molecular ion species were observed.

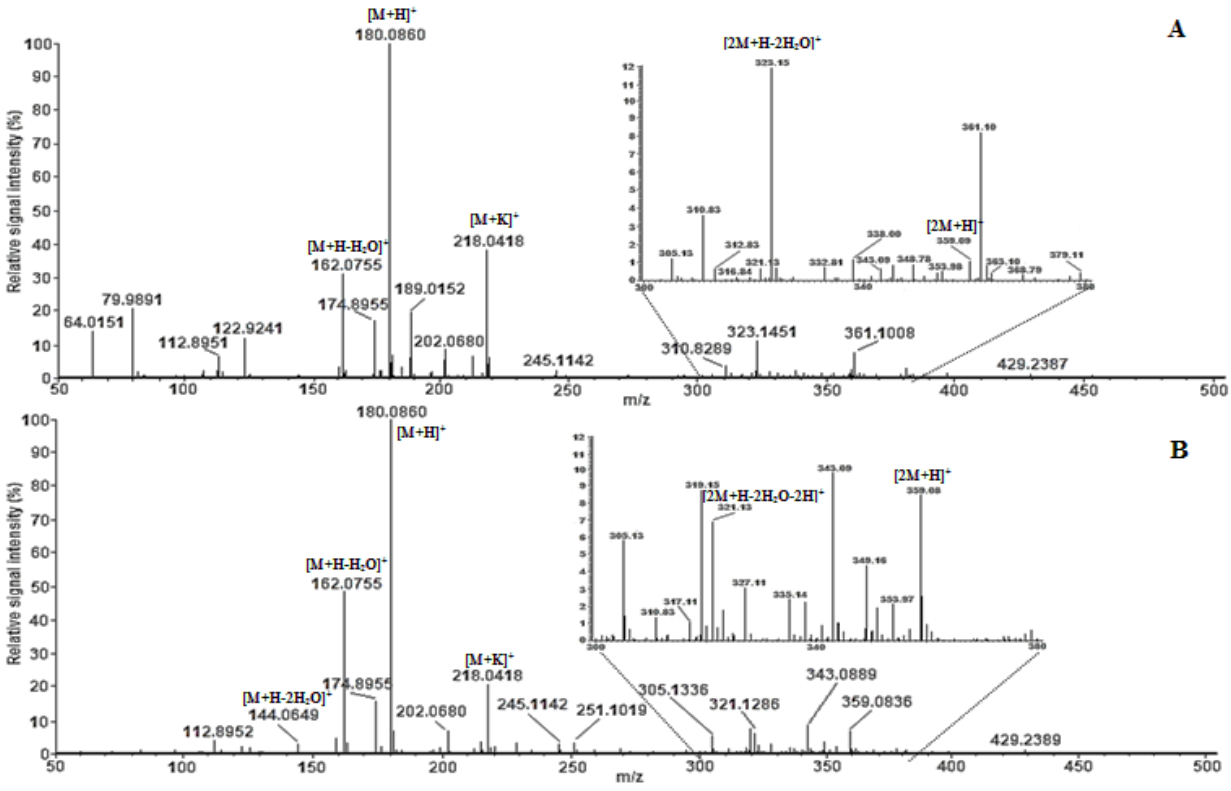

Figure 5.5. Mass spectrum of GlcN incubated at 0.5 (A) and 3 (B) days and directly infused into the LTQ Orbitrap – MS instrument. Inset: enlargement of the respective spectra in the range of m/z 300-380.

GlcN showed peaks at m/z 180.0860 corresponding to its protonated molecular ion $[M+H]^+$, m/z 162.0755 and 144.0649 corresponding to mono- and didehydrated GlcN, respectively. The m/z 218.0418 is likely due to GlcN`s potassium adduct $[M+K]^+$ while m/z 359.0836 corresponding to $[2M+H]^+$, possibly due to N-glycoside formation between two GlcN molecules. Remarkably, several other species with pseudo molecular weights higher than m/z 300 were present. These species are the result of cyclocondensation reaction (Figure 5.5), which results in pyrazine ring formation. One of the products of GlcN cyclocondensation, namely dihydrofructosazine [2,5-bis(arabino-tetrahydroxybutyl)dihydropyrazine)], was identified at m/z 323.1451 (Figure 5.5 A). This compound was originally identified and isolated by Candiano et al. (1988) during the incubation of lysine in the presence of GlcN at 37°C. The products at m/z 321.1286 and

305.1336 believed to be the products of dihydrofructosazine rearrangement, producing fructosazine and deoxyfructosazine, respectively. Similar products of GlcN incubation at m/z 321 and 323 were reported previously by Kashige et al. (1995) while studying the possible involvement of GlcN-derived dihydrofructosazine in breaking DNA. It is also apparent that many other cyclocondensation products may be produced as a consequence of the reaction between GlcN and α-DCs via the mechanism proposed by Klinger et al. (2013).

The proposed reaction mechanisms between the most abundant α-DCs found in this study and GlcN are reported in Figure 5.6. The term "symmetric cyclocondensation" indicates a reaction scheme that involves two identical GlcN (Figure 5.5 A1) or α-DC molecules (Figure 5.6 A2) and "asymmetric cyclocondensation" refers to a reaction that occurs between a specific α-dicarbonyl and GlcN (Figure 5.6 A3 and A4). Theoretically, the formation of all masses reported in the Figure 5.5 is possible. 0.9 to 16.8% of NH_3 released (refer to Appendix D) during incubation of GlcN could aid in the production of cyclocondensation products between α-DC. The mass spectra of underivatized GlcN (Figure 5.5 A and B) at 0.5 and 3 days show the presence of the peaks which correspond to both "symmetric" (Figure 5.6 A1, A2) and "asymmetric" (Figure 5.6 A3, A4) cyclocondensation products and in some cases the molecular weights of these products coincide (i.e. protonated m/z 305.1348; 321.1298; 323.1454).

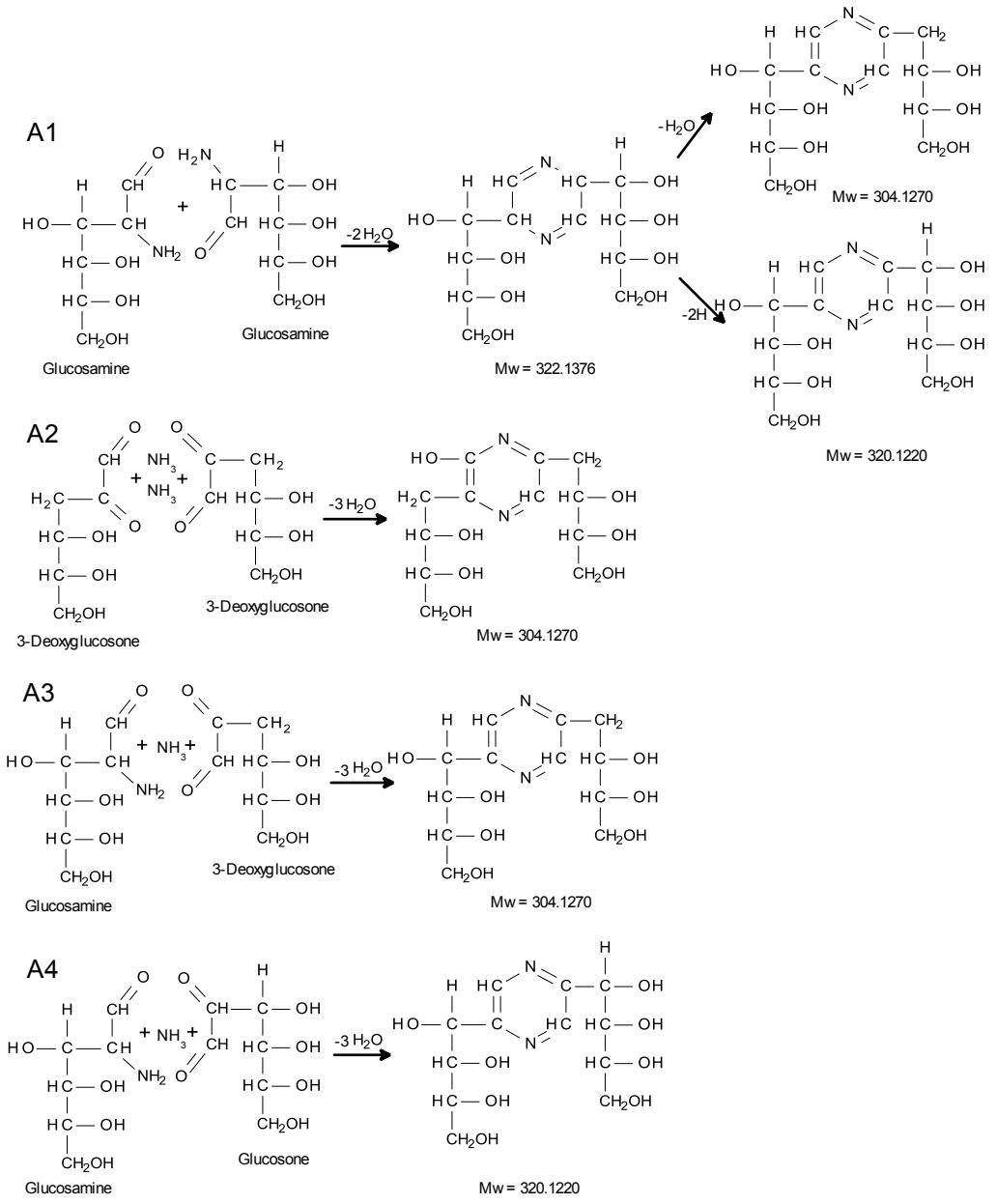

Figure 5.6. Proposed structures and theoretical monoisotopic molecular weights (M_w) of cyclocondensation products of GlcN only or GlcN and α-dicarbonyl compounds. Structures are shown as neutral molecules.

These data are also corroborated by the Figure 5.7, which represents the UV/Vis (Figure 5.7 A) and fluorescence emission (Figure 5.7 B) profile of equimolar mixture of G, 3-DG, GO and MGO with GlcN over a period of incubation from 0 to 48 h.

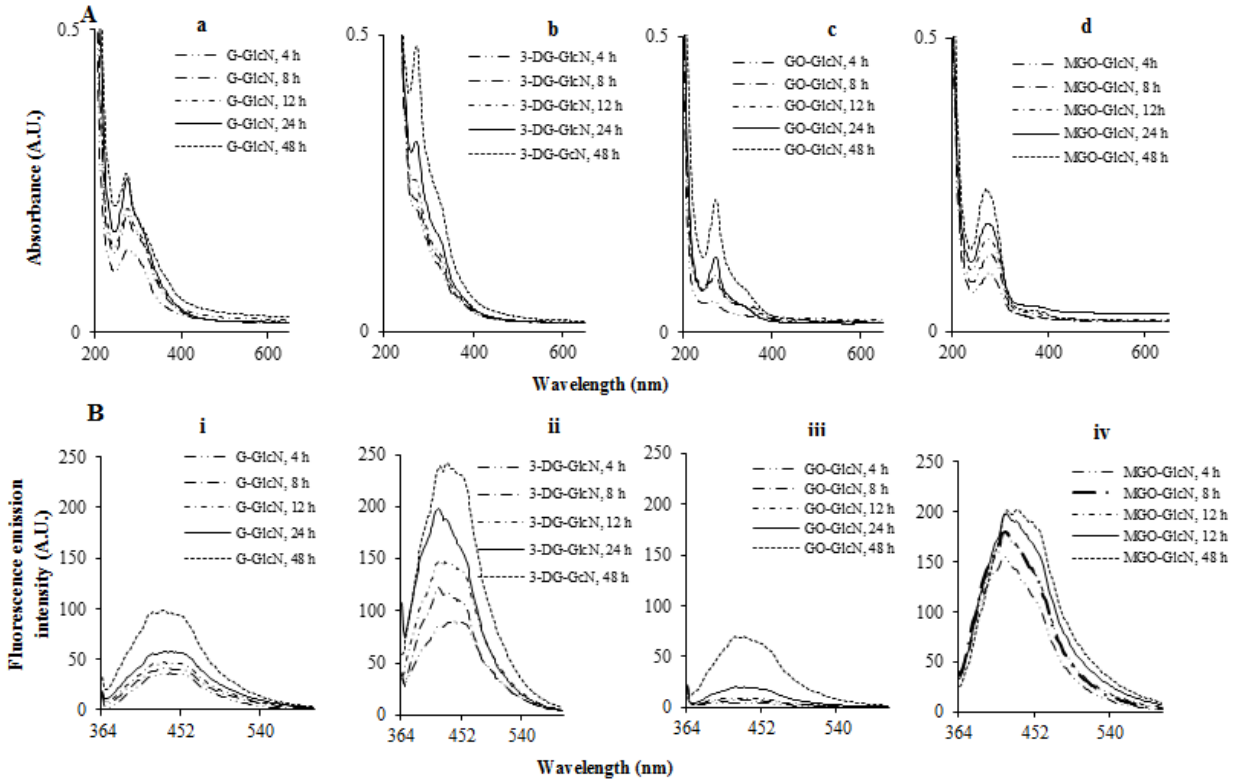

Figure 5.7. Absorbance (A) and fluorescence emission (B) spectra of incubated equimolar mixtures of GlcN and α-dicarbonyl compounds. Part (A): GlcN incubated with (a) G, (b) 3-DG, (c) GO and (d) MGO. Part (B): GlcN incubated with (i) G, (ii) 3-DG, (iii) GO and (iv) MGO.

In all cases absorbance and fluorescence emission intensities increased over time owing to the formation of cyclocondensation reaction products. Hence, GlcN possesses a trapping effect to the nascent α-DCs produced from its degradation. Fluorophore formation was also reported (Zhang et al. 2004) to represent the formation of heterocyclic compounds (i.e. pyrazines). Among four α-DCs tested, 3-DG appears to be the most reactive towards GlcN, judging from an extensive accumulation of fluorescence (240 units). 3-deoxyosones predominantly form pyrazines and imidazoles with ammonia, which in turn are responsible for the sugar coloring (Belitz, 2009). Therefore, the accumulation of 3-DG (Table 5.2) and its reaction products with GlcN (Figure 5.6) over time could be partially responsible for GlcN browning with extended incubation periods (Figure 5.2 3A inset).

5.4. Conclusions

In summary, this research demonstrated that GlcN, and not GlcNAc, is the unstable compound, producing 1 - 6 mg of α-dicarbonyl compounds per gram of GlcN depending on incubation time. The cause of this reactivity lays in the nature of GlcN, which is a Heyns (aldosamine) compound with the potential to generate many reactive α-dicarbonyls, precursors of fluorescent heterocyclic compounds such as pyrazines. By contrast, acetylation of GlcN decreases its reactivity by blocking the nucleophilicity of the free -NH_2 group. Considering the ubiquities of GlcNAc in animal tissues, enzymatic acetylation appears to play a crucial role in minimizing the less stable GlcN, which has the potential to form endogenous reactive α-DCs. Also, research interests on GlcN application in food products are dramatically increasing. For instance, Jia et al. (2014) proposed the bioconversion of GlcN to deoxyfructosazine and fructosazine in order to produce flavour compounds for the food industry. Uzzan et al. (2007) enriched milk with GlcN with the hope to produce a functional food product; however, the experiment was compromised due to aggregation of milk protein upon pasteurization. This may indicate the cross-linking effects of α-DCs generated from GlcN degradation (results described in Chapter 5 also showed GlcN-induced myoglobin aggregation at moderate temperatures). In North America, GlcN has a legislative status of "Natural Health Product" (or dietary supplement) and not of a food ingredient; for instance a specific dose of 1.5 g daily is recommended to treat osteoarthritis. The USDA does not recognize GlcN as "generally recognized as safe" due to lack of clinical studies that its consumption is safe in young children, pregnant women and diabetics (Kralovec and Barrow, 2008). Hence, more studies are necessary for the use of GlcN as a food ingredient for both technological and safety reasons.

CHAPTER 6. Rapid myoglobin aggregation through glucosamine-induced α-dicarbonyl formation

6.1. Introduction

Non-enzymatic modification of proteins through the Maillard reaction has recently gained new attention. This process produces neoglycoproteins with enhanced functionality (i.e. solubility, emulsification capacity, etc.) and melanoproteins with improved antioxidant activity (Liu et al. 2012; Tagliazucchi and Bellesia, 2015). The Maillard reaction is a complex reaction between protein and reducing sugars and can be reduced to three major steps; the formation of a keto- or aldosamine (Amadori or Heyns compound, respectively), an intermediate reactive compound like α-dicarbonyl compounds (α-DC), and a final stage where yellow and brown condensation products are formed (heterocyclic compounds and melonoidins/melanoproteins, respectively). Fogliano and Moralez (2011) reported that these melanoproteins can be divided into soluble and insoluble protein aggregates. Insoluble protein aggregates are resistant to protein digestion and would possibly represent a dietary fiber. However, to date, there are few studies reporting the nature of the Maillard protein aggregates in food systems. On the other hand, several *in vitro* studies have simulated physiological conditions to demonstrate the effect of high level of sugars or α-DC like glyoxal and methylglyoxal, on protein modification (Glomb and Monnier, 1995; Schwarzebbolz et al. 1997; Oya et al. 1999). Amyloid fibrils are insoluble protein aggregates deposited extracellularly in tissues that have a pathogenic effect leading to amyloid-like diseases including Alzheimer's disease, and the spongiform encephalopathies (Ranbaran and Serpell, 2008). Furthermore, extensive islet amyloid formation is induced by development of Type II diabetes mellitus and contributes to its progression (Höppener et al. 1999). Based on these considerations, it is important to distinguish the effect of the endogenous and exogenous Maillard reactions. The endogenous reaction may form modified protein structures that affect

cell metabolism, whereas the exogenous reaction occurs during food processing and confers positive qualities regarding flavour, colour, antimicrobial activity (Hauser et al. 2014) and also antioxidant capacity (Summa et al. 2008; Liu et al. 2014). Beside these positive effects, there is a controversy on the harmful consequences that some of the Maillard reaction products, advanced glycation end-products (AGEs) in particular, exert on human health. Well known examples of these compounds are acrylamide and 5-hydroxymethylfurfural, also referred as neo-formed contaminants (Capuano et al. 2011).

Glucosamine (GlcN) is an amino monosaccharide used by consumers as a dietary supplement to both reduce osteoarthritis pain and improve joint function (Block et al. 2010). GlcN supplementation may stimulate synovial production of hyaluronic acid (HA), a type of glycosaminoglycan responsible for the lubricating and shock-absorbing properties of synovial fluid in cartilage (Qu et al. 2006). In a previous study (Chapter 5) was found that 1 g of GlcN produces up to 6 mg of reactive α-DC, mainly glucosone, 1-and 3-deoxyglucosone during incubation at 37°C from 0 to 12 days. This because GlcN is a Heyns compound that, like the Amadori compound (fructosamine), can degrade rapidly under certain conditions. By contrast, the amide form of GlcN, *N*-acetyl-GlcN (GlcNAc), does not produce a significant amount of α-DC due to the stabilizing effect of the acetyl group on the nucleophilicity of the -NH_2 group. The possibility of producing a significant amount of the Heyns compound with a "simple" deacetylation process allows for an opportunity to design a model system to study how a first product of the Maillard reaction interacts with protein.

Equine myoglobin (Mb), a monomeric oxygen-binding protein found within muscle cells, was chosen since it is a readily available protein frequently used for *in vitro* studies and behaves similarly to Mb from meat-producing species (Tang et al. 2004). This study serves to understand

both the effect of the degradation products of GlcN on Mb structure and also how Mb affects the degradation of GlcN. Mb was incubated in the presence of GlcN at 37°C and the major changes in Mb structure were monitored by mass spectrometric (MALDI and ESI ionization), spectroscopic (circular dichroism and fluorescence) and microscopic techniques (TEM). GlcNAc and Glc were also incubated in the same conditions and used as comparison as reported in Chapter 5.

6.2. Materials and Methods

6.2.1. Materials

Myoglobin from equine skeletal muscle (95-100% purity, lyophilized powder), *N*-acetyl-D-glucosamine (≥99% purity), D-glucose (≥99.5% purity), D-glucosamine hydrochloride (≥99% purity), potassium phosphate monobasic and dibasic, sodium azide, HPLC-grade solvents (acetonitrile, methanol, formic acid, trifluoroacetic acid), glucosone (2-keto-D-glucose; ≥98.0% purity; M_W 178.14 Da), glyoxal (ethanedial; 40% in H_2O; M_W 58.04 Da), methylglyoxal (2-oxopropanal; 40% in H_2O; M_W 72.06 Da), diacetyl (butane-2,3-dione; ≥95.0% purity; M_W 86.09 Da), 1,2-diaminobenzene, DTPA and Thioflavin T were purchased from Sigma-Aldrich (St. Louis, MO). 3-deoxyglucosone (3-Deoxy-D-erythro-hexosulose; ≥95% purity; M_W 162.14 Da) was obtained from Cayman Chemical (Ann Arbor, MI). SPE tC-18 Sep-Pak Vac 6 cc columns were obtained from Waters (Milford, MA). Filtration membranes (0.22 μm) were from Millipore (Billerica, MA). 3,5-dimethoxy-4-hydroxycinnamic acid (sinapinic acid), ProMix3 (mass spectrometry protein standards) were obtained from LaserBiolabs. Standard ion calibration solution (Pierce LTQ) for electrospray ionization in positive mode was purchased from Thermo Scientific (Rockford, IL, USA). Milli-Q purified distilled water for buffers and reagents

preparations were purchased from Waters Millipore (Milford, MA, USA). All the reagents and chemicals used in the study were of analytical grade.

6.2.2. Experimental design

The non-enzymatic modifications of Mb in presence of GlcNAc, Glc and GlcN were evaluated over time at 0, 0.5, 1, 2, 3, 6 and 12 days in phosphate buffer at 37°C. In the first part of the study, mass spectrometric profiles were assessed over time to understand the major changes occurring during the reaction as dependent on the type of monosaccharide. In this regard, a total of 42 tubes (2 tubes × monosaccharide × incubation time) were randomly placed within the incubator and the reaction was monitored over time. At each time, 2 tubes per treatment were pooled and subjected to MS analysis. Next, α-dicarbonyl content was evaluated, where 3 tubes per treatment were incubated, resulting in 63 samples in total. Then 9 tubes per treatment were incubated, from which 3 tubes were used for Trp fluorescence analyses, 3 tubes to assess protein oxidation level and 3 tubes for circular dichroism. Finally, Thioflavin T fluorescence analyses were performed for all treatments and selected incubation times were used for microscopy.

6.2.3. Preparation of glycoforms of myoglobin

For the preparation of myoglobin-sugar conjugates, 5 mg/mL of horse skeletal muscle myoglobin was incubated at 37˚C (Thermoshaker Innova 44, New Brunswick Scientific, USA) in the presence of GlcNAc, Glc or GlcN (1:3 ratio, w/w) in 50 mM potassium phosphate buffer (pH 7.4) containing 0.02% NaN_3 as bacteriostat. Final pH values were adjusted to 7.4 when necessary. The controls were only protein and only sugars solutions at zero time and incubated. The samples aliquots were transferred into plastic screw-cap aliquot tubes and randomly arranged within an incubator (New Brunswick Scientific, Edison, NJ). After collection at 0.5, 1, 2, 3, 6 and 12 d, the samples were ultrafiltrated with Amicon Ultra 3K membrane (molecular

weight cut-off of 3.000 NMWL; Millipore Corporation, Bedford, MA, USA) to eliminate unreacted sugar. Incubations did not fluctuate by more than 0.1 pH units up to 12 days (Mb-Glc-NH_3) or 0.4 units (for Mb-GlcN). The ultrafiltration step was avoided for the samples subjected to the analyses of free α-dicarbonyl compounds and transmission electron microscopy.

6.2.4. Matrix asisted laser desorption/ionisation time-of-flight mass spectrometry (MALDI-TOF-MS)

MALDI-TOF-MS analyses were performed on a Bruker Ultraflextreme MALDI-TOF/TOF mass spectrometer (Bruker, Bremen, Germany) using positive ionization linear ion mode between 5 and 20 kDa and sinapinic acid as a matrix. The sample preparation protocol for MALDI-TOF/TOF MS is described as follows: a solution of the protein sample (1 μL) was spotted on a ground steel MALDI plate and acidified by spotting 1 μL of 0.1% trifluoroacetic acid (TFA) in water on top and air dried. A 1 μL aliquot of a stock solution of sinapinic acid (10 mg/mL) in 50% acetonitrile (ACN)/ 50% H_2O was spotted on top and air dried. Prior to each experiment the apparatus was calibrated using a reference protein solution (Sigma-Aldrich, St. Louis, MO). Data analysis was performed using the Bruker flex Analysis software package version 3.3.

6.2.5. Liquid chromatography–electrospray ionization mass spectrometry (LC-ESI-MS)

For protein molecular weight determination reverse phase high performance liquid chromatography followed by detection using ultraviolet absorption and mass spectrometry (RP-HPLC-UV-MS) was performed using an Agilent 1200 SL HPLC System with a Poroshell 300SB-C8, 5 micron particle size, 75 x 0.5 mm column (Agilent Technologies, USA), with Opti-pak trap cartridge kit, 5 μL BED, C8, thermostated at 60°C. A buffer gradient system composed 0.1% formic acid in water as mobile phase A and 0.1% formic acid in ACN as a mobile phase B. An aliquot of 5 μL of sample was loaded onto the column at a flow rate of 0.15 mL/min and an initial buffer composition of 95% mobile phase A and 5% mobile phase B. After injection, the

column was washed using the initial loading conditions for 3 minutes to effectively remove salts. Elution of the proteins was done by using a linear gradient from 5% to 60% mobile phase B over a period of 15 minutes, 60% to 80% mobile phase B over a period of 3 min, 80% to 98% mobile phase B over a period of 2 min. UV absorbance was monitored at 210, 214, 254 and 280 nm. Mass spectra were acquired in positive mode of ionization using an Agilent 6220 Accurate-Mass TOF HPLC-MS system (Santa Clara, CA, USA) equipped with a dual sprayer electrospray ionization source with the second sprayer providing a reference mass solution. Mass correction was performed for every individual spectrum using peaks at m/z 121.0509 and 922.0098 from the reference solution. Mass spectrometric conditions were drying gas 10 L/min at 325°C, nebulizer 20 psi, mass range 100-3000 Da, acquisition rate of ~1.03 spectra/sec, fragmentor 200 V, skimmer 65 V, capillary 3200 V, instrument state 4 GHz High Resolution. Data analysis was performed using the Agilent MassHunter Qualitative Analysis software package version B.03.01 SP3.

6.2.6. Assay of carbonyl formation

To understand glycation-induced carbonyl stress, carbonyl formation in Mb and glycated Mb forms was detected by reactivity with 2,4-dinitrophenylhydrazine (DNPH) to form protein hydrazones as described in Chapter 3 (section 3.2.5.). After subtraction of zero time values, the mean values were then plotted and fitted (except Mb-GlcN treatments) with the non-linear fitting using GraphPad Prism software (version 4.0, San Diego, CA, USA).

6.2.7. Extraction of α-dicarbonyl compounds

The extraction method was based on a three-step procedure described by Papetti et al. (2014). Briefly, collected aliquots of Mb-GlcNAc, Mb-Glc and Mb-GlcN (6.0 mL) were passed through a pre-conditioned SPE tC-18 Sep-Pak cartridge (Waters, Milford, MA, USA) at a flow rate close

to 2 mL/min as a clean-up step before derivatisation. Collected polar fraction was spiked with 0.006 g of 1,2-diaminobenzene (*O*-phenylenediamine (*o*-OPD)), the pH was adjusted to 3.00 ± 0.02 with HCl (4 N), and the fraction was derivatised at 37°C for 1 h in the presence of 11 mM diethylene triamine pentaacetic acid (DTPA) (Gensberg et al. 2012). The quinoxaline derivatives were eluted from another SPE cartridge with 4 mL of a MeOH/H_2O mixture (90/10 v/v). The first 1 mL was discarded, whereas the next 2 mL were used for analysis.

6.2.8. Separation of the quinoxalines derivatives of α-dicarbonyl compounds by UHPLC-UV

α-DC analysis was conducted using an Ultrahigh Performance Liquid Chromatography apparatus (Shimadzu, Columbia, MD) as described in Chapter 5 (section 5.2.5.2).

6.2.9. Identification and quantitation of quinoxaline derivatives

The identification of major α-DC was based on comparison of their retention times of the reference compounds (quinoxalines derivatives of G, 3-DG, GO, MGO and DA) and spectral characteristics. For unequivocal identification of the major α-DC, eight UHPLC peaks were manually collected and subjected to mass spectrometry analyses. The accurate mass and MS/MS fragmentation patterns were compared to authentic standards and to the reference data. Mass spectrometry analyses were performed in duplicates.

For quantitation external calibration was used. Each quinoxaline derivative was diluted to the final concentrations ranging from 60 - 2000 (G), 1.5 - 2000 (3-DG), 4.5 - 200 (GO), 1.0 - 25 (MGO), and 1.25 - 12 μM for DA. Each concentration was analyzed in triplicate. The peak area was plotted against concentration and the regression equations were calculated. The correlation coefficients for all calibration curves were $R^2 \geq 0.99$. The limit of detection (LOD) was calculated as 2.08 (G), 0.26 (3-DG), 0.13 (GO), 0.09 (MGO) and 0.20 μM (DA). The limit of quantification

(LOQ) was determined as 6.30 (G), 0.78 (3-DG), 0.40 (GO), 0.28 (MGO), and 0.61 μM (DA) by assuming a signal-to-noise ratio (S/N) 3:1 for LOD and S/N 10:1 for LOQ.

6.2.10. Direct infusion orbitrap mass spectrometry analyses (DIMS)

Collected α-DC fractions from UHPLC were subjected to DIMS. All Orbitrap measurements were carried out by using the Ion Max electron spray ionization (ESI) source (Thermo Fisher Scientific) mounted on a LTQ Orbitrap XL (Thermo Scientific, San Jose, CA, USA). The procedure was applied as described in Chapter 5 (section 5.2.5.4).

6.2.11. Determination of myoglobin forms

Control and glycoconjugated samples were diluted to 1 mg/mL with 50 mM potassium phosphate buffer (pH 7.4) and the absorption was recorded at 557, 582, 503 and 525 nm using a Shimadzu UV-2101 spectrophotometer (Kyoto, Japan) with cuvettes of 1 cm path length. The relative proportions of the myoglobin redox forms: deoxymyoglobin (DeoMb), oxymyoglobin (OxyMb) and metmyoglobin (MetMb) were calculated according to the modified Krzywicki's equation described by Tang et al. (2004) as follows:

$$[\text{DeoMb}] = -0.543R_1 + 1.594R_2 + 0.552R_3 - 1.329$$
$$[\text{OxyMb}] = 0.722R_1 - 1.432R_2 - 1.659R_3 + 2.599$$
$$[\text{MetMb}] = -0.159R_1 - 0.085R_2 + 1.262R_3 - 0.520$$

where $R_1 = A_{582}/A_{525}$, $R2 = A_{557}/A_{525}$ and $R3 = A_{503}/A_{525}$.

6.2.12. Soret absorbance spectroscopy

Soret absorption of the heme group was monitored on a Spectramax M5 (Molecular Devices, Sunnyvale, CA) spectrofluorometer by using 1 cm path length cell. The collected samples were 20-fold diluted and the readings taken in the range of 380-430 nm.

6.2.13. Circular dichroism (CD) spectra acquisition and analyses

Far-UV CD spectra of 0.2 mg/mL of unmodified and modified Mb in a 50 mM phosphate buffer (pH 7.4) were recorded at 20°C in the spectral range from 190 to 250 nm with spectral resolution of 2 nm on a OLIS DSM 17 UV-Vis-NIR CD spectrophotometer (Bogart, Georgia, USA). Spectra were recorded as averages of five scans. Quartz cuvettes with an optical path of 1 mm were used. The solvent reference (a protein-free buffer) spectrum was subtracted from each sample spectrum automatically after which the data were smoothed and converted to molar ellipticity (θ) units ($deg \cdot cm^2/dmol^{-1}$), as described by Yang et al. (2004). The amount of secondary structure associated with samples was estimated using the CONTIN/LL program in CDPro software.

6.2.14. Intrinsic fluorescence measurements

Recordings of fluorescence emission spectra were obtained immediately after incubation of control and treated solutions, diluted 20-fold, at specific time point. Spectra were recorded using quartzglass cuvettes (QS-1.000 Suprasil, HellmaGmbH & Co, Germany) (light path of 1 cm) at $\lambda_{excitation}$ of 280 nm and $\lambda_{emission}$ of 290–400 nm (Spectramax M5). Phosphate buffer (50 mM, pH 7.4) was used for samples dilution and baseline subtraction.

6.2.15. Thioflavin T (ThT) fluorescence spectroscopy

ThT stock solution was prepared by dispersing 8 mg of ThT into 10 mL of 50 mM phosphate buffer (pH 7.4) containing 150 mM NaCl and passed through a 0.22 μm Millipore filter. This stock solution was stored in the dark at 4°C. The stock solution was diluted by 50-fold in the same buffer on the day of analysis to produce the working solution. To prepare samples for spectrofluorometry, 50 μL of samples aliquots were mixed with 5 mL of ThT working solution and allowed to stand for 1 min. The fluorescence spectra of the mixtures were acquired (Spectramax M5) using the excitation wavelength of 460 nm and the emission wavelength at a

range of 480-550 nm (Mishra et al. 2007). The fluorescence spectrum of the ThT working solution and GlcN control were subtracted from the fluorescence spectra of the samples.

Followed subtraction of zero time values, data curves were plotted expressing the mean of triplicates with standard deviation. Curves were fitted with non-linear regression fit using GraphPad Prism software.

6.2.16. Transmission electron microscopy (TEM)

Myoglobin fibrils formation in the presence of different sugars was monitored by TEM. Control and conjugated aliquots of 50 µL were sampled from a protein solution of 5 mg/mL, diluted 100-fold with phosphate buffer pH 7.4 and deposited on 400-mesh formvar/carbon grid (Ted Pella, Redding, CA) and allowed to absorb for 3 min. The excess liquid was blotted gently on Kimwipes (Kimberly-Clark). A drop of stain, 1% aqueous uranyl acetate (Ted Pella, Redding, CA) made up fresh was placed on the grid for 1 min. After drying on the bench, the grids were visualized by a Philips EM 410 at 80 kv.

6.2.17. Statistical analyses

Data were tested for significance by analysis of variance (ANOVA) using the PROC MIXED procedure of SAS (v. 9.3, SAS Institute Inc., Cary, NC). Comparison among means was evaluated by performing Tukey's honestly significant difference test ($p < 0.05$). Data for carbonyl groups content and ThT fluorescence were plotted as a function of incubation time to generate curves. Data were fitted with the non-linear fitting using GraphPad Prism software.

6.3. Results

6.3.1. Mass spectrometric glycoform profiling of myoglobin

6.3.1.1. MALDI-TOF/TOF-MS

The power of mass spectrometric techniques for the identification of glycated proteins has been widely accepted. MALDI and ESI mass spectrometries, in particular, are validated by numerous studies on protein glycation. The combinatorial approach with both techniques allows using the advantages typical for both techniques obtaining complimentary information and a better understanding of the reaction evolution. MALDI-TOF/TOF-MS was applied initially to investigate Mb's *in vitro* glycation, performed by incubation at 37ºC (pH 7.4) with GlcNAc, Glc and GlcN from 0 to 12 days. Modifications were monitored through the increase in the molecular weight as a result of covalent sugar or glycation product addition. The MALDI spectrum from the different treatments is shown in Figure 6.1.

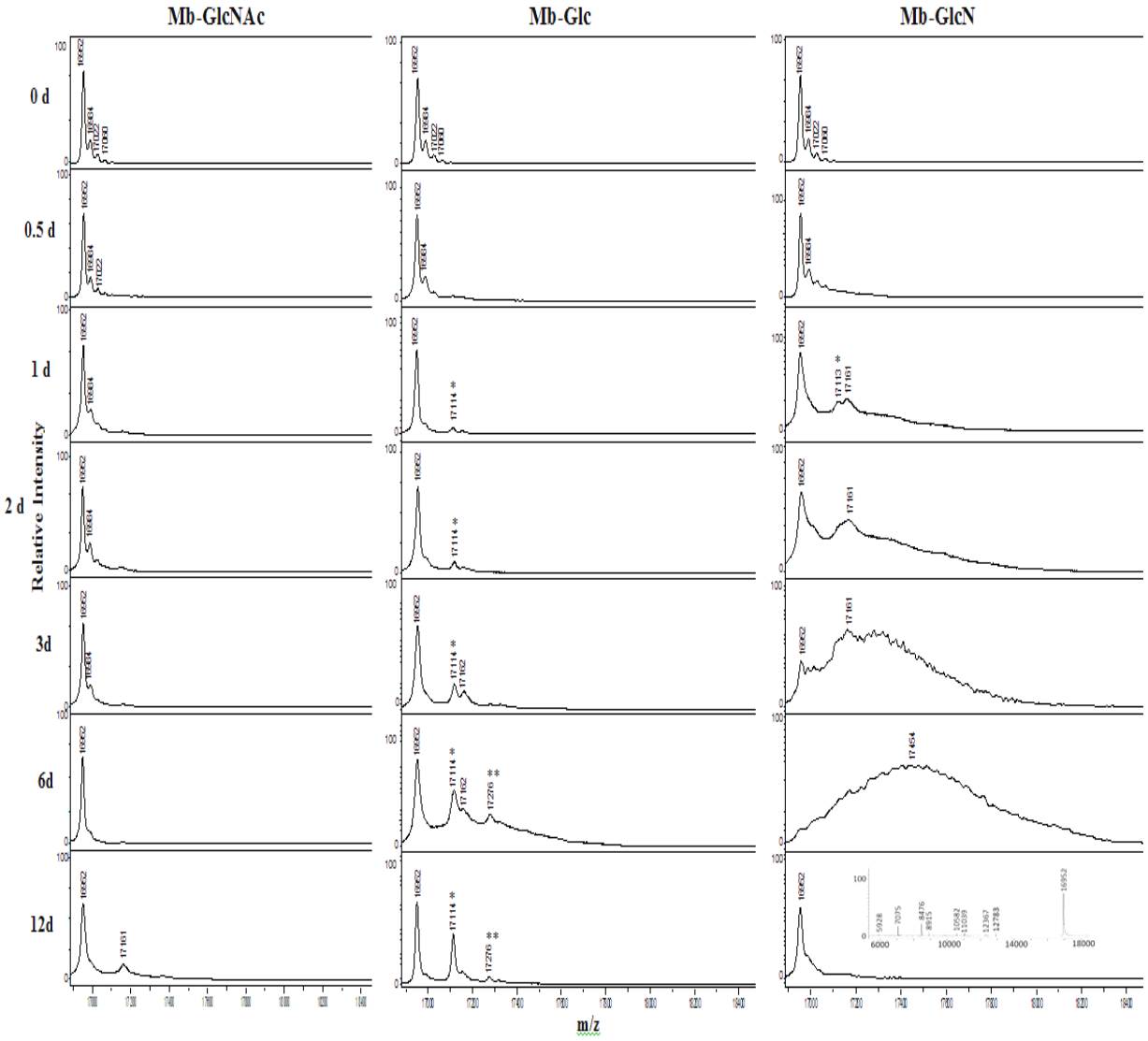

Figure 6.1. MALDI-TOF/TOF deconvoluted mass spectra of Mb incubated at 37ºC for various times in the presence of GlcNAc, Glc and GlcN. Sugar adducts are marked with a star, with the number of stars corresponding to the number of adducts.

The peak at 16952 Da, corresponding to a protonated apomyoglobin (apoMb) was found in all the spectra profiles. Heme-globin interactions are disrupted during desorption/ionization process resulting in extensive loss of the heme (Zehl and Guenter, 2004). Other peaks presented in all the profiles were at 16984 Da, which corresponds to an increment of 32 Da possibly due to double

oxidative adducts formation (Suckau et al. 2003) and the peaks at 17022 and 17060 Da are likely due to potassium adducts.

There were no major changes in the spectra Mb glycated with GlcNAc over time suggesting no glycation occurrence within the reaction period studied. The evaluation of blocked -NH_2 groups (refer to Appendix E) supports this assumption, since only 3.9% of -NH_2 was found to be modified at 12 reaction days, whereas for the Mb-Glc and Mb-GlcN treatments the percentage reached 32 and 49, respectively.

For Mb-Glc conjugates after 1 day of reaction a new peak at m/z 17114 arose, and corresponded to molecules produced by the condensation of one Glc molecule (+162 Da) (Roberts et al. 2001). With a prolonged reaction time the intensity of monoglycated peak increased and a peak at m/z 17276 was also observable starting from 6 reaction days, likely corresponding to a diglycated form with a mass shift of 324 Da (Amoresano et al. 2000).

In Mb-GlcN mixture after one reaction day GlcN monoadducts were identified at m/z 17113 (Δm = 161 Da). As the reaction progressed up to three days only broad and poorly resolved peaks were found, most likely due to both a large heterogeneity of the glycoforms (Roberts et al. 2001) and modifications caused by the high production of α-DC generated from the non-enzymatic degradation of GlcN (Chapter 5 Table 5.1). Furthermore, it is expected that in presence of proteins α-DC production would further increase (see α-DC section further). These extensive changes in MS profile were corroborated with the significant accumulation of AGEs (refer to Appendix F). By day 6 of reaction, only a large bell-shaped distribution of signal was observed and the disappearance of the signal from unmodified Mb, likely due to the increased formation of AGEs (Niwa, 2006). For instance, Zhang et al. (2004) demonstrated accumulation

of high molecular weight AGEs during glycation of fibrinogen and human serum albumin by GlcN at 37°C for 30 days.

Remarkably, slight protein precipitation was also observed by the naked eye after 3 days of glycation and became more significant after 6 and 12 days (see pictures in Figure 6 B). Bokiej et al. (2011) also reported un-interpretable MALDI mass spectra during the incubation of Mb with highly-reactive D-ribose- 5-phosphate (R5P) for longer than 18 h. Due to extensive precipitation of Mb-GlcN conjugates at 12 days, the MS analysis was mainly performed on the supernatant fraction, due to the inability to process the precipitated material. A significant protein fragmentation was observed, as evident from the appearance of smaller molecular weight fragments in the mass range m/z 6000-15000 Da, apart from double charged ion peak of Mb at m/z 8476 (Figure 6.1 A inset). These results were also observed on SDS-PAGE electrophoresis (data not shown), where high and low molecular bands were present for the same treatment starting from 3 days of glycation.

6.3.1.2. Electrospray ionization mass spectrometry (ESI-MS)

The MALDI-TOF/TOF-MS results indicated extensive heterogeneity but no discrete masses could be resolved efficiently. To improve the analysis of modified Mb, the focus was shifted from MALDI-TOF/TOF-MS to LC/ESI-MS. A dramatic improvement of spectral resolution was obtained particularly for longer incubation periods. A typical ESI deconvoluted mass spectrum over time with different sugars is shown in Fig. 6.2. Similar to a MALDI-TOF/TOF-MS spectrum the major peak at 16952 Da was associated with apoMb. Raw data spectra for Mb-GlcNAc (0 and 12 days), Mb-Glc (0 and 12 days) and Mb-GlcN (0 and 6 days) are shown in Appendices G, H and I, respectively. Under ESI-MS analysis heme loss occurs, resulting in apoMb with a molecular weight of 16950±2 Da [Upmacis et al. 1997].

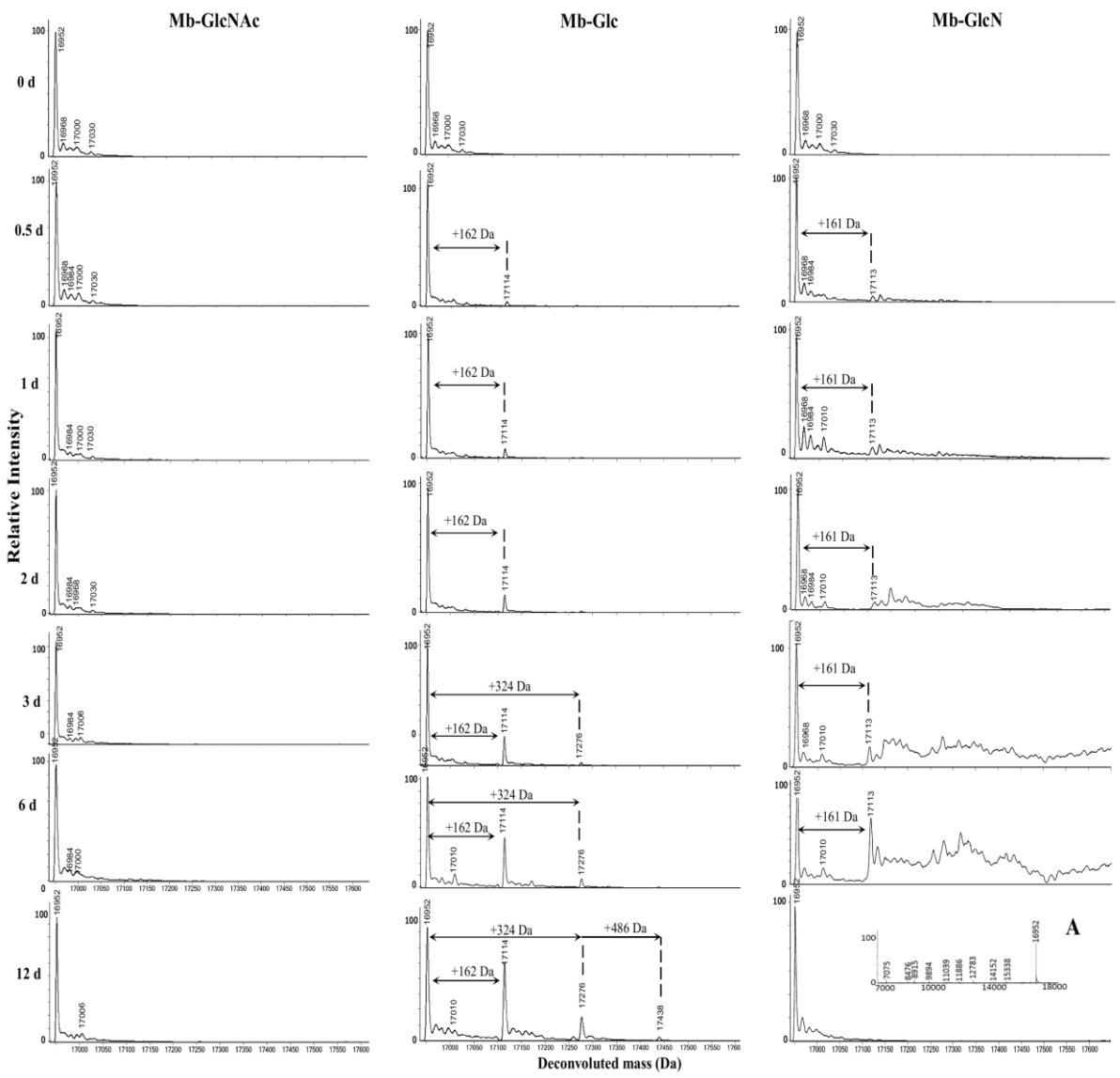

Figure 6.2. A deconvoluted ESI-MS spectra of Mb incubated at 37ºC for various times in the presence of GlcNAc, Glc and GlcN. The experimental conditions were the same as those used to obtain the spectra in Figure 6.1. Inset spectrum (A) shows the spectrum of GlcN incubated for 12 days in the region of 7000-18000 Da.

For Mb-Glc, a mass shift 162 Da upwards was observed incremental to the native apoMb already at 0.5 day and was assigned to a Glc (180 Da) adduct through elimination of water (−18 Da). The relative abundance of this peak at 17114 Da increased with incubation time, suggesting an increased concentration of sugar adducts over time. At 6 days of glycation the Mb's molecular

weight increased from 16952 Da to 17276 Da, corresponding to the condensation of two Glc units on Mb. The condensation of three Glc units was apparent by the peak at 17438 Da after 12 days of glycation. Both the increased abundance of glycated species and the presence of triglycated molecules clearly demonstrate the higher reactivity of glucose compared to GlcNAc. The deacetylation of the GlcN -NH_2 moiety makes it much more reactive towards Mb-GlcN conjugates, which showed progressively higher modifications over time. In the previous study (Chapter 5) glucosone (G) and 3-deoxyglucosone (3-DG) were the most abundant α-dicarbonyl compounds produced during GlcN incubation. Glucosone (Mw=178 Da) or 3-DG (Mw =162 Da) attachment to amino acid residues in Mb could possibly result in the mass shift upward 160 Da or 144 Da, respectively. For instance, the resulting mass difference between GlcN (+161 Da) or G (+160 Da) attachment to Mb is only 1 Da, which is not enough for accurate peak assignment in an intact protein. The complexity of Mb-GlcN reaction mixture leads to a large varieties of glycation combinations, so the discussion here of peak origins is not definitive. Moreover the complexity of the raw data (S5 Fig) also complicates exact peaks identification. Starting from ½ days until 6 days the peak at 17113 Da was likely due to monoglycation (Δm=161 Da). Many other peaks present in this spectra were attributed to the modification of Mb by various adducts, exact nature of which is unknown. The appearance of multiple peaks in the spectrum during prolonged incubation time refers to more numerous modifications, including the occurrence of oxidation/dehydration and possibly condensation (Chapter 5) reactions in the presence of GlcN. As mentioned earlier, mostly the supernatant was analyzed at 12 days of reaction due to substantial protein precipitation. The ESI-MS results corroborate with those of MALDI-TOF/TOF-MS, showing strong protein degradation, generating fragments with a molecular weight ranging from 7000 to 16000 Da. Protein fragmentation is most likely due to the

production of reactive oxygen species (ROS) generated in the Mb-GlcN model system (Bokiej et al. 2011). In this regard, at least three major sources can contribute to ROS production. The first is direct autoxidation of GlcN and the second is the Schiff base/Amadori compounds produced from both glycation of Mb with GlcN and α-DC condensation with Mb and GlcN, respectively (Mossine et al. 1999). Lastly, ROS production may be further facilitated by the presence of Mb, a biological Fenton reagent (Sadrzadeh et al. 1984). Human serum albumin scission to fragments of discrete sizes was also demonstrated over prolonged glycation in the presence of copper ions, proposed to cause fragmentation via free radical mechanism (Hunt and Wolff, 1991; Hunt et al. 1993).

Although MALDI-TOF/TOF-MS results showed the same trend of the extent of glycation with different sugars, the superior peak resolution of ESI (Hail et al. 2004) was obtained. Thus in this regard, in our study conditions, ESI-MS was better than MALDI-TOF-MS, especially for Mb-GlcN conjugates with higher glyco-heterogeneity.

6.3.2. Glycation induces myoglobin oxidative modifications through carbonyl formation

The Maillard reaction induces protein oxidation (Liggins and Furth, 1997). For instance, protein carbonylation is a type of protein oxidation that can be promoted by ROS, including hydrogen peroxide and free radicals, and usually refers to a process that forms reactive ketones or aldehydes (Wong et al. 2010). Lysine, arginine, proline, and threonine residues, among other amino acids are normally subjected to direct ROS attack forming carbonyl groups (Suzuki et al. 2010). As previously discussed in mass spectrometry section, it is expected that the reaction cocktail containing GlcN and Mb possesses all the triggers to produce an elevated concentration of ROS species. Figure 6.3 reports Mb carbonylation over time as a function of the different treatments.

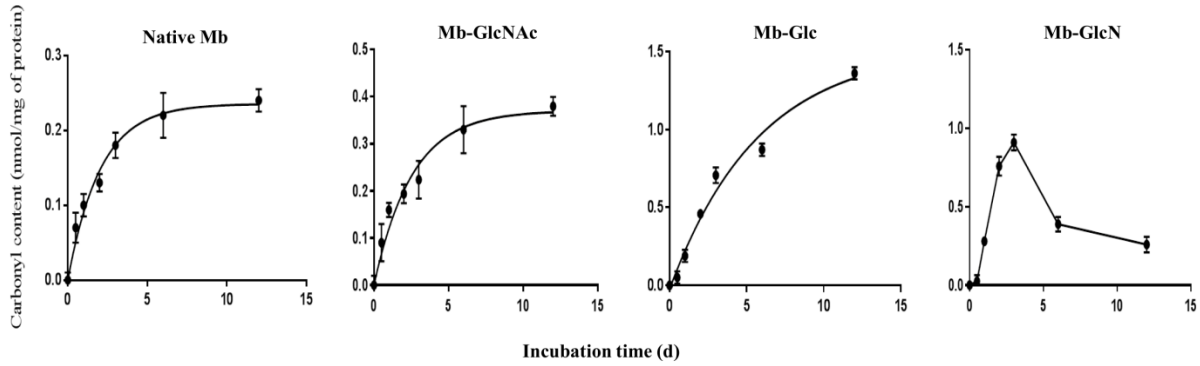

Figure 6.3. Protein oxidation (carbonyl content) in Mb and Mb conjugated with GlcNAc, Glc and GlcN from 0 to 12 days. The results are mean ± standard deviation of three independent experiments. Data were fitted (except Mb-GlcN) with the non-linear fitting by GraphPad Prism software using following exponential equation: $y = A(1-e^{-kt})$, where y is the product concentration, A is the initial value at t_0, k is the reaction rate, and t is time.

In the control (Mb incubated without reducing sugars) and GlcNAc treatments, carbonyl production increased slightly, reaching a plateau at concentrations of 0.23 and 0.37 nmol/mg protein, respectively. The same exponential fitting was applicable for Mb-Glc treatments withthe mean values of around 3.2 times higher as compared to Mb and Mb-GlcNAc, reaching a plateau at 1.56 nmol carbonyls/mg protein as estimated by the exponential fitting model. In addition, native Mb and Mb-GlcNAc mixtures showed a lower velocity of carbonyls development, as reflected by the plateau reached by 10-11 days of incubation, whereas in Mb-Glc conjugates the plateau level was reached at 12 days of glycation.

In Mb-GlcN treatment, carbonyls increased sharply up to 3 days incubation (1.01 nmol/mg protein), with a subsequent dramatic decrease (0.36 nmol/mg protein) at 6 days. This pattern was most likely due to the nature of GlcN which possess an $-NH_2$ that can condense (and thus "quench") with the carbonyl compounds on Mb. This also induces more glycation (see also Chapter 3) with subsequent detrimental effects on Mb structure, thus leading to rapid protein aggregation (see section on conformational changes). Therefore, the higher reactivity of GlcN

towards Mb compared to Glc and GlcNAc depends not only on the amount of α-DC produced at the beginning of the reaction (section α-DC formation), but also on the additional effect of the free -NH_2 group of GlcN reacting with the carbonyls formed during Mb oxidation (see also Chapter 3).

6.3.3. Identification and quantitation of the major α-dicarbonyl compounds in Mb-GlcN

In a previous study (Chapter 5) a significant formation of reactive α-DC from GlcN incubated at 37°C was reported. α-DC are up to 20,000-fold more reactive than Glc in inducing the Maillard reaction (Rabbani and Thornalley, 2008), which can explain the characteristic mass profile reported in Figures 6.1 and 6.2 for Mb-GlcN treatment. To investigate the amount of α-DC formed in Mb-GlcNAc/Glc/GlcN conjugates, the latter were trapped by reacting with *o*-OPD and the resulting quinoxaline derivatives were analyzed. However, there was no detectable α-DCs in Mb-GlcNAc conjugates up to 12 days of incubation, whereas α-DC were observed in Mb-Glc-NH_3 samples at 6 and 12 days of reaction, but at a lower level as compared to Mb-GlcN. Hence, attention was devoted mainly on identifying and quantifying the α-DC derived from the Mb-GlcN reaction mixture. Figure 6.4 B illustrates a UHPLC-UV representative chromatogram of Mb-GlcN conjugates incubated for 1 day. The identity of the peaks, determined by elution time, molecular mass and mass fragmentation pattern as compared to the standards (Figure 6.4 A) and /or literature (Papetti et al. 2014; Gensberg et al. 2012; Mavric et al. 2008) is reported in Table 6.1.

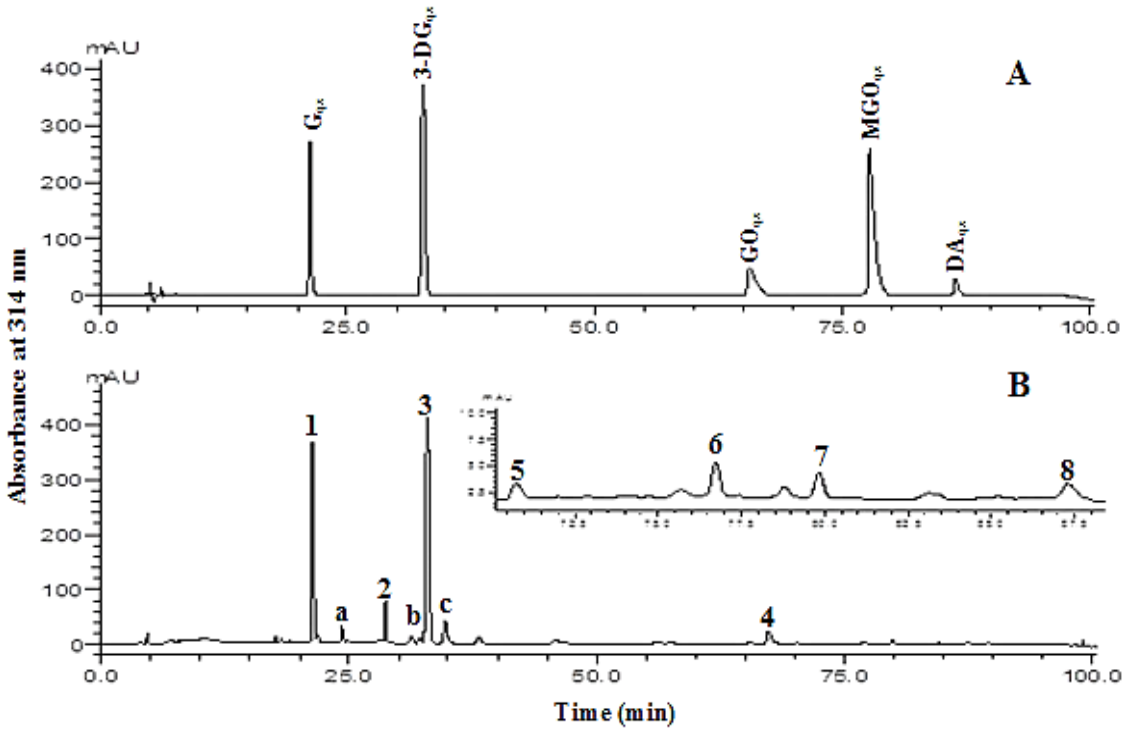

Figure 6.4. UHPLC analyses of quinoxaline derivatives of α-dicarbonyl compounds produced from Mb-GlcN conjugates over time. (A) Chromatograms of a reference quinoxaline mixture of glucosone (G), 3-deoxyglucosone (3-DG), glyoxal (GO), methylglyoxal (MGO) and diacetyl (DA). (B) Representative chromatogram of Mb-GlcN conjugate incubated for 1 d, derivatized with OPD and acquired by UHPLC with UV detection at 314 nm. Numbers indicate the peaks of the quinoxalines of (1) G, (2) unidentified, (3) 3-DG, (4) GO, (5) HPA, (6) 3,4- DGE, (7) MGO, (8) DA and a, b, c peaks corresponding to non-OPD derived GlcN condensation products.

Table 6.1. Retention time, structure, MS and MS/MS data of the α-dicarbonyl compounds detected Mb-GlcN conjugates.

Peak	Retention time (min)	Structure	Precursor ion $(M+H)^+$	MS/MS fragments
1	21.3	**Glucosone$_{qx}$** 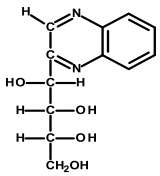	251.1038	251.0930 (2), 233.0923 (100), 215.0817 (30), 173.0710 (32), 161.0710 (15), 145.0553 (2)
2	28.5	Unidentified	235.0978	235.0977 (5), 217.1944 (20), 199.0865 (10), 187.0864 (21), 179.1057 (45), 175.1474 (100), 157.0774 (8), 145.0759 (10)
3	32.7	**3-Deoxyglucosone$_{qx}$** 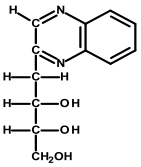	235.0991	235.0992 (10),217.0974 (100),199.0868 (52), 187.0867 (3), 171.0917 (5), 157.0760 (12), 145.0760 (7), 130.0437 (4)
4	66.5	**Glyoxal$_{qx}$** 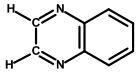	131.0614	131.0601 (100), 104.0492 (38),102.4872 (12), 77.0163 (10)
5	70.7	**Hydroxypyruvaldehyde$_{qx}$** 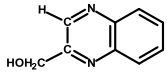	161.0722	161.0711 (7), 143.0602 (17), 139.1301 (10), 133.0760 (100), 119.0602 (87), 102.5203 (45), 71.1806 (12)
6	76.7	**3,4-Dideoxyglucosone-3-ene$_{qx}$** 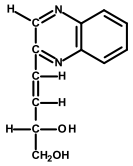	217.1712	217.1702 (100), 199.0869 (7), 181.1072 (7) 157.1234 (17), 145.0760 (7), 130.0729 (5)
7	79.8	**Methylglyoxal$_{qx}$** 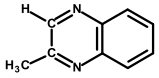	145.0773	145.0760 (100), 118 (12), 102.5180 (20), 77.2856 (5)
8	87.3	**Diacetyl$_{qx}$** 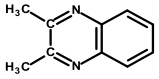	159.0933	159.0998 (15), 145.0932 (12), 131.0603 (100), 102.4846 (47)

As expected, the quinoxaline derivative of G eluted first as identified at m/z 251.1038. It was followed by the quinoxaline derivatives of 3- DG identified at 235.0991. GO derivatives eluted following HPA, 3,4-DGE, MGO and DA quinoxalines. After identifying the presence of major α-DC, five of them were quantified and the concentrations expressed in mg/L and are reported in Figure 6.5.

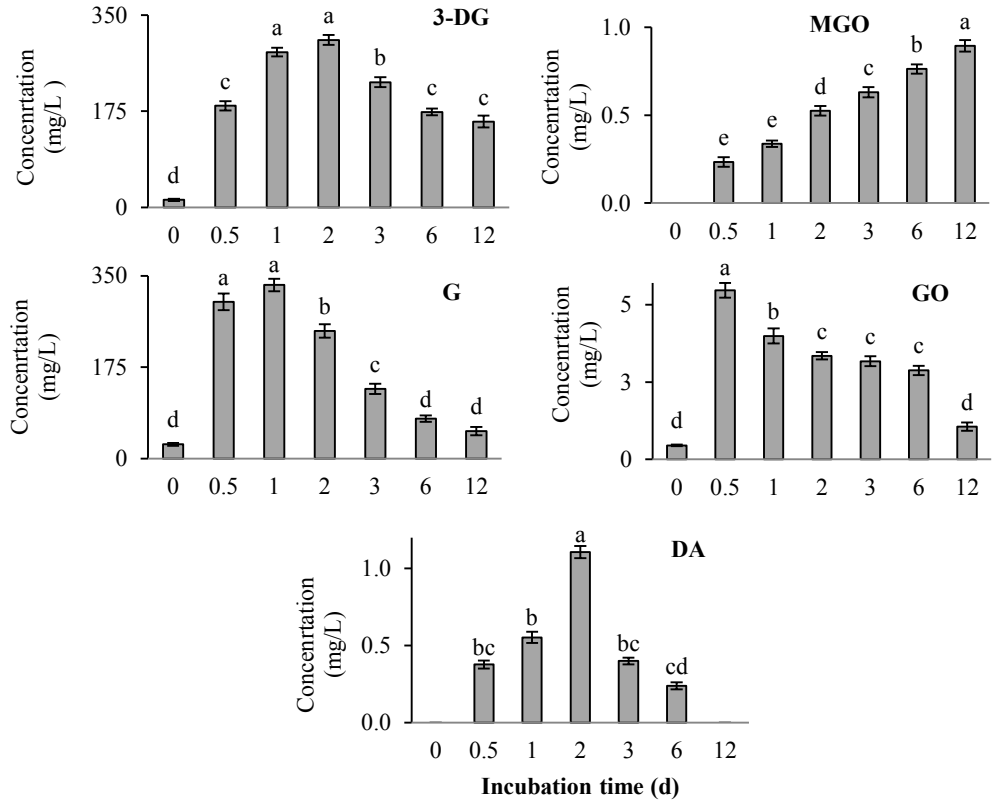

Figure 6.5. Concentration of the major α-dicarbonyl compound produced during incubation of Mb in the presence of GlcN from 0 to 12 days. The values are represented as mean ± standard deviation (calculated from three independent trials). G, glucosone; 3-DG, 3-deoxyglucosone; GO, glyoxal; MGO, methylglyoxal; DA, diacetyl. Different letters within each α-dicarbonyl compound indicate statistical significant difference ($p < 0.05$).

All α-DC, except MGO and DA were present in control samples, suggesting a partial degradation of GlcN while it was stored in powder form. Previously the presence of G, 3-DG and GO was also found in untreated GlcN (Chapter 5). Overall, G and 3-DG were the most abundant α-DC in Mb-GlcN conjugates, followed by GO, MGO and DA. At the beginning of the

incubation, G was the most abundant α-DC reaching the highest concentration at 0.5 and 1 day of the reaction (~332 mg/L on average). With prolonged reaction times its concentration dropped significantly ($p < 0.05$). 3-DG was the most abundant at 1 and 2 days of reaction, then decreased almost 2-fold by the end of the incubation time tested. At shorter reaction times (0.5 and 1 d) the amount of G was 1.3 times higher than 3-DG, however with prolonged times to 6 and 12 days 3-DG became more prevalent by 2.3-fold. This suggests that at the beginning of the reaction the oxidative pathway is the dominant, and by increasing the reaction time the enolization pathway becomes favourable. A similar trend was reported for GlcN incubation alone with similar conditions (Chapter 5), where the values for 3-DG were significantly ($p < 0.05$) lower for all studied times, except for 12 days, where the quantity of 3-DG reached 209 mg/L. When comparing G amount in GlcN incubated alone or Mb-GlcN conjugate at all incubation times, the presence of protein increased the amount of G produced. The opposite relationship was found between GO and MGO generation over time in the Mb-GlcN system. While the concentration of GO significantly ($p < 0.05$) decreased from 5.5 mg/L at 1 day to 1.1 mg/L after 12 d, the amount of MGO significantly ($p < 0.05$) increased from 0.2 to 0.9 mg/L. MGO derives from fragmentation of 3-DG by a retroaldol condensation reaction (Thornalley et al. 1999), whereas GO is produced at the very early stages of the Maillard reaction or as a result of C-2/C-3 scission of the G (Hofman et al. 1999).

For instance, at 0.5 day MGO accounted for 0.1% of 3-DG, whereas with incubation up to 12 days the percentage increased to 0.6. In comparison, MGO and GO derived from GlcN incubation was reported (Chapter 4) to follow a similar tendency of increasing and decreasing over time, respectively, however in quantities much lower than in Mb-GlcN conjugate.

DA reached the highest concentration at 2 days of incubation (1.1 mg/L), followed by a significant ($p < 0.05$) decrease by 6 days and was not detected at 12 days of incubation. A similar trend of the highest amount at 2 days was observed for DA produced from GlcN incubation, but with a concentration around 3.2-fold less as in Mb-GlcN conjugate.

In summary, the amount of α-DC produced in Mb-GlcN, particularly at the beginning of the reaction, was greater compared to the one observed in non-enzymatic degradation of GlcN alone (Chapter 5). The reason for this phenomenon is likely due to Mb supplying side chain amino groups for the Maillard reaction with GlcN; however it may also be due to the catalytic effect of heme iron on both GlcN and Amadori product oxidative degradation. In this regard, as shown in Figure 6.6 A about the Soret band, heme iron was displaced from the hydrophobic core of Mb during the course of glycation. This would increase its ability to catalyze the oxidation degradation of GlcN and Amadori intermediates to α-DC. Further investigations are required to confirm this phenomenon.

6.3.4. Mb-Fe^{3+}-reducing activity of GlcN

Of interest is the effect of GlcN on the oxidative status of iron in Mb (Figure 6.6). After 1 day of incubation the proportion of Mb-Fe^{2+} (deoxy- + oxyMb forms) relative to Mb-Fe^{3+} (metMb) increased by up to 50%. There are several theories to explain this phenomenon. For instance, Stepuro et al. (1997) observed reduction of ferriforms of cytochrome C and metMb by adding glycated amino acids or glycated albumin. The authors proposed it was due to the effects of a combination of $O_2^{\cdot -}$ and α-dicarbonyls in the reduction process. Gersten et al. (2010) reported that the reaction of bovine cytochrome C and R5P rapidly generated superoxide ($O_2^{\cdot -}$) that subsequently reduced ferri- to ferro-cytochrome C. Also these authors noted that the addition of amines to the cytochrome C-R5P system greatly increased the generation of $O_2^{\cdot -}$ at 37°C.

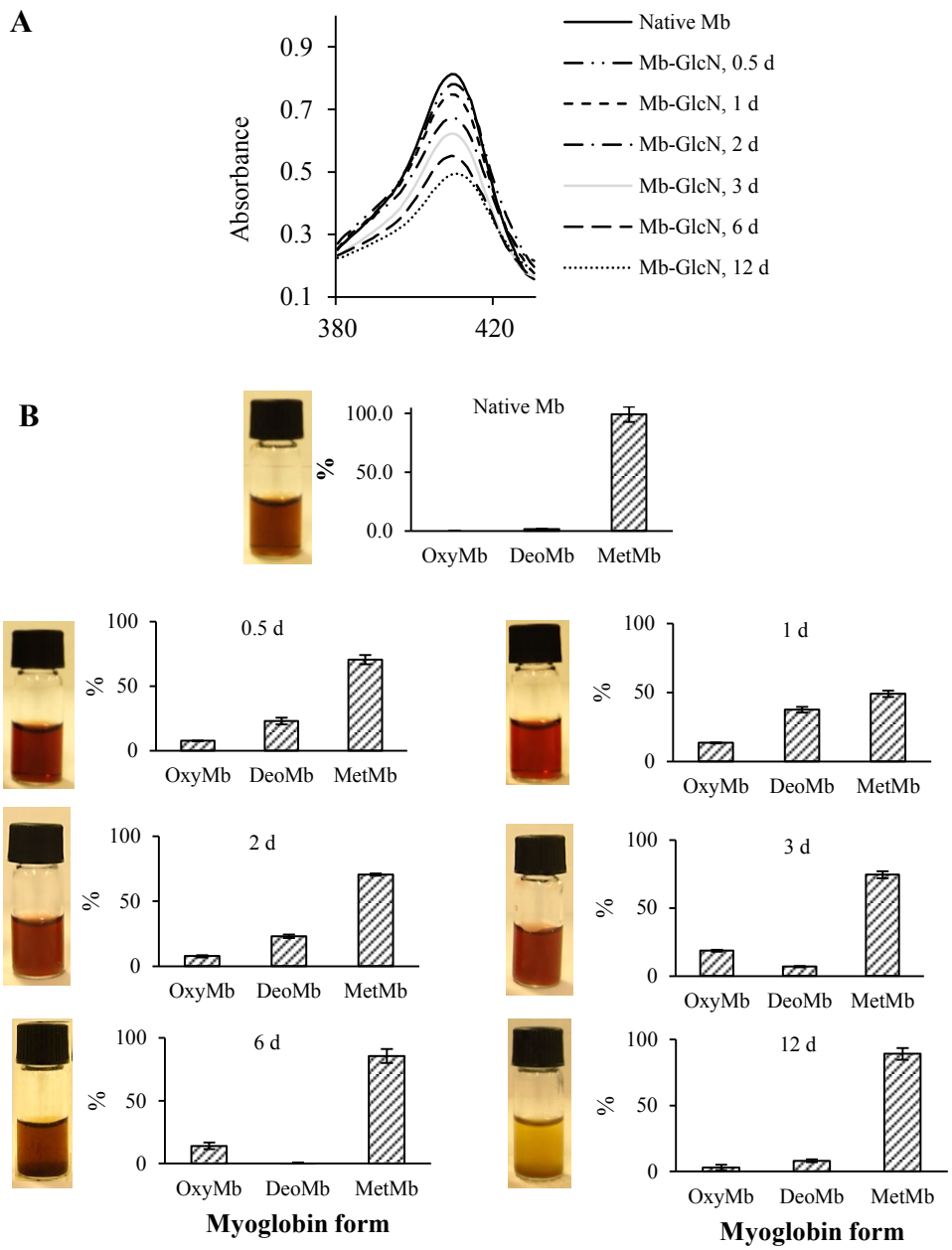

Figure 6.6. (A) Decrease in Soret band absorbance; (B) images and the percentages of metmyoglobin (MetMb), deoxymyoglobin (DeoMb) and oxymyoglobin (OxyMb) in native Mb and Mb-GlcN conjugates over glycation period from 0.5 to 12 days.

The reaction of R5P with metMb also resulted in the formation of oxyMb within 1-2 days of the reaction at 37°C and was ascribed to the rapid generation of $O_2^{\cdot -}$ from sugar which subsequently

reduced Mb`s state. Glycation can also generate “reductones”, which refers to compounds with an enediol structure next to a carbonyl, such as G and 1-DG (Kanzler et al. 2014). As a matter of interest, the production of G which was the highest one at 1 day (Figure 6.5), however, with time, this effect was lost and the deleterious effect of α-DC and ROS (i.e. H_20_2) on Mb structure became dominant. Finally, in the last stage of the Maillard reaction free and bound AGEs to protein are formed. Some AGEs, like for instance argpyrimidine, have been recognized to act as reducing agent inducing formation of oxyMb in fructated Mb (Bhattacherjee and Chakraborti, 2011). In addition, dihydroxyfructosazines deriving from GlcN cyclocondensation were also reported to carry a reducing power (Shimamura et al. 2003).

6.3.5. Conformational changes of myoglobin during glycation in the presence of glucosamine

6.3.5.1. Intrinsic fluorescence of glycated Mb

Fluorescence spectroscopy analyses were performed to examine the alterations in the molecular structure of glycated Mb. Mb-GlcNAc treatments did not show any significant impact on the protein structural arrangement. Even though glycation with Glc was found to occur, particularly at longer reaction times, the effect on conformation was significantly less as compared to GlcN. The following discussion focuses on the structural modification of Mb induced by GlcN. When excited at 280 nm, the protein tertiary structure is reflected, since this frequency of electromagnetic radiation excites Trp and Tyr. In the region of 290 to 400 nm, native Mb has one emission peak with a maximum intensity at 325 nm (Figure 6.7 A). Glycation markedly decreased emission intensity in relation to the native protein, after 0.5 days of reaction. This suggests a strong influence of GcN attachment on the local environment around Trp and Tyr residues. Even though changes in intrinsic fluorescence are symptomatic to the local changes in the Trp and Trp microenvironment, they are usually associated with larger structural rearrangements of the peptide chains, including protein polymerization. Mb contains two highly

conserved tryptophan residues located at positions 7 and 14 on the α-helix (Sirangelo et al. 2002). According to Tang et al. (2011) attachment of sugar moieties to protein causes Trp hydrophobic chromophores to become more buried within the molecules, resulting in a lower extent of interaction with quenching agents. Indeed, in folded Mb the Trp residues are partially quenched by the heme group (Roncone et al. 2004). Consequently, a decrease in Trp fluorescence in glycated Mb could correspond to a more closed structure where the Trp is closer to the heme group, increasing its quenching effect. On the other hand, Swamy and Surolia (1989) proposed that decrease in fluorescence results from the exposure of tryptophanyl residues to the solvent molecules that collide with fluorophores and consume fluorescence energy. The decrease could also be induced by oxidation, since the indole ring of Trp and side chain of Tyr are susceptible to oxidative damage by ROS (Villamena, 2013).

Upon incubation, the decrease in emission was accompanied by a progressive bathochromic shift (~15 nm) in the wavelength of maximum emission (λ_{max}). This shift usually corresponds to an exposure of intrinsic tryptophan residues of glycated protein to a more polar medium in the presence of carbohydrates (Nagy et al. 2009). Fluorescence emission of Trp7 is significantly quenched by Lys79 (EF2 helix), therefore a red shift in emission could be also due to the movement of this Lys away from Trp7 when the α-helix unfolds (Hargrove et al. 1994) as a result of glycation. At the same time glycation-induced conformational changes could increase the separation between two of Mb's Tyr residues (Tyr103 and 146) and energy acceptors, especially for Tyr 103, which is located in a close proximity to the heme. The same results of decreasing in fluorescence intensity along with a red shift were reported in the study of Tang et al. (2011), who performed glycation of phaseolin with Glc at 60˚C.

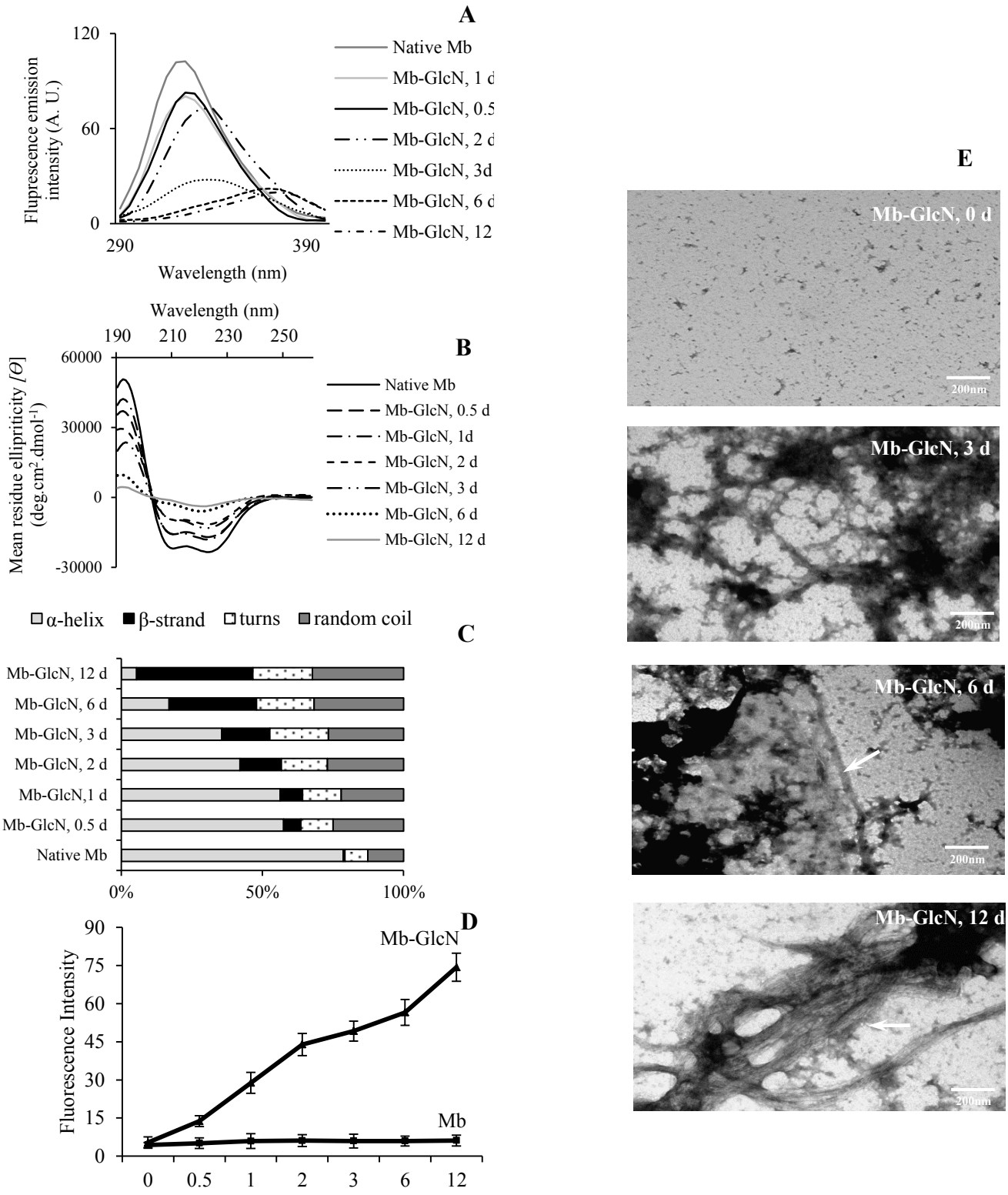

Figure 6.7. (A) Fluorescence emission spectra; (B) far-UV spectra analyses; (C) secondary structure fcomposition; (D) maximum fluorescence intensity of Thioflavin T (λ=482 nm). The data points all have SD bars, but some are illegible and lie within the symbols; (E) transmission electron micrographs of native Mb and Mb incubated in the presence of GlcN at specific time points.

Jin et al. (2013) also reported decrease in fluorescence concomitantly with red shift while investigating the deactivation of chloroperoxidase by different monosaccharide, attributing this to the uncoiling of α-helical structures in the presence of sugar and protein precipitation. In the current study, strong protein precipitation was observed when glycating with GlcN, observed at 6 days of reaction (Figure 6.7 E). This remarkable change in fluorescence emission suggests that glycation with GlcN causes substantial alterations in Mb`s tertiary structure along with displacement of heme from the hydrophobic pocket within Mb's interior (Figure 6 A).

6.3.5.2. Secondary structure fingerprint by circular dichroism spectropolarimetry

After confirming changes in tertiary conformation of Mb, it was attempted to detect whether the secondary structure was altered during glycation. The far-UV (190-260 nm) CD spectrum is an extremely sensitive probe for protein secondary structure, reflecting its structural features due to absorption of the peptide bond (Martin and Schilstra, 2008). The conjugation of sugar induced the changes in the secondary structure of Mb, as shown by the difference in CD spectra of native and glycated protein in far-UV CD region (Figure 6.7 B). The CD spectra of native Mb (control) displayed CD bands in a wavelength shorter than 240 nm, which is characterized by two negative bands (210 and 222 nm) and single positive (192 nm). The secondary structure of native Mb was 78.6 % α-helix, 0.6% β-strand, 8.1% turns and 12.7% random coil (Figure 6.7 C). Horse myoglobin consists of eight helical regions (named A to H), separated by non-helical segments (AB, BC, CD…GH) (Picotti et al. 2004). Compared to native Mb, Mb-GlcN conjugates showed a gradual decrease in negative ellipticity in the region 210–225 nm, associated with a decrease in α-helix content (Figure 6.7 C). This decrease in α-helix content of glycated Mb was compensated by an increase in β-sheets, random coiling and turns, suggesting the disruption of secondary structure by glycation. As shown (Figure 6.7 B, C) glycation over time greatly

impacted the secondary conformation of protein, evident already at 0.5 days. This corresponds to information obtained from ESI-MS, where the changes in Mb-GlcN conjugates were identifiable already at 0.5 days of glycation. Such major modifications of secondary structure composition over time result from the steric hindrance attained from the attachment of GlcN and/or its derivatives. They could be involved in protein unfolding and subsequent aggregation by the formation of intermolecular β-sheets. In 12 d, only 5.4% of Mb`s α-helical structure retained, while 41% of its chains attained a β-sheet conformation. This increased tendency to form highly insoluble fibrillar aggregates during glycation of an original α-helical structure into a predominantly β-sheet conformation was reported previously for different proteins, including apoMb (Iannuzzi et al. 2013), albumin (Bouma et al. 2003; Monacelli et al. 2013) and islet (Kapurniotu et al. 1998). Uzzan et al. (2007) in an attempt to produce a GlcN-enriched milk beverage reported that GlcN instantaneously destabilized the milk protein system at 100°C or higher, causing a rapid and drastic precipitation. In a search for evidence of a β-sheet conformation, implying the formation of amyloid-like aggregates, the glycated Mb preparations were analyzed by transmission electron microscopy and thioflavin T staining.

6.3.5.3. Aggregation propensity of Mb-GlcN conjugates: Th T fluorescence and TEM

In order to understand if aggregates formed in the presence of GlcN were amyloidogenic, a benzothiazole fluorescent dye (ThT) was added to the samples. ThT, as an extrinsic fluorescent probe molecule, once binding to amyloid fibrils, gives a characteristic fluorescent emission at ~480 nm with intensity proportional to the amount of amyloid fibrils present (Ma et al. 2014). As shown in Figure 6.7 D, the fluorescence of ThT at 482 nm slightly increased at 0.5 days incubation relative to the Mb control, whereas a marked increase was observed after 2 days. This suggests an onset of fibril formation. At the same time, Mb incubated with GlcNAc and Glc

(refer to the Appendix J) showed no significant changes in ThT fluorescence under the experimental conditions applied. The control Mb showed no changes in fluorescence intensity at 482 nm when exposed to the dye, and therefore Mb did not bind the dye (Figure 6.7 D). The GlcN-induced modification accelerated Mb aggregation and promoted the formation of amyloid fibrils. In addition, recent studies suggest that some protein molten globules are positive in ThT fluorescence. The increase at the beginning could correspond to a molten globular structure of Mb which over time transforms into fibril-like structures.

Using TEM the morphologies of Mb-GlcN aggregates were examined over time (Figure 6.7 D). Amorphous aggregates, possibly pre-fibrillar species, were observed at 3 days of incubation. Prolonged incubation up to 6 and 12 days resulted in observations of mature bundles of fibrous structures (indicated by arrows). Mb glycation with GlcN strongly affected aggregation behaviour of protein, producing amyloid fibrils within 6-12 days. This agrees with previous studies where glycation with D-ribose promoted rapid amyloid-like aggregation of bovine serum albumin (Wei et al. 2009), Tau (Chen et al. 2009) and α-Synuclein (Chen et al. 2010). Sirangelo et al. (2002) demonstrated that substitutions of both of apoMb's tryptophan residues endowed it with a high propensity to rapidly form fibrils under physiological conditions. This is corroborated with the fluorescence results (Figure 6.7 A), where a significant decrease was associated with changes in the environment of Trp and Tyr amino acid residues.

A specific sequence of events occur to induce the formation of amyloid in Mb, which involves modifications of amino groups at the exposed side of protein, that then stimulates its refolding from a globular state to fibrillar. Firstly, this could occur by the covalent binding of GlcN and derivatives (i.e. α-DC) to amino acids in a way that alters their environment causing partial unfolding. Another mechanism would be through extreme cross-linking due to the production of

α-DC. For instance, 3-DG rapidly reacts with protein amino groups to form AGEs, including imidazolone and pyrraline (Niwa and Tsukushi, 2001) MGO and GO also react with proteins rapidly and directly producing hydroimidazolones and variety of lysine-derived adducts (Thornalley et al. 2008). Lastly, numerous inter- and intramolecular AGE-bridged cross-linkages can exert mechanical stress on the polypeptide chain that facilitates its unfolding (Bouma et al. 2003). For instance, AGE-induced cross-linking of collagen during incubation with glucose at 37ºC was shown by Sajithlal et al. (1998). This variety of cross-links may promote diversity of new bonds between newly-exposed amino acids stimulating the formation of β-sheet structure, a prerequisite for amyloid fibril formation (Rondeau et al. 2011). The multimerization or condensation of glycated proteins into plaque has been reported for extracellular matrix proteins (i.e. fibrinogen and collagen) (Raj et al. 2000). In this way, α-DC and AGEs act as denaturants bringing together sequences that have a propensity to fold into β-sheet structure.

6.4. Conclusions

In conclusion, this study provides further evidence that GlcN is a highly reactive monosaccharide, leading to heme reduction, displacement and significant modifications of protein conformation, involving fragmentation and formation of amyloidal-type fibrils. Production of α-DC and AGEs are suggested to play a primary role in protein aggregation rapidly observed after 3 days of reaction. At the same time, GlcN`s acetylated counterpart, GlcNAc, did not induce significant changes to protein conformation within the timeline studied, confirming the involvement of $–NH_2$ group with the increased rate of modification.

CHAPTER 7. Conclusions, implications and future research

This Ph.D. work started with the aim of addressing a practical issue and ended with more theoretical studies. In the beginning the focus was on addressing the problem of reduced solubility of muscle proteins isolated through the isolecteric solubilization/precipitation process. Later, with an aim of better understanding the chemistry of glucosamine modification, the aminomonosaccharide proposed to create novel glycoproteins, a more detailed study on sugar degradation was performed. It was believed that this would allow for solving the issue of the reduced protein solubility. Overall this research will contribute knowledge to the following fields:

1. Glycoconjugation: evidences were provided that novel glycoproteins with enhanced functionality can be obtained in laboratory conditions at moderate temperatures using glucosamine by two approaches: chemical (the Maillard reaction) and enzymatic (via TGase-catalyzed glycosylation).

2. Technology of conjugation: Dry vs wet glycation: evidences were provided that glycation of muscle protein can be achieved in a liquid environment whereas the majority of the studies in the field have focused on protein glycation at low water activity (dry state).

3. Glucosamine chemistry and its effect protein modification: new results and theoretical aspects about the chemistry of glucosamine *in vitro* that helps to understand its reactivity toward muscle proteins were provided. To best of my knowledge, this is the only research that identifies and quantifies α-dicarbonyl compounds production during GlcN degradation.

4. Protein aggregation: it was demonstrated that glucosamine can induce rapid protein aggregation. Characterization of these aggregates using electron microscopic techniques and chemical assays was performed. Evidence that glucosamine may induce fibrous amyloid structures was provided.

5. Valorization of meat processing by-products: maximizing the use of proteins from the leftover of the meat processing is an industry priority. Retaining protein functionality during the process of extraction is of importance in order to fully use their potential in food formulations.

The results have important implications about the use of glucosamine in food applications. A debate exists between the uses of glucosamine as a natural health ingredient vs. food ingredient. For instance, in North America, glucosamine is regulated as a natural health products or dietary supplement (in US) and does not have the status of food ingredient. The US Food and Drug Administration (FDA) has not yet given GlcN the status of "generally recognized as safe" due to lack of clinical studies that its consumption is safe in young children, pregnant women and diabetics (Kralovec and Barrow, 2008). In light of the results obtained from this study, more studies are necessary to validate the use of GlcN as a food ingredient. For instance, a recommended dose of GlcN supplement is 1.5 g daily (Navarro et al. 2015), which according to the amount of α-dicarbonyls found in the present thesis (Chapter 5) corresponds to around 6 mg, and would put glucosamine at the "safe" level. Degen et al. (2012) made a comprehensive analysis on a total of 173 food items and estimated a total dietary intake of 3-deoxyglucosone between 20-160 mg/day, and methylglyoxal between 5-20 mg/day.

Yet it is still difficult to make strong conclusion about the toxicology of α-dicarbonyl compounds obtained from the diet due to lack of in depth studies in this field. A cautious approach similar to

the one adopted from the FDA should be employed in Canada as well; after all, the effect of the endogenous α-dicarbonyls on oxidative stress and diabetic complications are well-documented in the scientific literature (Rabanni and Thornalley, 2008, 2014; Sena et al. 2012). If glucosamine is allowed to be used in concentrations similar to regular table sugars (i.e. fructose syrup, sucrose), indeed, the amount of consumed α-dicarbonyl compounds will increase. For instance, a company could use a concentration of 5-10% in soft drinks (or other beverages), increasing significantly the amount of α-dicarbonyls, over already higher amount found in these beverages due to fructose. For instance Pepsi, Coca-Cola and Procter@Gamble manufactured glucosamine-fortified beverages, advertising these as supplements. This is why a clear definition of supplemental and regularly consumed beverages needs to be rationally established.

Besides α-dicarbonyl compounds, the effect of GlcN condensation products (i.e. fructosazines) on health needs to be taken in consideration. These compounds are flavouring agents in food, but at the same time they are found in cigarettes (Moldoveanu et al. 2011). Furthermore, *in vitro* studies show that dihydrofructosazines have an impact on DNA. It is therefore recommended that all the necessary experiments are conducted rigorously and reproduced adequately by the proper regulatory institutions before allowing the use of GlcN as a food ingredient.

In terms of future research related to this work, more exploration into the effect of glucosamine on protein aggregation at mild temperatures could be performed. For instance, it would be interesting to study the mechanistic aspects of amyloid formation in myoglobin-induced by GlcN. There must be some particular site in the myoglobin molecule that is highly susceptible to α-dicabronyls and ROS attack, triggering a cascade of events leading to the observed aggregation. This was attempted during my doctoral studies using a proteomic approach based

on peptide mapping modification. However, the complexity of the modifications generated in the model myoglobin-GlcN system was more difficult than expected and only a minor part of these modifications were tentatively identified (i.e. carboxymethylysine modification on Lys147). In addition, the quantification of glucosamine condensation products would be also of an important field of future investigation. Considering the relatively rapid degradation of GlcN over time (unpublished data from my study showed that up to 40% of GlcN degraded at 3 days), it would be necessary to identify and quantify more products of degradation. More time and resources would have been necessary to complete this research. Due to the inconclusive results, this partial and tentative identification has not been included in this thesis, however, this could be the starting point for future studies.

Bibliography

Akamittath, J.G.; Ball, H.R. Transglutaminase mediated polymerization of crude actomyosin refined from mechanically deboned poultry meat. *J. Muscle Foods*. **1992**, *3*, 1-14.

Akhtar, M.; Dickinson, E. Emulsifying properties of whey protein-dextran conjugates at low pH and different salt concentrations. *Colloids Surf., B*. **2003**, *31*, 125-132.

Ames, J. M. The Maillard reaction. In *Biochemistry of Food Proteins,* Hudson, B. J. F., Ed., London: Elsevier Science Publishers. **1992**, pp. 99-153.

Amoresano, A.; Andolfo, A.; Corsaro, M.M.; Zocchi, I.; Petrescu, I.; Gerday, C.; Marino, G. Structural characterization of a xylanase from psychrophilic yeast by mass spectrometry. *Glycobiology*. **2000**, *10*, 451-458.

Anderson, J.W.; Nicolosi, R.J.; Borzecella, J.F. Glucosamine effects in humans: a review of effects on glucose metabolism, side effects, safety considerations and efficacy. *Food Chem. Toxicol*. **2005**. *43*, 187-201.

Ando, H.; Adachi, M.; Umeda, K.; Matsura, A.; Nonaka, M.; Uchio, R.; Tanaka, H.; Motoki, M. Purification and characteristics of novel transglutaminase derived from microorganisms. *Agric. Biol. Chem.* **1989**, *53*, 2613-2617.

Arbia, W.; Arbia, L.; Adour, L.; Amrane, A. Chitin extraction from crustacean shells by biological methods – A review. *Food Technol. Biotechnol.* **2013**, *51*, 12-25.

Babiker, E.E. Effect of transglutaminase treatment on the functional properties of native and chymotrypsin-digested soy protein. *Food Chem*. **2000**, *70*, 139-145.

Ban, L.; Pettit, N.; Li, L.; Stuparu, A. D.; Cai, L.; Chen, W.; Guan, W.; Han, W.; Wang, P. G.; Mrksich, M. Discovery of glycosyltransferases using carbohydrate arrays and mass spectrometry. *Nat. Chem. Biol.* **2012**, *8*, 769-773.

Basman, A.; Köksel H.; Perry, K.W.N. Effects of increasing levels of transglutaminase on the rheological properties and bread quality of two wheat flours. *Eur. Food Res. Technol.* **2002**, *215*, 419-424.

Baudys, M.; Uchio, T.; Mix, D.; Wilson, D.; Kim, S.W. Physical stabilization of insulin by glycosylation. *J. Pharm. Sci.* **1995**, *84*, 28-33.

Bekedam, E.K.; Schols, H.A.; van Boekel, M.A.J.S.; Smith, G. High molecular weight melanoidins from coffee brew. *J. Agric. Food Chem*. **2006**, *54*, 7658-7663.

Belitz, H.-D; Grosch, W;· Schieberle, P. Carbohydrates. In *Food Chemistry*, edition 4; Belitz, H.-D., Grosch, W., Schieberle, P., Eds.; Springer-Verlag Berlin and Heidelberg GmbH: Germany, **2009**; pp. 248-337.

Benjakul, S.; Visessanguan, W.; Ishizaki, S.; Tanaka, M. Differences in gelation characteristics of natural actomyosin from two species of bigeye snapper, *Priacanthus tayenus* and *Priacanthus macracanthus*. *J. Food Sci.* **2001**, *66*, 1311-1318.

Betti, M.; Xu, Y. Protein compositions and methods of making and using thereof. US patent WO 2010136894 A1. Dec. 2, 2010.

BfR. Bundesinstitut für Risikobewertung. Glucosamine in food supplements: risky also for patients taking coumarin anticoagulants. URL http://www.bfr.bund.de/en/press_information/2012/07/glucosamine_in_food_supplements__risky_also_for_patients_taking_coumarin_anticoagulants-128855.html Accessed May, 1, 2015.

Bhattacherjee, A.; Chakraborti, A.S. Fructose-induced modifications of myoglobin: Change of structure from met (Fe3+) to oxy (Fe2+) form. *Int. J. Biol. Macromol.* **2011**, *48*, 202-209.

Black, C.; Clar, C.; Henderson, R.; MacEachern, C.; McNamee P.; Quayyum, Z.; Royle, P.; Thomas, S. The clinical effectiveness of glucosamine and chondroitin supplements in slowing or arresting progression of osteoarthritis of the knee: a systematic review and economic evaluation. *Health Technol. Assess.* **2009**, *52*, 1-148.

Block, J.A.; Oegema, T.R.; Sandy, J.D.; Plaas, A. The effects of oral glucosamine on joint health: is a change in research approach needed? *Osteoarthr. Cartilage*. **2010**, 18, 5-11.

Blonski, C.; De Moissac, D.; Perie, J.; Sygusch, J. Inhibition of rabbit muscle aldolase by phosphorylated aromatic compounds. *Biochem. J.* **1997**, *323*, 71-77.

Bokiej, M.; Livermore, A.T.; Harris, A.W.; Onishi, A.C.; Sandwick, R.K. Ribose sugars generate internal glycation cross-links in horse heart myoglobin. *Biochem. Biophys. Res*. Commun. **2011**, *407*, 191-196.

Bouma, B.; Kroon-Batenburg, L.M.; Wu, Y.P.; Brunjes, B.; Posthuma, G.; Kranenburg, O.; De Groot, P.G.; Voest, E.E.; Gebbink, M.F. Glycation induces formation of amyloid cross-beta structure in albumin. *J. Biol. Chem.* **2003**, *278*, 41810-41819.

Brands, C.M.J.; Alink, G.M.; van Boekel, M. A.J.S.; Jongen, W.M.F. Mutagenicity of heated sugar-casein systems: Effect of the Maillard reaction. *J. Agric. Food Chem.* **2000**, *48*, 2271-2275.

Brown, M. R.; Keith, T. J.; Knull, H. R. Decreased actin activated myosin ATPase activity by non-enzymatic glycation. In *The Maillard reaction in food processing human nutrition and physiology*, Finot, P.A., Aeschbacher, H.U., Hurrell, R.F., Liardon, R., Eds.; Birkha user Verlag: Basel, **1990**; pp. 487-492.

Burdett, N.; McNeil, J.D. Difficulties with assessing the benefit of glucosamine sulphate as a treatment for osteoarthritis. *Int. J. Evid. Based Healthc.* **2012**, *10*, 222-226.

Candiano, G.; Ghiggeri, G.M.; Gusmano, R.; Zetta, L.; Benfenati, E.; Icardi, G. Reaction of 2 amino-2-deoxyglucose and lysine: Isolation and characterization of 2,5 bis(tetrahydroxybutyl)pyrazine. *Carbohydr. Res.* **1988**, *184*, 67-75.

Cao, Y.; Xia, T.; Zhou, T.; Xu, X. The mechanism of high pressure-induced gels of rabbit myosin. *Innov. Food Sci. Emerg.* **2012**, *16,* 41-46.

Capuano, E.; Fogliano, V.Acrylamide and 5-hydroxymethylfurfural (HMF): A review on metabolism, toxicity, occurrence in food and mitigation strategies. *Food Sci. Technol.* **2011**, *44*, 793-810.

Chan, J.; Omana, D.A.; Betti, M. Effect of ultimate pH and freezing on the biochemical properties of proteins in turkey breast meat. *Food Chem*. **2011***, 127*,109-117.

Chen, L.; Wei, Y.; Wang, X.; He, R. D-Ribosylated Tau forms globular aggregates with high cytotoxicity. *Cell. Mol. Life Sci*. **2009**, *6*, 2559–2571.

Chen, L.; Wei, Y.; Wang, X.; He, R. Ribosylation rapidly induces alpha-synuclein to form highly cytotoxic molten globules of advanced glycation end products. *PLoS One*. **2010**, *5*, E9052.

Chesnokov, V.; Gong, B.; Sun, C.; Itakura, K. Anti-cancer activity of glucosamine through inhibition of N-linked glycosylation. *Cancer Cell Int.* **2014**, *14*, 45-55.

Chung, Y.C.; Tsai, C.F.; Li, C.F. Enhanced solubility and characterization of chitosan in aqueous solutions prepared by Maillard reaction. *Fish. Sci.* **2006**, *72*, 1096-1103.

Church, F.C.; Swaisgood, H.E.; Porter, D.H.; Catignani, G.L. Spectrophotometric assay using o-phthaldialdehyde for determination of proteolysis in milk and isolated milk proteins. J. Dairy Sci. **1983**, *66*, 1219-1227.

Colas, B.; Caer, D.;Fournier, E. Transglutaminase-catalyzed glycosylation of vegetable proteins. Effect on solubility of pea legumin and wheat gliadins. *J. Agric. Food Chem*. **1993**, *41*, 1811 1815.

Conti, M-A.; Adelstein, R.S. Nonmuscle myosin II moves in new directions. *J. Cell Sci*. **2008**, *121*, 11-18.

Cordoba, F.; Nimni, M.E. Chondroitin sulfate and other sulfate containing chondroprotective agents may exhibit their effects by overcoming a deficiency of sulfur amino acids. *Osteoarthr. Cartilage.* **2003**, *11*, 228–230.

Corzo-Martínez, M.; Soria, A. C.; Villamiel, M.; Olano, A.; Harte, F. M.; Moreno, F. J. Effect of glycation on sodium caseinate - stabilized emulsions obtained by ultrasound. *J. Dairy Sci*. **2011**, *94*, 51-58.

D'Ambrosio B.; Casa R.; Bompani G.; Scali M. Glucosamine sulfate: a controlled clinical investigation in arthrosis. *Pharmacotherpeutica.* **1981**, *2*, 504-508.

Damodaran, S. Amino acids, peptids and proteins. In *Fennema's Food Chemistry*, 4th ed.; Damodaran S., Parkin, K.L., Fennema, O.R. Eds.; New York: CRC Press, Taylor and Francis Group, **2008**; pp. 120–150.

Dave, A.C., Loveday, S.M.; Anema, S.G.; Jameson, G.B.; Singh, H. Glycation as a tool to probe the mechanism of β-lactoglobulin nanofibril self-assembly. *J. Agric. Food Chem*. **2012**, *62*, 3269–3278.

Davidek, T.; Davidek, J. Chemistry of the Maillard reaction in foods. In Chemical and functional properties of food saccharides. Tomasik, P., ED.; CRC Press: Boca Raton, FL, **2003**; Vol. 4, pp. 291-315.

Degen, J.; Hellwig, M.; Henle, T. 1, 2-dicarbonyl compounds in commonly consumed foods. *J. Agric. Food Chem*. **2012**, *60*, 7071-7079.

Del Duca, S.; Dondini, L.; Della Mea, M.; Munoz de Rueda, P.; Serafini Fracassi, D. Factors affection transglutaminase activity catalysing polyamine conjugation to endogenous substrates in the entire chloroplast. *Plant Phys. Biochem*. **2000**, *38*, 429-439.

DeWitt, C.A.M.; Gomez, G.; James, J.M. Protein extraction from beef heart using acid solubilisation. *J. Food Sci*. **2002**, *67*, 3335–3341.

Dills, W. L., Jr. Protein fructosylation: Fructose and the Maillard reaction. *Am. J. Clin. Nutr*. **1993**, *58*, 779S–787S.

Dobson, C. M. The structural basis of protein folding and its links with human disease. *Philos. Trans. R. Soc. London, Ser. B.* **2001**, *356*, 133-145.

Dutta, U.; Cohenford, M.A.; Dain, J.A. Monitoring the effect of glucosamine and glyceraldehyde glycation on the secondary structure of human serum albumin and immunoglobulin G: An analysis based on circular dichroism, thermal melting profiles and UV–fluorescence spectroscopy. *Anal. Chim. Acta.* **2006**, *558*, 187-194.

Dworschak E. Nonenzyme browning and its effect on protein nutrition. *Crit Rev Food Sci Nutr.* **1980**, *13*, 1-40.

Dykstra, M.J. *Biological electron microscopy: Theory, techniques and troubleshooting*. Plenum Press: New York, NY; **1992**, pp. 534.

Echlin, P. *Low Temperature Microscopy and Analysis*. Plenum Press: New York, NY.; **1992**.

EFSA. Scientific opinion of the panel on dietetic products nutrition and allergies on a request from the European Commission on the safety of glucosamine hydrochloride from *Aspergillus niger* as food ingredient. *EFSA* J. **2009**, *1099*, 1-19.

Egelansdal, B.; Freitheim, K.; Samejima, K. Dynamic rheological measurement on heat-induced myosin gels: effect of ionic strength, protein concentration and adenosine triphosphate or pyrophosphate. *J. Sci. Food Agric.* **1986**, *37*, 915-926.

Einbu, A.; Varum, K.M. Characterization of chitin and its hydrolysis to GlcNAc and GlcN. *Biomacromolecules*, **2008**, *9*, 1870–1875.

Elgawish, A.; Glomb, M.; Friedlander, M.; Monnier, V.M. Involvement of hydrogen peroxide in collagen cross-linking by high glucose in vitro and in vivo. *J. Biol. Chem.* **1996**, *22*, 12964-12971.

Evans, M.; Ratcliffe, I.; Williams, P.A. Emulsion stabilisation using polysaccharide–protein complexes. *Curr. Opin. Colloid Interface Sci*. **2013**, *18*, 272-282.

Fan, L.; Wu, H.; Zhou, X.; Peng, M.; Tong, J.; Xie, W.; Liu, S. Transglutaminase-catalyzed grafting collagen on chitosan and its characterization. *Carbohydr Polym.* **2014**, *105*, 253-259.

FDA (Food and Drug Administration). GRAS Notice No. GRN 000095. **2002**. Office of Food Additive Safety, Center for Food Safety and Applied Nutrition.

FDA (Food and Drug Administration). **2004**. GRAS Notice No. GRN 000147. http://www.fda.gov/ucm/groups/fdagov-public/@fdagov-foods gen/documents/document/ucm267843.pdf

Ferrer, E.; Alegria, A.; Farre, R.; Clemente, G.; Calvo, C. Fluorescence, browning index, and color in infant formulas during storage. *J. Agric. Food Chem*. **2005**, *53*, 4911-4917.

Fogliano, V.; Monti, S.M.; Musella, T.; Randazzo, G.; Ritieni, A. Formation of coloured Maillard reaction products in a gluten-glucose model system. *Food Chem*. **1999**, *66*, 293-299.

Fogliano, V.; Morales, F.J. Estimation of dietary intake of melanoidins from coffee and bread. *Food Funct*. **2011**, *2*, 117–123.

Folk, J. Mechanism of action of guinea pig liver transglutaminase. VI Order of substrate addition. *J. Biol. Chem*. **1969**, *244*, 3707-3713.

Folk, J.E. Mechanism and basis for specificity of transglutaminase catalyzed ε-(γ-glutamyl)-lysine bond formation. *Adv. Enzymol.* **1983**, *54*, 1-56.

French, S.J.; Harper, W.J.; Kleinholz, N.M.; Jones, R.B.; Green-Church, K.B. Maillard reaction induced lactose attachment to bovine β-lactoglobulin: Electrospray ionization and matrix-assisted laser desorption/ionization examination. *J. Agric. Food Chem*. **2002**, *50*, 820–823

Friedman, M. Food browning and its prevention: an overview. *J. Agric. Food Chem*. **1996**, *44*, 631–653.

Fu, Q.; Li, L.D.; Li, B. Formation of Nε-(Carboxymethyl)lysine in saccharide-lysine model systems by different heat treatments. *Int. J. Food Eng.* **2012**, *8.*

Fujiwara, K.; Oosawa, T.; Saeki, H. Improved thermal stability and emulsifying properties of carp myofibrillar proteins by conjugation with dextran. *J. Agric. Food Chem*. **1998**, *46*, 1257-1261.

Gatlin. L.A.; Auffret, T.; Shalaev, E.; Speaker, S.M.; Teagarden, D.L. Freeze-drying concepts: The basics. In *Protein Formulation and Delivery*, McNally, E.J, Hastedt, J.E, Eds.; Informa Healthcare: New York, NY, **2008**; Vol. 175, pp. 177-196.

Geirsdottir, M. Protein isolation from herring. Nordic Innovation Centre report report. **2006**, 39-06.

Gensberger, S.; Mittelmaier, S.; Glomb, M.A.; Pischetsrieder, M. Identification and quantification of six major α-dicarbonyl process contaminants in high-fructose corn syrup. *Anal. Bioanal. Chem*. **2012**, *403*, 2923-2931.

Gerrard, J.A. Protein–protein cross-linking in food: methods, consequences, applications. *Trends Food Sci. Technol.* **2002**, *13*, 391–399.

Gersten, R.A.; Gretebeck, L.M.; Hildrick-Smith, G.; Sandwick, R.K. Maillard reaction of ribose-5-phosphate generates superoxide and glycation products for bovine heart cytochrome C reduction. *Carbohydr. Res*. **2010**, *345*, 2499-2506.

Gervais, V.; Zerial, A. Oschkinat. NMR investigations of the role of the sugar moiety in glycosylated recombinant human granulocyte-colony-stimulating factor. *Eur. J. Biochem.* **1997**, *247,* 386-395.

Glomb, M.A.; Monnier, V.M. Mechanism of protein modification by glyoxal and glycolaldehyde, reactive intermediates of the Maillard reaction *J Biol Chem*. **1995**, *270*, 10017-10026.

Glomb, M.A.; Tschirnich, R. Detection of alpha-dicarbonyl compounds in Maillard reaction systems and in vivo. *J. Agric. Food Chem*. **2001**, *49*, 5543–5550.

Gobert, J.; Glomb, M.A. Degradation of glucose: reinvestigation of reactive α-dicarbonyl compounds. *J. Agric. Food Chem*. **2009**, *57*, 8591–8597.

Gornall, A.C.; Bardawill, C.J.; David, M.M. Determination of serum proteins by means of the biuret reaction. *J. Biol. Chem,* **1949**, *177*, 751-767.

Greenberg, C.S.; Birckbichler, P.J.; Rice, R.H. Transglutaminases: multifunctional cross-linking enzymes that stabilize tissues. *FASEB.* **1991**, *5,* 3071-3077.

Greene, T.W.; Wuts, P.G.M. *Protective groups in organic synthesis* (3rd ed.). New York: Wiley and Sons. **1999**, p.1100.

Griffith, A.; Bell E.D.; Kantor, J.W.; Lampe, Shen, D.D.; White, E. Use of glucosamine and chondroitin in relation to mortality. *Eur. J. Epidemiol*. **2012**, *27*, 593-603.

Hail, M.; Elliott, B.; Anderson, K. High-throughput analysis of oligonucleotides using automated electrospray ionization mass spectrometry. *Am. Biotechnol. Lab*. **2004**, *22*, 12–14.

Hamada, J.S. Deamidation of food proteins to improve functionality. *Crit Rev Food Sci Nutr.* **1994**, *34*, 283-92.

Hargrove, M.S.; Krzywda, S.; Wilkinson, A.J.; Dou, Y.; Ikeda-Saito, M.; Olson, J.S. Stability of myoglobin: a model for the folding of heme proteins. *Biochem*. **1994**, *33*, 11767–11775.

Hauser, C.; Müller, U.; Sauer, T.; Augner, K.; Pischetsrieder, M. Maillard reaction products as antimicrobial components for packaging films. *Food Chem*. **2014**, *145*, 608–613.

Hawkins, M.; Barzilai, N.; Chen, W.; Angelov, I.; Hu, M.; Cohen, P.; Rossetti, L. Increased hexosamine availability similarly impairs the action of insulin and IGF-1 on glucose disposal. *Diabetes*. **1996**, 45, 1734–1743.

Hayashi, T.; Namiki, M. Role of sugar fragmentation in the Maillard reaction. *Dev. Food Sci.* **1986**, *13*, 29–38.

Health Canada official website. URL http://webprod.hcsc.gc.ca/nhpidbdipsn/ingredReq.do?id=1573&lang=eng Accessed Apr. 16, 2015.

Heart, E.; Choi, W.S.; Sung, C.K. Glucosamine-induced insulin resistance in 3T3-L1 adipocytes. *Am. J. Physiol. Endocrinol. Metab*. **2000**, *278*, E101–E112.

Heller L. US glucosamine grows slow, lags global sales. **2009**. URL www.nutraingredients-usa.com/Consumer-Trends/US-glucosamine-grows-slow-lags-global-sales. Accessed April 17, 2015.

Hellwig, M.; Henle, T. Baking, ageing, diabetes: a short history of the Maillard reaction. *Angew. Chem. Int. Ed.* **2014**, *53*, 10316-10329.

Henle, T.; Deppisch, R.; Ritz, E. The Maillard reaction: from food chemistry to uremia research. *Nephrol. Dial. Transplant*. **2006**, *11*, 1718-1722.

Henrotin, Y.; Mobasheri, A.; Marty, M. Is there any scientific evidence for the use of glucosamine in the management of human osteoarthritis? *Arthriti Res. Ther.* **2012**, *14*, 201-211.

Heyns, K.; Hauber, R. Determination of structure of specific C-14 labeled brown polymerisates of sorbose by thermal fragmentations. *Justus Liebigs Ann. Chem.* **1970**, *733*, 159−169.

Heyns, K.; Koch, W. Über die bildung eines aminozuckers ausd-fruktose und ammoniak. *Z Naturforsch* [*B*]. **1952***, 7B,* 486–488.

Hodge, J. Chemistry of browning reactions in model systems. *J. Agric. Food Chem*. **1953**, *1*, 928-943.

Hofmann, T. Studies on melanoidin-type colorants generated from the Maillard reaction of protein-bound lysine and furan-2-carboxaldehyde. Chemical characterization of a red colored domain. *Zeitschrift fuer Lebensmittel-Untersuchung und -Forschung A: Food Res. Tech*. **1998**, *206*, 251-258.

Hofmann, T.; Bors, W.; Stettmaier, K. Radical-assisted melanoidin formation during thermal processing of foods as well as under physiological conditions. *J. Agric. Food Chem.* **1999**, *47*, 391-396.

Hofmann, T.; Heuberger, S. The contribution of coloured Maillard reaction products to the total colour of browned glucose/l-alanine solutions and studies on their formation. *Z. Lebensm. Unters. Forsch. A*. **1999**, *208*, 17–26.

Höppener, J.W.; Oosterwijk, C.; Nieuwenhuis, M.G.; Posthuma, G.; Thijssen, J.H.; Vroom, T.M.; Ahrén, B.; Lips, C.J. Extensive islet amyloid formation is induced by development of Type II diabetes mellitus and contributes to its progression: pathogenesis of diabetes in a mouse model. *Diabetologia*. **1999**. *42*, 427-434.

Horowitz, M.I. Nonenzymatic modifications of amino sugars in vitro. *Arch. Biochem. Biophys.* **1991**, *288*, 317-323.

Hrynets,Y.; Omana, D.A.; Xu, Y.; Betti, M. Effect of acid- and alkaline-aided extractions on functional and rheological properties of proteins recovered from mechanically separated turkey meat (MSTM). *J. Food Sci.* **2010**. *75*, E477-E486.

Hrynets,Y.; Omana, D.A.; Xu, Y.; Betti, M. Impact of Citric Acid and Calcium Ions on Acid Solubilization of Mechanically Separated Turkey Meat (MSTM): Effect on Lipid and Pigment Content. *Poultry Sci.* **2011a**, *90*, 458-466.

Hrynets,Y.; Omana, D.A.; Xu, Y.; Betti, M. Comparative study on the effect of acid- and alkaline-aided extractions on Mechanically Separated Turkey Meat (MSTM): Chemical and functional properties of recovered proteins. *Process Biochem.* **2011b**, *46*, 335-343.

Hrynets, Y.; Omana, D. A.; Betti, M. Improving the functionality of mechanically separated turkey meat protein isolates by enzymatic cross-linking using transglutaminase. **2011c**. Abstract. *Poultry Sci.* E-Suppl. 1. p. 184.

Hsu, D.; Zimmer, V. Canadian diabetes sssociation national nutrition committee technical review: advanced glycation end-products in diabetes management. *Can. J. Diabetes.* **2010**, *32*, 136-140.

Hu, X.; Ren, J.; Zhao, M.; Cui, C.; He, P. Emulsifying properties of the transglutaminase-treated crosslinked product between peanut protein and fish (*Decapterus maruadsi)* protein hydrolysates. *J. Sci. Food Agric.* **2011**, *91*, 578-585.

Hubbard, W.K. Associate Commissioner of Policy and Planning. **2012**. United States Department of Health and Human Services, Food and Drug Administration. http://www.fda.gov/Food/IngredientsPackagingLabeling/LabelingNutrition/ucm073400.htm

Hunt, J.V.; Bottoms, M.A.; Mitchinson., M.J. Oxidative alterations in the experimental glycation model of diabetes mellitus are due to protein-glucose adduct oxidation. Some fundamental differences in proposed mechanisms of glucose oxidation and oxidant production. *Biochem J.* **1993**, *291* (Pt 2), 529–535.

Hunt, J.V.; Wolff, S.P. Oxidative glycation and free radical production: a causal mechanism of diabetic complications. *Free Radic Res Commun*. **1991**, *12-13* (Pt 1), 115-123.

Hussain, M.R.; Iman, M.; Maji, T.K. Determination of degree of deacetylation of chitosan and their effect on the release behavior of essential oil from chitosan and chitosan-gelatin complex microcapsules. *Int. J. Adv. Eng. Appl.* **2013**, *12*, .4-12.

Iannuzzi, C.; Maritato, R.; Irace, G.; Sirangelo, I. Glycation accelerates fibrillization of the amyloidogenic W7FW14F apomyoglobin. *PLoS One*. **2013**, *8*, e80768.

IDF (International Dehydrated Foods). URL http://idf.com/dehydrated-chicken-protein-powder/. Accessed May 5, 2015.

Igaki, N.; Sakai, M.; Hata, H.; Oimomi, M.; Baba, S.; Kato, H. Effects of 3-deoxyglucosone on the Maillard reaction. *Clinic. Chem.* **1990**, *36*, 631-634.

Ihaka, R.; Gentleman, R. R: A language for data analysis and graphics. *J. Comput. Graph. Stat.* **1996**, *5*, 299-314.

Jacobson, A.; L., Henderson, J. Temperature sensitivity of myosin and actomyosin. *Can. J. Biochem.* **1973**, *51*, 71-86.

Jalal, A.F.; Risheed, C.M.; Ibrahim, B.M. Optimization of chitin extraction from chicken feet. *J. Anal. Bioanal. Tech.* **2012**, *3*, 1-5.

Jamin, N.; Lacapere, J-J. Circular dichroism: folding and conformational changes of membrane proteins. In *Biophysical analysis of membrane proteins: investigating structure and function*, Pebay-Peyroula, E., Ed.; Weinhem: John Wiley and Sons, **2007**; pp. 243-259.

Jaros, D.; Partschefeld, C.; Henle, T., Rohm, H. Transglutaminase in dairy products: chemistry, physics and applications. J. Texture Stud. **2006**, *37*, 113-155.

Jia, L.; Wang, Y.; Qiao, Y.; Qia, Y.; Hou, X. Efficient one-pot synthesis of deoxyfructosazine and fructosazine from D-glucosamine hydrochloride using a basic ionic liquid as a dual solvent-catalyst. *RSC Adv*. **2014**, *4*, 44253–44260.

Jiang, S.; Zhao, X. Transglutaminase-induced cross-linking and glucosamine conjugation in soybean protein isolates and its impacts on some functional properties of the products. *Eur. Food Res. Technol.* **2010**, *231*, 679-689.

Jimenez-Castano, L.; Lopez-Fandino, R.; Olano, A.; Villamiel, M. Study on β-lactoglobulin glycosylation with dextran: effect on solubility and heat stability. *Food Chem.* **2005**, *93,* 689-695.

Jin, R.; Li, C.; Zhi, L.; Jiang, Y.; Hu, M.; Li, S.; Zhai, Q. Deactivation of chloroperoxidase by monosaccharides (D-glucose, D-galactose, and D-xylose). *Carbohydr Res*; **2013**, *370*, 72-75.

Joao, H.C.; Scragg, I.G.; Dwek, R.A. Effects of glycosylation on protein conformation and amide proton exchange rates in RNase B. *FEBS Lett.* **1992**, *307*, 343-346.

Jorda, K.M.; Arden, N.K.; Doherty, M.; Bannwarth, B.; Bijlsma, J.; Dieppe, P.; Gunther, K.; Hauselmann, H.; Herrero-Beaumont, G.; Kaklamanis, P.; et al. EULAR Recommendations 2003: an evidence based approach to the management of knee osteoarthritis: report of a task force of the standing committee for international clinical studies including therapeutic trials (ESCISIT). *Ann. Rheum. Dis.* **2003**, *62*, 1145–1155.

Joseph, D.; Lanier, T.C.; Hamann, D.D. Temperature and pH affect transglutaminase-catalyzed "setting" of crude fish actomyosin. *J. Food Sci*. **1994**, *59*, 1018-1036.

Joubran Y.; Mackie A.; Lesmes, U.Impact of the Maillard reaction on the antioxidant capacity of bovine lactoferrin. *Food Chem.* **2013**, *141*, 3796–3802.

Jouppila, K. Mono- and disaccharides: selected physiochemical and functional aspects. In *Carbohydrates in Food*, Eliasson, A.-C., Ed.; CRC Press: Boca Raton, FL, **2006**; pp 41-88.

Jourdain, L.; Leser, M.E.; Schmitt, C.; Michel, M.; Dickinson, E. Stability of emulsions containing sodium caseinate and dextran sulfate: Relationship to complexation in solution. *Food Hydrocolloid.* **2008**, *22,* 647-659.

Jun, M.; Shao, Y.; Ho, C.T.; Koetter, U.; Lech, S. Structural identification of nonvolatile dimerization products of glucosamine by gas chromatography-mass spectrometry liquid chromatography-mass spectrometry and nuclear magnetic resonance analysis. *J. Agric. Food Chem.* **2003**, *51*, 6340-6346.

Jung, S.H.; Choi, S.J.; Kim, H.J.; Moon, T.W. Molecular characteristics of bovine serum albumin-dextran conjugates. *Biosci. Biotechnol. Biochem.* **2006**, *70,* 2064-2070.

Kantor, E. D.; Lampe, J.W.; Peters, U.; Shen, D.D.; Vaughan, T.L.; White, E. Use of glucosamine and chondroitin supplements and risk of colorectal cancer. *Cancer Cause Control*. **2013**, *24*, 1137–1146.

Kanzler, C.; Haase, P.T.; Kroh, L.W. Antioxidant capacity of 1-deoxy-D-erythro-hexo-2,3-diulose and D-arabino-hexo-2-ulose. *J. Agric. Food Chem*. **2014**, *62*, 2837-2844.

Kapurniotu, A.; Bernhagen, J.; Greenfield, N.; Al Abed, Y.; Teichberg, S.; Frank, R. W.; Voelter, W.; Bucala.Contribution of advanced glycosylation to the amyloidogenicity of islet amyloid polypeptide. *R. Eur. J. Biochem*. **1998**, *251*, 208–216.

Kashige, N.; Yamaguchi, T.; Mishiro, N.; Hanazono, H.; Miake, F.; Watanabe, K. Possible involvement of dihydrofructosazine in the DNA breaking activity of D-glucosamine. *Biol. Pharm. Bull*. **1995**, *18*, 653–658.

Katayama, J.; Shima, S.; Saeki, H. Solubility improvement of shellfish muscle protein by reaction with glucose and its soluble state in low-ionic-strength. *J. Agric. Food Chem.* **2002**, *50*, 4327-4332.

Katayama, S.; Haga, Y.; Saeki, H. Loss of filament-forming ability of myosin by nonenzymatic glycosylation and its molecular mechanism. *FEBS Lett*. **2004**, *575*, 9-13.

Katayama, S.; Saeki, H. Cooperative effect of relative humidity and glucose concentration on improved solubility of shellfish muscle protein by the Maillard reaction. *Fish Sci*. **2004**, *70*, 159-166.

Katayama S.; Saeki, H. Water solubilization of glycated carp and scallop myosin rods, and their soluble state under physiological conditions. *Fish Sci.* **2007**, *73*, 446-452.

Kato, A. Industrial applications of Millard-type protein– polysaccharide conjugates. *Food Sci. Technol. Res.* **2002***, 8*, 193–199.

Katsumata, T.; Nakakuki, H.; Tokunaga, C.; Fujii, N.; Egi, M.; Phan, T.H.; Mummalaneni, S.; DeSimone, J.A.; Lyall, V. Effect of Maillard reacted peptides on human salt taste and the amiloride-insensitive salt taste receptor (TRPV1t). *Chem. Senses*, **2008**, *33*, 665–680.

Kerler, J.; Winkel, C.; Davidek, T.; Blank, I. Basic chemistry and process conditions for reaction flavours with particular focus on Maillard-type reactions. In *Food Flavour Technology,* edition 2; Taylor, A. J., Linforth, R. S. T., Eds.; Blackwell Publishing Ltd: Chichester, UK, **2010**; Vol. 2, pp. 51–81.

Kerwin, J.L.; Whitney, D.L.; Sheikh, A. Mass spectrometric profile of glucosamine, glucosamine polymers and their catecholamine adducts. Model reactions and cuticular hydrolysates of *Toxorhynchites amboinensis* (Culicidae) pupae. *Insect Biochem. Mol. Biol.* **1999**, *29*, 599-607.

Khiari, Z.; Omana, D.A.; Pietrasik, Z.; Betti, M. Evaluation of poultry protein isolate as a food ingredient: physicochemical properties and sensory characteristics of marinated chicken breasts. *J. Food Sci*. **2013**, *78*, S1069-1075.

Khiari, Z.; Pietrasik, Z.; Gaudette, N.J.; Betti, M. Poultry protein isolate prepared using an acid solubilization/precipitation extraction influences the microstructure, the functionality and the consumer acceptability of a processed meat product. *Food Structure*. **2014**, *2*, 49-60.

Kieliszek, M.; Misiewicz, A. Microbial transglutaminase and its application in the food industry. A review. *Folia Microbiol (Praha).* **2014**, *59*, 241-250.

Kihlberg, J.; Elofsson, M. Solid-phase synthesis of glycopeptides: immunological studies with T cell stimulating glycopeptides. *Curr. Med. Chem.* **1997**, *4,* 85-117.

Kim, S.-H.; Carpenter, J.A.; Lanier, T.C.; Wicker, L. Polymerization of beef actomyosin induced by transglutaminase. *J. Food Sci*. **1993**, *58*, 473-474.

Kim, Y.S.; Park, J.W.; Choi, Y.J. New approaches for the effective recovery of fish proteins and their physicochemical characteristics. *Fisheries Sci*. **2003**, *69*, 1231–1239.

Klinger, K.M.; Liebner, F.; Fritz, I.; Potthast, A.; Rosenau, T. Formation and ecotoxicity of N heterocyclic compounds on ammoxidation of mono- and polysaccharides. *J. Agric. Food Chem*. **2013**, *61*, 9004−9014.

Kobayashi, E.; Hashiguchi, K.; Yikozeki, K.; and Yamanaka, S. Molecular cloning of the transglutaminase gene from *Bacillus subtilis* and its expression in *Escherichia coli*. *Biosci. Biotech. Biochem.* **1998**, *62*, 1109-1114.

Kohn, P.; Winzler, R.J.; Hoffmann, R.C. Metabolism of D-glucosamine and N-acetyl-D-glucosamine in the intact rat. *J. Biol. Chem*. **1962**, *237*, 304-308.

Kraehenbuehl, K.; Davidek, T.; Devaud, S.; Mauroux, O. Basic and acidic sugars as flavour precursors in Maillard reaction. In *Expression of multidisciplinary flavour science.*

Proceedings to 12th Weurman symposium, I. Blank, M., Wust, C., Yeretzian, C.; Eds.; Institut Für Chemie und Biologische Chemie. **2008**. pp. 267–271

Kralovec, A.; Barrow, C.J. Glucosamine production and health benefits. In *Marine Nutraceuticals and Functional Food,* edition1; Barrow, C., Shahidi, F, Ed.; CRC Press: Boca Raton, FL, **2008**; pp.198-227.

Krebs, M.R.; Bromley, E.H.; Donald, A.M. The binding of thioflavin-T to amyloid fibrils: localisation and implications. *J. Struct. Biol*. **2005**, *149*, 30–37.

Kristinsson, H.G.; Hultin, H.O. Changes in trout hemoglobin conformations and solubility after exposure to acid and alkali pH. *J. Agric. Food Chem*. **2004**, *52*, 3633–3643.

Kurita, K. Controlled functionalization of the polysaccharide chitin. *Prog. Polym. Sci*. **2001**, 26, 1921-1971.

Laemmli, U.K. Cleavage of structural protein during the assembly of the head of bacteriophage T4. *Nature,* **1970**, *277*, 680-685.

Lapolla, A.; Fedele, D.; Traldi, P. The role of mass spectrometry in the study of non-enzymatic protein glycation in diabetes. *Mass Spectrom. Rev.* **2000**, *19*, 279-304.

Leblanc, E.L.; Leblanc, R.J. Determination of hydrophobicity and reactive groups in proteins of cod (*Gadus morhua*) muscle during frozen storage. *Food Chem*. **1992**, *43*, 3–11.

Li, C.; Xiong Y.L.; Chen, J. Oxidation-induced unfolding facilitates myosin cross-linking in myofibrillar protein by microbial transglutaminase. *J. Agric. Food Chem.* **2012**, *60*, 8020-8027.

Liggins, J.; Furth, A.J. Role of protein-bound carbonyl groups in the formation of advanced glycation end-products. *Biochem. Biophys. Acta.* **1997***, 1361*, 123-130.

Lillard, J.S.; Clare, D.A.; Daubert, C.R. Glycosylation and expanded utility of a modified whey protein ingredient via carbohydrate conjugation at low pH. *J. Dairy Sci.* **2009**, *92,* 35-48.

Lim, L.-T.; Mine, Y.; Tung, M.A. Transglutaminase cross-linked egg white protein films: tensile properties and oxygen permeability. *J. Agric. Food Chem*. **1998**, 46, 4022-4029.

Lis. H.; Sharon, N. Protein glycosylation-structural and functional aspects. *Eur J Biochem*. **1993**, *218*, 1–27.

Liu, G.; Zhong, Q. Glycation of whey protein to provide steric hindrance against thermal aggregation. *J. Agric. Food Chem.* **2012**, *60,* 9754-9762.

Liu, J.; Ru, Q.; Ding, Y. 2012. Glycation a promising method for food protein modification: Physicochemical properties and structure, a review. *Food Res. Int*. **2012**, *49*, 170–183.

Liu, G.; Zhong, Q. Thermal aggregation properties of whey protein glycated with various saccharides. *Food Hydrocolloid*. **2013**, *32*, 87-96.

Liu, Q.; Li, J.; Kong, B.; Jia, N.; Li, P. Antioxidant capacity of Maillard reaction products formed by a porcine plasma protein hydrolysate-sugar model system as related to chemical characteristics. *Food Sci. Biotechnol*. **2014**, *23*, 33-41.

Loveday, S. M.; Su, J.; Rao, M. A.; Anema, S. G.; Singh, H. Whey protein nanofibrils: the environment–morphology–functionality relationship in lyophilization, rehydration, and seeding *J. Agric. Food Chem*. **2012**, *60*, 5229-5236.

Luthra, M.; Balasubramanian, D. Nonenzymatic glycation alters protein structure and stability. *J. Biol. Chem.* **1993**, *24*, 18119-18127.

Ma, G.; Zhang, H.; Guo, J.; Zeng, X.; Hu, X.; Hao, W. Assessment of the inhibitory effect of rifampicin on amyloid formation of hen egg white lysozyme: thioflavin T fluorescence assay versus FTIR difference spectroscopy. *J. Spectroscopy*. **2014**. *2014*, p.1-5.

Maillard, L.-C. Action des acides amines sur les sucres: formation des melanoidines par voie methodique. *C.R. Hebd. Seances Acad. Sci*. **1912**, *154*, 66–68.

Maitena, U.; Katayama, S.; Sato, R.; Saeki, H. Improved solubility and stability of carp myosin by conjugation with alginate oligosaccharide. *Fish Sci*. **2004**, *70*, 896–902.

Martin, S.R.; Schilstra, M.J. Circular dichroism and its application to the study of biomolecules. *Methods Cell Biol*. **2008**, *84*, 263-293.

Matsudomi, N.; Tsujimoto, T.; Kato, A.; Kobayashi, K. Emulsifying and bactericidal properties of a protamine-galactomannan conjugate prepared by dry heating. *J. Food Sci*. **1994**, *59*, 428-431.

Mavric, E.; Wittmann, S.; Barth, G.; Henle, T. Identification and quantification of methylglyoxal as the dominant antibacterial constituent of Manuka (*Leptospermum scoparium*) honeys from New Zealand. *Mol. Nutr. Food Res.* **2008**, *52*, 483-489.

Meltretter, J.; Pischetsrieder, M. Application of mass spectrometry for the detection of glycation and oxidation products in milk proteins. *Ann. N Y Acad. Sci.* **2008**, *1126*, 134-140.

Milosavic, N.B. Enzymes in organic chemistry: transglycosylation. J. Microb. Biochem. Tech. 2012, *4*, e109.

Mishra, R.; Sörgjerd, K.; Nyström, S.; Nordigärden, A.; Yu, Y.C. Hammarström, P. Lysozyme amyloidogenesis is accelerated by specific nicking and fragmentation but decelerated by intact protein binding and conversion. *J. Mol. Biol*. **2007**, *366*, 1029-1044.

Mittelmaier, S.; Fünfrocken, M.; Fenn, D.; Fichert, T.; Pischetsrieder, M. Identification and quantification of the glucose degradation product glucosone in peritoneal dialysis fluids by HPLC/DAD/MSMS. *Anal. Bioanal. Chem*. **2011**, *401*, 1183–1193.

Moldoveanu, S.C.; Byrd, C.H.; Gerardi, A.R. Analysis of certain nitrogenous compounds in Tobacco. Part 1: Adenosine, 2,5- and 2,6-Deoxyfructosazines, mannosamine and glucosamine. Beiträge zur Tabakforschung International/*Contributions to Tobacco Research,* **2011**, *24*, 233-242.

Monacelli, F.; Storace, D.; D'Arrigo, C.; Sanguineti, R.; Borghi, R.; Pacini, D.; Furfaro, A.L.; Pronzato, M.A.; Odetti, P.; Traverso, N. Structural alterations of human serum albumin caused by glycative and oxidative stressors revealed by circular dichroism analysis. *Int. J. Mol. Sci.* **2013**, *14*, 10694-10709.

Montero, P.; Jimenez-Colmenero, F.; Borderias, J. Effect of pH and the presence of NaCl on some hydration properties of collagenous material from trout (*Salmo irideus Gibb*) muscle and skin. *J. Sci. Food Agric.* **199**1, *54*, 137-146.

Morgan, F.; Leonil, J.; Molle, D.; Bouhallab, S. Modification of bovine β-lactoglobulin by glycation in a powdered state or in an aqueous solution: Effect on association behavior and protein conformation. *J. Agric. Food Chem.* **1999**, *47*, 83–91.

Mossine, V.V.; Linetsky, M.; Glinsky, G.V.;Ortwerth, B.J.; Feather, M.S. Superoxide free radical generation by Amadori compounds: the role of acyclic forms and metal ions. *Chem. Res. Toxicol.* **1999**, *12*, 230–236.

Mottram, D.S.; Wedzicha, B.L.; Dodson, A.T. Food chemistry: Acrylamide is formed in the Maillard reaction. *Nature.* **2002**, *419*, 448-449.

Mottram, D.S.; Elmore, J.S. Control of the Maillard reaction during the cooking of food. In *Controlling Maillard Pathways To Generate Flavors*, edition 3; Mottram, D. S., Taylor, A. J., Eds.; ACS Symposium Series 1042. American Chemical Society: Washington, DC, **2010**; pp. 143-155.

Moure, A.; Dominquez, H.; Zuniga, M. E.; Soto, C.; Chamy, R. Characterization of protein concentrates from pressed cakes of *Guevina Avellana* (Chilean hazelnut). *Food Chem.* **2002**, *78*, 179-186.

Munanairi, A.; O'Banion, S.K.; Gamble, R.; Breuer, E.; Harris, A.; Sandwick, R.K. The miultipole Maillard reactions of ribose and deoxyribose sugars and sugar phosphates. *Carbohydr. Res.* **2007**, *342*, 2575-2592.

Nagy, A.; Darmochwal, K.M.; Stanislaw, K.; Mierzejewska, D.; Kostyra, H.; Gelencser, E. Influence of glycation and pepsin hydrolysis on immunoreactivity of albumin/globulin fraction of herbicide resistant wheat line. *Czech J. Food Sci.* **2009***, 27*, 320–329.

Nakamura, M.; Barber, A.J.; Antonetti, D.A.; LaNoue, K.F.; Robinson, K.A.; Buse, M.G.; Gardner, T.W. Excessive hexosamines block the neuroprotective effect of insulin and induce apoptosis in retinal neurons. *J. Biol. Chem.* **2001**, *276*, 43748-43755.

Nakamura, A.; Yoshida, R.; Maeda, H.; Furuta, H.; Corredig, M. Study of the role of carbohydrate and protein moieties of soy soluble polysaccharides in their emulsifying properties. *J. Agric. Food Chem.* **2004**, *52,* 5506-5512.

Nakamura, A.; Watanabe, K.; Ojima, T.; Ahn, D.H.; Saeki, H. Effect of Maillard reaction on allergenicity of scallop tropomyosin. *J. Agric. Food Chem.* **2005**, *53*, 7559–7564.

Navarro, S.L.; White, E.; Kantor, E.D.; Zhang, Y.; Rho, J.; Song, X.; Milne, G.L.; Lampe, P.D.; Lampe, J.W. Randomized trial of glucosamine and chondroitin supplementation on inflammation and oxidative stress biomarkers and plasma proteomics profiles in healthy humans. *PLoS One.* **2015**, *10*, e01175.

Nishimura, K.; Murakoshi, M.; Katayama, S.; Saeki, S. Changes in solubility and thermal stability of chicken myofibrillar protein by glycosylation. *Food Sci. Technol. Res*. **2011**, *17*, 69-75.

Niu, L.; Jiang, S.; Pan, L.; Zhai, Y. Characteristics and functional properties of wheat germ protein glycated with saccharides through Maillard reaction. *Int. J. Food Sci. Technol.* **2011**, *46*, 2197–2203.

Niwa, T.; Tsukushi, S. 3-deoxyglucosone and AGEs in uremic complications: inactivation of glutathione peroxidase by 3-deoxyglucosone. *Kidney Int. Suppl*. **2001**, *78*, S37-41.

Niwa, T. Mass spectrometry for the study of protein glycation in disease. *Mass Spectrom. Rev.* **2006**, *25*, 713–723.

Noguchi, K.; Ishikawa, K.; Yokoyama, K.; Ohtsuka, T.; Nio, N.; Suzuki, E. Crystal structure of red sea bream transglutaminase. *J. Biol. Chem*. **2001**, *276,* 12055-12059.

Nursten, H. The chemistry of nonenzymic browning In *The Maillard Reaction: Chemistry, Biochemistry and Implications,* edition 1; Nursten, H., Ed.; Royal Society of Chemistry: Cambridge, UK, **2005**; pp. 5-30.

Oboroceanu, D.; Wang, L.; Magner, E.; Auty, M. A. E. Fibrillization of whey proteins improves foaming capacity and foam stability at low protein concentrations. *J. Food Eng*. **2014**, *121*, 102– 111.

Oh, S.; Catignani, G.; Swaisgood, H. Characteristics of an immobilized form of transglutaminase: A possible increase in substrate specificity by selective interaction with a protein spacer. *J. Agric. Food Chem*. **1993**, *41*, 1337-1342.

Oliveira, F.C.; Coimbra, J.S.; de Oliveira, E.B.; Zuñiga, A.D.; Rojas, E.E. Food protein-polysaccharide conjugates obtained via the Maillard reaction: A review. *Crit Rev Food Sci Nutr*. **2014**. DOI: 10.1080/10408398.2012.755669.

Oliver, C.M.; Melton, L.D.; Stanley, R.A. Creating proteins with novel functionality via the Maillard reaction: A review. *Crit. Rev. Food Sci.Nutr*. **2006**, *46*, 337-350.

Oliver, C.M. Insight into the glycation of milk proteins: an ESI- and MALDI-MS perspective (review). *Crit. Rev. Food Sci. Nutr.* **2011**, *51*, 410-431.

Omana, D.A.;Pietrasik, Z.; Betti, M. Evaluation of poultry protein isolate as a food ingredient: Physicochemical characteristics of low fat turkey bologna. *Poultry Sci.* **2012a***, 91,* 3223-3229.

Omana, D. A.; Pietrasik, Z.; Betti, M. Use of poultry protein isolate as a food ingredient: Sensory and color characteristics of low fat poultry bologna. *J. Food Sci.* **2012b***, 77,* S274-S280.

Oya, T.; Hattori, N.; Mizuno, Y.; Miyata, S.; Maeda, S.; Osawa, T.; Uchida, K. Methylglyoxal modification of protein. *J. Biol. Chem*. **1999**, *274*, 18492-18502.

Papetti, A.; Mascherpa, D.; Gazzani, G. Free α-dicarbonyl compounds in coffee, barley coffee and soy after in vitro digestion. *Food Chem*. **2014**, *164*, 259-265.

Pearson, A.M.; Young, R.B. *Muscle and Meat Biochemistry*. Academic Press: San Diego, CA; **1989**, pp. 457.

Pfeifer, Y.V.; Kroh, L.W. Investigation of reactive alpha-dicarbonyl compounds generated from the Maillard reactions of L-methionine with reducing sugars via their stable quinoxaline derivatives. *J. Agric. Food Chem*. **2010**, *58*, 8293-8299.

Picotti, P.; Marabotti, A.; Negro, A.; Musi, V.; Spolaore, B.; Zambonin, M.; Fontana, A. Modulation of the structural integrity of helix F in apomyoglobin by single amino acid replacements. *Protein Sci.* **2004**, *13*, 1572-1585.

Pillai, C.K.S.; Paul, W.; Sharma, C.P. Chitin and chitosan polymers: Chemistry, solubility and fiber formation. *Prog. Polym. Sci*. **2009**, *34*, 641-678.

Popova, E.A.; Mironova, R.S.; Odjakova, M.K. Non-enzymatic glycosylation and deglycating enzymes. *Biotechnol. Biotechnol. Equip*. **2010**, *24*, 1928-1935.

Porta, R.; Mariniello, L.; Pierro, P.D.; Sorrentino, A.; Giosafatto, C.V.L. Transglutaminase crosslinked pectin- and chitosan-based edible films: A review. *Crit. Rev. Food Sci. Nutr*. **2011**, *51*, 223-238.

Proliver. Functional chicken proteins. URL http://www.proliver.be/nl/chicken-protein-isolate-13.htm. Accessed May 5, 2015.

Prospector. Chicken protein isolates. URL https://www.ulprospector.com/en/la. Accessed May 5, 2015.

Qi, J.; Yang, X.; Liao, J. Improvement of functional properties of acid-precipitated soy protein by the attachment of dextran through Maillard reaction. *Int. J. Food Sci. Technol.* **2009**, *44*, 2296 – 2302.

Qu, C-J.; Karjalainen, H.M.; Helminen, H.J.; Lammi, M.J. The lack of effect of glucosamine sulphate on aggrecan mRNA expression and (35)S-sulphate incorporation in bovine primary chondrocytes. *Biochim. Biophys. Acta*. **2006**, *4*, 453–459.

Qu, C.J.; Rieppo, J.; M.M. Hyttinen, M.J.; Lammi, I.; Kiviranta, J.; Kurkijarvi, J.; Jurvelin, J.S.; Töyräs, J. Human articular cartilage proteoglycans are not undersulfated in osteoarthritis. *Connect. Tissue Res*. **2007**, *48*, 27–33.

Rabbani, N.; Thornalley, P.J. Dicarbonyls linked to damage in the powerhouse: glycation of mitochondrial proteins and oxidative stress. *Biochem. Soc. Trans*. **2008**, *36* (Pt 5), 1045-1050.

Rabbani, N.; Thornalley P.J. The critical role of methylglyoxal and glyoxalase 1 in diabetic nephropathy. *Diabetes.* **2014**, *63*, 50-52.

Raj, D.S.; Choudhury, D.; Welbourne, T.C.; Levi, M. Advanced glycation end products: a Nephrologist's perspective. *Am. J. Kidney Dis*. **2000**, *35*, 365–380.

Rambaran, R.N.; Serpell, L.C. Amyloid fibrils: abnormal protein assembly. *Prion*. **2008**, *2*, 112–117.

Roberts, N.B.; Amara, A.B.; Morris, M.; Green, B.N. Long-term evaluation of electrospray ionization mass spectrometric analysis of glycated hemoglobin. *Clin. Chem*, **2001**, *47*, 316-321.

Roncone, R.; Monzani, E.; Nicolis, S.; Casella, L. Engineering and prosthetic-group modification of myoglobin: peroxidase activity, chemical stability and unfolding properties. *Eur. J. Inorg. Chem.* **2004**, 2203-2213.

Rondeau, P.; Armenta, S.; Caillens, H.; Chesne, S.; Bourdon, E. Assessment of temperature effects on β-aggregation of native and glycated albumin by FTIR spectroscopy and PAGE: Relations between structural changes and antioxidant properties. *Arc. Biochem. Biophys.* **2007**, *460,* 141-150.

Rondeau, P; Navarra, G; Militello, V; Bourdon, E. On the aggregation of albumin: influences of the protein glycation. In *Protein Aggregation,* edition 1; Stein, D.A. Ed.; Nova Science Publishers, Inc: New York, NY, **2011**; pp.139-159.

Roseman, S. Reflections on glycobiology. *J. Biol. Chem*. **2001**, *276*, 41527-41542.

Saberi, A.H.; Kadivar, M.; Keramat, J. Improvement of functional properties of glutens extracted from two Iranian wheat varieties (Sardari and Mahdavi) employing chemical and enzymatic modifications. *J. Agric. Sci. Technol.* **2008,** *10*, 243-252.

Sadrzadeh, S.M.; Graf, E.; Panter, S.S.; Hallaway, P. E.; Eaton, J. W. Hemoglobin: a biologic Fenton reagent. *J. Biol. Chem*. **1984**, *259*, 14354-14356

Saeki, H. Preparation of neoglycoprotein from carp myofibrillar protein by Maillard reaction with glucose: biochemical properties and emulsifying properties. *J. Agric. Food Chem*. **1997**, *45*, 680-684.

Saeki, H.; Inoue, K. Improved solubility of carp myofibrillar proteins in low ionic strength medium by glycosylation. *J. Agric. Food Chem*. **1997**, *45,* 3419–3422.

Saeki, H.; Tanabe, M. Change in solubility of carp myofibrillar protein by glycosylation with ribose. *Fish Sci*. **1999**, *65*, 967–968.

Saeki, H. Protein–saccharide interaction. In *Food proteins and peptides: Chemistry, functionality, interactions, and commercialization,* Hettiarachchy, N. S., Sato K., Marshall M. R., Kannan, A., Eds.; London: CRC Press, **2012**, pp. 230–253.

Saha, B.C.; Hayashi, K. Debittering of protein hydrolysates. Research review paper. *Biotech. Adv.* **2001**, *19*, 355-370.

Sajithlal, G.B.; Chithra, P.; Chandrakasan, G. The role of metalcatalyzed oxidation in the formation of advanced glycation end products: an in vitro study on collagen. *Free Radic. Biol. Med*. **1998**, *25*, 265–269.

Sakamoto, H.; Kumazawa, Y.; and Motoki, M. Strength of protein gels prepared with microbial transglutamin ase as related to reaction conditions. *J. Food Sci*. **1994**, *59*, 866-871.

Salazar, J, Bello, L, Chávez, M.; Anez, R.; Rojas, J.; Bermudez, V. Glucosamine for osteoarthritis: biological effects, clinical efficacy, and safety on glucose metabolism. *Arthritis*. **2014**, *2014*, 432463.

Sanmartin, E.; Arboleya, J.C.; Villamiel, M.; Moreno, F.J. Recent advances in the recovery and improvement of functional proteins from fish Processing by-products: use of protein glycation as an alternative method. *Compr. Rev. Food Sci. Tech*. **2009**, *8*, 332-344.

Sarkar, N.K.; Clarke, D.D.; Waelsch, H. An enzymatically catalyzed incorporation of amines into proteins. *Biochim. Biophys. Acta.* **1957**, *25*, 451-452.

Sato, R.; Sawabe, T.; Kishimura, H.; Hayashi, K.; Saeki, H. Preparation of neoglycoprotein from carp myofibrillar protein and alginate oligosaccharide: improved solubility in low ionic strength medium. *J. Agric. Food Chem*. **2000**, *48*, 17-21.

Sato, R.; Katayama, S.; Sawabe, T.; Saeki, H. Stability and emulsion-forming ability of watersoluble fish myofibrillar protein prepared by conjugation with alginate oligosaccharide. *J. Agric. Food Chem*. **2003**, *51*, 4376-4381.

Sato, R.; Sawabe, T.; Saeki, H. Characterization of fish myofibrillar protein by conjugation with alginate oligosaccharide prepared using genetic recombinant alginate lyase. *J. Food Sci.* **2005**, *70*, C58-62.

Schleicher, E. D.; Weigert, C. Role of the hexosamine biosynthetic pathway in diabetic nephropathy. *Kidney Int. Suppl*. **2000**, *77*, S13-8.

Schwarzenbolz, U.; Henle, T.; Haeßner, R.; Klostermeyer, H. On the reaction of glyoxal with proteins. *Z. Lebensm. Unters. Forsch. A*. **1997**, *205*, 121-124.

Sena, C.M.; Metafome, P.; Crisostomo, J.; Rodrigues, L.; Fernandes, R. Pereira, P.; Seica, R.M. **2012**. Methylglyoxal promotes oxidative stress and endothelial dysfunction. *Pharmacol Res.* 65, 497-506.

Shaviklo, G.R.; Arason, S.; Thorkelsson, G.; Sveinsdottir, K.; Martinsdottir, E. Sensory attributes of haddock balls affected by added fish protein isolate and frozen storage. *J Sens Stud*. **2010a**, *25*, 316–331.

Shaviklo, G.R.; Thorkelsson, G.; Arason, S. The influence of additives and frozen storage on functional properties and flow behaviour of fish protein isolated from haddock (*Melanogramms aeglefinus*). *Turk. J. Fish Aquat. Sci.* **2010b**, *10*, 333–340.

Shibamoto, T. Diacetyl: occurrence, analysis, and toxicity. *J. Agric. Food Chem.* **2014**, *62*, 4048−4053.

Shimamura, T.; Takamori, A.; Ukeda, H.; Sawamura, M. Reduction mechanism of tetrazolium salt XTT by a glucosamine derivative. *Biosci. Biotechnol. Biochem*. **2003**, *67*, 295-299.

Shu, Y.; Nakamura, S.; Kato, A. The role of polysaccharide chain attachment to lysozyme in the excellent emulsifying properties of polymannosyl lysozyme. *Nahrung-Food.* **1998**, *42*, 68-70.

Sibi, G.; Dhananjaya, K.; Ravikumar, K. R.; Mallesha, H.; Venkatesha, R. T. Preparation of glucosamine hydrochloride from crustacean shell waste and it's quantitation by RP-HPLC. *American-Eur. J. Sci. Res.* **2013**, *8*, 63-67.

Silván, J.M.; Assar, S.H.; Srey, C.; del Castillo, M.D.; Ames, J.M. Control of the Maillard reaction by ferulic acid. *Food Chem*. **2011**, *128,* 208-213.

Sirangelo, I.; Malmo, C.; Casillo, M.; Mezzogiorno, A,; Papa, M.; Irace, G.Tryptophanyl substituions in apomyoglobin determine protein aggregation and amyloid-like fibril formation at physiological pH. *J. Biol. Chem*. **2002**. *277*, 45887-45891.

Smith, D.M. Functional properties of muscle proteins in processed poultry products. In *Poultry Meat Processing*. Sams, A.R., Ed.; CRC Press: Boca Raton, FL, **2001**; pp.181-194.

Sola, R.J.; Rodriquez-Martinez, J.A., Griebenow, K. Modulation of protein biophysical properties by chemical glycosylation: biochemical insights and biomedical implications. *Cell. Mol. Life Sci.* **2007**, *64*, 2133-2152.

Song, C-L.; Zhao, X-H. A Review on the glycosylation of food proteins by Maillard reaction or transglutaminase-catalyzed reaction. *J. Food Sci*. **2013**, *34*, 369-374.

Song, K.-H.; Kang, J.-H.; Woo, J.-K.; Nam, J.-S.; Min, H.-Y.; Lee, H.Y.; Kim, S.-Y.; Oh, S.-H. The novel IGF-IR/Akt–dependent anticancer activities of glucosamine. *BMC Cancer*. **2014**, *14*, 31.

Soyer, A.; Ozalp, B.; Dalmis, U.; Bilgin, V. Effects of freezing temperatures and frozen storage time on lipid and protein oxidation in chicken meats. *Food Chem.* **2010**, *120*, 1025-1030.

Stepuro, I.I.; Chaikovskaya, N.A.; Vodoevich, V.P.; Vinogradov, V.V. Reduction of methemoglobin and ferricytochrome C by glycosylated amino acids and albumin. *Biochem* (Moscow). **1997**, *62*, 967–972.

Strasburg, G.; Xiong, Y.; Chiang, W. Physiology and chemistry of edible muscle tissues. In *Fennema's Food Chemistry,* 4th ed.; Damodaran, S., Parkin, K., Fennema, O.R., Eds.; CRC Press Taylor and Francis Group: Boca Raton FL, **2008**; pp. 923-973.

Suckau, D.; Resemann, A.; Schuerenberg, M.; Hufnagel, P.; Franzen, J.; Holle, A. A novel MALDI LIFT-TOF/TOF mass spectrometer for proteomics. *Anal. Bioanal. Chem*. **2003**, *376*, 952–965.

Summa, C.; McCourt, J.; Cammerer, B.; Fiala, A.; Probst, M.; Kun, S.; Anklam, E.; Wagner, K. Radical scavenging activity, anti-bacterial and mutagenic effects of cocoa bean Maillard reaction products with degree of roasting. *Mol. Nutr. Food Res.* **2008**. *52*, 342 – 351.

Sunde, M.; Blake, C. The structure of amyloid fibrils by electron microscopy and X-ray diffraction. *Adv. Protein Chem*. **1997**, *50*, 123–159.

Suzuki, Y.J.; Carini, M.; Butterfield, D.A. Protein carbonylation. *Antioxid. Redox Signal*. **2010**, *12*, 323–325.

Swamy, M.J.; Surolia, A. Studies on the tryptophan residues of soybean agglutinin. Involvement in saccharide binding. *Biosci Rep*. **1989**, *9*, 189-198.

Syrovy, I.; Hodny, Z. Non-enzymatic glycosylation of myosin: Effect of diabetes and aging. *Gen. Physiol. Biophys*. **1992**, *11*, 301-307.

Tagliazucchi, D.; Bellesia, A. The gasto-intestinal tract as the major site of biological action of dietary melanoidins. *Amino Acids*. **2015**. DOI:10.1007/s00726-015-1951-z.

Tahergorabi, R.; Jaczynski, J. Physicochemical changes in surimi with salt substitute. *Food Chem.* **2012**, *132*, 1281-1286.

Takeda, H.; Iida, T.; Okada, A.; Ootsuka, H.; Ohshita, T.; Masutani, E.; Katayama, S.; Saeki, H. Feasibility study on water solubilization of spawned-out salmon meat by conjugation with alginate oligosaccharide. *Fish Sci*. **2007**, *73*, 924-930.

Tanabe, M.; Saeki, H. Effect of Maillard reaction with glucose and ribose on solubility at low ionic strength and filament-forming ability of fish myosin. *Agric. Food Chem*. **2001**, *49*, 3403-3407.

Tanaka, M.; Kunisaki, N.; Ishizaki, S. Improvement of emulsifying and antibacterial properties of salmine by the Maillard reaction with dextran. Fisheries Sci. **1999**, *65*, 623–628.

Tang, J., Faustman, C., & Hoagland, T. A. Krzywicki revisited: Equations for spectrophotometric determination of myoglobin redox forms in aqueous meat extracts. J. *Food Sci.* **2004**, *69*, 717–720.

Tang, C-H.; Sun, X.; Foegeding E.A. Modulation of physicochem-ical and conformational properties of kidney bean vicilin (Phaseolin) by glycation with glucose: implications for structure–function relationships of legume vicilins. *J. Agric. Food Chem*. **2011**. *59*, 10114–10123.

Tauer, A.; Elss, S.; Frischmann, M.; Tellez, P.; Pischetsrieder, M. Influence of thermally processed carbohydrate/amino acid mixtures on the fermentation by *Saccharomyces cerevisiae. J. Agric. Food Chem.* **2004**, *52, 2042-2046.*

Thornalley, P.J.; Langborg, A.; Minhas, H.S. Formation of glyoxal, methylglyoxal and 3-deoxyglucosone in the glycation of proteins by glucose. *Biochem. J.* **1999**, *344*, 109-116.

Thornalley, P.J. Protein and nucleotide damage by glyoxal and methylglyoxal in physiological systems - role in ageing and disease. *Drug Metabol. Drug Interact*. **2008**, *23*, 125–150.

Totosaus, A.; Montejano, J. G.; Salazar, J. A.; Guerrero, I. A review of physical and chemical protein-gel induction. *Int. J. Food Sci. Technol.* **2002**, *37*, 589−601.

Traoré, F.; Meunier, J. Cross-linking of caseins by human placental factor XIIIa. *J. Agric. Food Chem*. **1991**, *39*, 1892-1896.

Tressl, R., Wondrak, G.T.; Krüger, R.P.; Rewicki, D. New melanoidin-like Maillard polymers from 2-Deoxypentoses. *J. Agric. Food Chem.* **1998***,* 46, 104-110.

Uitterlinden, E.J.; Koevoet, J.L.; Verkoelen, C.F.; Bierma-Zeinstra, S. M.; Jahr, H.; Weinans, H.; Verhaar, J.A.; van Osch, G.J. Glucosamine increases hyaluronic acid production in human osteoarthritic synovium explants. *BMC Musculoskelet. Disord*. **2008**, *9*, 120-127.

Upmacis, R.K.; Hajjar, D.P.; Chait, B. T.; Mirza, U.A. Direct observation of nitrosylated heme in myoglobin and hemoglobin by electrospray ionization mass spectrometry *J. Am. Chem. Soc.* **1997**, *119*, 10424–10429.

US Market report **2014**. Global glucosamine market analysis and segment forecasts to 2020. URL http://www.grandviewresearch.com/industry analysis/glucosamine-market. Accessed April 17, 2015.

Uzzan, M.; Nechrebeki, J.; Labuza, T.P. Thermal and storage stability of nutraceuticals in a milk beverage dietary supplement *J. Food Sci.* **2007**, *72*, E109-114.

van der Kraan, P.M.; de Vries, B.J.; Vitters, E.L.; van den Berg, W.B.; van de Putte, L.B. Inhibition of glycosaminoglycan synthesis in anatomically intact rat patellar cartilage by paracetamol-induced serum sulfate depletion. *Biochem. Pharmacol*. **1998**, *37*, 3683–3690.

Venugopal, V. Polysaccharides: their characteristics and marine sources. In Marine Polysaccharides: Food Applications. CRC Press: Boca Raton, FL; **2011**. pp. 396.

Vigetti, D.; Viola, M.; Karousou, E.; De Luca, G.; Passi, A. Metabolic control of hyaluronan synthases. *Matrix Biol.* **2014**, *35*, 8-13.

Villamena, F. Protein posttranslational modification. In *Molecular Basis of Oxidative Stress*: *Chemistry, Mechanisms, and Disease Pathogenesis*, edition 1; John Wiley and Sons Ltd: UK, **2013**.

Visessanguan, W.; An, H. Effects of proteolysis and mechanism of gel weakening in heat-induced gelation of fish myosin. *J. Agric. Food Chem.* **2000**, *48,* 1024-1032.

Vosseller, K.; Wells, L.; Lane, M.D.; Hart, G.W. Elevated nucleocytoplasmic glycosylation of O-GlcNAc results in insulin resistance associated with defects in Akt activation in 3T3-L1 adipocytes. *PNAS*. **2002**, *99*, 5313–5318.

Wahyuni, M.; Ishizaki, S.; Tanaka, M. Improvement of thermal stability of fish water soluble proteins with glucose-6-phosphate through the Maillard reaction. *Fish Sci.* **1998**, *64*, 973-978.

Wahyuni, M.; Ishizaki, S.; Tanaka, M. Improvement of functional properties of fish water soluble proteins with glucose-6-phosphate through the Maillard reaction. *Fish Sci*. **1999**, *65*, 618–622.

Weenen, H. Reactive intermediates and carbohydrate fragmentation in Maillard chemistry. *Food Chem*. **1998**, *62*, 393–401.

Wei, Y.; Chen, L.; Chen, J.; Ge, L.; He, R.Rapid glycation with D-ribose induces globular amyloid-like aggregations of BSA with high cytotoxicity to SH-SY5Y cells. *BMC Cell Biol*. **2009**, *10*, 10.

Weimer, S.; Priebs, J.; Kuhlow, D.; Groth, M.; Priebe, S.; Mansfeld, J.; Merry, T.L.; Dubuis, S.; Laube, B. et al. D-Glucosamine supplementation extends life span of nematodes and of ageing mice. *Nat. Commun*. **2014**, *5*, 3563.

Wellen, K.E.; Lu, C.; Mancuso, A.; Lemons, J.M.S.; Ryczko, M.; Dennis, J.W.; Rabinowitz, J.D; Coller, H.A.; Thompson, C.B. The hexosamine biosynthetic pathway couples growth factor-induced glutamine uptake to glucose metabolism. *Genes Dev*. **2010**. *24*, 2784-2799

Wells, L.; Vosseller, K.; Hart, G.W. A role for N-acetylglucosamine as a nutrient sensor and mediator of insulin resistance. *Cell Mol. Life Sci*. **2003**, *60*, 1-7.

Wong, C.M.; Marcocci, L.; Liu, L.; Suzuki, Y. Cell Signaling by Protein Carbonylation and Decarbonylation. *Antioxid. Redox Signal*. **2010**, *12*, 393–404.

Wong, B.T.; Li, D.; Augustin, M.A. Deamidated heat protein-dextran Maillard conjugates: effect of size and location of polysaccharide conjugates on steric stabilization of emulsions at acidic pH. *Food Hydrocolloid.* **2011**, *25,* 1424-1432.

Worratao, A.; Yongsawatdigul, J. Cross-linking of actomyosin by crude tilapia (*Oreochromis niloticus*) transglutaminase. *J. Food Biochem*. **2003**, *27*, 35-51.

Wrolstad, R.E.; Acree, T.E.; Decker, E. A.; Penner, M.H.; Reid, D.S.; Schwartz, S. J.; Shoemaker, C.F.; Smith, D.; Sporns, P. Functionality of proteins. In *Handbook of food analytical chemistry, water, proteins, enzymes, lipids, and carbohydrates*. John Willey and Sons: New Jersey, **2005**; Vol. 2. pp. 289-323.

Wu, S.; Hu, J.; Wei, L.; Du, Y.; Shi, X.; Zhang, L. Antioxidant and antimicrobial activity of Maillard reaction products from xylan with chitosan/chitooligomer/glucosamine hydrochloride/taurine model systems. *Food Chem.* **2014**, *148*, 196-203.

Xiong, Y.L.; Blanchard, S.P. Myofibrillar protein gelation: viscoelastic changes related to heating procedures. *J. Food Sci.* **1994**, *59,* 734-738.

Xiong, Y.L. Structure-function relationship of muscle proteins. In *Food Proteins and Their Applications*, Damodaran, S., Paraf, A., Eds.; Marcel Dekker: New York, NY, **1997**; pp. 341-392.

Yanagimoto, T.; Tanaka, M.; Nagashima, Y.; Taguchi, T. Changes in the antibacterial activity of salmine during its Maillard reaction. Nippon Suisan Gakkaishi. **1992**, *58*, 2153–2158.

Yang, Y.; Shao, Z.; Chen, X.; Zhou, P. Optical spectroscopy to investigate the structure of regenerated bombyx mori silk fibroin in solution. *Biomacromolecules.* **2004**, *5*, 773-779.

Yaylayan, V.A.; Keyhani, A. Origin of carbohydrate degradation products in L-alanine/D-[13C]glucose model systems. *J. Agric. Food Chem*. **2000**, *48*, 2415–2419.

Yongsawatdigul, J.; Park, J.W. Thermal aggregation and dynamic rheological properties of Pacific whiting and cod myosins as affected by heating rate. *J. Food Sci.* **1999**, *64,* 679-683.

Yongsawatdigul, J.; Park, J.W. Effects of alkali and acid solubilization on gelation characteristics of rockfish muscle proteins. *J. Food Sci*. **2004**, *69*, 499-505.

Zehl, M.; Guenter, A. Ultraviolet matrix-assisted laser desorption/ionization time-of-flight mass spectrometry of intact hemoglobin complex from whole human blood. *Rapid Commun. Mass Spectrom*. **2004**, *18*, 1932-1938.

Zhang, X.; Ma, Y.; Liu, H.; De Sa, P.F.; Brown, P.R.; Dain, J.A. Capillary electrophoresis separation of autocondensation glycation products of glucosamine. *J. Capill. Electrophor. Microchip. Technol.* **2003**, *1-2*, 33-37.

Zhang, X.; Ma, Y.; Liu, H.; De Sa, P.F.; Brown, P.R.; Dain, J.A. Monitoring the formation of Maillard reaction products of glucosamine with fibrinogen and human serum albumin using capillary electrophoresis. *Anal. Biochem.* **2004**, *325*, 255-259.

Zhang, W.; Moskowitz, RW.; Nuki, G.; Abramson, S.; Altman, RD.; Arden, N.; Bierma-Zeinstra, S.; Brandt, K.D.; Croft, P.; Doherty, M.; et al. OARSI recommendations for the management of hip and knee osteoarthritis, Part II: OARSI evidence-based, expert consensus guidelines. *Osteoarth. Cartilage*. **2008**, *16*, 137-162.

Zhang, X.; Tong, N.; Li, Y. Concurrently using rosiglitazone prevents glucosamine-induced islet and beta Cell apoptosis and dysfunction. *Cell Biochem. Funct*. **2010,** *28*, 509-514.

Zheng, J.; Zanuy, D.; Haspel, N.; Tsai, C.J.; Aleman, C.; Nussinov, R. Nanostructure design using protein building blocks enhanced by conformationally constrained synthetic residues. *Biochem.* **2007**, *46,* 1205-1218.

Zhu, D.; Damodaran, S.; Lucey, J.A. Formation of whey protein isolate (WPI)–dextran conjugates in aqueous solutions *J. Agric. Food Chem*. **2008**, *56*, 7113–7118.

Zhu, D.; Damodaran, S.; Lucey, J.A. Physicochemical and emulsifying properties of whey protein isolate (WPI)-dextran conjugates produced in aqueous solution. *J. Agric. Food Chem.* **2010**, *58*, 2988–2994.

Zhuo, X.Y.; Qi, J.R., Yin, S.W.; Yang, X.Q.; Zhu, J.H.; Huang, L.X. Formation of soy protein isolate–dextran conjugates by moderate Maillard reaction in macromolecular crowding conditions. *J. Sci. Food Agric.* **2013**, 93-316-3.

Appendix A. Schematic flow diagram of the isoelectric solubilization/precipitation process.

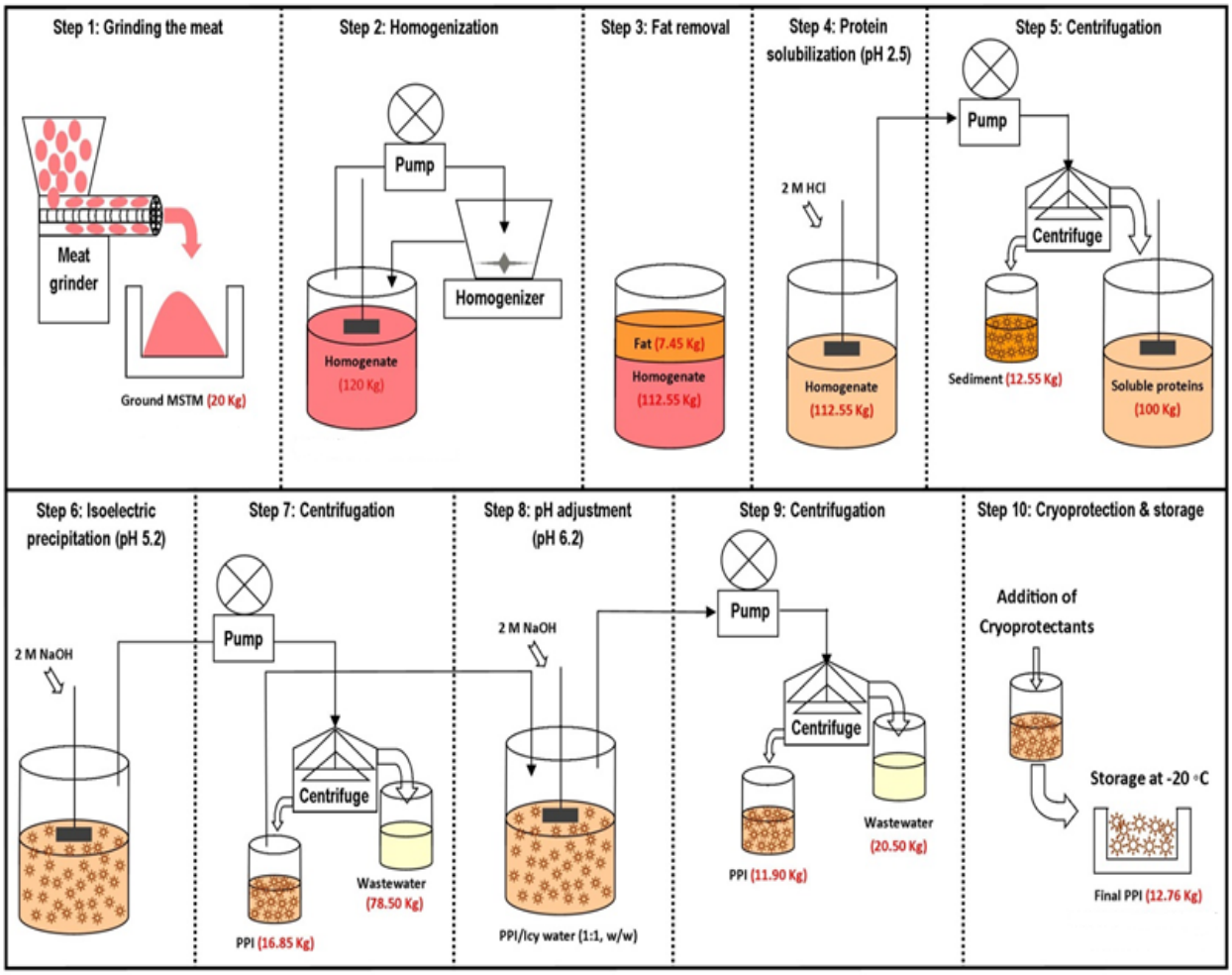

Reproduced from Khiari et al. 2014 with minor modifications.

Appendix B. MS/MS spectra and tentative structures of the peaks (9) and (10) shown in the Figure 5.2. (9) 2-amino-2-deoxy-4-glucosyl-5,6-dihydroxy-2-oxohexanal (4-GlcN-3-DG) and (10) 4-glucosyl-5,6-dihydroxy-2-oxohexanal (4-Glc-3-DG).

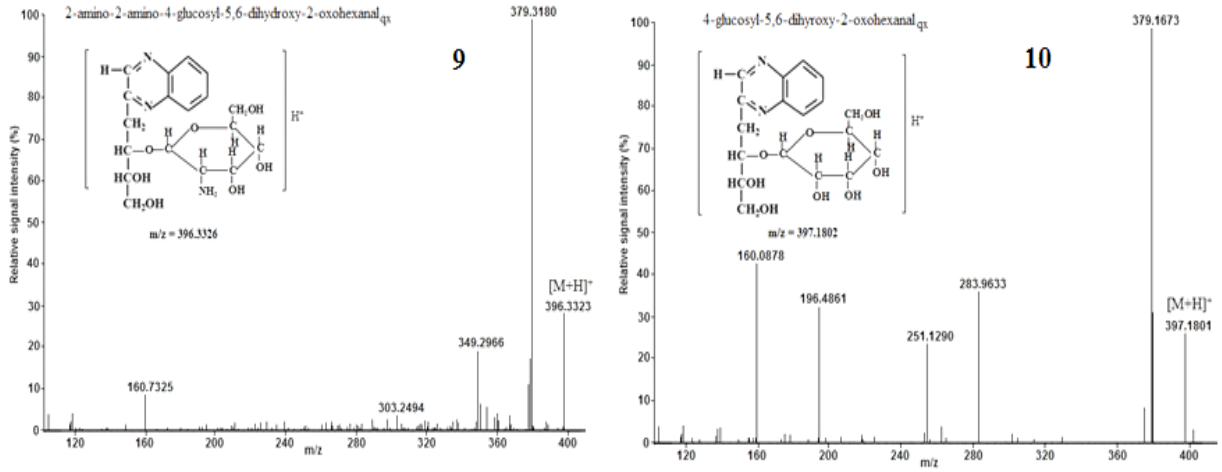

Appendix C. Precursor ions of the peaks (a), (b) and (c) indicated as non-OPD derived α-dicarbonyl compounds in UHPLC-UV chromatogram (Figure 5.2 II).

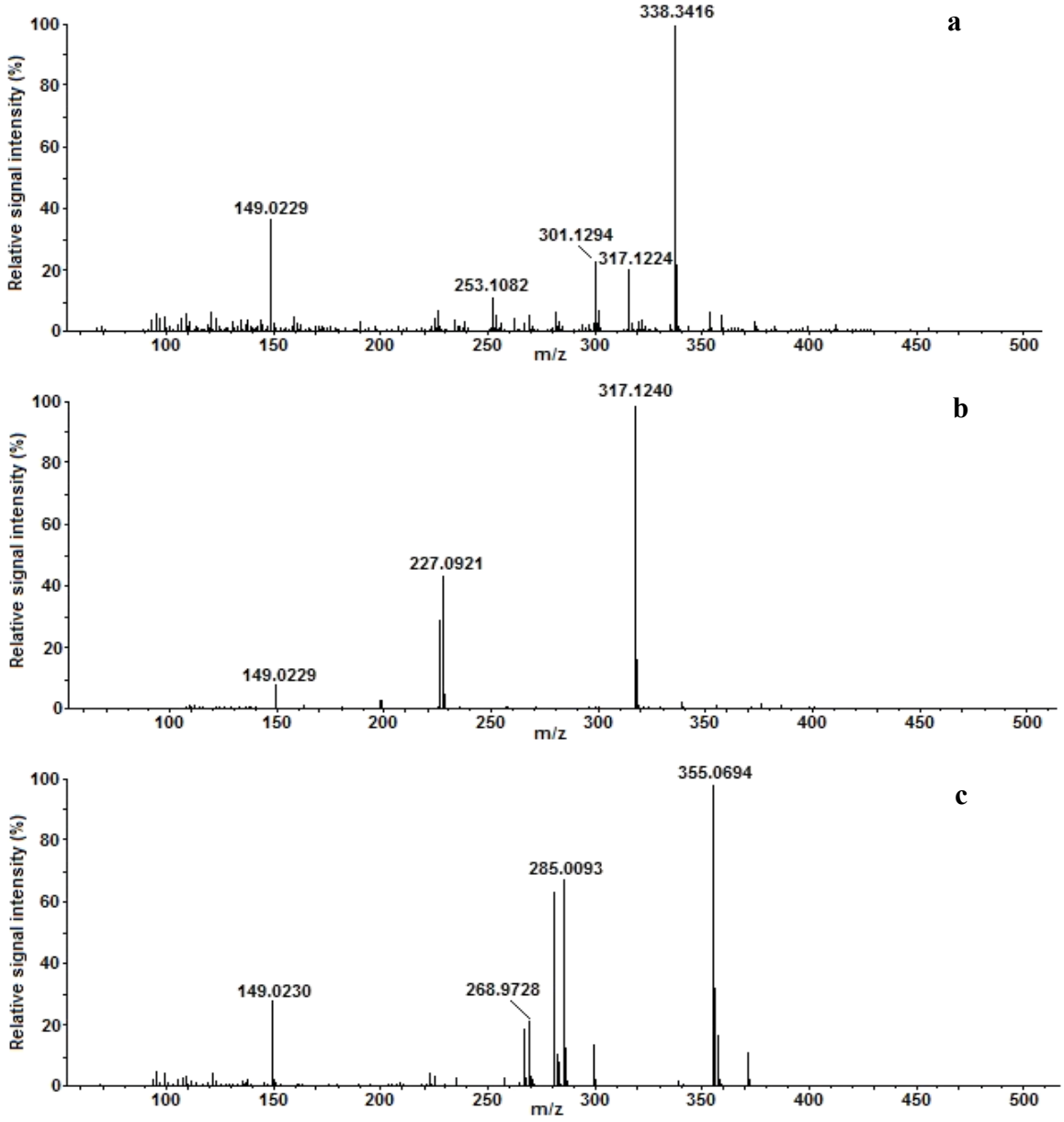

Appendix D. Percentage of NH_3 released during incubation of glucosamine from 0 to 12 days at 37°C.

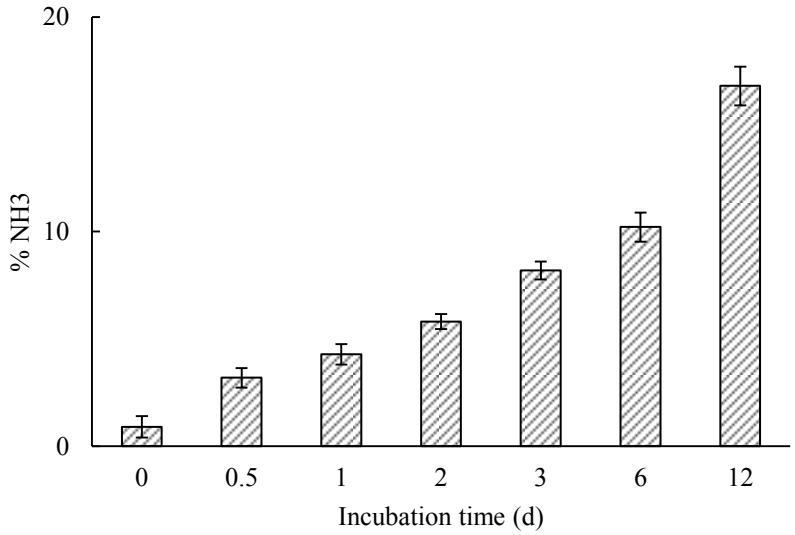

Appendix E. Blocked amino groups upon glycation of Mb with GlcNAc, Glc and GlcN through the Maillard reaction for various incubation periods (0.5, 1, 2, 3, 6 and 12 d).

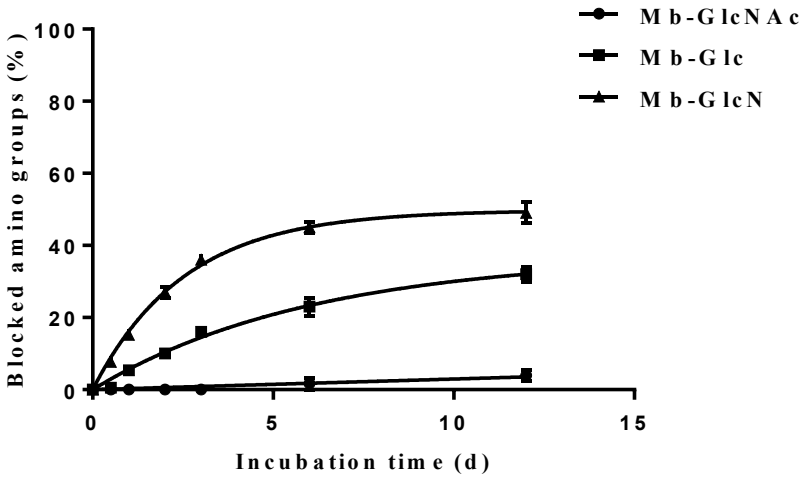

Determination of available amino groups

The quantity of free amino groups in control and glycated samples was determined by the ortho-phthaldialdehyde (OPA) method described in Jiang and Brodkorb (2012). The OPA reagent was prepared fresh daily by mixing 25 mL of 0.1 M sodium tetraborate, 2.5 mL of 20% w/w sodium dodecyl sulfate (SDS), 100 µl of β-mercaptoethanol and 40 mg OPA (dissolved in 1 mL of methanol) and adjusting the final volume to 50 mL with distilled water. Fifty µL of protein solution (0.5 mg/mL in 50 mM potassium phosphate buffer, pH 7.4) was added to 1 mL of OPA reagent and incubated for 2 min at room temperature. The absorbance was red at 340 nm against a blank containing the OPA reagent. A calibration curve was obtained by using 0.25-2.00 mM L-leucine as a standard. Untreated myoglobin (control) was assumed to have 100% available amino groups.

Appendix F. Total (A) and free (B) AGEs in Mb-GlcNAc, Mb-Glc and Mb-GlcN mixtures incubated for various periods (0.5, 1, 2, 3, 6 and 12 d) at 37˚C. Each bar is the mean and standard deviation of triplicate measurements.

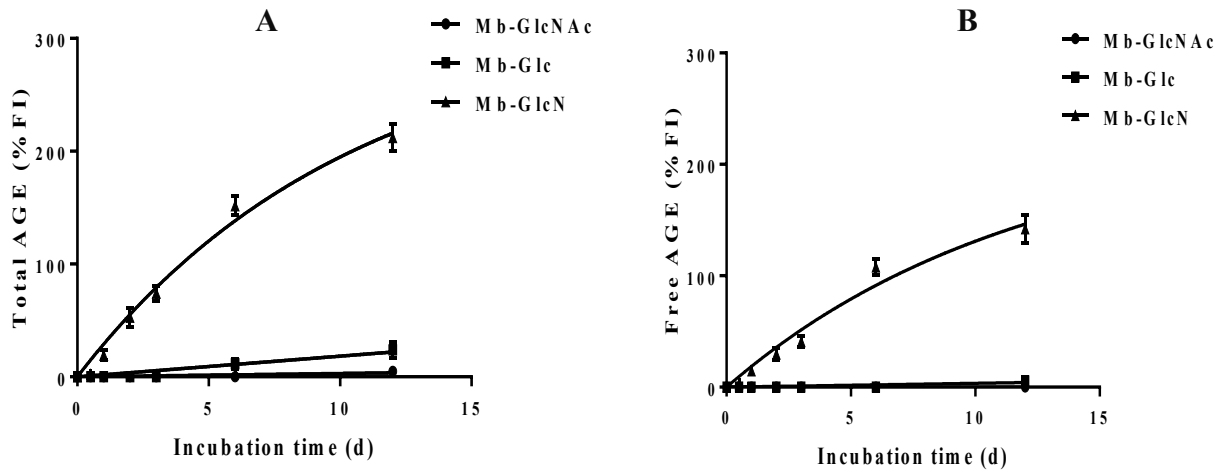

Determination of advanced reaction products

To assess the production of AGEs, glycated Mb was diluted with a phosphate buffer (pH 7.4) to a final concentration of 2 mg/mL (the samples were not subjected to ultrafiltration followed glycation reaction in order to avoid the loss of AGEs). According to the method of Ferrer et al. (2005), for measuring free fluorescence, 2 mL of samples were deprotoinized by addition of 2 mL of 24% (w/v) TCA. For determination of the total fluorescence, enzymatic hydrolysis with 20 U/mL Pronase E (from *Streptomyces griseus* (≥3.5 U/mg, EC 3.4.24.4)), at 25˚C for 30 min was carried out. Solutions corresponding to free and total AGEs were centrifuged at 13000*g* for 10 min at room temperature and 100 μL of the resulting supernatants were diluted in 5 mL of 50 mM saline phosphate buffer (pH 7.4). The spectra were recorded at 347 nm excitation and 370–600 nm emission. Maxima of emission were found at 430 nm, thus this wavelength was chosen for AGEs detection (Hayase, 2000). The spectra values derived from GlcN control incubated at tested times were subtracted. Results were expressed as relative fluorescence intensity (%FI) with respect to the fluorescence of a 0.5 μg/mL quinine sulfate standard in 0.1 N sulfuric acid. Emission spectra were recorded in quartzglass cuvettes with a path length of 1 cm using SpectraMax M3 (Molecular Devices, USA).

Appendix G. Multiple-charged ions spectrum of Mb-GlcNAc control and incubated mixtures acquired on an Agilent 6220 ESI-TOF MS. A) Full spectrum at 0 days. B) Zoomed in spectrum at Z = 21-18. C) Full spectrum at 12 days. D) Zoomed in spectrum at Z = 21-18.

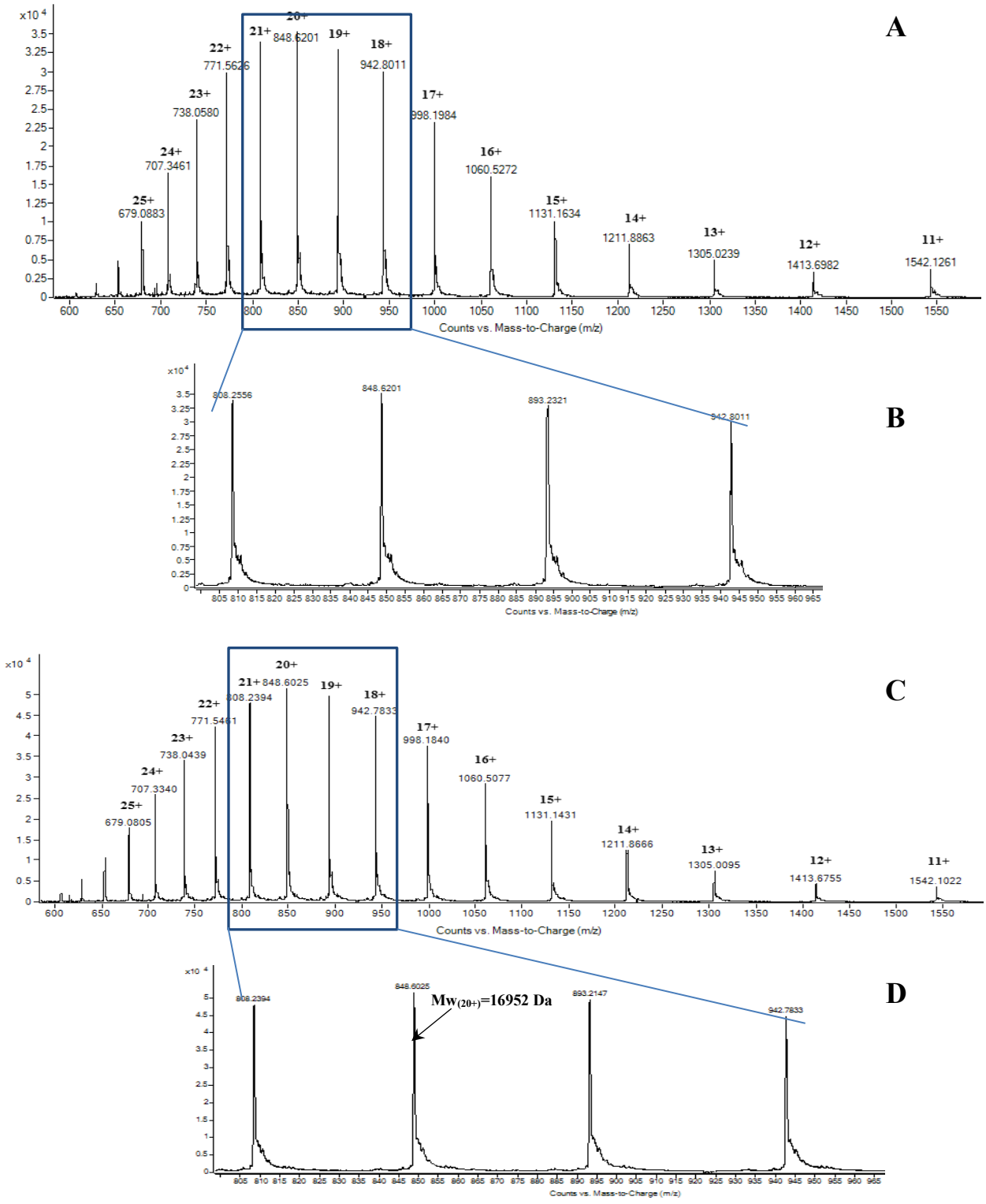

Appendix H. Multiple-charged ions spectrum of Mb-Glc control and incubated mixtures acquired on an Agilent 6220 ESI-TOF MS. A) Full spectrum at 0 days. B) Zoomed in spectrum at Z = 21-18. C) Full spectrum at 12 days. D) Zoomed in spectrum at Z = 21-18.

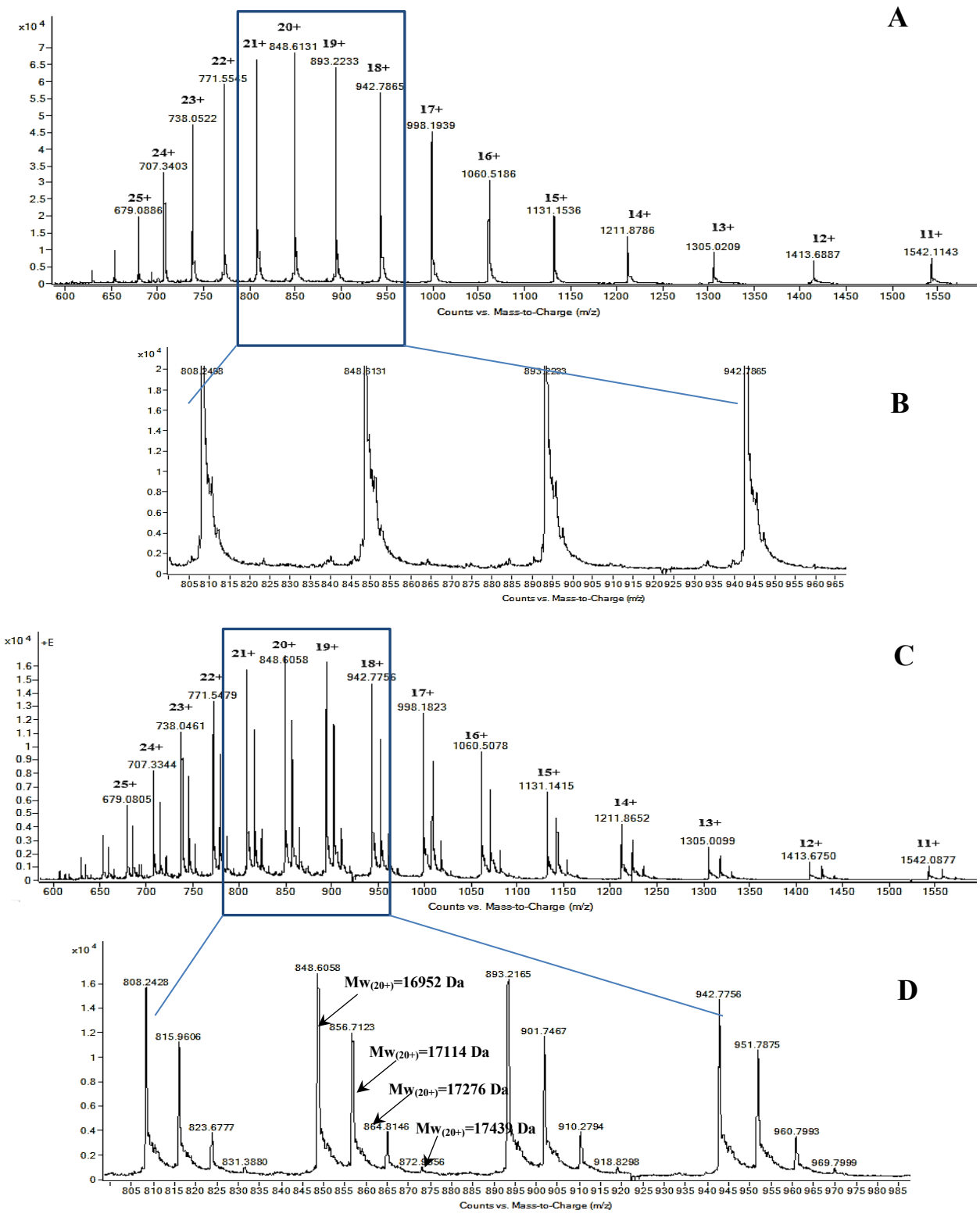

Appendix I. Multiple-charged ions spectrum of Mb-GlcN control and incubated mixtures acquired on an Agilent 6220 ESI-TOF MS. A) Full spectrum at 0 days. B) Zoomed in spectrum at Z = 21-18. C) Full spectrum at 6 days. D) Zoomed in spectrum at Z = 21-18.

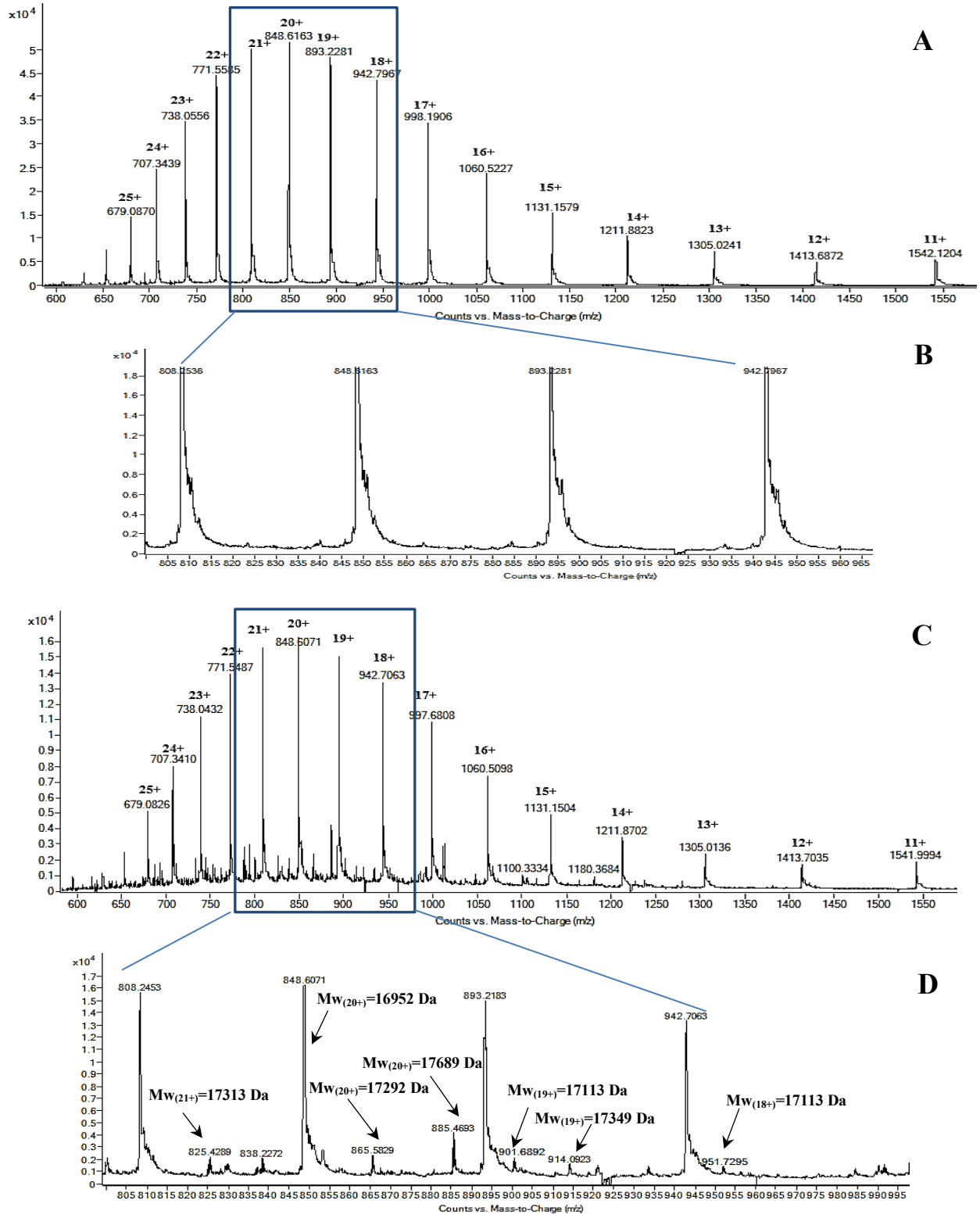

Appendix J. The mean of triplicate Thioflavin T fluorescence measurements (λ=482 nm) in Mb control, Mb-Glc and Mb-GlcNAc treatments. The data points all have SD bars, but some are illegible and lie within the symbols.